

Hozy 3

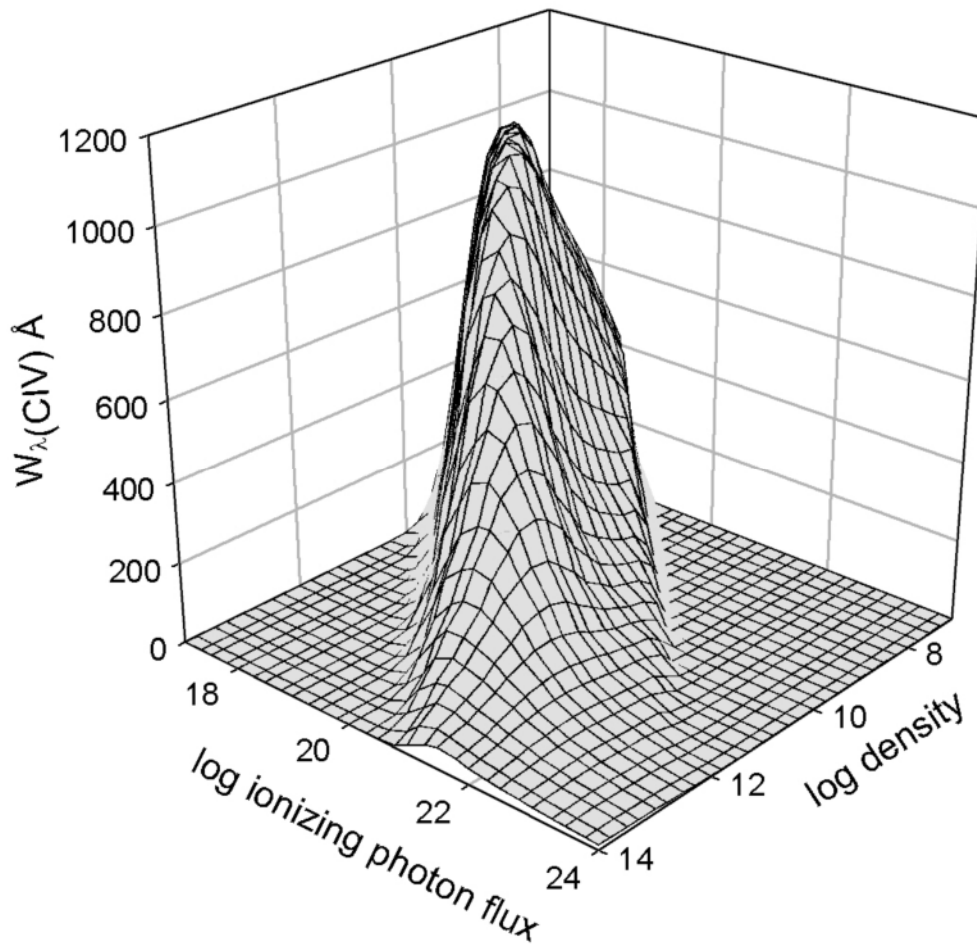
a brief introduction
to Cloudy 96

results, environment

G.J. Ferland

*Department of Physics and Astronomy
University of Kentucky, Lexington*

<http://www.pa.uky.edu/~gary/cloudy>



Use of this program is not restricted provided each use is acknowledged upon publication. The bibliographic reference to this version of Cloudy is "version 96 of the code last described by Ferland, G.J., et al 1998, PASP, 110, 761-778.

Portions of this document have been published, and are copyrighted by, the American Astronomical Society, the Astronomical Society of the Pacific, and the Royal Astronomical Society. The remainder of this document, and the code Cloudy, are copyright 1978-2004 by Gary J. Ferland.

Cloudy is an evolving code. Updates are made on a roughly quarterly basis, while major revisions occur roughly every three years. You should confirm that you have the most recent version of the code by checking the web site <http://www.nublado.org> or by asking to be placed on the Cloudy mailing list.

CLOUDY 96

G. J. Ferland

Department of Physics and Astronomy

University of Kentucky

Lexington

Table of Contents

1 OTHER DETAILS	401
1.1 Overview	401
1.2 Overall Code Structure.....	401
1.2.1 The main program	401
1.2.2 Routine cdDrive	401
1.2.3 Routine Cloudy	401
1.2.4 The convergence ladder	402
1.2.5 ConvPresTempEdenIoniz converge pressure	402
1.2.6 ConvTempEdenIoniz - converge temperature	402
1.2.7 ConvEdenIon - converge the electron density	403
1.3 Line radiative transfer routines.....	406
1.4 Geometry.....	406
1.5 Physical Conditions	407
1.5.1 Densities	407
1.5.2 Temperatures.....	408
1.5.3 Structure	408
1.6 Optical depths and iterations	409
1.6.1 RTOptDepthInit	409
1.6.2 RTOptDepthIncre	409
1.6.3 RTOptDepthReset.....	409
1.6.4 lgTauOutOn.....	409
1.7 Zones and Iterations	409
1.8 Search phase?.....	410
1.9 Composition variables.....	410
1.10 Covering factors	411
1.10.1 Geometric covering factor	411
1.10.2 Radiative transfer covering factor	411
1.11 Floating Point Environment	412
1.12 Reliability in the face of complexity	412
2 RUNNING A SINGLE MODEL	413
2.1 Running a single model with a shell script	413
2.2 Running a single model from the command line.....	413
3 CLOUDY AS A SUBROUTINE.....	414
3.1 Overview	414
3.1.1 Creating a new main program.....	415

3.1.2	The cddrive.h header file.....	415
3.1.3	The cddefines.h header file	415
3.1.4	A note on return conditions.....	415
3.2	Initializing the code.....	415
3.3	Handling input and output.....	416
3.3.1	cdTalk - produce output??	416
3.3.2	cdOutp - sending output to a file.....	416
3.3.3	cdRead - entering Commands.....	416
3.4	Executing the code.....	417
3.4.1	cdDrive - calling the Code.....	417
3.4.2	cdNoExec - checking without Computing	417
3.5	Checking Predictions	418
3.5.1	cdLine - emission lines intensities.....	418
3.5.2	cdDLine - emergent line intensities	419
3.5.3	cdGetLineList - special arrays of emission lines	419
3.5.4	cdEmis - emissivity of lines.....	420
3.5.5	cdColm - the computed column densities	420
3.5.6	cdH2_colden - column density in H ₂	421
3.5.7	cdCO_colden - column density in CO.....	421
3.5.8	cdIonFrac - the computed ionization fractions	421
3.5.9	cdTemp - the computed mean temperature.....	422
3.5.10	cdGetCooling_last, cdGetHeating_last - last zone's cooling or heating	423
3.5.11	cdGetTemp_last - the temperature of the last zone.....	423
3.5.12	cdGetPressure_last - pressure of the last zone	423
3.5.13	cdGetnZone - how many zones in the last iteration?	423
3.5.14	cdGetPressure_depth - pressure structure of the last iteration.....	423
3.5.15	cdGetDepth_depth - returns the depth structure of the previous iteration	423
3.5.16	cdTimescales - several timescales.....	423
3.5.17	cdSPEC - get predicted spectrum.....	423
3.6	Other information.....	424
3.6.1	cdDate(cdString).....	424
3.6.2	cdVersion(cdString)	424
3.6.3	double cdExecTime(void)	424
3.7	Printing the comments.....	424
3.7.1	Were comments generated?.....	424
3.7.2	Printing the comments.....	425
3.7.3	cdErrors(FILE *io) - printing a summary of any problems	425
3.7.4	cdPrintCommands(FILE *io) - print the command stack	425
3.7.5	setbuf or the no buffering command	425
3.8	Example Call as a Subroutine	426
3.9	Computing Grids of Calculations	426
3.10	Storing Grids of Calculations.....	427
4	OUTPUT.....	429
4.1	Overview.....	429

4.2 Header Information	429
4.2.1 Initial Information.....	429
4.2.2 Properties of the Continuum.....	429
4.3 Chemical composition.....	432
4.4 Zone Results.....	432
4.4.1 Line 1	432
4.4.2 [Optional] wind parameters.....	433
4.4.3 [Optional] radiation pressure.....	433
4.4.4 Line 1 - Hydrogen I.....	433
4.4.5 Line 2 - Hydrogen II	433
4.4.6 Line 3 - Helium.....	434
4.4.7 Line 4 - Atomic Helium.....	434
4.4.8 Line 5 - Ionized Helium	434
4.4.9 Pressure	434
4.4.10 Optional Grains.....	435
4.4.11 Molecules	435
4.4.12 Li, Be, B.....	435
4.4.13 Carbon	435
4.4.14 Nitrogen	435
4.4.15 Oxygen	435
4.4.16 Fluorine, Neon.....	435
4.4.17 Remaining Elements.....	435
4.5 Calculation Stopped Because	436
4.5.1 ... because of radiation pressure	436
4.5.2 ... because lowest EDEN reached.....	436
4.5.3 ... because low electron fraction.....	436
4.5.4 low H ₂ /H fraction.....	436
4.5.5 ... because wind veloc too small.....	437
4.5.6 ... because code returned BUSTED	437
4.5.7 ... because DRAD small - set DRMIN	437
4.5.8 ... because DR small rel to thick.	437
4.5.9 ... because optical depth reached.	437
4.5.10 ... because outer radius reached.....	437
4.5.11 ... because column dens reached.....	437
4.5.12 ... because lowest Te reached.	438
4.5.13 ... because highest Te reached.	438
4.5.14 ... because NZONE reached.....	438
4.5.15 ... because line ratio reached.....	438
4.5.16 ... because internal error - DRAD.	438
4.5.17 ... because initial conditions out of bounds.....	438
4.5.18 Because zero electron density	438
4.5.19 ... because reason not specified.	438
4.6 Geometry.....	439
4.7 Warnings, Cautions, Surprises, and Notes.....	439
4.8 Optional Plot.....	440
4.9 Final Printout.....	441

4.9.1 Emission-Line Spectrum.....	441
4.9.2 Thermal balance.....	442
4.9.3 Column densities, et al.	443
4.9.4 Averaged Quantities.....	444
4.9.5 Grains.....	446
4.9.6 Continuum optical depths.....	446
4.9.7 Line optical depths.....	447
4.9.8 Column density.....	447
4.9.9 Mean ionization.....	447
4.9.10 Continuum.....	448
5 OBSERVED QUANTITIES.....	450
5.1 Overview.....	450
5.2 Incident and Diffuse Continua.....	450
5.3 Line Equivalent Widths.....	450
5.4 Emission Line Asymmetries.....	451
5.5 Line to Continuum Contrast.....	451
5.6 Surface Brightness.....	452
5.7 Flux to luminosity.....	453
5.8 Flux at the Earth.....	453
5.9 Relative hydrogen line intensities.....	453
5.10 Helium line intensities.....	454
5.11 Line Intensities in a dusty open geometry.....	454
5.12 Continuum pumping contribution to line intensities.....	455
5.13 Column densities.....	455
5.14 A synthetic spectrum.....	455
5.15 Line profiles.....	455
6 THE EMISSION LINES.....	457
6.1 Overview.....	457
6.2 The main emission line printout.....	457
6.2.1 Blocks of lines.....	458
6.2.2 General properties.....	458
6.2.3 Continua.....	458
6.2.4 Molecules.....	459
6.2.5 Grains.....	459
6.2.6 H-like iso-seq.....	460
6.2.7 He iso-sequence.....	461
6.2.8 level 1 lines.....	461
6.2.9 Recombination.....	462
6.2.10 Level 2 lines.....	462
6.3 The transferred lines.....	462
6.3.1 Punch line data output.....	462
6.3.2 Output produced for the transferred lines.....	463
6.4 Forbidden Lines.....	464
6.5 Atomic data sources.....	470

7 CODING CONVENTIONS	487
7.1 Variable names and strong typing	487
7.1.1 Integers	487
7.1.2 Double or float variables	487
7.1.3 Character strings	487
7.1.4 Logical variables	487
7.2 Structure names	488
7.3 Braces	488
7.4 Changes to the code	488
7.5 Atomic data references	489
7.6 Sanity checks and asserts	489
7.7 Code in need of attention	489
7.8 Version numbers	490
8 PROBLEMS	491
8.1 Overview	491
8.2 Thermal stability and temperature convergence	491
8.2.1 Types of thermal maps	491
8.2.2 No Temperature Convergence	492
8.2.3 Thermal Stability	494
8.2.4 Thermal fronts	494
8.2.5 Map Output	495
8.3 Floating Point Errors	496
8.4 Optical depth convergence problems	496
8.5 Negative populations of H-like and He-like ions, and molecules	496
8.6 I can't fix it if I don't know it's broken.	496
9 REVISIONS TO CLOUDY	498
9.1 Overview	498
9.2 Cloudy and Moore's Law	498
9.3 Major Past Versions	498
9.4 Version 96 vs 94	501
9.4.1 Commands	501
9.4.2 Physics	501
9.4.3 Miscellaneous	501
9.5 Version 94 versus 90	501
9.5.1 Commands	501
9.5.2 Hydrogen	501
9.5.3 Grains	502
9.5.4 Other changes	502
9.6 Version 90 versus 84	502
9.6.1 Commands	502
9.6.2 Continuum Transport	502
9.6.3 Hydrogen	502
9.6.4 The helium ion	502
9.6.5 Heavy elements	503
9.6.6 Free-free, line heating and cooling	503
9.6.7 Excited state photoionization cross sections	503

9.6.8 The O ⁺ photoionization cross section.....	503
9.7 Version 84 versus 80.....	504
9.7.1 Commands	504
9.7.2 Mg II λ 2798.....	504
9.7.3 General Results	505
9.8 Known Modes for Cloudy 96.....	505
9.9 Making a Revision.....	505
9.9.1 The code.....	505
9.9.2 Printing Hazy.....	505
10 COMPARISON CALCULATIONS	507
10.1 Overview.....	507
10.2 Cool HII Region	508
10.3 Paris HII Region.....	509
10.4 Blister HII Region	511
10.5 Paris Planetary Nebula	513
10.6 Paris NLR Model	516
10.7 Lexington NLR Model	518
10.8 The DQ Her Shell.....	520
10.9 The Kwan and Krolik Standard Model	521
10.10 Rees, Netzer, and Ferland, low density.....	522
10.11 Rees, Netzer, and Ferland, high density	523
11 THE TEST SUITE	524
11.1 Gas phase H ₂ balance	Error! Bookmark not defined.
12 REFERENCES.....	529
13 INDEX.....	540

List of Figures

main's structure.	401
Cloudy's structure.	403
ConvPresTempEdenIoniz 's structure.....	404
ConvTempEdenIoniz's structure.	405
ConvEdenIoniz's structure.....	406
Line radative transfer structure.....	406
A grid of model calculations.....	414
Reflected continuum	451
Reflected continuum	454
Ccooling function for low density photoionized gas.	491
Cooling function for low density collisionally ionized gas.....	492
Temperature as a function of density for photoionized gas.	493
Thermal front in cooling flow cloud.....	494
Cloudy's size as a function of time.....	498
O ⁺ photoionization cross section	504

List of Tables

Excited state column densities	420
Cool HII Region.....	508
Cool HII Region vs Cloudy	508
Paris meeting HII region.....	509
Paris HII region vs cloudy	510
Blister HII Region.....	511
Blister HII Region vs Cloudy.....	512
Paris meeting planetary nebula	514
Paris planetary vs Cloudy.....	515
Paris meeting NLR model.....	516
Paris NLR model vs CLOUDY.....	517
Lexington NLR Model.....	518
Lexington NLR vs Cloudy	519
DQ Her Shell.....	520
Kwan and Krolik Standard Model	521
Rees, Netzer, Ferland low density BLR	522
Rees, Netzer, Ferland high density BLR.....	523
Single model test cases	524

1 OTHER DETAILS

1.1 Overview

This section largely outlines internal details of code variables, and how these relate to overall quantities. These are described only after the relevant portion of the code has become fairly mature, and not likely to undergo further major revision.

1.2 Overall Code Structure

This section outlines the flow control in the higher levels of the code.

1.2.1 The main program

When used as a stand-alone program, control passes to program *main* contained in `maincl.c`, which initializes the code by calling *cdInit*. It then reads the input stream (from standard input) and passes the line images into the code by calls to *cdRead*. The main routine calls *cdDrive* to compute the model, then checks whether any problems occurred during the calculation (by calling *cdNwcns*). It then prints a brief summary of what happened and stops. The organization is shown in Figure 1.

There actually is no difference in the way the stand-alone and subroutine versions of the code work. The main routine simply reads standard input and passes the command strings into the code through calls to routine *cdRead*. The one difference is that the main routine includes logic to identify whether the input stream is the header of a previous calculation.

1.2.2 Routine *cdDrive*

cdDrive is called to execute the code, both in the stand-alone and subroutine versions. *cdDrive* decides whether to compute a single model or try to optimize a model by varying a set of parameters by checking whether the keyword **vary** occurred on a command line. If the keyword did not appear then it simply calls routine *cloudy* to compute a single model. If the keyword **vary** occurred then *cdDrive* calls *DoOptimize*, the routine to optimize parameters to match a set of observations.

1.2.3 Routine *Cloudy*

Most of the actual work performed in the computation of a model is done in the main subroutine *Cloudy* (Figure 2). This routine controls the zone and iteration variables *nzone* and *iter*.

At its outermost level the routine controls the number of iterations and stops when the simulation is complete. Within this loop is an inner loop that determines whether a particular

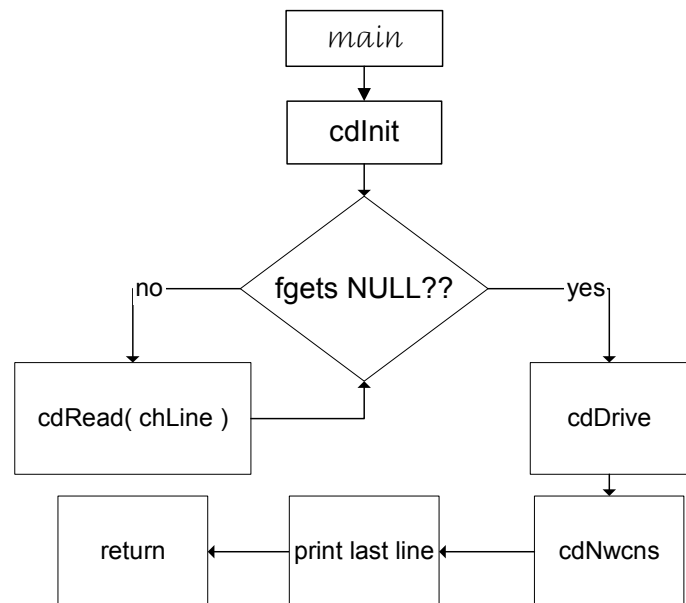


Figure 1 This shows the structure of the main program.

iteration is complete. This inner loop controls the integration over zones and checks stopping criteria to determine whether the structure is complete.

1.2.4 The convergence ladder

Many quantities must be simultaneously converged. The following table, and the following sections, outlines the nested group of routines that converges each type of ingredient. At the highest level the pressure is converged, and that solver assumes that the temperature, ionization, etc, are known. Below that is the temperature solver, which is not concerned with the pressure, but assumed that the ionization and electron density are known. Below that is the electron density solver, which assumes that the level of ionization, and the OTS rates, are known.

Routine	Ionization OTS	Electron density	Temperature	Pressure	Trace convergence keyword
ConvPresTempEdenIoniz	Stable	Stable	Stable	Solve	Pressure
ConvTempEdenIoniz	Stable	Stable	Solve	NA	Temperature
ConvEdenIoniz	Stable	Solve	NA	NA	Eden
ConvIoniz	Solve	NA	NA	NA	ioniz
ConvBase	Drive	NA	NA	NA	

1.2.5 *ConvPresTempEdenIoniz* converge pressure

ConvPresTempEdenIoniz, shown in Figure 3, is the routine that converges the local pressure or satisfies some other specification of the gas density. Its major loop calls routine *PressureChange*, which determines what the local density/pressure should be, changes the density if necessary, and sets the variable *conv.lgConvPres* to true if the current pressure is correct. It then calls routine *ConvTempEdenIoniz* to determine the local temperature, electron density, and level of ionization at the new density. *ConvPresTempEdenIoniz* loops until the pressure is declared converged (by the value of the flag *conv.lgConvPres*) as determined by routine *PressureChang*.

1.2.6 *ConvTempEdenIoniz* - converge temperature

ConvTempEdenIoniz is the routine that calls *ConvEdenIoniz* to converge the electron density and ionization, and simultaneously determines the electron temperature by balancing heating and cooling. An overview is shown in Figure 4. *Ionte* totally controls the value of *lgDoPhoto*. When *lgDoPhoto* is true the code completely reevaluates all opacities and photoionization rates. When false the rates are left at previous values, safe for second iterations.

ConvTempEdenIoniz returns when the heating and cooling match (the variable *conv.lgConvTemp l* is set TRUE), or a temperature failure occurs (*tfail* is set true). The Boltzmann factors are evaluated next in routine *boltgn*.

A great deal of the code within *ConvTempEdenIoniz* deals with identifying temperature oscillations or problems in obtaining temperature convergence. The upshot of this is an estimate of the partial derivative of the difference in heating and cooling with respect to temperature. Many tricks are used to establish this estimate. Routine *MakeDeriv* can recall previous values of the heating and cooling and make numerical estimates of their change with respect to temperature. Analytical

estimates are also made from the functional form of various heating and cooling constituents.

1.2.7 *ConvEdenIon* - converge the electron density

The electron density is actually converged by routine *ConvEdenIon*, called by *ConvTempEdenIon* as described above. The structure of the routine is shown in Figure 5.

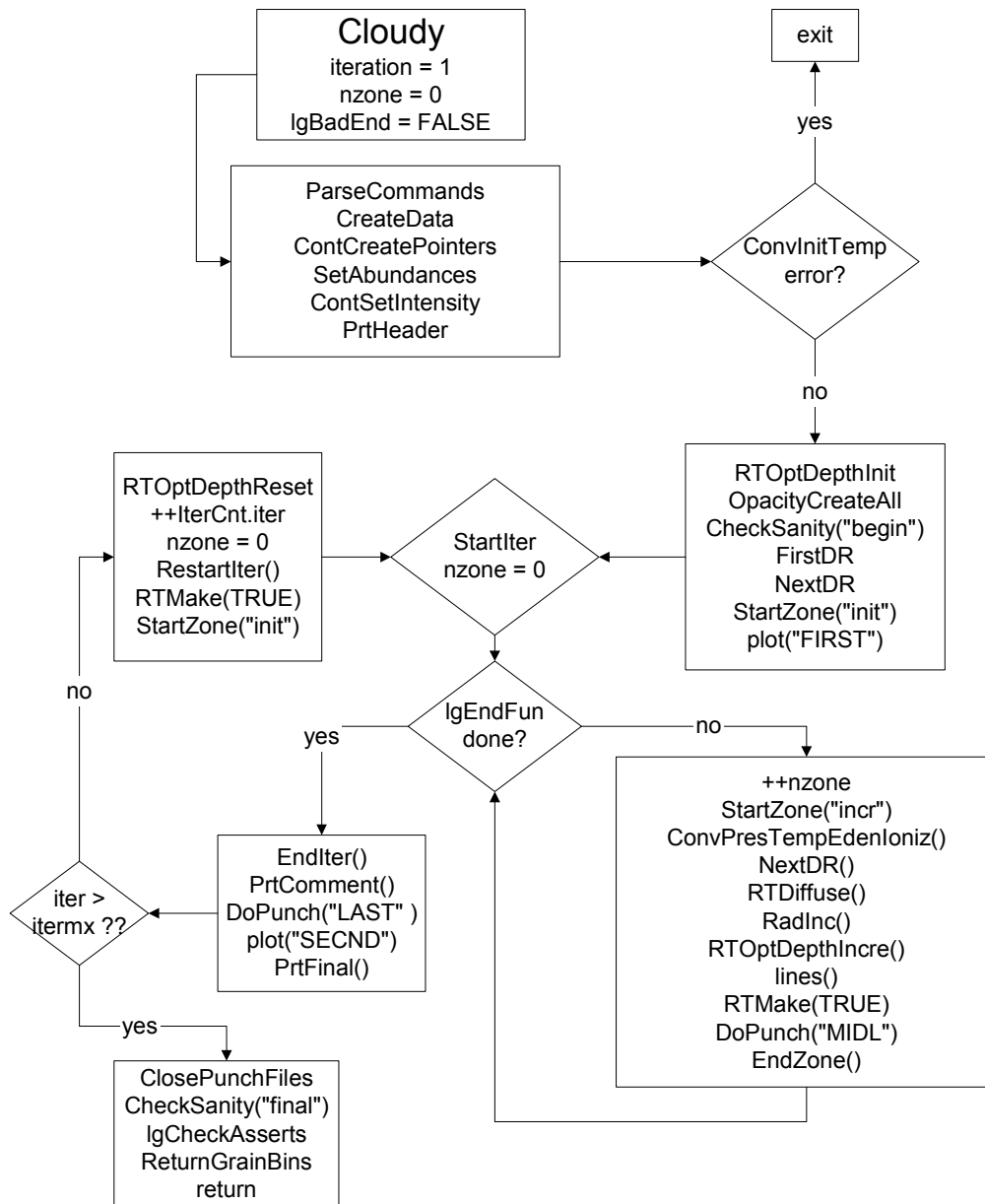


Figure 2 This figure shows the structure of subroutine Cloudy.

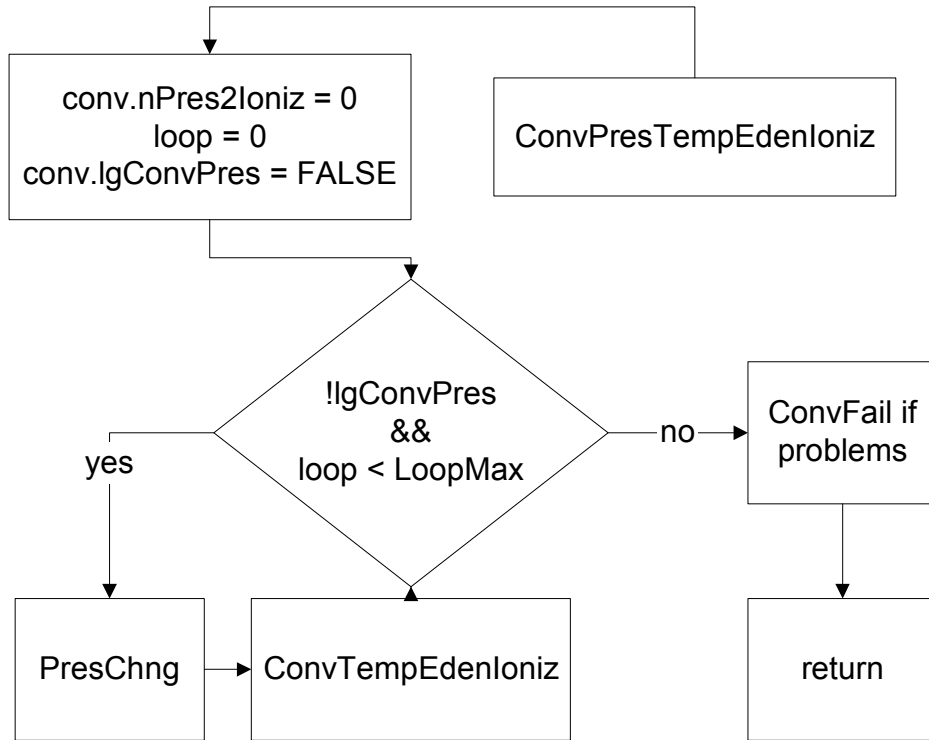


Figure 3 This figure shows the structure of routine ConvPresTempEdenloniz..

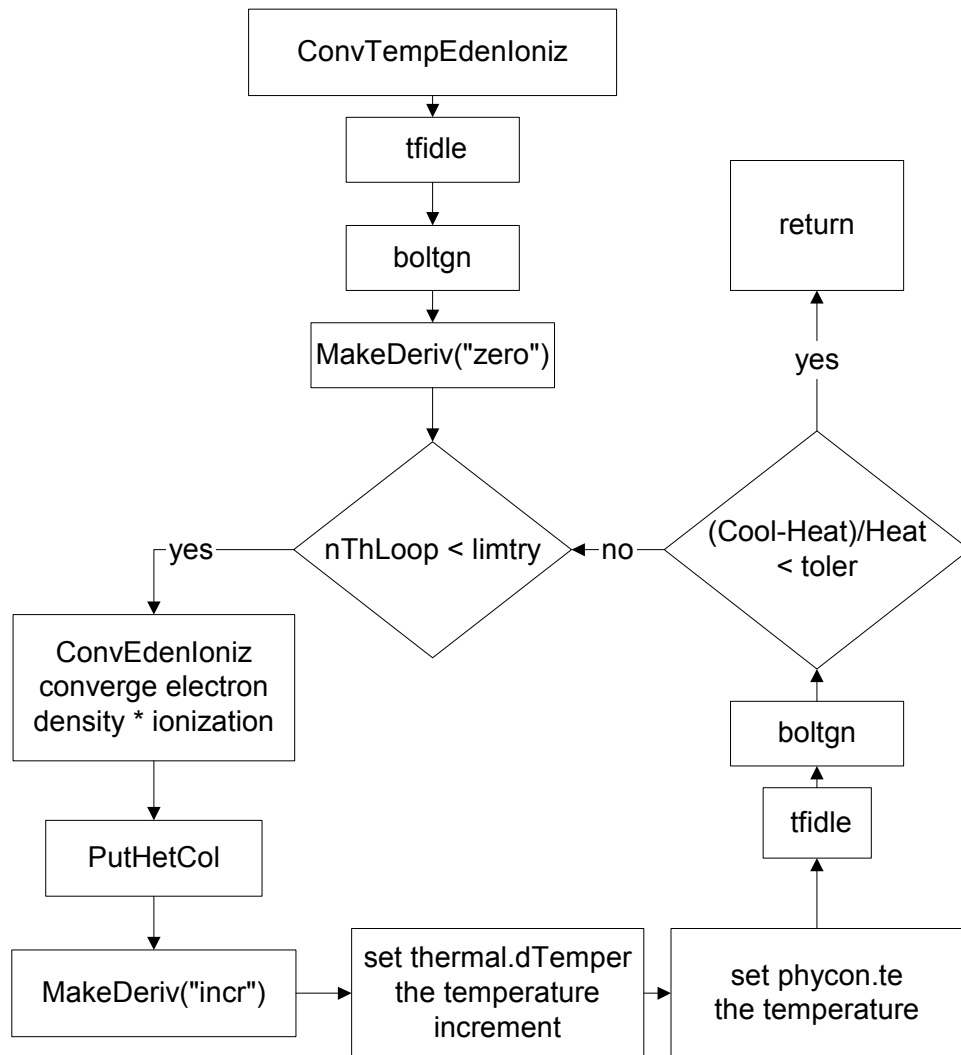


Figure 4 This figure shows the structure of routine ConvTempEdenIoniz.

1.3 Line radiative transfer routines

Figure 6 shows the series of routines that are called to evaluate line radiative transfer.

1.4 Geometry

This section defines the internal variables used to describe the geometry. The geometry is always spherical, but can be made effectively plane parallel by making the inner radius of the cloud much larger than its thickness.

Most variables having to do with the geometry members of the structure *radius*, contained in *radius.h*, and are set and incremented in routine *StartZone*. The following gives the variable name and a brief description of its intentions. Variables are contained within the structure *radius*.

rinner, r_o This is the separation between the center of symmetry (i.e., the center of the central object) and the inner edge of the cloud. It remains constant throughout the calculation. If an inner radius is not specified then it is given the default value of 10^{30} cm. This will usually result in a plane parallel geometry.

drad, δr This is the thickness of the current zone. Note that the zone size changes continuously throughout the calculation. Upper or lower limits to *drad* can be set with the *drmax* and *drmin* commands, described in Part I.

radius, r This is the distance between the center of symmetry and the *outer* edge of the current zone. For the first zone, *radius* has the value *rinner* + *drad*.

depth, Δr This is the distance between the inner edge of the cloud and the *outer* edge of the current zone. For the first zone, *depth* has the value *drad*.

A problem can arise under certain extreme circumstances. The depth variable *depth* must

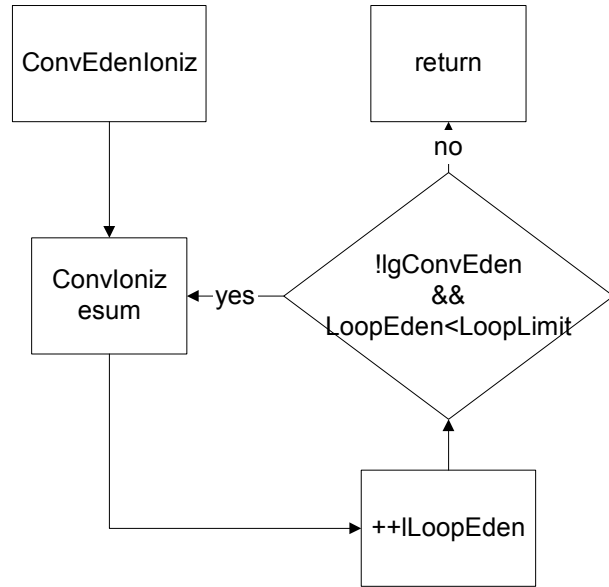


Figure 5 The structure of routine *ConvEdenIoniz*.

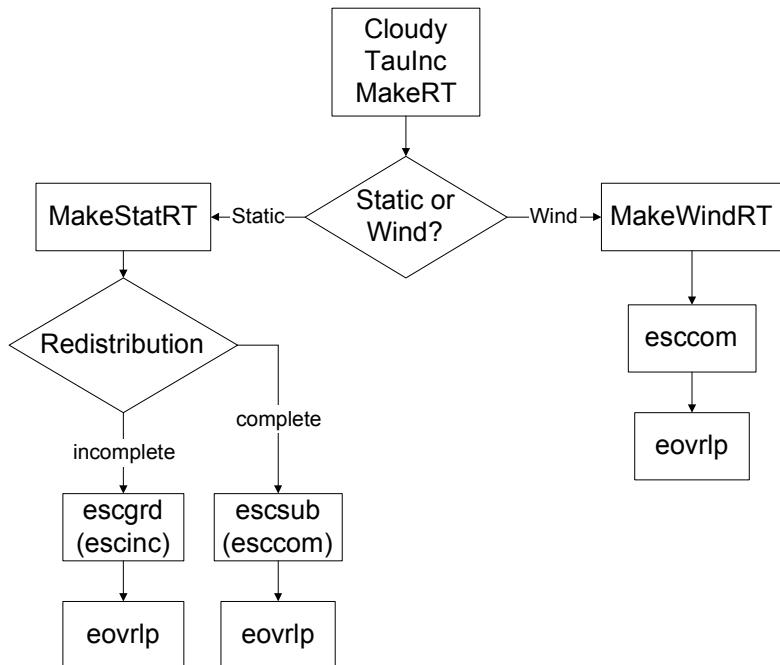


Figure 6 This figure shows the structure of the radiative transfer routines. radtrn

be increased for every zone by adding the zone thickness *drad*. Both variables are double precision. If the ratio *drad/depth* falls below $\sim 10^{-14}$ then the depth cannot be updated on most machines. The problem is that the sum *depth + drad* will be equal to *depth* because of numerical underflow. If this occurs (i.e., the zone thickness *drad* falls below *depth/10¹⁴*) the code will stop, with the comment that the zone thickness is too small relative to the depth. There is no obvious solution to this problem.

drNext This will be the thickness of the next zone. The thickness of the zones is adjusted continuously during a calculation. Adaptive logic is used to ensure that the zones are large enough to be economical, but small enough to follow changes in the physical conditions across the nebula. This choice of the next zone thickness is done in routine *NextDR*. The logic behind the choice of the zone thickness can be followed with either the **trace dr** or **punch dr** commands.

router[iteration] This is the limit to the outer radius of the structure, as set before the calculation begins. The default value is effectively infinite, actually 10^{31} cm.

r1r0sq This is the sphericity ratio

$$R1R0SQ = \left[\frac{\text{outer radius of zone}}{\text{radius of face}} \right]^2 = \left(\frac{\text{RADIUS}}{\text{RINNER}} \right)^2 \quad (1)$$

dReff This is the effective radius, $\delta r_{\text{eff}} = \delta r \times f(r)$ where *f(r)* is the filling factor.

dVeff This is the effective volume relative to the inner radius. The units of *dVeff* are cm, and it is equal to *dReff* if the geometry is plane parallel.

$$dVeff = \left(\frac{\text{radius} - dRad / 2}{rinner} \right) \left(\frac{\min(\text{radius} - dRad / 2, \text{cylind})}{rinner} \right) dRad \times f(r) \quad (2)$$

Structure *fourpi* has the following:

pirsq This is the log of the inner area ($4\pi r_o^2$).

lgFourPi - set true if quantities like line intensities are into 4π sr.

1.5 Physical Conditions

1.5.1 Densities

These are contained in structure *dense*.

xMassDensity The gas mass density in gm cm⁻³.

pden This is the number of particles per cubic centimeter. It is evaluated in *TotalPressure*.

wmole This is a quantity related to the mean molecular weight, the mean AMU per particle. It is evaluated in *TotalPressure*.

$$wmole = \frac{\sum n_i m_i}{n_{\text{tot}}} \quad (3)$$

With these definitions the density *densty* (gm cm⁻³) is the product of *pden* and *wmole*.

TotalNuclei – total number of nuclei

eden This is the electron density, as evaluated in routine *esum*. *eden* is also controlled by other parts of the code, which allow it to change only gradually while looking for a new solution.

EdenTrue This is the correct electron density, and is evaluated in *esum*. The electron density has converged when *EdenTrue* and *eden* are within *EdenError* of one another. *EdenError* is set in the large block data to 0.01. This variable is the sole member of the common block of the same name.

edensqte This is the ratio

$$edensqte = (n_e + n_H 10^{-4}) T_e^{-0.5} \quad (4)$$

used in many collision rate equations across the code. It is evaluated in routine *tfidle*. The second term in parenthesis approximately accounts for neutral collisions.

cdsqte This is the ratio

$$cdsqte = edsqte \times 8.629 \times 10^{-6} = (n_e + n_H 10^{-4}) T_e^{-0.5} 8.629 \times 10^{-6} \quad (5)$$

used in many collision rate equations across the code. It is evaluated in routine *tfidle*.

1.5.2 Temperatures

These are all contained in structure *phycon*.

te This is the local electron temperature.

tlast is the final temperature of the last computed zone. It is only meaningful for the second or greater zone.

alogte, *alogete* These are the base 10 and natural logs of the electron temperature. The array *telogn* contains powers of the base 10 log of the temperature.

telogn[i] This is a vector dimensioned 7 long. The n^{th} member of the array contains $\log(T_e)^n$.

alogete is the natural log of the temperature.

Routine *StartZone* will propose a temperature for the next zone, the variable *TeProp*, if the model is a constant density model. Routine *tfidle* sets all ancillary variables related to the temperature, such as *alogte*.

1.5.3 Structure

The *struc* structure. This saves information about the structure of the model. It has several elements, each containing a saved quantity for a zone.

ednstr The electron density of each zone is saved in this vector.

hiistr The H^+ density of each zone is saved in this vector.

histr The H^0 density of each zone is saved in this vector.

heatsrt This is the total heating.

pdenstr This save the total number of particles per cubic centimeter.

radstr The effective thickness *dReff* (cm) of each zone is saved in this vector. This includes a filling factor if one was specified.

testr The temperature structure of the nebula is saved in this vector.

volstr The volume dV_{eff} (cm^3) of each zone is saved in this vector. This includes a filling factor if one was specified.

1.6 Optical depths and iterations

1.6.1 *RTOptDepthInit*

Routine *RTOptDepthInit* is called soon after the initial boundary conditions are established, to estimate the initial total line and continuum optical depths. It uses various methods to estimate these.

1.6.2 *RTOptDepthIncr*

Routine *RTOptDepthIncr* is called once during each zone to increment the optical depth scale.

1.6.3 *RTOptDepthReset*

Routine *RTOptDepthReset* is after the iteration is complete to reset the optical depth scale.

1.6.4 *lgTauOutOn*

This logical variable indicates whether or not the outward optical depths have been estimated. It is false on the first iteration and true thereafter.

1.7 Zones and Iterations

iteration This global variable is the counter for the current iteration. It is set to one at the start of the first iteration, and is incremented in routine *Cloudy* after the last printout, just after the limiting optical depths are updated by calling routine *RTOptDepthReset*. The calculation stops when *iteration* is greater than *itermx* after the iteration is complete, but before the counter is incremented.

ITRDIM This is the limit to the total number of iterations that can possibly be performed. It is used to declare the dimension of the vectors that store iteration information. It currently is set to 200.

itermx This is the limit to the number of iterations to be performed and is set by the user. *itermx* is part of the structure *IterCnt*. *itermx* is initialized to 0 so that the code normally stops after the first iteration. The value of *itermx* can be changed with the **iterate** command. *itermx* is set equal to the number entered on the command *minus one*. This is so that “**iterate 1**” will cause the code to stop after a single iteration (*iteration* is equal to 1 at the end of the first iteration, and the code will only stop if *iteration* is greater than *itermx* after the iteration is complete).

nzone This is a global variable and gives the current zone number. It is equal to one for the first zone. *nzone* is set and incremented in routine *Cloudy*. *nzone* is equal to zero during the search for the initial conditions, on all iterations. After the search has identified a solution the conditions in the first zone are computed with *nzone* set to unity.

nend[I] This is the limit to the number of zones in the current (i^{th}) iteration and is part of the structure *ZoneCnt*. It is a vector of dimension 200 (as set by *ITRDIM*).

Individual elements of the vector are set with the **stop zone** command. The current iteration stops when *nzone* is greater than or equal to *nend[iteration]*.

lgLastIt This logical variable indicates whether (true) or not this is the last iteration. It is controlled by routine *startr* and is set true if *iter* is greater than *itermx*, and false otherwise.

1.8 Search phase?

The logic used during the search for the initial conditions at the illuminated face of the cloud is quite different from that used when going from zone to zone across the cloud. Usually no good estimate of the initial conditions exists, but within the cloud conditions do not vary by much from zone to zone. One way to check whether the code has a valid estimate of the physical conditions, or whether the first step in the initial search for parameters is taking place, is to check the status of the variable *conv.lgSearch*. The initial search is underway if this variable is true. Another is to check whether *nzone* is greater than 0.

Some quantities are totally unknown while the various routines are being called for the very first time during a calculation. The variable *nPres2Ioniz*, part of *conv*, is zero before the ionization has been determined the first time, since it counts the number of times the pressure routine has called the ionization routine.

1.9 Composition variables

All variables that hold information concerning abundances and composition are contained in the structure *abund*, defined in the header file *abundances.h*.

Routine *SetAbundances* is called by routine *cloudy* after all commands have been entered. This routine sets the final abundances to be used in the first zone of the calculation. The following variables are used.

Routine *SetAbundances* first modifies the contents of *solar* by the scale factors. The helium abundance is altered by both *depset* and *scalem*, while all heavier elements are modified by these and *dmetal* as well. Then *abund.gas_phase[nelem]* is set to the density (cm^{-3}) of each element, the product *hden* and *solar[nelem]*. This is the total abundance of that element, in all stages of ionization and molecular forms.

The initial chemical composition is printed by routine *PrintElem*, which is called by *SetAbundances*.

Default abundances are stored in several arrays. Solar abundances are stored in the array *SolarSave[nelem]*, where *nelem* is the atomic number on the C scale. Other mixtures, such as ISM, HII Region, etc, are also entered in this structure, in other arrays. Each array is dimensioned *LIMELM* (currently 30), the number of elements included in the code.

When the code is initialized the contents of *SolarSave* are copied to the array *solar*, which will contain the initial abundance mix for the current calculation. Gas phase depletion factors, used to modify the final abundance, are stored in the array *depset[nelem]* and are set to unity in routine *zero* when the calculation is initialized. The final contents of *solar* will be absolute abundances by number, on a scale with hydrogen at unity.

When an element with atomic number $nelem+1$ is turned off, the logical variable `lgElmtOn[nelem]` is set to false.

ScaleMetals This is the scale factor entered with the **metals** command when a number but no keyword appears on the line. This multiplies the abundances of all elements heavier than helium. It has no effect on hydrogen or helium.

depset If the **metals** command is entered and no numbers appear, but the keyword **deplete** occurs instead, then this array of scale factors is set to the contents of the array *deplon*.

ScaleElement This is an array of *LIMELM* scale factors, and is set when the **element scale** command is entered.

lgAbnSolar This logical variable is false if the default abundances have been altered, and is true if they are left at the default solar mixture. It is used for sanity checks within the code.

xIonDense This is a two dimensional vector containing the gas-phase ionic abundances. $xIonDense[nelem][n]$ is the gas-phase density of the n th ionization stage of that element, where the atom is 0.

1.10 Covering factors

Two covering factors enter into the calculations. These are referred to as the geometric covering factor, and the radiative transfer covering factor. All covering factors are part of the structure *sphere*, defined in the header file *sphere.h*.

1.10.1 Geometric covering factor

This covering factor linearly affects the luminosity of emission lines. The nebula intercepts a fraction $\Omega_{geo} / 4\pi$ of the luminosity radiated by the central object. Within the code the geometric covering factor is referred to by the variable *covgeo*.

The code actually works in units of intensity radiated by a unit area of illuminated face of the cloud to avoid exponential range problems with IEEE machines. If the predicted intensity of a line ($\text{erg s}^{-1} \text{cm}^{-2}$) is given by I then the line luminosity will be

$$L = 4\pi r_{inner}^2 \frac{\Omega_{geo}}{4\pi} I \quad [\text{erg s}^{-1}] \quad (6)$$

where r_{inner} is the inner radius.

The default value of the geometric covering factor is unity, and it can be changed with the **covering factor** and **sphere** commands.

1.10.2 Radiative transfer covering factor

The radiative transfer covering factor has only second order effects on the intensity of emission lines. This is the covering factor which takes into account interactions with diffuse fields produced on the symmetric far side of the nebula. Within the code it is referred to by the variable *covrt*.

The default value of the radiative transfer covering factor is zero, appropriate for an open geometry. For a closed geometry it is set to unity. The radiative transfer covering factor only affects the model through the diffuse fields. For a closed geometry all radiation is included in the outward beam, and for an open geometry

only half. This covering factor has no effects on the calculations, other than the amount of diffuse fields transferred outward. Physically for an open geometry the fraction of radiation escaping in the inward direction is then lost to the system. In an open geometry the nebula is symmetric, and escaping radiation is exactly matched by radiation impinging from the far side of the geometry.

1.11 Floating Point Environment

The floating-point environment should be set to ignore floating-point underflow but crash on any other floating-point error. Floating-point underflow is an unavoidable consequence of the attenuation of radiation as a beam of light is extinguished by an absorbing medium; underflow error checking should be disabled.

Floating point overflow or division by zero *must never* occur, nor should library function domain errors (i.e., the log of a negative number). I would appreciate hearing about these errors. I can't fix it if I don't know it is broken. My email address is gary@pa.uky.edu. Please send the input file and version number.

1.12 Reliability in the face of complexity

The real challenge in software development is to prevent mistakes from happening in the first place, catch mistakes as soon as they are produced, then validate all results every time anything changes (Ferland 2001b). You can help by keeping on the lookout for suspicious results.

2 RUNNING A SINGLE MODEL

2.1 Running a single model with a shell script

Cloudy is often used to read in the parameters for a single model and compute the result. The easiest way to do this is to create a small file that contains the input commansa for that model. As a typical case consider a simple planetary nebula:

```
hden 4 // this is the log of the hydrogen density (cm^-3)
radius 17 // log of the inner radius in cm
black body 100,000K, luminosity 38 // black body temperature and total luminosity
```

Assume this is saved as the file *pn.in*. Note that Cloudy stops reading the input steam when it reaches either an empty line or the end of file. No special end of input sentinel is needed.

I created a shell script with the name *run* which is in my “bin” directory, which I include on my path. The shell script *run* consists of the following:

```
echo reading input file $1.in
case $# in
0) echo there must be an input file ;;
1) /homeb/uwc0/gary/cloudy/c.sun4<$1.in >$1.out
   echo created output file $1.out ;;
2) /homeb/uwc0/gary/cloudy/c.sun4 < $1.in >$2.out
   echo created output file $2.out ;;
esac
echo $p
exit
```

If *run* is executed with no input parameters it will complain that at least one argument is needed and then stop. If there is one parameter it is treated as the name of the input and output files. So in the above example, typing

```
run pn
```

would read the input stream in *pn.in* and create an output file of results called *pn.out*. When two parameters occur the first is the name of the input stream and the second is the name of the output steam. The example

```
run pn test
```

would read the file *pn.in* and create the file *test.out*.

2.2 Running a single model from the command line

The code also has a command line option that will accomplish the same thing as the shell script described in the previous section. If you create an executable called *cloudy.exe*, then the command

```
cloudy.exe -p model
```

will read input from *model.in*, write output to *model.out*, and add the prefix *model* to all the punch files. This option was added by Robin Williams.

3 CLOUDY AS A SUBROUTINE

3.1 Overview

It is possible to use Cloudy as a subroutine of other, much larger, codes. When used this way a series of subroutine calls, described next, are used to initialize the code, specify the initial conditions, drive the code, and finally examine the predictions.

It is said to be possible to call a C program like Cloudy from Fortran programs by using the *cfortran.h* header file described at <http://www-zeus.desy.de/~burow/cfortran/>

A common strategy is to call the code to compute line intensities for a large matrix of parameters. The results of one such calculation is shown in Figure 7 (Baldwin et al. 1995). Such grids can be computed in a few dozen hours on modern workstations, and offer far greater insight to physical effects of changing model parameters, than does a single model.

This Chapter gives an overview of all the routines that are intended to be “public” (needed to be accessed by programs that will call Cloudy). The definitions for all public routines are contained in the header file *cdrive.h*, which gives the best current description of all these routines. That file is the definitive reference source for all of

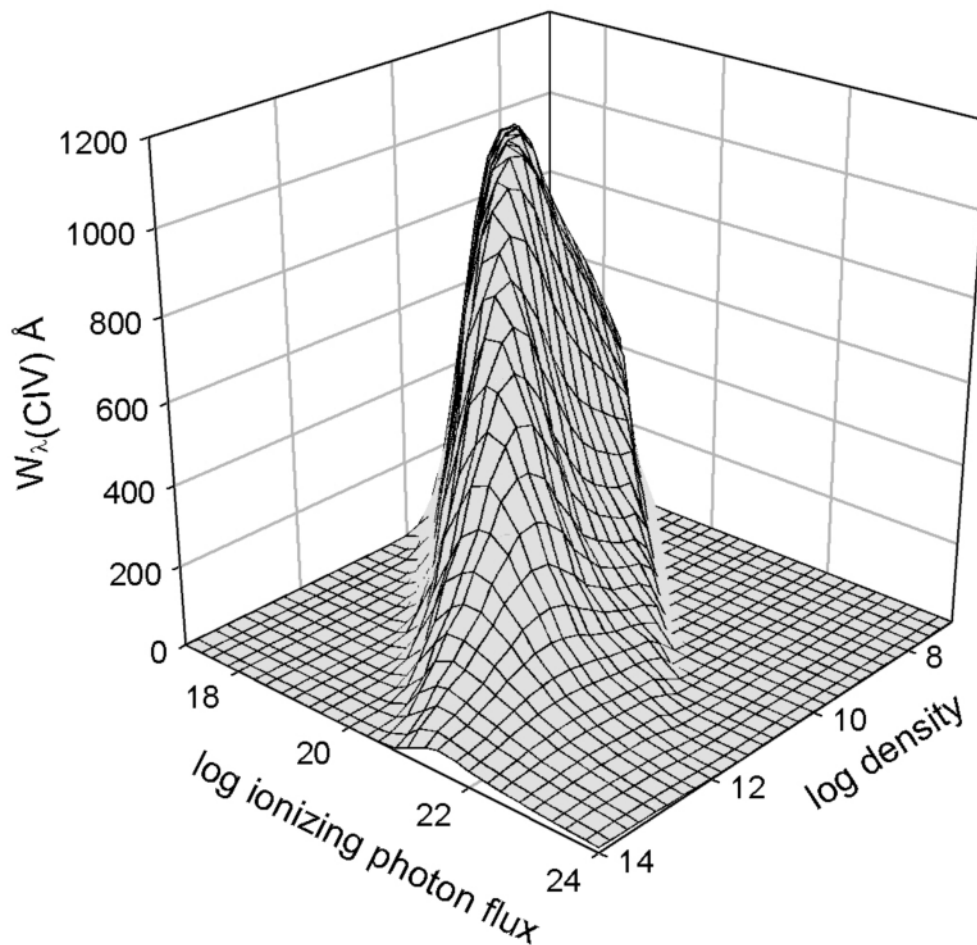


Figure 7 The results of a large grid of model calculations are shown. The x-y plane shows the logs of the hydrogen density (cm^3) and flux of ionizing photons ($\text{cm}^2 \text{s}^{-1}$). The z axis is the predicted line equivalent width.

the material in this chapter.

3.1.1 Creating a new main program

In C there must be exactly one main program, called *main*. This routine is within the file *maincl.c* in the source downloaded from the web. You need to replace the existing Cloudy main program with one that you write. The file *maincl.c* that is included in the distribution must be deleted so that the program you write will be loaded instead. The remaining routines are then compiled with a command like the following:

```
gcc -c *.c
```

which will create a large number of object files. Often the new main program will be linked with these object files with a command something like

```
gcc newmain.c *.o -lm
```

The following subsections outline how to write code for this new main program.

3.1.2 The *cddrive.h* header file

The file *cddrive.h* contains definitions of all public routines, the routines that a user would call to drive Cloudy. That file is the definitive reference for the material contained in this section and is more up to date than this document. Comments within that file explain all routines and their parameters.

3.1.3 The *cddefines.h* header file

While it is not absolutely necessary to include this header file, it is a good idea to include this before *cddrive.h*, since it includes many definitions and includes the standard C header files that are needed to drive the code.

3.1.4 A note on return conditions

Some of the routines return a value to indicate success or failure. I try to follow the C and Unix conventions to indicate success with zero and trouble with a non-zero return. This rule is not always followed, however, and *cddrive.h* should be consulted to make sure the return conditions are understood.

3.2 Initializing the code

Many variables must be initialized at the beginning of the calculation. Calling routine *cdInit* does this.

```
cdInit();
```

Routine *cdInit* must be called every time a new calculation is to be performed, *before* calling any of the following subroutines, but after the results of any previous calculations have been read. (The results of any previous calculations are lost when *cdInit* is called.)

cdMPI When the code is executed using MPI (Message Passing Interface, used on parallel machines) the code must call a specific exit handler, *MPI_finalize*, upon exit. To enable this routine *cdMPI* should be called after *cdInit* but before the main program is called.

3.3 Handling input and output

3.3.1 *cdTalk* - produce output??

Cloudy normally speaks what's on its mind, but this can generate a lot of output in a large grid. It does have a quiet mode in which nothing at all is printed. This quiet mode is set by the logical argument to subroutine *cdTalk*.

```
#include "cddefines.h"
#include "cddrive.h"
/*set no output at all*/
cdTalk( FALSE )
/*have the code produce the normal printout*/
cdTalk( TRUE )
```

The default is for Cloudy to produce output, and *cdTalk* does not have to be called if this is desired. However, it does need to be called with the logical variable *FALSE* if the quiet mode is desired. (*TRUE* and *FALSE* are defined in *cddrive.h*).

3.3.2 *cdOutp* - sending output to a file

Cloudy normally writes its standard output on the system's **stdout**. This can be changed to another stream by calling routine *cdOutp*, which has a file handle to an open file as its single argument. By combining this redirection with the C **fopen** statement it is possible to have the standard output sent into any file.

```
#include "cddefines.h"
#include "cddrive.h"
/* this defines a standard C file handle */
FILE *ioData ;

/* open the file output.txt for writing */
ioData = fopen("output.txt","w");

/* ioData is equal to NULL if we failed to open the file */
if( ioData==NULL )
{
    exit(1);
}

/* send output to this file*/
cdOutp( ioData ) ;
- - - code goes here
/* at end of calculation we need to close the file */
fclose(ioData);
```

3.3.3 *cdRead* - entering Commands

Command lines are entered by successive calls to routine *cdRead*. The argument of *cdRead* is a null-terminated string containing valid commands. The commands must obey all the rules outlined in Part I.

In the examples below some commands are directly entered as strings (this works when the string is a constant) while others are created by writing variables through *sprintf* (a standard C io function – this is necessary when the value of a variable needs to be placed into a string).

```

char chLine[132];/* this vector will hold the command lines we will generate*/

/* this example sends the string straight to cdRead */
nleft = cdRead("title a series of constant pressure models" );

/* this example writes a variable to a string then sends the string to cdRead
*/
hden = 5.4;
sprintf( chLine , "hden %5.2f ", hden );
nleft = cdRead(chLine );

/* this example sends a string that contains double quotes,
* and so must "escape" them with doubled backslashes */
nleft = cdRead("set path\"d:\\projects\\cloudy\\ccloudy\\data\" " );

sprintf( chLine , "coronal %5.2f ", temp );
nleft = cdRead(chLine );

nleft = cdRead("stop zone 1 " );

```

cdRead returns the number of commands that can still be entered before exceeding the size of the storage arrays. So this routine is an exception to the general rule that a zero return condition indicates success – here it indicates a problem – no further commands can be entered. The return value was ignored in the examples above.

It is not now possible to read in more than 4000 command lines because of limits to the size of the character arrays used to store them. This limit is stored as the variable *NKRD*. If more than 4000 lines are read in by calling *cdRead* then *cdRead* will stop after explaining why. It will be necessary to increase *NKRD* if more than 4000 command lines are needed.

3.4 Executing the code

3.4.1 *cdDrive* - calling the Code

The calculation is performed when routine *cdDrive* is called. *cdDrive* returns an int indicating whether the calculation was successful. The value 0 indicates a successful calculation. The following shows an example of its use.

```

int lgOK;
if( cdDrive() )
{
    printf("problems!\n");
    exit(1);
}

```

If problems occurred and the results cannot be trusted then the return value is non-zero. This will only be set if the calculation suffered a complete meltdown. Routine *cdNwcns* (page 424) can be called to find out about any problems.

3.4.2 *cdNoExec* - checking without Computing

If routine *cdNoExec* is called after *cdInit* but before *cdDrive* then only the initial parts of a calculation will be performed when routine *cdDrive* is called.

```
cdInit();

/*read in commands */
cdRead( . . .);

/*tell it not to execute */
cdNoExec();

/*call the code */
lgBad = cdDrive();
```

When *cdDrive* is called after *cdNoExec* the code will generate the incident continuum, set the initial density, and the chemical composition. It will then stop just before the initial search for the physical conditions in the first zone. All of the initial printout, summarizing properties of the composition and continuum, will be generated. This provides a quick way to check that a large grid of models will be specified correctly, without actually fully computing the grid.

3.5 Checking Predictions

3.5.1 *cdLine* - emission lines intensities

The predicted line intensities or luminosities for all lines with non-zero values are stored within a set of structures which also contain the line identifiers, a four character label and the wavelength in Angstroms. These are normally printed at the end of the calculation. You can obtain the line intensity by calling subroutine *cdLine*. The label and wavelength of the line are specified in the call, and the routine returns the relative intensity and the log of the absolute intensity or luminosity.

```
#include "cddefines.h"
#include "cddrive.h"
double relint , absint;
*
if( cdLine( "totl" , 4861 , &relint , &absint ) <= 0)
    printf("did not find this line\n");
```

The first variable in the call is the line label, the four-character null-terminated string (upper or lower case) as used by the code to identify the line. The second variable gives the wavelength of the line in Angstroms. Both of these must exactly match the label and wavelength used by Cloudy to identify the line (see the chapter "Lines" for a full description). The third variable (*relint* in the above example) is a pointer to the relative intensity of the line (relative to the normalization line, usually H β , but set with the **normalize** command). The log of the intensity (erg cm⁻² s⁻¹) or luminosity (erg s⁻¹) of the line is returned as a double precision variable (*absint* in the above example). If the intensity of the line is zero or the line was not found then this variable will be set to -37.

If *cdLine* finds the line it returns the index of the line within the stack of emission lines. So a positive return value indicates success. It returns the negative of the total number of lines in the stack if the line is not found. This may occur if the line wavelength or label were mistyped. This is an exception to the normal, C-like, function return convention in which a normal return is zero and an abnormal return non-zero. A positive value indicates a successful return.

The emission lines returned by this routine are the only ones printed when grains are not present, and those with the heading *Intrinsic Intensities* in the printout when grains are present.

3.5.2 *cdDLine - emergent line intensities*

This form of the *cdLine* routine has the same arguments and return values, but returns the intensity emergent from the illuminated face of a layer in front of an optically thick scattering/absorbing layer. These are the lines that are printed with the heading *Emergent Line Intensities*. They are only predicted for an open geometry when grains are present and are discussed on page 454 below.

3.5.3 *cdGetLineList - special arrays of emission lines*

The routine *cdGetLineList* provides a way to access a large number of emission lines in an automatic manner.

A list of emission lines can be entered into a data file. When routine *cdGetLineList* is called with the name of this file a series of lines will be entered into a pair of vectors. One vector will give the set of line labels, a set of character strings like "H 1". The second vector gives the corresponding wavelengths. The lists can then be used to call *cdLine* to obtain intensities of the lines.

cdInit must be called to initialize needed variables before *cdGetLineList* is called. Next *cdGetLineList* is called, and finally, the actual grid of calculations begins with another call to *cdInit*. The predicted intensities of a set of lines are extracted by calls to *cdLine*. So the first call to *cdInit* followed by a call to *cdGetLineList* rather than the actual execution of the code.

The first argument to routine *cdGetLineList* is the name of the file containing the line list. A set of files is included in the data directory of the distribution files. They have names *LineList*.dat*. The last part of the name indicates its purpose. If a null string is passed ("") then *LineList_BLR.dat* is used. The code will first try to open the file in the current directory, and if is not present, will then try on the path as set with the **path** command, or in *path.c*.

The second two parameters are a pair of pointers that are defined by the calling program. When routine *cdGetLineList* is called it uses these pointers to create a pair of vectors giving the labels and wavelengths. Space for the lines is allocated by *cdGetLineList* after it determines how many lines are in the file. These string and integer vectors contain the label and wavelength used to identify the lines. The function returns the number of lines in the list. If problems occurred then a -1 is returned.

The following shows an example of getting the lines from *LineList_BLR.dat*, executing the code, and then obtaining the predicted intensities of all lines listed in *LineList_BLR.dat* by calling *cdLine*.

```

/* define variables */
char **chLabel;
float *wl;
/* initialize the code */
cdInit();
/* get list of lines from standard data file */
if( ( nLines=cdGetLineList("", &chLabel, &wl) ) < 0 )
{
    /* this is the error exit - could not obtain
the lines */
    exit(1);
}
- - - - -
/* now set up the actual call to the code */
cdInit();
/* missing commands here, then call the code */
- - - - -
cdDrive();
/* missing commands here */
/* now print the emission lines that were in the file into
the array pred */
for( n=0; n<nLines; ++n )
{
    lgOK = cdLine( cdGetchLabel[n], cdGetnWL[n] , &relative , &absolute );
    if( lgOK<= 0 )
    {
        fprintf(stderr, "did not find
%4s%5li\n", cdGetchLabel[n], cdGetnWL[n]);
        fprintf(ioDATA, "\ndid not find line.\n");
    }
    print("%.3e\n", relative);
}

```

Table 1 Excited state column densities

Label	column
He1*	He ⁰ 2 ³ S
CII*	C ⁺ J = 3/2
C11*	C ⁰ J = 0
C12*	C ⁰ J = 1
C13*	C ⁰ J = 2
C30*	C ²⁺ J = 0
C31*	C ²⁺ J = 1
C32*	C ²⁺ J = 2
O11*	O ⁰ J = 0
O12*	O ⁰ J = 1
O13*	O ⁰ J = 2
Si2*	Si ⁺ J=3/2

3.5.4 *cdEmis* - emissivity of lines

cdEmis functions much the same as *cdLine* (page 418 above) but returns the local emissivity (erg cm⁻³ s⁻¹ for unit filling factor) of the line for the last computed zone. The return value is the index of the line within the line stack if it was found, and the negative of the number of lines in the stack if the line could not be found.

3.5.5 *cdColm* - the computed column densities

The predicted column densities can be accessed by calling the routine *cdColm*.

```

/* want C+2 */
if(cdColm("carb", 3 , &column))
{
    printf(" could not find C+2\n");
}
else
{
    printf("The predicted C+2 column density is %e\n", column );
}

```

The routine returns zero if it found the species, and 1 if it could not. It returns the predicted column density (linear, cm⁻²) as the third argument. The first argument *chLabel* is a four-character identifier that must agree with the first four characters (upper or lower case) of the name used to indicate the element in the printout. It can be upper or lower case, or a mixture of the two. The integer variable *ion* is the spectroscopic designation of the level of ionization, i.e., 1 indicates C⁰, 3 indicates C²⁺, etc.

The ion stage of 0 indicates a special case, a molecule or excited level of an atom or ion. In this case the routine will examine the label to decide which species is desired.

The labels "H2__", "CO__", "OH__", "H2O__", "O2__", "SiO__", and "OH__", where the underscore represents a space, are possible molecules. Column densities of states within the ground term of some ions are also available. In this case the label will include the ion designation, perhaps followed by an indication of which level within the term is desired, and the symbol "*" to indicate the excited state. The cases now recognized are listed in Table 1.

3.5.6 *cdH2_colden* - column density in H₂

This routine returns various column densities in the ground electronic state of molecular hydrogen. This command only works when the large H₂ molecule is turned on. It has two integer arguments, the vibration and rotation quantum numbers. If both are zero or greater the routine returns the column density in that level. If the vibration quantum number is negative then a summed column density are turned. In this case if the rotation quantum number is 0 it returns the total H₂ column density, if 1 the ortho column density, and if 2 the para column density. If the indices do not make sense the routine prints a message and returns -1.

Here are some examples:

```
/* total H2 column density */
total = cdH2_colden( -1 , 0 );
/* ortho column density */
ortho = cdH2_colden( -1 , 1 );
/* para column density */
para = cdH2_colden( -1 , 2 );
/* column density in 0, 0 */
total00 = cdH2_colden( 0 , 0 );
```

3.5.7 *cdCO_colden* - column density in CO

This routine returns the column density of a rotation level within the ground vibrational level of CO. It has two arguments, the carbon isotope, which must be 12 or 13, and the rotation quantum number. It returns the column density in that rotation level. Some caveats - the chemistry network does not independently solve for the ¹³CO abundance, but rather it uses a preset ¹³CO/¹²CO ratio (see the description of the atom co command), and only the ground vibrational state is done. Any number of rotation states can be done. The routine has two integer arguments. The first is the carbon isotope and the second is the rotation level.

```
/* total column density in J=0 of 13CO*/
total = cdCO_colden( 13 , 0 );
/* total column density in J=2 of 12CO */
ortho = cdCO_colden( 12 , 2 );
```

3.5.8 *cdIonFrac* - the computed ionization fractions

The predicted ionization fractions¹, averaged over radius or volume, can be accessed by calling the subroutine *cdIonFrac*.

¹ Before version 96 the ionization fractions only included atoms and ions. They now also include molecules. The sum of the atomic and ionic fractions will not add up to unity if a significant fraction of the element is in molecules.


```

/* FALSE below means to not include electrons in the mean */
if( cdIonFrac( "carb" , 2 , &frac , "radius" , FALSE) )
{
    exit(1);
}
printf("The predicted ionization fraction over radius is is%g\n", frac);
/* TRUE below means to include electrons in the mean */
if( cdIonFrac( "carb" , 2 , &frac , "radius" , TRUE) )
{
    exit(1);
}
printf("Ionization fraction wrt radius end elec den is is%g\n", frac);

```

The routine returns the predicted ionization fraction A_{ion}/A_{tot} . *chLabel* is a four-character identifier that must agree with the first four characters (upper or lower case) used to indicate the element in the printout. The integer variable *ion* is the spectroscopic designation of the level of ionization, i.e., 1 indicates C^0 or the atom, 3 indicates the second ion C^{+2} , etc. *chWeight* is a six-character variable (plus end of string sentinel) which must be either "radius" or "volume" (either upper or lower case). This string determines whether the ionization fraction returned is weighted with respect to radius or volume. The last variable determine whether (TRUE) or not (FALSE) the ionization fraction is also weighted with respect to the electron density. The function returns zero if the ion was found and non-zero if an error occurred.

The ionization stage of zero will request the ionization fraction of a molecule. If the element name is "H2 " (the letters H2 followed by two spaces) then the fraction of hydrogen in H_2 , $2n(H_2)/n(H_{tot})$, will be returned.

3.5.9 *cdTemp* - the computed mean temperature

Routine *cdTemp* returns the computed mean temperature. The first parameter is a four character null-terminated string giving the first four letters (upper or lower case) of the name of the element as spelled by the code. The second parameter is the ionization stage, with 1 for the atom, 2 the first ion, etc. The third parameter will be the computed mean temperature. The last parameter is a six character null terminated string, either "radius" or "volume" that says whether the temperature should be weighted with respect to radius or volume. The routine returns 0 if it finds the species, and 1 if it could not find the species.

```

if( cdTemp( "carb" , 2 , &temp , "radius") )
{
    exit(1);
}
printf("The mean temperature is%g\n", temp);

```

21 cm-related temperatures: If the ion stage is zero then the routine will return one of three temperatures related to 21 cm observations. The label "21cm" will return the mean of n_H/T_{kin} , the harmonic mean gas kinetic temperature weighted with respect to the atomic hydrogen density, averaged over radius. The label "spin" will return the mean of n_H/T_{spin} , the harmonic mean of the 21 cm spin temperature weighted with respect to the atomic hydrogen density, averaged over radius. The spin temperature T_{spin} is calculated with $L\alpha$ radiative processes included. Finally the label "opti" returns the temperature derived from the ratio of $Ly\alpha$ to 21 cm optical depths. This is the temperature measured by combined 21 cm - $L\alpha$ observations.

Molecular hydrogen: The label “**H2__**” will return the mean weighted with respect to the H₂ density.

3.5.10 *cdGetCooling_last, cdGetHeating_last - last zone's cooling or heating*

The total cooling and heating rates ($\text{erg cm}^{-3} \text{s}^{-1}$) for the last computed zone is obtained by called the functions *cdGetCooling_last* and *cdGetHeating_last*. In equilibrium the cooling and heating rates are equal.

3.5.11 *cdGetTemp_last - the temperature of the last zone*

The electron temperature of the last computed zone is obtained by called the function *cdLastTemp*. The function has no arguments and its return value is the predicted temperature.

3.5.12 *cdGetPressure_last - pressure of the last zone*

The pressure for the last computed zone is obtained by calling routine *cdGetPresure_last*. This routine has three arguments, pointers to the total (gas plus radiation) pressure, the gas pressure, and the radiation pressure. All are double precision variables.

3.5.13 *cdGetnZone - how many zones in the last iteration?*

This routine's return value is the number of zones in the previous iteration.

3.5.14 *cdGetPressure_depth - pressure structure of the last iteration*

The pressure as a function of depth, for the last iteration, is obtained by calling routine *cdGetPressure_depth*. This routine has three arguments, pointers to vectors giving the total (gas plus radiation) pressure, the gas pressure, and the radiation pressure. All are double precision vectors, and the calling routine must have allocated space for these before calling this routine. The number of zones in the last iteration, and so the total number of elements needed for each vector, is obtained by calling routine *cdGetnZone*.

3.5.15 *cdGetDepth_depth - returns the depth structure of the previous iteration*

This routine returns the depth structure (in cm) of the previous iteration. The code uses adaptive logic to control the radial zoning of the model. Neither the number of depth points nor their structure is known in advance. This routine is called with a double precision vector with enough space to hold the structure. The number of depth points is determined by calling *cdGetnZone* and space is allocated by the calling routine. Each element of the vector is the depth from the illuminated face to the center of zone n .

3.5.16 *cdTimescales - several timescales.*

This routine has three arguments, pointers to doubles, that return the timescales [s] for several processes. These are the thermal timescale, the hydrogen recombination timescale, and the H₂ formation timescale.

3.5.17 *cdSPEC - get predicted spectrum*

This routine provides an interface between Cloudy and Keith Arnaud's X-Ray spectral analysis program XSPEC. It is called after *cdDrive* has computed a model. Depending on which option is used, it will return the incident continuum, the

attenuated incident continuum, the reflected continuum, the diffuse continuous continuum, outward direction diffuse continuous emission, reflected lines, outward lines. All are $4\pi \nu J_\nu$ and have units of $\text{erg cm}^{-2} \text{s}^{-1}$.

All lines and continua emitted by the cloud assume full coverage of the continuum source. Details are given in *cddrive.h*.

3.6 Other information

3.6.1 *cdDate(cdString)*

The date when the current version of the code was released will be placed as a null terminated string. The string is passed as an argument and the calling program must have allocated enough room in the string.

3.6.2 *cdVersion(cdString)*

The code's version number will be placed as a null-terminated string into the string passed as an argument. The version number is a string rather than a float since it can end with a letter of the alphabet. The calling program must allocate enough room in string.

3.6.3 *double cdExecTime(void)*

This returns the time that has elapsed since the previous call to *cdInit*.

3.7 Printing the comments

After the calculation is complete, but before the emission lines are printed, the code generates a series of statements that indicate warnings, cautions, comments, and surprises. These should be examined to confirm that the calculation is likely to be all right. A series of public routines allows the driving code to determine whether these comments were generated, what type they were, and to print them into an arbitrary open file.

3.7.1 *Were comments generated?*

Routine *cdNwcns* will return the number of warnings, cautions, surprises, notes, and temperature and pressure failures:

```
cdNwcns( &lgAbort , &nw , &nc , &nn , &ns , &nte , &npe , &niOne, &neden )
```

where the first variable is a flag indicating whether the calculation aborted, *nw* is the number of warnings generated (if this number is non-zero, then the calculation has serious problems), *nc* is the number of cautions generated (these are less severe than warnings, but are still a cause of concern), and *nn* and *ns* are the number of notes and surprises. The next two arguments are the number of temperature and pressure failures. The last two are the number of ionization and electron density failures. All failures will add up to zero in a successful calculation.

If either of the first two variables are non-zero then the code returned with an indication of serious failure. An abort is far more serious than a warning since it indicates catastrophic meltdown. I would appreciate learning about these.

3.7.2 *Printing the comments.*

The comments that normally appear after the last zone may be printed into any file by calling the series of subroutines described here. In all cases the routines take as an argument a file handle, which must point to a file open for writing.

```

/* output the comments into a file, but first open it */
/* first define the file handle, then open the file for writing */
FILE *ioOUT;
If( (IoOUT = fopen( "comments.txt", "w" ) ) == NULL )
{
    printf("error creating comments.txt file\n");
    exit(1);
}
/*print the reason the calculation stopped, and geometry*/
cdReasonGeo( ioOUT )
/*print the warnings*/
cdWarnings(ioOUT)
/*next print the cautions*/
cdCautions(ioOUT)
/*now print any surprising results*/
cdSurprises(ioOUT)
/*now print the notes
cdNotes(ioOUT)

```

cdReasonGeo (FILE *io). It is very important to understand why the calculation stopped. The first two lines after the last zone results give the reason the calculation stopped, and the type of geometry. This information will be printed on the file whose handle is the argument.

cdWarnings(FILE *io) All warnings will be printed on the output file.

cdCautions (FILE *io) All cautions will be printed on the output file.

cdSurprises(FILE *io) All surprises (denoted by a "!") are printed on the output file.

cdNotes(FILE *io) The notes concerning the calculation will be printed on the output file.

3.7.3 *cdErrors(FILE *io) - printing a summary of any problems*

Routine ***cdErrors(FILE *io)*** will generate a summary of any problems that happened during a calculation. The argument is a file pointer to the output file where the summary will be placed. If problems occurred in the calculation, such as temperature or pressure failures, warnings, or cautions, these will be printed following the title for the calculation.

3.7.4 *cdPrintCommands(FILE *io) - print the command stack*

The entire series of input commands will be written into the file. The single argument is a file handle that points to a previously opened file. The commands are preceded and followed by lines that begin with "c =====" to easily identify the start and end.

3.7.5 *setbuf or the no buffering command*

Programs produce output by writing into a buffer, which places information on disk once it is full. If a C program crashes before this buffer is "flushed" the information within the buffer will be lost. This poses a problem if the printout generated just before the crash is needed for debugging. The C io library provides a

routine, *setbuf*, that can turn buffering off. The following sequence would open a file and turn buffering off:

```
ioDATA = fopen("d:\\projects\\cloudy\\run2\\test.out","w");
/* turn off buffering so we see results as then happen */
setbuf( ioDATA , NULL );
```

The **no buffering** command will accomplish the same thing. Note that turning off buffering has a severe performance penalty – the code will run far more slowly.

3.8 Example Call as a Subroutine

The following is an example of a very simple use of Cloudy as a subroutine.

```
/*main program that calls cloudy when used as a stand-alone program */
#include "cddefines.h"
#include "cddrive.h"

int main( void )
{
    int lgOK ;

    /* first create an open file */
    FILE *ioDATA ;
    ioDATA = fopen("d:\\projects\\cloudy\\run2\\test.out","w");
    if( ioDATA == NULL )
    {
        printf(" could not open test.out for writing.\n");
        exit(1);
    }

    /* initialize the code */
    cdInit();
    /* divert the output to this file */
    cdOutp(ioDATA);
    /* enter commands for this run */
    cdRead( "hden 10.5 ");
    cdRead( "agn 6.00 -1.40 -0.50 -1.0 ");
    cdRead( "phi(h) 23 ");
    cdRead( "stop column density 21.860889 ");
    cdRead( "*constant temper 727,000 ");
    cdRead( "background z=0 ");
    cdRead( "failures 3 no map ");
    /* actually call the code */
    lgOK = cdDrive();
    /* close the file then exit */
    fclose( ioDATA);
    exit(0);
}
```

3.9 Computing Grids of Calculations

Today I usually use the code to compute results, extract information on the fly, and then save desired quantities. The following example illustrates producing a series of models with increasing stellar temperature, in which the stellar temperature and the [O III]/H β ratio are written to a file.

In the following only one call to *cdLine* is made to get results for a single line. In practice all desired lines are usually extracted at this stage and stored in a format where it can be read by other software. A call to *cdGetLineList* (page 419 above) provides an easy way to obtain large numbers of lines whose labels are stored in a file.

```

/* very simple main program to call cloudy as a stand-alone program */
#include "cddefines.h"
#include "cddrive.h"

/*int main( int argc, char *argv[] )*/
int main( void )
{
    /* this will hold images of the command lines */
    char chCard[200];
    double TStar , rel , absol;
    int lgFail;
    int nFail;
    FILE *ioDATA ;

    /* open file for writing some results */
    if( (ioDATA = fopen("1DGrid.out","w")) == NULL )
    {
        printf(" could not open 1DGrid.out for writing.\n");
        exit(1);
    }

    TStar = 3e4;
    nFail = 0;
    while( TStar < 5e4 )
    {
        /* initialize the code */
        cdInit();
        /* redirect output to the file we opened above */
        cdOutp(ioDATA);
        /* but also say we want to output by passing 0, for FALSE */
        cdTalk( 0 );
        /* write variables into strings and send string as input file */
        cdRead( "hden 5 ");
        cdRead( "ionization parameter -2 ");
        cdRead( "stop zone 1 ");
        /* this is example of writing a variable into the string then passing
        * the string to cloudy */
        sprintf( chCard , "blackbody, T= %f" , TStar );
        cdRead( chCard );
        /* actually call the code */
        lgFail = cdDrive();
        if( lgFail )
        {
            printf("Beware: Cloudy returned error condition, so exit with 1.\n");
            /* this counts how many failures occurred */
            ++nFail;
        }
        /* now increment TStar by 5000K */
        TStar += 5000.;
        /* get intensity of [OIII] relative to Hbeta - remember cdLine is different
        * from most cd routines since it returns element within line stack, 0 for failure */
        if( !cdLine( "o 3" , 5007 , &rel , &absol ) <=0 )
        {
            printf("could not find 5007\n");
            exit(1);
        }
        /* now print stellar temperature and 5007/Hbeta ratio */
        fprintf(ioDATA , "%.0f %.2f\n", TStar , rel );
    }
    /* exit with number of error returns - this should be zero */
    exit(nFail);
}

```

3.10 Storing Grids of Calculations²

This subsection describes a strategy for creating and analyzing a large grid of models. In this strategy all results are saved to a file, which is then read in later.

² This method is seldom used today and will be removed in a future version of the code.

The **punch results last** command is described in Part I. The line intensities and column densities computed by the code will be written into a file when this command is entered. Any post-processing software can read this file, but reading this file is facilitated by routine *cdGett*, described next.

The output produced by the **punch results last** command can be read with routine *cdGett*. *cdGett* has one argument, a pointer to the file containing the results of the **punch results** command. Its return value indicates whether (TRUE) or not (FALSE) the end of file was encountered when the model results were read. If the logical variable is TRUE then the end of file was encountered and no results were read. If it has not been encountered then there may be more models further down the input stream. The next model in the grid will be accessed by the next call to *cdGett*.

Once *cdGett* has been called the routines *cdLine*, *cdIonf*, and *cdColm* routines can be used to obtain emission line intensities, ionization fractions, or column densities from the stored file. A structure, *getpar*, is associated with *cdGett*. This contains information concerning the initial parameters of the current model, as specified in the input stream.

This method is seldom used today and will be removed removed. The method described in the previous section is far simpler.

4 OUTPUT

4.1 Overview

This section defines the output produced by Cloudy. Each section begins with a sample of the output described, and then goes on to describe the meaning of the printout in greater detail. The output actually shown is from the Meudon (Péquignot 1986) and Lexington (Ferland et al 1995) meetings Planetary Nebula test case (*parispn.in*).

4.2 Header Information

Several lines of output echo the input commands and outline some properties of the initial continuum.

4.2.1 Initial Information

```

Cloudy 96.00
*****01Feb01*****
*
* title "New" Paris meeting Planetary nebula
* c recompute "standard" FN model of the Pequignot Meudon Conference
* init file="c84.ini"
* elements read
* sphere
* black body, T=150,000K radius = 10
* hden = 3.4771213
* radius = 17
* abund -1 C-3.523 N-4. 0-3.222 ne-3.824 na=-10 mg-4.523 al=-10
* continue si-4.523 s-4.824 ar-10 ca=-10 fe-10 ni=-10
* plot continuum range .1
* punch overview last 70
* c parispn.in
* c Sun
*****

```

This begins with the version number of Cloudy. Major revisions, which have noticeable effects on the emission-line spectrum, or which reflect significant improvements in the physics, are denoted by integer increases in the version number, while minor changes increment the revision number by 0.01. In a static version of the code, small changes (usually minor bug fixes) are denoted by letters (i.e., .02a). The following line gives the date this version was created.

All of the input command lines, with the exception of those starting with a #, %, or *, are echoed before the calculation begins, and are saved to be reprinted after the calculation is completed.

4.2.2 Properties of the Continuum

1568Cell Peak3.83E+00	Lo 1.00E-05=0.9108cm	Hi-Con:7.63E+01 Ryd	E(hi):7.35E+06Ryd	E(hi): 100.01 MeV
L(nu>1ryd): 37.5396	Average nu:2.935E+00	L(X-ray): 31.4007	L(BalC): 36.1444	Q(Balmer C): 46.9767
Q(1.0-1.8): 47.1613	Q(1.8-4.0): 47.4535	Q(4.0-20): 47.0522	Q(20--): 40.7275	Ion pht flx:4.312E+12
L(gam ray): 0.0000	Q(gam ray): 0.0000	L(Infred): 34.4845	Alf(ox): 0.0000	Total lumin: 37.5571
log L/Lsun: 3.9743	Abs bol mg: -5.1858	Abs V mag: 2.4170	Bol cor: -7.6028	nuFnu(Bbet): 34.5868
U(1.0----):4.794E-02	U(4.0----):9.977E-03	T(En-Den):3.354E+01	T(Comp):1.436E+05	nuJnu(912A):2.908E+01
Occ(ParIR):2.354E-10	Occ(H n=6):8.468E-14	Occ(1Ryd):1.342E-15	Occ(4R):3.707E-17	Occ(Nu-hi):0.000E+00
Tbr(ParIR):3.757E-10	Tbr(H n=6):3.703E-10	Tbr(1Ryd):2.120E-10	Tbr(4R):2.351E-11	Tbr(Nu-hi):0.000E+00

This section gives a synopsis of the incident continuum, evaluated at the illuminated face of the cloud. The first line gives the number of numerical frequency cells in the continuum, followed by the energy (in Ryd) of the hydrogen-ionizing continuum³ with the largest flux density per unit energy interval (f_{ν}). Next is the energy of the low-energy limit of the continuum, both in Ryd and cm. The last two

³ The printed number was incorrect in versions 80 through 88.01, but had no other effects on computed results.

numbers are the energies of the high-energy limit of the present version of the code, in Ryd and keV.

The intensity or luminosity of the continuum will be given within this header. A luminosity will be given if the code has enough information to predict it. It must know an inner radius for this to occur. The units will be energy radiated by the central object into 4π sr. If an inner radius is not set then predictions will be emission per unit area of cloud surface, loosely called the intensity, but more formally $4\pi J$ where J is the proper mean intensity ($\text{erg cm}^{-2} \text{s}^{-1} \text{sr}^{-1}$ for an emission line; Mihalas 1978).

The second line gives the log of the energy ($\text{erg s}^{-1} \text{cm}^{-2}$ or erg s^{-1} , depending on whether a flux or luminosity was specified) in the hydrogen-ionizing continuum ($1 \text{ Ryd} \leq h\nu < 100 \text{ MeV}$), and the average energy of the hydrogen ionizing continuum, in Ryd, weighted by photon number;

$$\langle h\nu \rangle = \frac{\int_{1 \text{ Ryd}}^{\infty} 4\pi J_{\nu} d\nu}{\int_{1 \text{ Ryd}}^{\infty} 4\pi J_{\nu} / h\nu d\nu} [\text{Ryd}]. \quad (400)$$

The log of the energy in the X-ray continuum ($20.6 \text{ Ryd} \leq h\nu \leq 7676 \text{ Ryd}$), the log of the energy ($\text{erg s}^{-1} \text{cm}^{-2}$ or erg s^{-1}), and the number of photons ($\text{cm}^{-2} \text{s}^{-1}$ or s^{-1}) in the Balmer continuum (0.25 Ryd to 1.0 Ryd) is then printed.

The third line gives the log of the number of photons ($\text{cm}^{-2} \text{s}^{-1}$ or s^{-1}) in four frequency bins ($1.0 \text{ Ryd} \leq h\nu < 1.807 \text{ Ryd}$, $1.807 \text{ Ryd} \leq h\nu < 4.0 \text{ Ryd}$, $4.0 \text{ Ryd} \leq h\nu < 20.6 \text{ Ryd}$, and $20.6 \text{ Ryd} \leq h\nu < 7676 \text{ Ryd}$). The last number “Ion pht flx” is the flux of hydrogen ionizing photons;

$$\Phi(H) = \frac{Q(H)}{4\pi r^2} [\text{cm}^{-2} \text{s}^{-1}]. \quad (401)$$

In this equation $Q(H)$ is the total number of hydrogen-ionizing photons emitted by the central object (s^{-1}), and r is the separation between the center of the central object and the illuminated face of the cloud. Unlike the majority of the quantities printed in the header, $\Phi(H)$ (per unit area) is always printed, never $Q(H)$ (into 4π sr).

The fourth line of the header gives some information about the low and high energy portions of the incident continuum. The first number is the log of the luminosity or intensity in the gamma-ray ($100 \text{ keV} \sim$ to $\sim 100 \text{ MeV}$) continuum. The second number on the line is the log of the number of photons over this energy range. The third number is the log of the luminosity in the continuum between 0.25 Ryd and the lowest energy considered, presently an energy of $1.001 \times 10^{-5} \text{ Ryd}$. All of these entries are either per unit area, or radiated into 4π sr, depending on how the continuum was specified.

The next entry, “Alf(ox)”, is the spectral index α_{ox} , defined as in Zamorani et al. (1981), except for the difference in sign convention. This is the spectral index which

would describe the continuum between 2 keV (147 Ryd) and 2500Å (0.3645 Ryd) if the continuum could be described as a single power-law, that is,

$$\frac{f_\nu(2 \text{ keV})}{f_\nu(2500 \text{ \AA})} = \left(\frac{\nu_{2 \text{ keV}}}{\nu_{2500 \text{ \AA}}} \right)^\alpha = 403.3^\alpha \quad (402)$$

The definition of α_{ox} used here is slightly different from that of Zamorani et al. since implicit negative signs are *never* used by Cloudy. Typical AGN have $\alpha_{\text{ox}} \sim -1.4$. If no X-rays are present then $\alpha_{\text{ox}} = 0$. The last number on the line is the log of the total energy in the continuum between 1.001×10^{-8} Ryd and 100 MeV.

The next line is optional, depending on whether the continuum is specified as the total luminosity or photon number radiated into 4π sr, or as an incident surface flux. This optional line is generated if the continuum is specified in absolute terms, i.e., the luminosity or photon number radiated into 4π sr. The first quantity is the log of the total luminosity in the continuum, in solar units. The absolute bolometric magnitude, absolute V magnitude, and the bolometric correction, are then given, followed by the log of the continuum specific luminosity (νF_ν) at the wavelength or frequency of H β (the units of $\nu F_\nu(\text{H}\beta)$ are erg s^{-1}).

The next line begins with two ionization parameters. The first is the dimensionless ratio of ionizing photon to hydrogen densities, defined as

$$U \equiv \frac{\Phi(H)}{n_H c} \quad (403)$$

where n_H is the total hydrogen density. The second number is defined in a similar way, but the numerator is the number of photons with energies greater than 4 Ryd (i.e., helium-ionizing). The third number is the equivalent black body temperature corresponding to the energy density u at the illuminated face of the cloud, from the incident continuum and Stefan's radiation density constant a ; $T_u \equiv (L / 4\pi r^2 a c)^{1/4}$, and the next quantity is the Compton temperature of the incident radiation field⁴. The last number on the line is $4\pi \nu J_\nu(912 \text{ \AA})$, the flux at 912Å ($\text{erg cm}^{-2} \text{ s}^{-1}$). In this equation J_ν is the mean intensity of the incident continuum as defined by Mihalas (1978).

The next two lines give dimensionless photon occupation numbers $\eta(\nu)$, for the incident continuum at several energies. This is defined as

$$\eta(\nu) \equiv J_\nu(\nu) \left(\frac{2h\nu^3}{c^2} \right)^{-1}, \quad (404)$$

⁴For a blackbody radiation field T_{Compton} is roughly 4% lower than the blackbody color temperature T_{color} when the energy density temperature T_u is $\ll T_{\text{color}}$. Only when $T_u \equiv T_{\text{color}}$ does induced Compton heating cause $T_{\text{Compton}} \equiv T_{\text{color}}$. If $T_u > T_{\text{color}}$ then $T_{\text{Compton}} > T_{\text{color}}$ because of induced Compton heating. All of the relevant physics is included in the Compton temperature printed here.

and the incident continuum brightness temperature $T_b(\nu)$, (K), defined as

$$T_b(\nu) \equiv J_\nu(\nu) \left(\frac{2k\nu^2}{c^2} \right)^{-1} \quad [\text{K}], \quad (405)$$

for five energies. These energies correspond to the lowest frequency considered (presently an energy of 1.001×10^{-8} Ryd); the ionization potential of the $n = 6$ level of hydrogen ($1/36$ Ryd); an energy of one Rydberg; four Rydbergs, and the high energy limit of the incident continuum (this depends on the continuum shape; the energy is given by the fifth number on the first line of the continuum output).

4.3 Chemical composition

```

Chemical Composition
H : 0.0000 He: -1.0000 C : -3.5230 N : -4.0000 O : -3.2220 Ne: -3.8240 Mg: -4.5230 Si: -4.5230 S : -4.8240
Ar: -10.0000 Fe: -10.0000

```

The continuum information is followed by the chemical composition of the gas. There are three blocks of numbers, the first giving the gas phase abundances of the elements, the second the abundances contained in grains, and the third the number of each type of grains per unit hydrogen. The numbers are the logs of the number densities of the elements, relative to the gas phase hydrogen abundance of unity (so, 0 on the log scale). Only the active elements are included (those turned off with the **elements off** command are not printed). If grains are not present then the second two blocks are not printed.

4.4 Zone Results

```

#### 1 Te:1.118E+06 Hden:1.000E+05 Ne:1.197E+05 R:9.258E+18 R-R0:4.534E+12 dR:9.068E+12 NTR: 5 Htot:2.638E-12 T912: 9.97e+07###
Hydrogen 1.40e-08 1.00e+00 H+o/Hden 1.00e+00 0.00e+00 H- H2 0.00e+00 0.00e+00 H2+ HeH+ 0.00e+00 Ho+ CoLD 1.27e+10 9.07e+17
Helium 6.60e-12 1.88e-06 1.00e+00 He I2SP3 5.53e-15 1.72e-22 Comp H,C 9.73e-15 5.17e-16 Fill Fac 1.00e+00 Gam1/tot 3.20e-01
He singlet 6.59e-12 6.96e-16 1.02e-21 1.85e-21 3.65e-21 7.01e-21 He tripl 1.11e-14 1.72e-22 6.50e-24 1.89e-23 1.10e-24
Pressure NgasTgas 2.57e+11 P(total) 3.67e-05 P( gas ) 3.54e-05 P(Radtn) 1.22e-06 Rad accl 2.14e-06 ForceMul 2.04e-02
Texc(La) 5.04e+03 T(contn) 4.50e+02 T(diffs) 5.44e+01 nT (c+d) 1.22e+08 PRad/Gas 3.44e-02 Pmag/Gas 3.22e-02
DustTemp 8.36e+02 Pot Volt 1.59e+02 Chrg (e) 9.19e+02 drf cm/s 1.02e+06 Heating: 9.92e-13 Frac tot 3.76e-01
Sil-ISM 1.01e+03 Pot Volt 1.62e+02 Chrg (e) 9.36e+02 drf cm/s 8.22e+05 Heating: 1.62e-12 Frac tot 6.13e-01
Carbon 4.50e-26 1.33e-19 8.48e-15 3.91e-10 3.40e-06 3.26e-03 9.97e-01 H2O+O 0.00e+00 OH+Otot 0.00e+00 Hex(tot) 0.00e+00
Nitrogen 5.07e-29 1.52e-22 1.88e-17 2.89e-13 3.14e-09 1.83e-05 8.77e-03 9.91e-01 O2/Otot1 0.00e+00 O2+Otot 0.00e+00
Oxygen 9.69e-31 2.65e-24 5.25e-19 7.66e-15 7.75e-12 2.46e-08 9.51e-05 2.07e-02 9.79e-01 sec ion: 0.00e+00
Neon 0.00e+00 5.48e-28 2.06e-22 1.10e-17 8.18e-14 6.46e-11 3.81e-09 2.03e-06 1.73e-03 8.17e-02 9.17e-01
Magnesium 0.00e+00 1.55e-30 7.71e-25 6.08e-21 1.31e-17 4.90e-14 2.84e-11 6.33e-09 5.84e-07 8.35e-05 1.66e-02 2.18e-01 7.65e-01
Silicon 2 1.34e-29 4.38e-25 1.58e-20 1.83e-16 2.18e-13 1.03e-10 1.73e-08 1.20e-06 3.23e-05 1.40e-03 8.61e-02 3.99e-01 5.13e-01
Sulphur 4 1.92e-23 6.45e-20 4.28e-16 6.33e-13 2.82e-10 4.80e-08 2.22e-06 4.79e-05 5.55e-04 1.14e-02 2.58e-01 4.73e-01 2.56e-01
Argon 6 6.64e-19 3.90e-16 1.13e-12 4.53e-10 6.40e-08 3.95e-06 8.45e-05 8.49e-04 4.99e-03 4.74e-02 4.65e-01 3.83e-01 9.85e-02
Iron 14 6.72e-07 6.01e-06 3.52e-04 4.72e-03 2.97e-02 1.20e-01 2.01e-01 2.47e-01 1.88e-01 1.05e-01 9.68e-02 7.34e-03 1.86e-04

```

The results of calculations for the first and last zones are always printed. Results for intermediate zones can be printed if desired (see the **print every** command). The following is a line-by-line description of the output produced for each printed zone.

4.4.1 Line 1

The line begins with a series of # characters, to make it easy to locate with an editor. The zone number is the first number, followed by the electron temperature of the zone ("Te"). A lower case u will appear before the "Te" if the temperature solution is possibly thermally unstable (i.e., the derivative of the net cooling with respect to temperature is negative. See the section on thermal stability problems starting on page 491 below). The total hydrogen ("Hden") and electron ("Ne") densities (cm^{-3}) follow. The next number ("R") is the distance to the center of the zone, from the center of the central object. The depth, the distance between the illuminated face of the cloud and the center of the zone, ("R-R0", or $r-r_0$), and the thickness of the zone ("dR", or δr), (all are in cm), follow. The inner edge of the zone

is $(r - r_o) - \delta r / 2$ from the illuminated face of the cloud. The line ends with a number indicating how many ionization iterations were needed for this zone to converge (NTR), followed by the total heating⁵ (“Htot”; photoelectric and otherwise, $\text{erg cm}^{-3} \text{s}^{-1}$), and the optical depth between the *illuminated* face of the cloud and the *outer* edge of the zone at the Lyman limit (T912; the number is the *total absorption* optical depth at 912\AA , and *not* the hydrogen Lyman limit optical depth).

4.4.2 [Optional] wind parameters

A line describing the velocity and acceleration of the zone is printed if the **wind** option is used. The numbers are the wind velocity at the outer edge of the current zone (km s^{-1}), inward gravitational acceleration (cm s^{-2}), total outward radiative acceleration (cm s^{-2}), and the fraction of this acceleration caused by the incident continuum, line driving, and the gradient of the radiation pressure.

4.4.3 [Optional] radiation pressure

If the ratio of line radiation to gas pressure, $P(\text{radiation})/P(\text{gas})$, is greater than 5%, then a line describing the source of the radiation pressure is generated. The line begins with the label **P(Lines)** and continues with the fraction of the total radiation pressure produced by that emission line, the spectroscopic designation of the line, and its wavelength. Up to twenty lines can be printed, although in most cases only $\text{L}\alpha$ and a few others will dominate.

4.4.4 Line 1 - Hydrogen I

The line begins with the abundance of neutral and ionized hydrogen relative to all atomic-ionic hydrogen (i.e., the ratios $H^0/(H^0+H^+)$ and $H^+/(H^0+H^+)$ where H^0 is the population in all bound levels of hydrogen. If **print h-like departure coefficients** has been specified then departure coefficients are also printed on the following line. Neutral hydrogen H^0 is defined to be the total population of atomic hydrogen in all explicitly computed bound levels. Next comes “H+o/Hden”, the ratio of the density of hydrogen in atomic or ionic form (this is indicated by the label “H+o”) to the total hydrogen density in all forms (including molecular).

The following five numbers are abundances of the negative hydrogen ion and several molecules (H^- , H_2 , H_2^+ , and HeH^+) relative to the total hydrogen abundance. The total hydrogen density is usually referred to by the label *hden*, and is the sum $\text{H}^0 + \text{H}^+ + \text{H}^- + 2\text{H}_2 + 2\text{H}_2^+ + 3\text{H}_3^+$. Note that, with this definition of the hydrogen density a fully molecular gas will have $n(\text{H}_2)/n(\text{H})=0.5$. These molecular abundances are also expressed as departure coefficients if this option is set with the **print departure coefficients** command. The last number on the line is the total hydrogen column density (cm^{-2}).

4.4.5 Line 2 - Hydrogen II

This information is only printed if it is explicitly requested with the **print H-like levels** command. The first two numbers are the populations of the H^0 2s

⁵Cloudy defines heating as the energy input by the freed photoelectron, or $h\nu - \text{IP}$, where IP is the ionization potential of the atom or ion, and $h\nu$ is the energy of the photon. See Osterbrock (1989) for more details.

and $2p$ levels relative to the ionized hydrogen density. The next numbers are populations of excited levels, again relative to the ionized hydrogen density. All of these populations usually are relative to the ionized hydrogen density, but can also be printed as LTE departure coefficients if the `print departure coefficients` command is given.

4.4.6 Line 3 - Helium

The first three numbers are the total populations of the three ionization stages of helium, relative to the total helium abundance. The population of atomic helium is the sum of the total population in the triplets and singlets, including the population of all explicitly computed levels of each. These populations can also be expressed as departure coefficients if this option is set with the `print departure coefficients` command. The population of He 2^3S , relative to the total helium abundance, follows. The Compton heating and cooling rates (both $\text{erg cm}^{-3} \text{ s}^{-1}$) are next, followed by the gas filling factor. The last number is the fraction of the total hydrogen ionizations that are caused by photoionization from the ground state.

4.4.7 Line 4 - Atomic Helium

The first group are the level populations of the populations of the $n=1$ to 6 levels of the He 0 singlets. Level two is actually resolved into $2s$ and $2p$, but the total population of 2 is printed. The next group consists of populations of the $2s$, $2p$, and $n=3s, p, d$ levels of the He 0 triplets. Both sets of populations are relative to the total helium abundance. Departure coefficients are also printed if requested.

4.4.8 Line 5 - Ionized Helium

The populations of the $2s$, $2p$, and $n=3$ to 6 levels are indicated. There are relative to He $^{++}$; departure coefficients are also printed if requested. The ratio of radiation pressure to gas pressure follows.

4.4.9 Pressure

Some information concerning the pressure is printed. The gas equation of state includes thermal gas pressure, the radiation pressure due to trapped line emission, magnetic pressure, and the radiation pressure due to absorption of the incident continuum. The first number is the gas pressure $n_{\text{gas}} T_{\text{gas}}$ (with units $\text{cm}^{-3} \text{ K}$), followed by the total pressure (dynes cm^{-2}), and followed by the gas pressure ($n_{\text{gas}} kT_{\text{gas}}$) in dynes cm^{-2} . The radiation pressure follows. The second to last number is the radiative acceleration (cm s^{-2}) at the inner edge of this zone. The radiative acceleration is computed with all continuous scattering and absorption opacities included. The last number is a force multiplier, defined as in Tarter and McKee (1973), and is the ratio of total opacity to electron scattering opacity.

The second line gives further information. The line starts with "Texc(La)", the excitation temperature T_{exc} of $L\alpha$, defined as

$$\frac{n(2p)/g(2p)}{n(1s)/g(1s)} = \exp(-h\nu/kT_{\text{exc}}) \quad (406)$$

is given. This is followed by the temperature corresponding to the energy density of the attenuated incident continuum ("T(contn)"), and the diffuse continua ("T(diffs)").

This includes all trapped lines and diffuse continuous emission. The entry “ nT (c+d)” is the energy densities of the sum of these two continua expressed as an equivalent pressure nT . The line ends with the ratios of the radiation to gas pressure, “Prad/Gas”, and the ratio of magnetic to gas pressure “Pmag/Gas”.

4.4.10 *Optional Grains*

If grains are present, then some properties of the grain populations are printed. Each line gives the results of calculations for a specific type and size of grain. Normally, a type of graphite and silicate are included when grains are present. There will be one line of output for each grain species. Each line begins with the name of the grain, and an asterisk appears if quantum heating was important for the species. Normally quantum heating is only computed if it is significant due to its computational expense. The remainder of the line gives the equilibrium temperature of the grain, the potential in volts, the charge, the drift velocity, followed by the gas heating ($\text{erg cm}^{-3} \text{ s}^{-1}$) due to grain photoionization, and the dimensionless fraction of the total gas heating due to grain photoionization. For quantum-heated grains the temperature is the average weighted by T^4 .

4.4.11 *Molecules*

A line giving relative abundances of some molecules is printed if the molecular fraction is significant. All molecular abundances are relative to either the total carbon or total oxygen abundance (this is indicated in the label for each). In order, the molecules are CH, CH⁺, CO, CO⁺, H₂O, and OH.

4.4.12 *Li, Be, B*

Abundances of each stage of ionization relative to the total gas phase abundance of the element are printed across two lines.

4.4.13 *Carbon*

The abundances of the seven stages of ionization of carbon relative to the total carbon abundance begin the line. The abundance of H₂O⁺ and OH⁺ relative to the total oxygen abundance follows.

4.4.14 *Nitrogen*

The relative populations of the eight ionization stages of nitrogen are printed first. The relative abundance of O₂ and O₂⁺ (relative to the total oxygen abundance) follows.

4.4.15 *Oxygen*

The oxygen ionization stages are followed by the extra heat added at this zone ($\text{erg cm}^{-3} \text{ s}^{-1}$) due to cosmic rays, turbulence, etc, and the log of the effective hydrogen recombination coefficient ($\text{cm}^3 \text{ s}^{-1}$).

4.4.16 *Fluorine, Neon*

The fluorine and neon relative ionization balances are printed across the line.

4.4.17 *Remaining Elements*

There are too many ionization stages to print across the line. Although all stages with non-trivial abundances are computed, only the highest twelve stages of ionization are printed. The first number is an integer indicating how many stages are

“off the page to the left”. If the number is 2, then the first printed stage of ionization is twice ionized, i.e., Fe⁺².

4.5 Calculation Stopped Because ...

```
Calculation stopped because lowest Te reached.      Iteration 1 of 1
The geometry is spherical.
!Non-collisional excitation of [OIII] 4363 reached 2.08% of the total.
!AGE: Cloud age was not set. I cannot check whether the time-steady assumption is ok.
Derivative of net cooling negative and so possibly thermally unstable in 4 zones.
Photoionization of He 2TriS reached 17.1% of the total rate out, 10.6% of that was Ly $\alpha$ .
Grains were not present but might survive in this environment (energy density temperature was 3.35E+01K)
The ratio of radiation to gas pressure reached 1.65E+01. Caused by Lyman alpha.
Line radiation pressure capped by thermalization length.
```

A series of messages will appear after the printout of the last zone.

The first will say why the calculation stopped. In a valid calculation the model will stop because one of the specified stopping criteria specified was met. If no other criteria are specified then the calculation usually stops when the default lowest temperature of 4000 K is reached. If the code stops because of an unintended reason (i.e., internal errors, or the default limit to the number of zones) then a warning is printed saying that the calculation may have halted prematurely.

Only one stopping criterion message will be printed. The possible messages, and their interpretations, are:

4.5.1 ... because of radiation pressure

The default density law is for a constant density. If constant pressure is specified instead (with the **constant pressure** command), then Cloudy will try to keep the total pressure, particle and radiation, constant. The radiation pressure is small at the boundaries of the cloud, so the cloud will be unstable if the ratio of radiation to total pressure exceeds 0.5. The calculation stops, and this message is generated, if $P_{rad}/P_{tot} > 0.5$ occurs after the first iteration.

4.5.2 ... because lowest EDEN reached.

The calculation can be forced to stop when the electron density (**eden**) falls below a certain value, as set by the **stop eden** command. This can be used to stop the calculation at an ionization front. The default lowest electron density is negative, so this stopping criterion applies only when the command is entered.

4.5.3 ... because low electron fraction.

The calculation can be forced to stop when the ratio of electron to hydrogen densities falls below a certain value, as set by the **stop efrac** command. This can be used to stop the calculation at an ionization front when the hydrogen density there is not known (for instance, in a constant pressure model). The default lowest electron density is negative, so this stopping criterion applies only when the command is entered.

4.5.4 low H₂/H fraction

The calculation can be forced to stop when the ratio of densities of molecular hydrogen to total hydrogen falls below a certain value, as set by the **stop mfrac** command. The molecular fraction is defined as $2n(H_2)/n(H_{tot})$. This can be used to stop the calculation at some depth into a PDR. The default lowest molecular density is negative, so this stopping criterion applies only when the command is entered.

4.5.5 ... *because wind veloc too small*

The code can perform a wind calculation which includes the outward force due to radiation pressure and the inward force of gravity. This message is printed if the gas is decelerated to a stop.

4.5.6 ... *because code returned BUSTED*

The calculation stopped because something bad happened. The results are suspect. I would appreciate learning about this - please send the input script and version number.

4.5.7 ... *because DRAD small - set DRMIN*

The Strömngren radius of the H⁺ zone is estimated at the start of the calculation, and the smallest allowed zone thickness is then set as a very small fraction of this. The calculation will stop if the zone thickness falls below this smallest thickness. This can occur because of any of several logical errors within Cloudy (adaptive logic is used to continuously adjust the zone thickness), although it can rarely occur for physical reasons as well. The smallest thickness can be reset to any number with the **set drmin** command, but it should not be necessary to do this. I would appreciate learning about this - please send the input script and version number.

4.5.8 ... *because DR small rel to thick.*

The depth into the cloud is stored as the double precision variable *depth* and the zone thickness is stored as the double precision variable *drad*. If the zone size becomes too small relative to the depth ($drad/depth < 10^{-14}$) then the depth variable will underflow such that $depth + drad = depth$. The calculation will stop in this case and give the above reason if this problem prevents the density from being properly evaluated. This is a fundamental numerical problem with no clear solution.

4.5.9 ... *because optical depth reached.*

The default value of the largest allowed continuous absorption optical depth is unphysically large, and can be reset with the **stop optical depth** command. The command specifies both the absorption optical depth, and the energy at which it is to be evaluated. All absorption opacity sources included in the calculation contribute to the computed optical depths and scattering opacities are not included. If the calculation stops because the largest continuum optical depth is reached, then this line is printed. This line is also printed if the **stop effective column density** command is used to stop the calculation, since this command is actually a form of the **stop optical depth** command.

4.5.10 ... *because outer radius reached.*

The default outer radius is unphysically large, but can be changed with the **radius** or **stop thickness** commands. If the calculation stops because the outer radius set by one of these commands is reached, then this line is printed.

4.5.11 ... *because column dens reached.*

The default values of the largest allowed neutral, ionized, and total hydrogen column densities are unphysically large. They can be reset with the commands **stop column density**, **stop neutral column density**, or **stop ionized**

column density. This message will be printed if one of these criteria stops the calculation.

4.5.12 ... because lowest Te reached.

The default value of the lowest temperature allowed is 4000 K. This is reasonable when only optical emission lines are of interest. The limit can be changed with the **stop temperature** command. This message is printed if the calculation stops because the lowest temperature is reached.

4.5.13 ... because highest Te reached.

The default value of the highest temperature allowed is 10^{10} K. The limit can be changed with the **stop temperature exceeds** command. This message is printed if the calculation stops because the highest allowed temperature is exceeded.

4.5.14 ... because NZONE reached.

The default condition is for up to 800 zones to be computed. This can be reset with the **stop zone** command. This message is printed if the calculation stops because the limiting number of zones is reached. A warning will be printed at the end of the calculation if it stops because it hits the default limit to the number of zones allowed, presently 800, since this was probably not intended.

The default limit to the number of zones can be increased, while retaining the check that the default limit is not hit, by using the **set nend** command.

4.5.15 ... because line ratio reached.

It is possible to set a limit to the largest value of an emission-line intensity ratio with the **stop line** command. This message is printed if the calculation stops because the largest value of the ratio is reached.

4.5.16 ... because internal error - DRAD.

An internal logical error caused this message to be printed. Please send the command lines and the version number of Cloudy to me (gary@pa.uky.edu).

4.5.17 ... because initial conditions out of bounds.

The temperature of the first zone was not within the temperature bounds of the code. This is probably due to the incident continuum not being set properly.

4.5.18 Because zero electron density

The electron density fell to zero. There is no source of ionization at all. This is unphysical and usually occurs because the cloud boundary conditions were not set properly. Consider adding the **cosmic ray background** command, to include their effects.

4.5.19 ... because reason not specified.

I would appreciate learning about this internal error. Please send the command lines and the version number of Cloudy to me (gary@pa.uky.edu).

4.6 Geometry

After saying why the calculation stopped, Cloudy will say whether the geometry is plane parallel ($\Delta r/r_o < 0.1$), a thick shell ($\Delta r/r_o < 3$), or spherical ($\Delta r/r_o \geq 3$), where r_o is the inner radius and Δr is the thickness of the cloud.

4.7 Warnings, Cautions, Surprises, and Notes

The next, optional, messages fall into four categories: warnings, which begin with W-; cautions, which begin with C-; surprising results, which begin with an explanation mark (!), and notes.

Cloudy checks that its range of validity was not exceeded in the calculation and does many internal sanity checks (Ferland 2001b). Warnings are issued to indicate that the program has not treated an important process correctly. For instance, warnings occur if the temperature was high enough for the electrons to be relativistic, if the global heating - cooling balance is off by more than 20%, or if the code stopped for an unintended reason. I would like to hear about warnings (gary@pa.uky.edu). Cautions are less severe, and indicate that Cloudy is on thin ice. Examples are when the optical depths in excited states of hydrogen change during the last iteration. Surprises begin with “!” and indicate that, while the physical process has been treated correctly, the result is surprising. An example is when induced Compton heating is more than 5 percent of the total Compton heating. Notes indicate interesting features about the model, such as maser effects in lines or continua, or if the fine structure lines are optically thick. The messages are usually self-explanatory.

4.9 Final Printout

4.9.1 Emission-Line Spectrum

```

*****> Cloudy 95.03 <*****
* title parispn.in Meudon Planetary nebula
* punch helium triplets "parispn.hel" last
* init file="ism.ini"
* sphere
* c standard" PN model of the Pequignot Meudon Conference
* dielec Kludge 0
* black body, T=150,000K radius = 10
* hden = 3.4771213
* radius = 17
* normalize to "Ca b" 4861
* abund he -1 C-3.523 N-4. O-3.222 ne-3.824 mg-4.523
*****> Log(U): -1.32 <*****

Emission Line Spectrum. Constant Density Model. Closed geometry. Iteration 1 of 1.
Luminosity (erg/s) emitted by shell with full coverage.

general properties..... Ca A 2511A 34.042 0.0392 C 2 2325A 33.805 0.0227 S 4 10.51m 35.761 2.0506
TOTL 4861A 35.453 1.0110 Ca A 1.012m 34.371 0.0836 C 2 2324A 33.496 0.0111 TOTL 1406A 33.440 0.0098
TOTL 1216A 36.889 27.5426 Ca A 6560A 34.075 0.0423 C 2 2328A 33.824 0.0237 S 4 1405A 32.541 0.0012
Inci 0 37.557 128.3691 Ca A 5412A 33.837 0.0244 C 2 2327A 34.358 0.0812 S 4 1417A 32.992 0.0035
TotH 0 37.248 62.9526 Ca A 4860A 33.639 0.0155 C 2 2325A 34.587 0.1374 S 4 1406A 33.048 0.0040
TotC 0 37.248 63.0276 Ca A 1.864m 33.907 0.0288 C 2 1335A 34.527 0.1199 TOTL 1198A 33.538 0.0123
BFH1 0 37.101 44.9165 Ca A 1.163m 33.672 0.0167 REC 1335A 34.450 0.1004 S 5 1199A 33.129 0.0048
BFHe 0 36.607 14.3953 Ca A 9345A 33.468 0.0105 C 3 977.0A 34.489 0.1098 S 5 1188A 33.323 0.0075
TotM 0 35.925 2.9977 Ca A 8237A 33.294 0.0070 C3 R 977.0A 34.274 0.0669 S 5 786.5A 32.792 0.0022
CT H 0 35.255 0.6400 Ca B 1640A 35.802 2.2585 P386 977.0A 33.436 0.0097 TOTL 933.0A 33.302 0.0071
H FB 0 35.844 2.4868 Ca B 1215A 35.302 0.7141 TOTL 1909A 35.676 1.6887 S 6 944.5A 32.879 0.0027
HFBC 0 35.844 2.4868 Ca B 1085A 34.958 0.3229 C 3 1911A 35.293 0.6988 S 6 933.4A 33.096 0.0044
continua..... Ca B 1025A 34.695 0.1762 C 3 1907A 35.444 0.9899 recombination.....
Bac 3646A 36.603 14.2567 Ca B 4686A 34.962 0.3264 C3 R 1909A 34.116 0.0465 C 2 4267A 32.690 0.0017
cout 3646A 36.603 14.2567 Ca B 3203A 34.594 0.1396 C 3 1176A 33.935 0.0307 C 2 1761A 32.647 0.0016
thin 3646A 36.603 14.2609 Ca B 2733A 34.315 0.0734 Rec 1175A 33.932 0.0305 C 3 4069A 32.633 0.0015
Inci 4860A 34.587 0.1375 Ca B 2511A 34.091 0.0439 TOTL 1549A 35.819 2.3485 C 3 1923A 33.289 0.0069
Inci 1215A 36.254 6.3864 Ca B 1.012m 34.385 0.0863 C 4 1551A 35.345 0.7879 C 3 4649A 32.612 0.0015

```

The final printout begins by reprinting the input commands. The box surrounding it gives both the version number of Cloudy (at the top) and the log of the ionization parameter (the ratio of ionizing photon to hydrogen densities) at the bottom.

The line following the box summarizes some properties of the model and output. The first part of the line indicates whether the energy in the emission lines is given as the luminosity radiated by a spherical shell covering Ω sr (erg s^{-1} ; $\Omega/4\pi$ is the covering factor) or the intensity produced by a unit area of gas ($\text{erg s}^{-1} \text{cm}^{-2}$). Which of the two choices is printed is determined by whether the luminosity of the continuum was specified as the luminosity radiated by the central object into 4π sr or the intensity ($4\pi J$) of the incident continuum ($\text{erg cm}^{-2} \text{s}^{-1}$) at the illuminated face of the cloud. If the model is spherical and the incident continuum specified per unit area, then the emergent emission-line spectrum will be per unit area in units of the inner radius r_o (that is, the total line luminosity radiated by a shell covering 4π sr will be the listed intensity $4\pi J$ times $4\pi r_o^2$). The second part of this line indicates the density structure of the model (i.e., wind, constant density, constant pressure, constant gas pressure, power-law density distribution, etc). The next section tells whether the geometry was open or closed (these are defined in Part I of this document). The last part indicates which iteration this is.

Next comes a series of predictions, mainly emission line intensities. The set of printed emission lines also includes other predicted quantities. Some continua, and various indications of contributors to lines and continua, are mixed in what follows. The section of the document describing observed quantities (page 450 below) tells how to convert these into some observed quantities. Not all are printed by default – the **print** commands described in Part I and also in section 6.3.2 starting on page 463 tell how to get more or fewer predictions. This list of emission lines can also be sorted by wavelength or intensity, and can be printed as a single column so that they

can be entered into a spreadsheet (see the **print lines** command in Part I of this document).

The organization and meaning of the different of lines in the printout is discussed on page 457 below.

A list of emission lines with negative intensities may follow the main block of lines. These are lines, which heat rather than cool the gas (heating is negative cooling). This is not a problem, but occurs if the line de-excitation rate exceeds the line excitation rate. The most common reason for this to occur is if the line is radiatively excited but collisionally de-excited.

4.9.2 Thermal balance

```
Cooling:  0 3 5007:0.245  0 3 4959:0.082
Heating:  BFH1  0:0.720  BFHe  0:0.233

IONIZE PARMET:  U(1-) -1.3193  U(4-) -2.0010  U(sp): -2.51  Q(ion):  43.458  L(ion):  33.712  Q(Low): 49.69  P(Low)  37.341
ENERGY BUDGET:  Heat:  37.222  Coolg:  37.222  Error:  0.2%  Rec Lin:  37.064  WorkF:  37.437  F-F  H 21.885  RadBetaMax:1.65E+01  G0:1.2e-3
```

Cooling: This line indicates the fraction of the total cooling (defined here as in Osterbrock 1989; that is, the energy of the freed photoelectron) carried by the indicated emission lines. The designation of the line is given as in the emission-line spectrum, and this is followed by the ratio of the energy in the line to the total cooling. This is an important indication of the fundamental power-losses governing conditions in the model. The labels used are the same as those in the line array.

Heating: This line indicates the fraction of the total heating produced by various processes. The labels used are the same as those in the line array.

IONIZE PARMET The line begins with the log of the H “U(1-)” and He⁺ “U(4-)” ionization parameters defined in the header. The third number “U(sp)” is the log of a spherical ionization parameter often used in spherical geometries, such as H II regions or planetary nebulae. It is defined as

$$U_{sph} = \frac{Q(H)}{4\pi R_s^2 n_H c} \quad (407)$$

where R_s is the Strömngren radius, defined as the point where the hydrogen neutral fraction falls to $H^0/H_{tot} = 0.5$. If no ionization front is present, then U_{sph} is evaluated at the outer edge of the computed structure. The next two numbers are the log of the number of hydrogen ionizing photons ($h\nu \geq 1$ Ryd) exiting the nebula “Q(ion)”, and the log of the energy in this ionizing continuum “L(ion)”. The next two numbers are the equivalent quantities, for non-ionizing ($h\nu < 1$ Ryd) radiation. These are either per unit area or by a shell covering 4π sr. These have been corrected for the r^{-2} dilution if per unit area, and so are directly comparable with the numbers given at the start of the calculation. The last number “G0” gives the intensity of the ultraviolet radiation field relative to the background Habing value, as defined by Tielens & Hollenbach (1985).

ENERGY BUDGET This line gives an indication of the energy budget of the nebula. The first number “Heat” is the log of the total heating (in ergs s⁻¹, but again either into 4π sr or cm⁻²). The second number “Coolg” is the log of the total cooling, in the same units. Cooling, as defined in Osterbrock (1989), is the total energy in collisionally excited lines and part of the recombination energy, but *does not* include

recombination lines. The percentage error in the heating-cooling match “Error” follows. The next number “Rec Lin” is the log of the total luminosity in recombination lines. The number indicated by “WorkF” is an indication of the work function (that is, the log of the energy needed to remove bound electrons from the atom or ion) of the cloud. The work function and the total cooling do not add up to the total energy absorbed from the incident continuum because some recombination lines of helium and heavy elements contribute to both. The next number “F-F H” is the log of the amount of energy deposited by free-free heating, and the last number “RadBetaMax” is the largest value of the ratio of radiation to gas pressures which occurred in the calculation.

4.9.3 Column densities, et al.

```
Column density  Htot:9.024E+20  H II:8.704E+20  HI:3.204E+19  H-: 1.445E+12  H2: 9.379E+11  H2+:2.190E+11  He H+:4.187E+12
                CH:0.000E+00  CH+:0.000E+00  OH:0.000E+00  OH+: 0.000E+00  O2: 0.000E+00  C2:0.000E+00  CO:0.000E+00
                CO+:0.000E+00  H2O:0.000E+00H2O+:0.000E+00  O2+: 0.000E+00  C2+: 0.000E+00  H3+:0.000E+00  H3O+:0.000E+00
                CH2+:0.000E+00  CH2:0.000E+00  CH3:0.000E+00MoH2O 0.000E+00
Col (Heff):      1.717E+04  snd travl time 1.73E-06 sec  Te-low: 1.00E+04  Te-hi:1.00E+04  T(21cm/Ly a):1.11E+16
Emiss Measure   n(e)n(p) dl      2.388E+08  n(e)n(He+)dl      2.014E+06  En(e)n(He++) dl      2.189E+07
He/Ha:9.71E-02  = 0.97*true  Lthin:2.79E+04  itr/zn: 4.50  File Opacity: F  <nH/T>:1.00E+04  Mass: 32.985
<a>:0.00E+00  erdeFe2.8E+21  Tcompt6.11E+05  Tthr1.02E+08  <Tden>: 1.00E+04  <dens>:2.38E-20  <Mol>:6.24E-01
Mean Jeans l (cm) 5.14E+19  M(sun)8.48E+05  smallest:      len(cm):5.14E+19  M(sun):8.48E+05  Alf(ox-tran): -1.4086
Hatom level 16  Nhtopoff: 10  HatomType: add  HInducImp F  He sin level: 9  He2 level: 16  ExecTime 20.894
ConvgError(%) <eden> 0.002  MaxEden 0.002  <H-C>107.512  Max(H-C) 107.52  <Press> 0.000  MaxPres 0.000
```

Column density This line lists the column densities (cm^{-2}) of some ions and molecules. The first number “Htot” is the total hydrogen column density (including atoms, ions, and molecules). The following two numbers are the column densities in H^+ and H^0 only. The last four numbers are column densities in four ions and molecules (H^- , H_2 , H_2^+ , and HeH^+). The next three lines give column densities in various molecules containing heavy elements.

Col (Heff) The effective column density “Col(Heff)”, as defined in the section on the **stop effective column density** command, is printed. This is followed by “snd travl time”, the sound travel time across the nebula in seconds. Constant pressure is only valid if the cloud is static for times considerably longer than this. The last two numbers are the lowest “Te-low” and highest “Te-hi” electron temperatures found in the computed structure. The last number is the temperature derived from the ratio of $\text{Ly}\alpha$ to 21 cm optical depths.

Emiss Measure This gives several line-of-sight emission measures. The definition of the line of sight emission measure of a species X is

$$E(X) = \int n(e) n(X) f(r) dr \quad [\text{cm}^{-5}] \quad (408)$$

where $f(r)$ is the filling factor. This is given for H^+ , He^+ , and He^{2+} .

He/Ha This line gives some quantities deduced from the predicted emission-line spectrum. The first (He/Ha) number is the apparent helium abundance He/H , measured from the emission-line intensities using techniques similar to those described in Osterbrock (1989);

$$\left(\frac{\text{He}}{\text{H}}\right)_{\text{apparent}} = \frac{0.739 \times I(5876) + 0.078 \times I(4686)}{I(\text{H}\beta)}. \quad (409)$$

The intensity of both $\text{H}\beta$ and $\text{HeI } \lambda 5876$ are the total predicted intensities, and includes contributions from collisional excitation and radiative transfer effects. The intensity of $\text{He II } \lambda 4686$ is taken from Case B results, which are better than those of

the model atom at low densities. The second number (i.e., 1.07*true), is the ratio of this deduced abundance to the true abundance. This provides a simple way to check whether ionization correction factors, or other effects, would upset the measurement of the helium abundance of the model nebula. This is followed by the longest wavelength in centimeters "Lthin" at which the nebula is optically thin. Generally the largest FIR opacity source is brems, and the number will be 10^{30} if the nebula is optically thin across the IR. The number "itr/zn" is the average number of iterations needed to converge each zone. "Mass" gives the log of the total mass of the computed structure in grams if the inner radius was specified. If the inner radius was not specified then this is the log of the mass per unit area, gm cm⁻².

Temps(21 cm) This line gives various quantities related to the H I 21 cm line. "T(21cm/Ly a)" gives the temperature deduced from the ratio of the 21 cm to Ly α lines. The opacity within the 21 cm line is proportional to $n(H^0)\chi/kT$ where χ is the excitation energy of the line. "T(<n(H0)/T>)" gives the harmonic mean temperature

$$\langle T \rangle = \frac{\int T n(H^0)\chi/kT dr}{\int n(H^0)\chi/kT dr} \quad (410)$$

The number "TB21cm" is the brightness temperature of the 21 cm line as viewed from the illuminated face of the cloud. "<Tspin>" gives the mean spin temperature of the 21 cm transition. This is the mean of the actual ratio of populations of the ground fine structure levels, which is computed including the effects of Ly α scattering.

<a> The mean radiative acceleration (cm s⁻²) is printed if the geometry is a wind model and zero otherwise. This is followed by some time scales. The first "erdeFe" is the time scale, in seconds, to photoerode Fe (Boyd and Ferland 1987; this number is 0s if the γ -ray flux is zero). The next two are the Compton equilibrium timescale "Tcompt", and the thermal cooling timescale "Tthr". Both are in seconds. The density (gm cm⁻³) weighted mean temperature "<Tden>", radius weighted mean density "<dens>" (gm cm⁻³), and mean molecular weight "<Mol>" follow.

Mean Jeans This line gives the mean Jeans length "l(cm)" (cm) and Jeans mass "M(sun)" (in solar units), followed by the smallest Jeans length "smallest len(cm)" and the smallest Jeans mass "M(sun)" which occurred in the calculation. The last quantity "Alf(ox-tran)" is the spectral index α_{ox} defined as in the header, but for the transmitted continuum (attenuated incident continuum plus emitted continuum produced by the cloud).

H and He atoms This line gives the number of levels of the model hydrogen atom, the "topoff" level, above which the remainder of the recombination coefficient is added, the type of topping off used for this calculation, and the number of levels used for the helium singlets and ion. The last number on the line is the execution time in seconds.

4.9.4 Averaged Quantities

Averaged Quantities
Te Te (Ne) Te (NeNp) Te (NeHe+) Te (NeHe2+) Te (NeO+) Te (NeO2+) NH Ne (O2+) Ne (Np)

```

Radius: 1.334E+04 1.358E+04 1.363E+04 1.109E+04 1.542E+04 1.115E+04 1.139E+04 3.000E+03 3.339E+03 3.429E+03
Volume: 1.179E+04 1.207E+04 1.214E+04 1.100E+04 1.446E+04 1.115E+04 1.117E+04 3.000E+03 3.305E+03 3.294E+03
Peimbert T(OIIIr)1.15E+04 T(Bac)1.21E+04 T(Hth)1.14E+04 t2(Hstrc) 2.72E-02 T(O3-BAC)1.15E+04 t2(O3-BC) 1.81E-03 t2(O3str) 7.36E-03

```

This begins with several temperature and density averages, over either radius or volume. The volume averages are only printed if the **sphere** command is entered. The quantity which is printed is indicated at the top of each column. The averaged quantity is the first part of the label, and the weighting used is indicated by the quantity in parenthesis. For instance, **Te (NeO2+)** is the electron temperature averaged with respect to the product of the electron and O²⁺ densities.

Peimbert This series of quantities deal with temperature fluctuations (t^2 , Peimbert 1967). The code attempts to analyze the predicted emission line and continuum spectrum using the same steps that Manuel outlined in this paper. The code does not attempt to correct the predicted emission line intensities for collisional suppression or reddening, so this line is only printed if the density is below the density set with the **set tsqden** command - the default is 10^7 cm^{-3} . This code does not attempt to deredden the spectrum: a caution is printed if grains are present.

The nature of temperature fluctuations is, in my option, the biggest open question in nebular astrophysics. Theory (Cloudy too) predicts that they should be very small, because of the steep dependence of the cooling function on the temperature, while some observations indicate a very large value of t^2 (see Liu et al. 1995, and Kingdon and Ferland 1995 for a discussion). If something is missing from our current understanding of the energy source of photoionized nebulae then the entire nebular abundance scale (for both the Milky Way and the extragalactic nebulae) is in error by as much as 0.5 dex.

Two fundamentally different t^2 s enter here - the “structural” t^2 and the “observational” t^2 . The structural value comes from the computed ionization and thermal structure of the nebula, while the observational value comes from an analysis of the predicted emission line spectrum following the methods outlined in Peimbert’s 1967 paper.

The structural t^2 for the H⁺ ion is defined as

$$t^2(H^+) = \left\langle \left[\frac{T(r) - \langle T \rangle}{\langle T \rangle} \right]^2 \right\rangle = \frac{\int [T(r) - \langle T \rangle]^2 n_e n_{H^+} f(r) dV}{\langle T \rangle^2 \int n_e n_{H^+} f(r) dV} \quad (411)$$

where $\langle T \rangle$ is the density-volume weighted mean temperature

$$\langle T \rangle = \frac{\int T(r) n_e n_{H^+} f(r) dV}{\int n_e n_{H^+} f(r) dV}. \quad (412)$$

This quantity is given in the averaged quantities block as the column “Te(NeNp)”.

The observational t^2 - related quantities are the following: “T(OIIIr)” is the electron temperature indicated by the predicted [OIII] 5007/4363 ratio in the low-density limit. This number is meaningless for densities near or above the critical density of these lines. “T(Bac)” is the hydrogen temperature resulting from the predicted Balmer jump and H β . “T(Hth)” is the same but for optically thin Balmer continuum and case B H β emission. “t2(Hstrc)” is the structural H II t^2 . The entries

“T(O3-BAC)” and $t_2(\text{O3-BC})$ ” are the mean temperature and t^2 resulting from the standard analysis of the [O III] and H I spectra (Peimbert 1967). Finally “ $t_2(\text{O3str})$ ” is the structural t^2 over the O^{2+} zone. Only the structural t^2 s are meaningful for high densities. This section was developed in association with Jim Kingdon, and Kingdon and Ferland (1995) provide more details.

4.9.5 Grains

```
Average grain Properties:
Gra-Ori      Sil-Ori
<Tdust>:    1.540E+02  1.218E+02
<Vel D>:    3.635E+04  2.891E+04
<Pot D>:    1.337E+00  1.419E+00
Total dust to gas ratio (by mass) is 6.277e-03, A(V)/N(H) = 3.999e-22, R = 3.753e+00
```

The next lines give some information concerning grains if these were included in the calculation. These lines give the mean temperature, drift velocity, and potential, for all of the grain populations included in the calculation. An asterisk will appear to the right of the name of any species with quantum heating included. In this case the mean temperature is weighted by T^4 .

The last line gives some information related to the grain abundance and optical properties. The first number is the dust to gas ratio by mass. The next is the total visual extinction per unit hydrogen column density. The last is the ratio of total to selective extinction.

4.9.6 Continuum optical depths

```
Contin Optical Depths: COMP: 6.80E-04  H-: 5.59E-05  R(1300): 2.14E-04  H2+ 1.50E-06  HeTri:6.09E-04
Pfa:3.40E-04  Pa:3.40E-04  Ba:3.65E-04  Hb:3.60E-04  La:1.29E-01  lr:4.995E+07  1.8:1.19E+07  4.:1.738E+06
Line Optical Depths: 10830: 1.23E+02  3889: 5.24E+00  5876: 3.29E-06  7065: 1.82E-06  2.06m 2.54E-03
```

Contin Optical Depths The first two lines give the continuum optical depths at various energies. These are the total optical depths, including the correction for stimulated emission, and will be negative if maser action occurs. These include grain opacity if grains are present. The labels, and their interpretation, are as follows. COMP is Thomson scattering. H- is the negative hydrogen ion at maximum cross section. R(1300) is Rayleigh scattering at 1300Å, H_2^+ is the molecular hydrogen ion. HeTri is the helium triplet at threshold. The next line gives total continuous optical depths at the energies of various hydrogen and helium ionization edges and lines. These are the Pfund α , Paschen α , Balmer α and β , $L\alpha$, and the ionization edges of hydrogen, atomic helium, and the helium ion.

Heavy element line optical depths are printed also if the **print line optical depths** command is entered.

```
Old hydro optical depths:  1 9.99E+07  2 1.00E-20  3 1.00E-20  4 1.00E-20  5 1.00E-20  6 1.00E-20  7 1.00E-20
Old H Lines: 2-1 9.96E+19 3-2 3.34E-02 4-3 3.33E-04 5-4 1.66E-05 6-5 2.56E-06 7-6 2.56E-07 8-7 2.56E-08
New hydro optical depths:  1 4.99E+07  2 1.46E-05  3 2.82E-05  4 6.80E-06  5 1.25E-12  6 3.05E-12  7 6.49E-12
New H Lines: 2-1 2.02E+06 3-2 9.37E-03 4-3 1.98E-09 5-4 6.50E-10 6-5-5.01E-09 7-6-2.94E-08 8-7-1.81E-07
Old He I optical depths:  1 2.38E+07  2 1.00E-20  3 1.00E-20  4 1.00E-20  5 1.00E-20  6 1.00E-20  7 1.00E-20
Old He I Lines: 2-1 9.96E+19 3-2 1.00E-20 4-3 1.00E-20 5-4 1.00E-20 6-5 1.00E-20 7-6 1.00E-20 8-7 1.00E-20
New He I optical depths:  1 1.19E+07  2 1.46E-05  3 2.83E-05  4 6.06E-06  5 1.41E-12  6 3.33E-12  7 6.93E-12
New He I Lines: 2-1 6.15E+04 3-2 1.12E-03 4-3 3.50E-11 5-4-2.59E-11 6-5-1.25E-10 7-6 5.98E-09 8-7 2.36E-08
Old He II optical depths:  1 3.41E+06  2 9.75E+07  3 1.00E-20  4 1.00E-20  5 1.00E-20  6 1.00E-20  7 1.00E-20
Old He II Lines: 2-1 9.96E+19 3-2 1.00E-20 4-3 1.00E-20 5-4 1.00E-20 6-5 1.00E-20 7-6 1.00E-20 8-7 1.00E-20
New He II optical depths:  1 1.70E+06  2 4.88E+07  3 1.89E-04  4 1.39E-05  5 2.16E-05  6 2.75E-05  7 2.72E-05
New He II Lines: 2-1 1.13E+06 3-2 9.14E-05 4-3 1.36E-11 5-4-4.73E-11 6-5-2.17E-10 7-6 5.52E-09 8-7 2.11E-08
```

Hydrogen and helium optical depths in continua and $\alpha(n \rightarrow n-1)$ transitions follow. The first two lines are the optical depths assumed at the start of the present iteration, and the second pair of lines gives the newly computed total optical depths. Negative optical depths indicate maser action. For each of the pairs of lines, the first line is the optical depth at thresholds of the first seven levels of hydrogen. The second line gives the optical depths in the first seven of the $\alpha(n \rightarrow n-1)$ transitions of hydrogen or helium.

4.9.7 Line optical depths

Line optical depths are not normally printed, but will be if the **print line optical depths** command is entered.

The last line gives column densities for some excited states. The label gives the element, ionization stage, and level within the ground term. The meaning of the labels is given in Table 1 on page 420 above.

4.9.8 Column density

```

Hydrogen  -1.117 -0.035
Helium    -1.454 -0.163 -0.556
Lithium   -3.801 -0.106 -0.722 -1.560
-----
Zinc      0.000 -9.140 -6.755 -5.236 -4.412 -3.639 -3.399 -3.681 -4.676 -5.987 -7.438 -8.975
Exc state CII* -1.785 CII* -5.897 CII* -5.677 OII* -5.992 OII* -6.311 Si2* -2.582

```

The column densities of all constituents will be printed if the **print column density** command is included in the input stream. Column densities within certain excited states, listed in Table 1 on page 420 above, are also printed.

4.9.9 Mean ionization

```

Hydrogen  -1.103 -0.036 -9.105 (H2)
Helium    -1.460 -0.181 -0.515
Carbon    -3.666 -0.845 -0.306 -0.653 -0.853
Nitrogen  -1.442 -0.818 -0.359 -0.537 -1.148 -1.884
Oxygen    -1.133 -0.889 -0.264 -0.770 -1.115 -2.248 -4.093
Neon      -2.225 -1.368 -0.153 -0.792 -1.077 -2.502 -5.649
Magnesium -2.887 -0.679 -0.307 -0.777 -0.912 -2.159 -4.911
Silicon   -4.300 -0.559 -0.559 -0.595 -0.718 -2.696 -5.810
Sulphur   -4.310 -0.960 -0.477 -0.553 -0.659 -1.304 -2.099 -7.773
Argon     -1.651 -1.552 -0.347 -0.567 -0.891 -1.086 -1.746 -3.513 -5.918
Iron      -4.522 -0.901 -0.913 -0.368 -0.917 -0.912 -1.142 -2.136 -4.077

      1      2      3      4      5      6      7      8      9     10     11     12     13     14     15     16     17

Hydrogen  -1.435 -0.016 -9.462 (H2)
Helium    -1.802 -0.378 -0.248
Carbon    -3.977 -1.155 -0.470 -0.594 -0.473
Nitrogen  -1.791 -1.129 -0.500 -0.433 -0.753 -1.325
Oxygen    -1.477 -1.186 -0.404 -0.540 -0.703 -1.692 -3.437
Neon      -2.580 -1.685 -0.321 -0.566 -0.665 -1.940 -4.989
Magnesium -3.171 -0.972 -0.472 -0.611 -0.542 -1.629 -4.275
Silicon   -4.577 -0.849 -0.705 -0.581 -0.407 -2.191 -5.175
Sulphur   -4.628 -1.288 -0.718 -0.624 -0.451 -0.869 -1.517 -7.006
Argon     -2.004 -1.887 -0.587 -0.623 -0.672 -0.691 -1.207 -2.876 -5.215
Iron      -4.849 -1.236 -1.192 -0.536 -0.827 -0.660 -0.718 -1.569 -3.419

Hydrogen  -1.458 -0.015 -10.265 (H2)
Helium    -1.992 -0.191 -0.461
Carbon    -3.785 -1.049 -0.295 -0.614 -0.796
Nitrogen  -2.057 -0.927 -0.339 -0.496 -1.091 -1.826
Oxygen    -1.544 -0.946 -0.243 -0.715 -1.058 -2.190 -4.034
Neon      -3.174 -1.698 -0.156 -0.738 -1.020 -2.443 -5.590
Magnesium -2.963 -0.808 -0.294 -0.726 -0.855 -2.101 -4.852
Silicon   -4.344 -0.663 -0.540 -0.560 -0.665 -2.639 -5.751
Sulphur   -4.444 -1.217 -0.484 -0.524 -0.608 -1.247 -2.040 -7.714
Argon     -2.450 -1.890 -0.364 -0.536 -0.836 -1.028 -1.688 -3.454 -5.860
Iron      -4.675 -1.167 -0.925 -0.349 -0.868 -0.857 -1.085 -2.077 -4.018

      1      2      3      4      5      6      7      8      9     10     11     12     13     14     15     16     17

Hydrogen  -1.796 -0.007 -10.648 (H2)
Helium    -2.338 -0.406 -0.220
Carbon    -4.114 -1.363 -0.480 -0.577 -0.443
Nitrogen  -2.425 -1.257 -0.502 -0.413 -0.724 -1.295
Oxygen    -1.906 -1.265 -0.408 -0.512 -0.673 -1.662 -3.407
Neon      -3.552 -2.005 -0.340 -0.539 -0.635 -1.910 -4.958
Magnesium -3.264 -1.110 -0.482 -0.586 -0.513 -1.598 -4.245
Silicon   -4.641 -0.965 -0.709 -0.567 -0.379 -2.161 -5.144
Sulphur   -4.782 -1.556 -0.748 -0.619 -0.425 -0.840 -1.486 -6.976
Argon     -2.827 -2.236 -0.625 -0.615 -0.644 -0.661 -1.177 -2.845 -5.184
Iron      -5.025 -1.521 -1.230 -0.544 -0.804 -0.632 -0.688 -1.538 -3.389

Hydrogen  3.963 4.089 3.744 (H2)
Helium    3.915 4.047 4.158
Carbon    4.032 4.000 4.058 4.101 4.184
Nitrogen  3.900 4.036 4.062 4.111 4.186 4.215
Oxygen    3.953 4.049 4.057 4.157 4.190 4.214 4.231
Neon      3.820 3.961 4.054 4.155 4.190 4.215 4.232
Magnesium 4.039 4.019 4.052 4.139 4.182 4.209 4.228
Silicon   4.049 4.028 4.058 4.088 4.164 4.203 4.228
Sulphur   4.029 3.988 4.052 4.065 4.143 4.194 4.219 4.249
Argon     3.868 3.972 4.048 4.069 4.156 4.189 4.212 4.228 4.239
Iron      4.026 3.989 4.060 4.047 4.122 4.162 4.193 4.216 4.231

      1      2      3      4      5      6      7      8      9     10     11     12     13     14     15     16     17

Hydrogen  3.968 4.134 3.745 (H2)
Helium    3.919 4.051 4.184
Carbon    4.034 4.006 4.067 4.130 4.203
Nitrogen  3.902 4.038 4.073 4.145 4.205 4.227
Oxygen    3.955 4.050 4.064 4.175 4.208 4.227 4.238
Neon      3.821 3.969 4.063 4.174 4.208 4.228 4.239
Magnesium 4.041 4.023 4.057 4.159 4.202 4.224 4.236
Silicon   4.050 4.032 4.068 4.117 4.192 4.221 4.236
Sulphur   4.031 3.992 4.052 4.081 4.170 4.211 4.230 4.250
Argon     3.869 3.975 4.048 4.083 4.173 4.205 4.225 4.236 4.243
Iron      4.028 3.992 4.059 4.047 4.137 4.180 4.210 4.228 4.238

Hydrogen  4.022 4.093 3.802 (H2)
Helium    3.998 4.051 4.159

```

Carbon	4.048	4.040	4.060	4.103	4.185												
Nitrogen	3.980	4.050	4.063	4.113	4.187	4.215											
Oxygen	4.011	4.056	4.057	4.157	4.190	4.214	4.231										
Neon	3.894	4.026	4.058	4.155	4.190	4.215	4.232										
Magnesium	4.050	4.046	4.053	4.140	4.182	4.209	4.228										
Silicon	4.056	4.051	4.059	4.090	4.165	4.204	4.228										
Sulphur	4.047	4.036	4.054	4.066	4.144	4.194	4.219	4.249									
Argon	3.932	4.022	4.052	4.070	4.157	4.189	4.212	4.228	4.239								
Iron	4.044	4.033	4.061	4.047	4.123	4.162	4.193	4.216	4.231								
	1	2	3	4	5	6	7	8	9	10	11	12	13	14	15	16	17
Hydrogen	4.027	4.138	3.803 (H2)														
Helium	4.002	4.054	4.184														
Carbon	4.049	4.043	4.068	4.132	4.203												
Nitrogen	3.982	4.051	4.075	4.147	4.205	4.227											
Oxygen	4.013	4.056	4.065	4.176	4.208	4.227	4.238										
Neon	3.896	4.030	4.067	4.175	4.208	4.228	4.239										
Magnesium	4.050	4.047	4.058	4.160	4.202	4.224	4.236										
Silicon	4.056	4.051	4.069	4.119	4.192	4.222	4.236										
Sulphur	4.048	4.037	4.054	4.083	4.171	4.211	4.230	4.250									
Argon	3.933	4.024	4.051	4.085	4.173	4.205	4.225	4.236	4.243								
Iron	4.045	4.034	4.060	4.048	4.138	4.180	4.210	4.228	4.238								

The two large blocks of output give the mean ionization, averaged over volume, and over radius. The numbers printed are the log of the mean ionization fraction in the various stages. The volume average ionization fraction for ion i of element a is given by

$$\left\langle \frac{n_a^i}{n_a} \right\rangle_{vol} = \frac{\int n_a^i f(r) dV}{\int n_a f(r) dV}. \quad (413)$$

and the radius average by

$$\left\langle \frac{n_a^i}{n_a} \right\rangle_{rad} = \frac{\int n_a^i f(r) dr}{\int n_a f(r) dr}. \quad (414)$$

The means are over molecules, atoms and ions of the element a , but does not include any atoms that are in grains. Similar blocks of information will give the mean ionization weighted by electron density and radius or volume, and mean electron temperature weighted by volume, radius, and electron density and volume and radius.

4.9.10 Continuum

This is only printed if the `print continuum` command is included. Then the following tables, all related to the transmitted continuum, will be printed.

X-Ray Continuum. The next line gives the photon fluxes ($\text{cm}^{-2} \text{s}^{-1}$) in various x-ray bands, if the continuum extends to x-ray energies. The units of the energy bands are keV. The numbers are the numbers of photons exiting the cloud, integrated over the energy bands. This is the net continuum, that is, the incident continuum, less attenuation, with diffuse re-emission from the cloud added on.

Normalized Continuum. This block is a set of ordered pairs giving the emergent Balmer continuum, relative to the continuum which entered the cloud. The first number of each pair is the frequency in Rydbergs. The second is the ratio of the emergent continuum to the incident continuum (i.e., that which went into the cloud). In the absence of optical depth or diffuse emission effects, this block will be equal to 1.000 throughout.

Emergent Continuum. This block gives ordered pairs of energy (in Rydbergs) and the emergent continuum. It is expressed as photon fluxes ($\text{phot Ryd}^{-1} \text{cm}^{-2}$)

corrected for r^2 dilution , so as to be directly comparable with the continuum which went into the cloud.

5 OBSERVED QUANTITIES

5.1 Overview

This section describes how to convert the quantities actually used or predicted by Cloudy into commonly observed ones.

5.2 Incident and Diffuse Continua

The emission line printout gives the intensity of the incident continuum (λF_λ or νF_ν) at 4860 and 1215 Å. These appear with the label **Inci** followed by the wavelength. The entire incident continuum can be obtained with the output of the **punch continuum** command.

The diffuse continuum, the continuum emitted by the cloud, is not normally included in the line output. The **print diffuse continuum** command will add the total emitted continuum to the emission line list. These are in units λF_λ or νF_ν at the indicated wavelengths and have the label **nFnu**. The entry with the label **nTnu** is the sum of the reflected plus attenuated incident continuum. The inward total emission and the reflected incident continua will be printed if this command appears together with the **print line inward** command. Two contributors to the inward emission are predicted. That labeled **InwT** is the total inwardly emitted continuum, and includes both diffuse emission and the back-scattered incident continuum. The component labeled **InwC** is the back-scattered incident continuum alone.

5.3 Line Equivalent Widths

The equivalent width of an emission or absorption line is defined as the number of Ångstroms of the continuum that is equivalent to the energy in the line. It can be defined as

$$W_\lambda = \int \frac{F_\lambda^c - F_\lambda^l}{F_\lambda^c} d\lambda \approx -\lambda \frac{F_{line}}{\lambda F_\lambda^c} \quad [\text{units of } \lambda] \quad (415)$$

where the fluxes are in the interpolated continuum (F_λ^c) and the integrated line (F_{line}). By this convention the equivalent width of an emission line is negative.

The code predicts the integrated fluxes of all lines. It also predicts the product λF_λ^c for the incident continuum at a few wavelengths. These are given the label **Inci** and the wavelength where it is evaluated follows. The entry **Inci 4860** is the intensity of the incident continuum at a wavelength near H β . The units of this incident continuum are either $\text{erg cm}^{-2} \text{s}^{-1}$ or erg s^{-1} depending on whether the incident continuum was specified as a flux or luminosity. The fluxes of lines and these continuum points can be read from the output, or obtained by software calling the *cdLine* routine. The continuum flux at any wavelength can be obtained with the **punch continuum** command. If the line intensity is given by F_{line} and the continuum intensity λF_λ^c , then the equivalent width of a line relative to the continuum where λF_λ^c is specified will be given by the last term in equation 415.

A covering factor will complicate this slightly. (Covering factors are defined in the section *Definitions* in Part I of this document.) If luminosities are predicted then partial coverage of the source is taken into account with the **covering factor** command, and the luminosities are correct for this coverage. The ratio of line to continuum given in equation 415 will represent what is observed. If intensities are predicted then the line intensity is given per unit area of cloud, no matter what covering factor is specified. In this second case the ratio in equation 415 must be scaled by the covering factor.

5.4 Emission Line Asymmetries

The inward fraction of the total emission of each line is always predicted by the code, but not normally printed out. Many lines are significantly inwardly beamed, and this can lead to emission line asymmetries if the envelope is expanding. The inward part of the lines will be printed if the **print line inward** command is entered. The effects of this line beaming are very geometry dependent.

5.5 Line to Continuum Contrast

The code has several **punch** commands that will produce ancillary files containing the predicted line and continuum spectra. There is an ambiguity in how strong the lines should appear to be relative to the continuum in a plot where the lines are not resolved. This is described in Part I of this document where the **punch continuum** and **set PunchLWidth** commands are introduced.

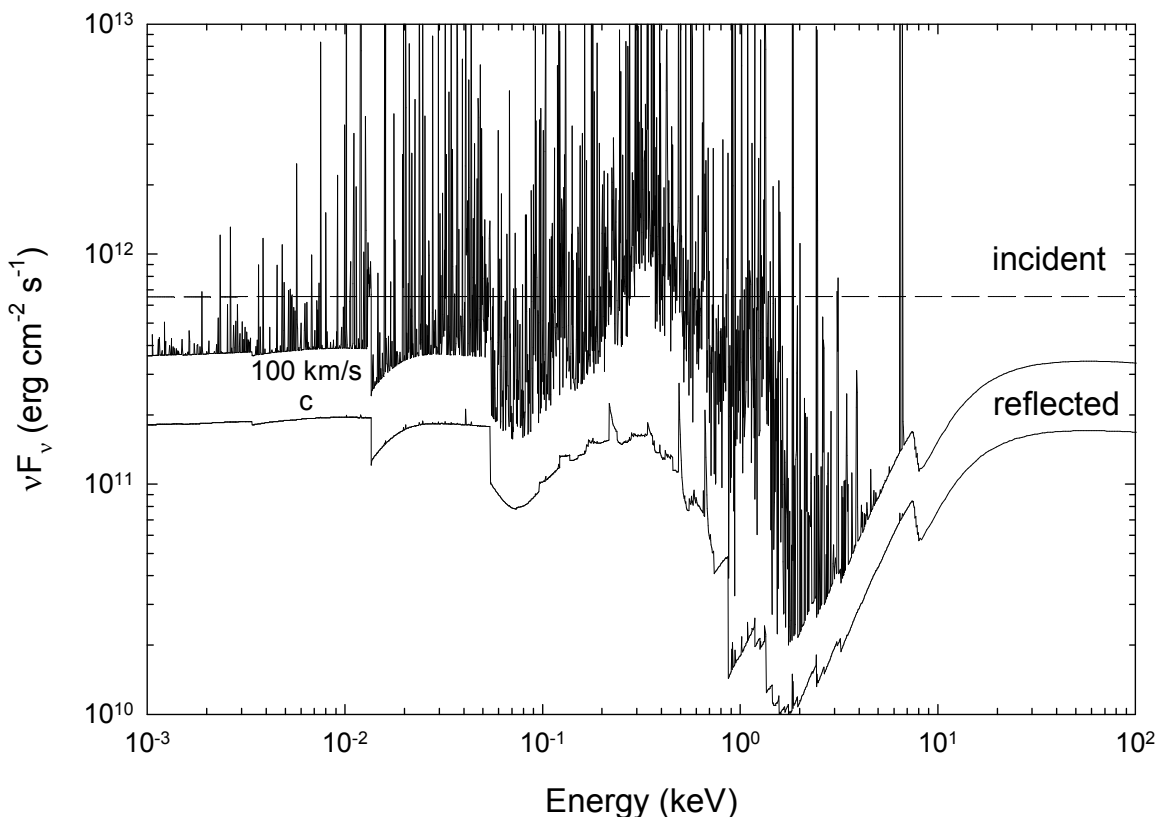


Figure 8 This shows the continua predicted by the input file reflector.in. The lowest curve has been divided by two and shows the total spectrum produced by setting the line width to the speed of light The middle curve shows the 100 km s⁻¹ case. The upper curve shows the incident continuum. reflector

Figure 8 shows the continuum predicted with the `reflector.in` test case. The upper curve is the incident continua and the two lower curves give the reflected continua for cases where the linewidth is 100 km/s and the speed of light⁶. Here lines are added to the continuum such that the difference between νF_ν at the line peak and νF_ν for the underlying diffuse continuum is equal to the line flux. As a result the resulting line to continuum contrast is very small. The middle curve shows the same model but with the line contrast enhanced by entering the command `set PunchLWidth 100 km/sec`. The entire spectrum of the c linewidth case is shifted by a factor of two to make the two continua appear separated. The default line width is 1000 km s⁻¹.

The only effect of the `set PunchLWidth` command is to change the contrast in the punch output. The computed results and line intensities in other output are not affected. If the width is set to the speed of light then the intensities in the punch output will be correct but the line to continuum contrast too small. If the width is set to a small value the contrast is increased but the total intensity in the punch output will be greater than the actual emission. (Energy *will not* appear to have been conserved in this punch output).

5.6 Surface Brightness

Cloudy will normally predict a line's intensity as $4\pi J$, the intensity radiated into 4π sr by a unit area of cloud, with units erg s⁻¹ cm⁻². Observations of resolved sources often measure the surface brightness, with units erg s⁻¹ cm⁻² arcsec⁻². Be careful! Some workers may report surface brightness with units erg s⁻¹ cm⁻² arcsec⁻² sr⁻¹. Remove the sr⁻¹ before continuing by multiplying by 4π .

To obtain the predicted surface brightness we must divide the intensity $4\pi J$ by the number of square seconds of arc in 4π sr. One radian is $360/2\pi = 57.29578$ deg, so 1 sr is $(180/\pi)^2 = 3282.806$ deg². There are $(60 \times 60)^2$ square seconds in a square degree, so there are 5.3464×10^{11} square arc seconds in 4π sr. The surface brightness (per square second of arc) is the intensity $4\pi J$ multiplied by the inverse of this, or 1.8704×10^{-12} arcsec⁻².

Note that this is only correct for a line that is emitted isotropically, because the code predicts $4\pi J$ while an observer measures I along a particular direction. (The code does predict the fraction of a line that is emitted from the illuminated face of the cloud.) This discussion is only formally correct if $I = J$.

There is a `print line surface brightness` command, described in Part I of this document, which will change the intensity into surface brightness units. By default the final units will then be erg s⁻¹ cm⁻² sr⁻¹, but the command has an `arcsec` keyword to specify the surface brightness in erg s⁻¹ cm⁻² arcsec⁻².

⁶ This was the default for version 90.00 through version 90.03. In C90.04 the default was changed to 1000 km/s. Before version 90 the line to continuum contrast depended on the cell width at the particular energy.

5.7 Flux to luminosity

The luminosity is the flux of a line multiplied by the total area of the shell. For full coverage this is $4\pi r^2$ where r is the radius of the shell. If the shell only partially covers the continuum source then this should be multiplied by the covering factor.

5.8 Flux at the Earth

If the distance to the object is specified with the **distance** command, and the simulation specifies enough information for the source luminosity to be predicted, then the flux observed at the Earth will be predicted if the **print flux at Earth** command also appears.

5.9 Relative hydrogen line intensities

Hydrogen line intensities can be predicted with great precision when Case B applies. Ferguson and Ferland (1997) describe Cloudy's hydrogen atom. It gives good results for levels below 10 in the code's default state, which uses a 15 level atom. The number of levels can be increased by using the **atom h-like levels** command, and this gives better results at the expense of more compute time. The larger atom should give results accurate to better than 5% for lines arising from below principal quantum number 10, and 10% accuracy for lines with upper levels between 10 and 15. The accuracy decreases for upper levels higher than 15 although the total recombination efficiency of the atom is computed to high precision.

The major compromise in this atom is that all levels except for 2s and 2p are assumed to be well l-mixed. So no attempt to resolve the n levels into l states is made. This approximation should be nearly exact at medium to high densities ($n_H > 10^6 \text{ cm}^{-3}$) but is approximate (but certainly better than 10%) at low densities, as Ferguson and Ferland (1997) describe.

For pure recombination lines you can easily get better predicted relative intensity than those predicted by Cloudy. The code is limited by the size of the model hydrogen atom that can be computed on the fly. The definitive calculation for hydrogen recombination is that of Hummer and Storey (1987), who used a 1000 level atom with all l-states explicitly considered (that works out to something like a million levels!). Storey and Hummer (1995) placed a program on the web that will interpolate on their tables of case B hydrogen emission, for any temperature and density they computed. The best way to obtain a very high-quality hydrogen optically thin recombination spectrum is to get the mean H^+ temperature and the electron density (perhaps those predicted by Cloudy) and then use their interpolating code to provide the hydrogen spectrum for these conditions. The code does print the Case A and Case B Storey & Hummer predictions within the main emission line list.

The Hummer and Storey (1987) calculation is for case B conditions, which assume that many processes are unimportant (see Ferguson and Ferland 1997). Neglected processes include collisional excitation from the ground or first excited states, induced processes where the incident continuum causes the atom to fluoresce, and line transfer in all non-Lyman lines. This is an excellent assumption for conventional

nebulae, such as planetary nebular or H II regions. They are questionable for gas denser than 10^6 cm^{-3} or when x-rays are present. When any of these processes are important the hydrogen spectrum is far more model dependent and Cloudy's results are more realistic than the case B results. 454 below

5.10 Helium line intensities

The code includes a model of the He^0 atom that is applied all along the helium isoelectronic sequence, and which can be made to have an arbitrarily large number of levels. The predictions become more exact as the number of levels is increased. This model does not collapse L and S levels into single n levels, so its predictions should be exact if the atom is made large enough.

5.11 Line Intensities in a dusty open geometry

Two sets of line intensities are printed when a dusty open geometry is computed. The second block of lines (with the title *Intrinsic Intensities*) is the conventional set of intrinsic emission line intensities. When grains are present these intensities would need to be corrected for line of sight reddening to be compared with observations.

The first block of emission-line intensities (with the title *Emergent Intensities*) would be that emitted from the illuminated face of a molecular cloud. The geometry is appropriate for the Orion Nebula, a blister H II region on the surface of Orion Molecular Cloud 1 (OMC1). An idealized geometry is shown in Figure 9. The code computes the fraction of the line emission that is directed towards the illuminated face. The remainder is emitted towards the neutral gas, which is assumed to have an infinite optical depth due to grains. The local albedo of the gas-grain mixture is computed, and the fraction reflected is passed back towards the illuminated face. The total intensities are roughly half what would be expected were the cloud emitting from both sides. Something like 10% of the light striking the molecular cloud will be reflected back to the observer, and so slightly more than 50% of isotropically emitted lines will emerge from the illuminated face.

So, for the illustrated blister the first block of lines gives what would be seen by an observer a large distance off to the left.

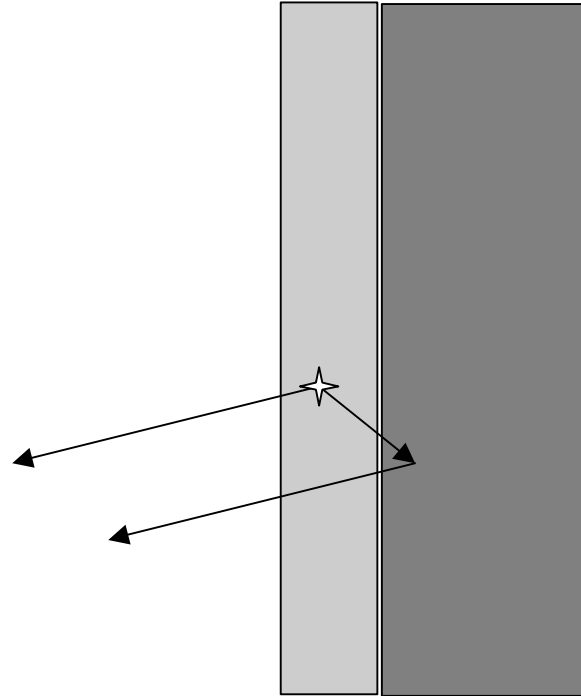


Figure 9 This shows the geometry assumed when computing the first block of lines in an open dusty geometry. The light area in the center is the H II region, which is assumed to be a layer on the surface of an infinitely optically thick molecular cloud, the dark area on the right. Light can be emitted towards, and freely escape from, the illuminated face of the cloud. A fraction of the light emitted towards the molecular cloud is reflected back towards the illuminated face.

5.12 Continuum pumping contribution to line intensities

Continuum pumping or fluorescence is included for all lines. The contribution is usually not explicitly printed, but will be if the **print line pump** command is entered. Whether or not this contribution actually adds to the observed line emission depends on the geometry. Continuum pumping increases the line emission if no related continuum absorption occurs. This will be the case if the continuum source is either not observed or not covered by absorbing gas. If absorbing gas covers an observed continuum source then the situation is like the P Cygni problem, and pumping may not increase the net intensity of the line at all (the absorption component will have the same equivalent width as the associated emission). The printed line intensity includes this contribution unless the **no induced processes** command is entered. (The **no induced processes** command has many other effects and so should not be used except as a test.)

The output produced by the **punch continuum** commands does not include the pumped part of the line contribution. This is correct if the continuum source is included in the beam, but is not if only the gas is observed.

5.13 Column densities

The column densities of all constituents are saved and printed at the end of the calculation. Column densities within many excited states are also printed. In the column density printout the excited states are identified with a '*', while the table that accompanies the description of the *cdColm* command, see Table 1 on page 419 above, identifies the various labels.

5.14 A synthetic spectrum

The code normally produces a table of emission-line intensities. Sometimes a synthetic spectrum, rather than a table, is desired. Very coarse spectra can be generated with the **punch continuum** or **punch spectrum** commands, but a detailed synthetic spectrum is not the main purpose of this output.

The best course is to save the emission-line spectrum at the end of the calculation, and then post-process this data using your own software. Then blends of lines can be synthesized at any spectral resolution desired. This can be done two ways. The main block of emission-line intensities in the final printout can be printed as a single column, which can be sorted by intensity or intensity (see the **print lines** command in Section 1 of this document). The **punch spectrum** command includes a set of all lines with non-zero intensities. Write a small program or script to read these tables and create a final synthesized spectrum.

5.15 Line profiles

The observed line profile can be predicted by integrating the emissivity of the line over the computed structure, taking the local velocity structure into account. The emissivity is obtained with the **punch lines emissivity** command, described in Part 1 of this document. This gives the net emission, with units $\text{erg cm}^{-3} \text{s}^{-1}$, emitted by a unit volume of gas and emergent from the cloud surface. The total emission is

the integrated sum of this emission. An integral over radius will give the line surface brightness while an integral over volume will give the luminosity.

The observed profile will depend on the velocity field at each point in the integration. For static models this will be the Voigt function at the local temperature and microturbulence. For a dynamical model it will include bulk motion of the gas. The net observed line profile will be

6 THE EMISSION LINES

6.1 Overview

The following sections outline the emission lines predicted by Cloudy. Before version 90 of the code all lines were listed in the sub-section immediately following this section. The code is being modified to bring all lines into a common line class, as the code moves to C++ and objects. This chapter will remain incomplete until this work is finished.

6.2 The main emission line printout

The main emission line printout was briefly described on page 441 above. This section goes into more detail.

Output organization. The printed list is sorted into four large groups of columns, with each large column sub-divided into four smaller sub-columns. The first sub-column is either the spectroscopic designation of the ion producing the line or an indication of how the line is formed. The second sub-column is the line wavelength, with a 0 to indicate a continuum. The third sub-column is the log of the power in the line, in the units given in the header (erg s^{-1} into either $4\pi\text{sr}$ or cm^{-2}). The last sub-column is the intensity of the line relative to the reference line, usually $\text{H}\beta$, unless this is reset with the **normalize** command.

These lines can be printed as a single large column, and can be sorted by wavelength or intensity. These options are controlled by the **print line** command described in Part I of this document.

Line intensities when grains are present. The computed emission-line spectrum follows. Emission lines are divided into two large groups. The first includes the effects of grain scattering and absorption, and is indicated by the header “Emergent Line Intensities”. This first group is only printed if grains are present and the geometry is open (i.e., **sphere** not set). The intensities are the *total* intensities observed from the illuminated face, including both absorption and scattering by grains. This is discussed on page 454 above.

The second, larger, group of lines, called “Intrinsic line intensities”, is always printed. This usually gives the intrinsic intensity of the lines, and does not include the reddening effects of internal grains due to the photon's passage out of the nebula (unlike the first group). This second group usually gives the total intrinsic intensity of the lines. Although reddening effects of internal (or external) dust are not taken into account, photon destruction by background opacity sources during the transfer process is. This distinction is only important for forbidden lines, which have no local destruction since they are optically thin, but can be absorbed along their way out. This predicted spectrum should be compared with the reddening-corrected observed spectrum.

Line wavelengths. These are given in various units. Numbers ending in “A” are wavelengths in Ångstroms. For instance, $\text{H}\beta$ is given by “H 1 4861A”. Wavelengths in microns are indicated by “m”, an example, the strong [O III] IR line, is “O 3 51.80m”.

The code follows the contention that wavelengths longward of 2000Å are given in air and shorter wavelengths in vacuum. Continua are usually indicated by a wavelength of zero.

6.2.1 Blocks of lines....

Within each column lines are organized by common origin with a comment beginning the section. As an example, the first commented block of lines begins with "general properties.....". The following subsections give overviews of the lines.

6.2.2 General properties....

This mainly summarizes heating and cooling agents for the model.

TOTL 4861 and *TOTL 1216*, are the total intensities of H β and L α , as predicted by the multi-level H atom. These intensities are the results of calculations that include all collisional, radiative, and optical depth effects.

Inci - The total energy in the incident continuum.

TotH and *TotC* give the total heating and cooling. These will be nearly equal in equilibrium.

BFH1 and *BFHx* are the heating due to photoionization of ground state and excited state hydrogen respectively.

He1i, *3He1*, heating due to ground state He and the triplets.

BFHe and *TotM* are the heating due to helium and metal photoionization.

Pair - heating due to pair production.

ComH, *ComC*, - Compton heating, cooling.

CT H *CT C* - charge transfer heating and cooling.

extH *extC* "extra" heating or cooling added to model.

e-e+ 511 The positron line.

Expn, expansion, or adiabatic, cooling

H FB, H radiative recombination cooling

HFBC, *HFBC*, hydrogen net free-bound cooling and heating

Iind, cooling due to induced recombination of hydrogen

3He2, cooling due to induced recombination of fully ionized helium

Cycln, cyclotron cooling

6.2.3 Continua....

These give intensities of various continua. These are either the total integrated continuum or the product νF_ν at certain energies.

Bac 3646 residual flux at head of Balmer continuum, νF_ν

cout 3646 cref 3646, outward, reflected continuum at peak of Balmer Jump

thin 3646, residual flux at head of Balmer continuum, optically thin limit

Inci 4860, *Inci 1215*, incident continua near H β and L α

Ba C 0, integrated Balmer continuum

PA C 0, integrated Paschen continuum

HeFF 0, He brems emission

HeFB 0, He recombination cooling

MeFB 0, heavy element recombination cooling

MeFF 0, metal brems emission

ToFF 0, total brems emission

FF x, part of H brems, in x-ray beyond 0.5KeV

eeff, electron - electron brems

nFnu 122m, *nInu 122m*, *InwT 122m*, *InwC 122m*, a large list of continua at selected wavelengths will be printed if the **print diffuse continuum** command is entered. The first is the total continuum at the wavelength, given as νF_ν . *nInu* is the transmitted and reflected incident continuum. *InwT* is the total reflected continuum. *InwC* is the reflected incident continuum.

6.2.4 Molecules....

H2 l 2 is the intensity of the H₂ lines near 2 μ m.

H2dC, is the cooling due to collisional dissociation of H₂.

H2dH, heating by H₂ dissociation by Lyman continuum

H2vH, heating by coll deexcit of vib-excited H₂

H2vC, cooling by coll deexcit of vib-excited H₂

H2 v, line emission by vib-excited H₂

H-FB and *H-FF* are the free-bound and free-free continua of the H⁻ ion.

H-CT 6563, H-alpha produce by H- mutual neutralization

H- H 0, H- heating

H-Hc 0, H- heating

H2+ and *HEH+* are the cooling due to formation of H₂⁺ and HeH⁺.

Codh, carbon monoxide photodissociation heating

CO C, old cooling due to collisions of vibrational rotational levels (used pre-c95)

CO 12, C12O16 cooling

CO 13, C13O16 cooling

12CO 2588m, *Inwd 2588m*, *Coll 2588m*, *Pump 2588m*, *Heat 2588m*, et al. Next follows intensities and contributors to the ¹²CO and ¹³CO lines included in the calculation.

6.2.5 Grains....

Information in this block concerns emission, absorption, heating, and cooling by any grains included in the calculation.

GrGH, gas heating by grain photoionization

GrTH, gas heating by thermionic emissions of grains

GrGC, gas cooling by collisions with grains

GraT, This is the total grain heating by all sources, lines, collisions, incident continuum. If the grain emission is optically thin limit then this is equal to the total intensity in grain emission.

GraI, grain heating by incident continuum

GraL 1216, grain heating due to destruction of Ly alpha

GraC, grain heating due to collisions with gas

GraD, grain heating due to diffuse fields, may also have grain emission

Grain emission is included in the predicted total emitted continuum. The continuum is not printed by default (it makes the printout longer) but can be included in the emission line array with the **print continuum** command, described in Part I of this document. A machine readable form of the continuum can be produced with the punch continuum command, also described in Part I of this document.

6.2.6 H-like iso-seq...

This block includes all hydrogen-like isoelectronic species.

HFFc 0, net free-free cooling, nearly cancels with cooling in lte

HFFh 0, net free-free heating, nearly cancels with cooling in lte

H FF 0, H brems (free-free) cooling

FF H 0, total free-free heating

Clin 912, total collisional cooling due to all hydrogen lines

Hlin 912, total collisional heating due to all hydrogen lines

Cool 1216, collisionally excited La cooling

Heat 1216, collisionally de-excited La heating

Crst 960, cooling due to n>2 Lyman lines

Hrst 960, heating due to n>2 Lyman lines

Crst 4861, cooling due to n>3 Balmer lines

Hrst 4861, heating due to n>3 Balmer lines

Crst 0, cooling due to higher Paschen lines

Hrst 0, heating due to higher Paschen lines

LA X 1216, la contribution from suprathreshold secondaries from ground

Ind2 1216, "Ly alpha" produced by induced two photon

Pump 4861, H-beta produced by continuum pumping in optically thin ld limit

CION 0, net col ionz-3 body heat collision ionization cooling of hydrogen

3bHt 0, heating due to 3-body recombination

Strk 1216, Stark broadening component of line

Dest 1216, part of line destroyed by background opacities

Fe 2 1216, part of La absorbed by Fe II

Q(H) 4861 is the intensity of H β predicted from the total number of ionizing photons, Q(H), assuming that each hydrogen-ionizing photon produces one hydrogen atom recombination.

Q(H) 1216 indicates the $L\alpha$ intensity produced if each hydrogen ionizing photon results in one $L\alpha$ photon in the high density limit (i.e., no two-photon emission).

CaBo 4861 These are the “old” case B predictions, as printed in versions 90 and before of the code.

Ca B 6563A The entries starting with Ca B are the Case B intensities computed from the actual model ionization and temperature structure, but assuming that H β emits with its case B emissivity.

Next the predicted intensities of all lines of the hydrogenic iso-electronic sequence are given. The lines have labels that identify the species and stage of ionization, such as H 1, He 2, Li 3, C 6, etc. The entries with a wavelength of zero are the total intensities of the 2s-1s two-photon emission.

6.2.7 He iso-sequence....

Atoms and ions of the helium-like iso-electronic sequence are treated as multi-level atoms. All species and stages of ionization are specified by labels like He 1, Li 2, C 5, etc. A wavelength of zero indicates the two-photon continuum.

6.2.8 level 1 lines....

In the current version of the code, the lines printed under this title include both the lines that have been moved to the new common *EmLine* class, but also older lines that are still scalar quantities. This part of the code is still in a state of flux, and this is reflected in the current documentation. The remaining part of this subsection outlines the methods used for most of the heavy element atoms. The method for producing a list of transferred lines, those that have been moved to the *EmLine* class, is described in the section beginning on page 462 below. The old-style scalar lines are described in the section beginning on page 464 below, although this is not totally up to date.

These lines have accurate collision strengths and wavelengths. Many are two-level atoms, but some are the result of multi-level atoms. The following is a summary of the general approach.

Li-sequence. Examples include C IV λ 1549, O VI λ 1034, and Mg II λ 2798. A three level atom, with full treatment of optical depths and collisional excitation, is used. The “TOTL” intensity is the sum of both lines in the doublet, and is followed by the individual intensities of each member.

Be-sequence. Examples include C III] λ 1909, O V] λ 1215, and Si III] 1895. A four level atom, solving for populations of the individual 3P_j states, is used. The first printed intensity is the total intensity of the multiplet (both $j=0,1$ decays), and this is followed by the intensities of individual lines. The intensity of the permitted $^1P_0 - ^1S$ transition is also calculated. Optical depth and collisional effects on both the permitted and intercombination lines are included.

B-sequence. Examples include C II and O IV. The ground term is treated as a two level atom, with optical depth and collisional effects included, when the gas is too cool to excite the UV lines. The $^4P - ^2P_0$ lines are also predicted with a full multi-level atom that resolves fine structure. The TOTL intensity printed is the total intensity of the multiplet and is followed by individual lines.

³P- ground term. Examples include such spectra as [O III] and [O I]. The infrared fine structure lines are computed with full treatment of collisional and optical depth effects. A comment is printed at the end of the model if these lines merge or become optically thick. The populations of ¹D and ¹S are computed with a three-level atom. The intensity of the ¹D - ³P transition is only that of the individual line (i.e. 5007), not the doublet.

⁴S⁰ - ground term. Examples include [O II] and [S II]. They are treated as a five level atom. Intensities of all individual lines, as well as co-added multiplets, are given.

6.2.9 Recombination . . .

These are a set of heavy-element recombination lines that are predicted assuming that they are optically thin. This consists of all recombination lines of C, N., and O, with coefficients taken from Nussbaumer and Storey (1984) and Péquignot, Petitjean, and Boisson (1991).

These are all predictions for optically thin pure recombination. These should be accurate for classical nebulae, such as planetary nebulae and H II regions. They will not be accurate for dense environments where optical depths and collisional effects come into play. There are several instances where more than one line of an ion will have the same wavelength due to the integer Ångstrom format used for wavelengths. The worst case is O V 4953, where three lines of the same multiplet have the same wavelength.

6.2.10 Level 2 lines . . .

These are resonance lines that use Opacity Project wavelengths, which are generally accurate to about 10%. These lines have g-bar collision strengths, which are not very accurate at all.

6.3 The transferred lines

The group of “transferred lines” includes all those that have been moved to the *EmLine* class, in anticipation of the code’s move to C++ and objects.

In versions of HAZY for Cloudy versions 90 and before, this section included descriptions of all predicted lines, and was automatically generated by the code. Today there is no limit to the number of lines the code is capable of predicting, since the iso-electronic sequences can now have a nearly arbitrarily large number of levels. Rather than waste paper by including the iso-electronic sequences here, instructions are given for creating your own automatic list of lines.

6.3.1 Punch line data output

To generate a line list, set up a calculation with the atoms set to whatever size is desired (see the **atom** command in Part I). Then execute this script with the **punch line data** command included (described in Part I). The punch output will include the line list. This will include the level 1, level 2, CO, and recombination lines, but not the scalar forbidden lines. These are described in a list following this subsection.

In previous versions of this document a large list of emission lines appeared here. This list is now far too large to include here. Rather, the list can be generated by executing the code with the command **punch line data "filename.txt"** included. This will create a file that includes the full set of lines that are predicted. Note that the lines that are output are only those that exist when the code is run. It is possible to make many of the model atoms and molecules as large or small as you like, and the actual lines that exist when the punch command is entered will be output.

This contains several groups of lines. All quantities were evaluated at 10^4 K. The description of the command in Part I of this document explains how to evaluate the quantities at other temperatures.

The ion is the first column of the table. This is in a uniform format, beginning with the two character element symbol and followed by an integer indicating the level of ionization. "C 2" is C^+ or C II. This is followed by the integer wavelength label used to identify the line in the printout. The third column, with the label "WL", is the correct wavelength of the line, with units of microns ("m"), Angstroms ("A"), or cm ("c"). The remaining columns give the statistical weights of the lower and upper levels, the product of the statistical weight and the oscillator strength, and then the transition probability.

The last column is the electron collision strength. Exceptions are lines whose collision strengths are only evaluated for temperatures far from 10^4 K, for instance, a Fe XXV transition. Usually these collision strengths are for only the indicated transition, although in some cases (the Be sequence) the value is for the entire multiplet.

6.3.2 Output produced for the transferred lines

Because the lines have a common format within their storage vectors, the output has a common format too. Generally only the total intensity of the transition, the result of the solution of a multi-level atom with all processes included, is printed. The approach used to compute the level populations is described in Part II of Hazy, and includes continuum pumping, destruction by background opacities, and trapping.

The total intensity of the transition is printed in a form like "C 2 1335", with the spectroscopic identification given by the first part, as found in the first column of the table, and the wavelength as indicated by the number in the second column of the table.

In a few cases (for instance, the C 4 $\lambda\lambda$ 1548, 1551 doublet), a total intensity is also derived. In these cases the label "Totl" will appear together with an average wavelength (1549 in this case). These lines are all explicitly shown in a following section.

It is possible to break out various contributors to the lines with options on the **print line** command, described in Part I of this document and in the following. These contributors are printed following the total intensity.

print line heating An emission line will heat rather than cool the gas if it is radiatively excited but collisionally de-excited. The print out will include this agent, with the label "Heat", when this command is given.

print line collisions The collisional contribution to the lines will be printed, with the label "Coll".

print line pump The contribution to the total line, produced by continuum pumping, is printed with the label "Pump". What is observed? Whether or not this is a net emission process contributing to the observed line intensity depends on the geometry, mainly whether or not continuum source is in the beam. At some velocities within the line profile this can be a net emission process, due to absorption at other velocities. If the continuum source is in the beam and gas covers it, this is not a *net* emission process, since photons are conserved.

print line inward The inwardly directed part of the total emission is printed with the label "Inwd". This can be greater than half of the line intensity if the line is optically thick since these lines tend to be radiated from the hotter illuminated face of the cloud.

print line optical depths At the end of the calculation the optical depths for all optically thick lines will be printed. This is not done by default since it can be quite long.

6.4 Forbidden Lines

These are a series of entries that contain most of the optical forbidden lines, some continua, and identify various contributors to the main lines. These are older lines that have not yet been moved to the *EmLine* class. This description is not totally up to date since this is a part of the code that is slowly being removed as lines go to the new style.

For this set of lines, the first column gives the four character label printed in the final array listing and the second column gives the wavelength of the line, using the conventions described above. The label in the first column is the one used to access the line using the *cdLine* routine described elsewhere.

The third character indicates whether the entry in the column is a heat source (indicated by h), a coolant (c), a recombination line (r), or an intensity entered for information only (i). The last column gives a brief description of the meaning of the line prediction.

Label	λ	Description
Mion	0 c	cooling due to collisional ionization of heavy elements
Li3r	19 i	these lines added to outlin in metdif - following must be false
Be4r	19 i	these lines added to outlin in metdif - following must be false
Bo5r	19 i	these lines added to outlin in metdif - following must be false
REC	1656 i	C 1 1656 recomb; n.b. coll deexcitation not in
C Ic	9850 c	C 1 9850, coll excit
C Ir	9850 i	was a big mistake
TOTL	9850 i	total intensity, all processes, C I 9850
C 1	8727 c	C 1 8727; equivalent to 4363
C 1	4621 c	1S - 3P
Phot	2326 i	photoproduction, Helfand and Trefftz
REC	1335 i	C 2 1335 recombination,
C II	3134 c	C 2 intercombination line with same upper state as 1335

C3 R 977 i dielectronic recombination contribution to C 3 977
 P386 977 r C 3 977 pumped by continuum near 386A

 TOTL 1909 i C 3 1909 collision, both lines together
 C 3 1907 i C 3 1908 j-2 to ground
 C3 R 1909 i C 3 1909 recombination from Storey
 Phot 1909 i C 3 1909 following relax following inner shell photoionization
 Rec 1175 i dielectronic recombination contribution to C 3 1175

 TOTL 1549 i total intensity of C 4 1549, all processes
 Inwd 1549 i inward part of C 4
 DEST 1549 i part of line destroyed by photoionization of Balmer continuum
 C4 r 1549 i recombination C 4 1549 from CV
 C 6r 34 i these lines added to outlin in metdif - following must be false

 N 1 5200 i N 1 5200, both 5198, 5200, collisions and recombination
 Coll 5200 c N 1 5200, both 5198, 5200, collisions and recombination
 REC 5200 i recombination contributon to [NI] 5200
 N 1 3466 c [N 1] 3466, 3 - 1 transition, whole multiplet
 N 1 10400 c [N 1] 10400 3 - 2 transition, whole multiplet

 N 2 6584 c N 2 6584 alone
 N 2 6548 c N 2 6548 alone
 REC 6584 i N 2 6584 alone, recombination contribution
 N 2 5755 i N 2 5755 total, collisions plus charge transfer
 Coll 5755 c N 2 5755 collisional contribution

 C T 5755 c N 2 5755 charge transfer contribution
 Rec 1085 i dielectronic recombination contribution to N 2 1085
 N2cn 1 i continuum pumped N 2 6584
 N2cn 5755 i continuum pumped N 2 5755
 N3cn 4640 i continuum pumped "Bowen" N 3, optically thin excited line

 N3cn 4634 i continuum pumped "Bowen" N 3, optically thin excited line
 N3cn 4642 i continuum pumped "Bowen" N 3, optically thin excited line
 extr 990 i total N 3 990, both electron excitation and continuum pumping
 rec 990 i part of N 3 990 due to recombination
 N 3p 990 r N 3 989.8, continuum pumped

 TOTL 1486 i N 4] 1486, total intensity of both lines
 N 4 1485 i the N 4] slow transition by itself
 rec 765 i N 4 765 recombination,
 TOTL 1240 i N 5 1240, total emission, collisions plus pumping
 Inwd 1240 i inward part of N 5

 N 7r 25 i these lines added to outlin in metdif - following must be false
 Fl7r 19 i these lines added to outlin in metdif - following must be false
 O 1 6300 c total Oxygen I 6300, including line optical depth
 O 1 6363 c total Oxygen I 6363, including line optical depth
 O 1 5577 c auroral OI

 TOIc 0 c total collisional cooling due to 6-level OI atom
 TOIh 0 h total collisional heating due to 6-level OI atom
 6lev 8446 i be moved to call PutLine
 6lev 1304 i OI 1304 from six level atom
 6lev 1039 i OI 1039 from six level atom

 6lev 4368 i OI 4368 from six level atom
 6lev 13 i OI 1.3 micron from six level atom
 6lev 11 i OI 1.1 micron from six level atom
 6lev 29 i OI 2.9 micron from six level atom
 6lev 46 i OI 4.6 micron from six level atom

 TOTL 3727 c O II 3727, all lines of multiplet together
 TOTL 7325 c O II 7325, all lines of multiplet together
 IONZ 3727 i line produced by photoionization of Oo; already in TOTL
 IONZ 7325 i line produced by photoionization of Oo; already in TOTL
 O II 3729 i five level atom calculations; D5/2 - S3/2

 O II 3726 i D3/2 - S3/2 transition
 O II 2471 c both 2P 1/2 and 3/2 to ground
 O II 7323 i P1/2-D5/2 and P3/2-D5/2 together
 O II 7332 i P1/2-D3/2 and P3/2-D3/2 together
 TOTL 1665 i total intensity of OIII] 1665, all processes

 Phot 1665 i contribution to OIII] 1665 due to inner shell (2s²) ionization

6 THE EMISSION LINES

Augr 1665 i contribution to OIII 1665 due to K-shell ionization
 O 3 5007 c fac = c5007/(1.+1./2.887)
 O 3 4959 c O III 4959 alone, collisions, tot OIII is this times 4
 LOST 5007 i O III 5007 lost through excit photo

 TOTL 4363 i O III 4363, sum of rec, coll, ct excitation
 Coll 4363 c O III 4363, collisions from five level atom
 Rec 4363 i O III 4363 recombination, coef from Burgess and Seaton
 O 3 2321 c collisional excitation of 2321, 5-level atom
 C EX 4363 i charge exchange, Dalgarno+Sternberg ApJ Let 257, L87.

 C EX 5592 i charge exchange rate, D+S
 rec 835 i O III 834A, dielectronic recombination only
 InSh 1401 i inner shell photoionization, relaxation
 rec 789 i O IV 789A, dielectronic recombination only
 rec 630 i O V 630A, dielectronic recombination only

 TOTL 1218 i O V 1218], total intensity of both lines
 O 5 1211 i the slow transition by itself
 O 5 5112 i BS O V 5112, recombination
 TOTL 1035 i O VI 1035, total of pumping and collisional excitation
 Inwd 1035 i inward part of OVI line

 O 8r 19 i recombination from fully stripped ion
 Ne 3 3869 c Ne III 3869, of 3968+3869 doublet
 Ne 3 3968 c Ne III 3968, of 3968+3869 doublet
 Ne 3 3343 c NeIII auroral line
 Ne 3 1815 c NeIII auroral line

 Ne 4 2424 c Ne IV 2424, collisional excitation
 Ne 4 4720 c Ne IV N=3 lines, three level atom approx
 Ne 4 1602 c Ne IV N=3 lines, three level atom approx
 Ne 5 3426 c Ne V 3426 of 3426, 3346 doublet
 Ne 5 3346 c Ne V 3346 of 3426, 3346 doublet

 Ne 5 2976 c auroral line
 Ne 5 1575 c collisionally excited
 Ne 5 1141 c both components of 5S-3P 1146.1, 1137.0 doublet
 TOTL 895 i Ne VII 895, collisionally excited, both lines
 Ne 7 890 i Ne VII 890, single line

 TOTL 774 i Ne VIII 774, collisionally excited
 Inwd 774 i inward part of NeVIII 774 line
 NeLr 12 i these lines added to outlin in metdif - following must be false
 Na 5 1365 c [NaV] 1365, sum of 1365.1+1365.8; cs only guess
 Na 5 2067 c [NaV] 2067, sum of 2066.9+2068.4; cs only guess

 Na 5 4017 c [NaV] 4017, sum of 4010.9+4016.7+4022.7; cs only guess
 Na 6 2569 c [Na VI] 2568.9
 Na 6 1357 c [Na VI] 1356.6
 Na 6 2972 c [Na VI] 2971.9
 Na 6 2872 c [Na VI] 2872.7

 NaLr 10 i these lines added to outlin in metdif - following must be false
 TOTL 2798 i Mg II 2798
 Inwd 2798 i inward part of Mg II 2798
 Mg 6 1806 c MG VI
 TOTL 615 i Mg 10 614.9 bothof doublet, li seq 2s 2p

 MgLr 7 i these lines added to outlin in metdif - following must be false
 totl 2665 i total emission in Al II] 2669.7, 2660 doublet
 Al 2 2660 i emission in Al II] 2669 alone
 TOTL 1860 i Al III
 Inwd 1860 i inward part of AlIII line

 Al 6 2428 c [Al VI] 2428.4
 Al 6 2601 c [Al VI] 2601.0
 Al 6 1170 c [Al VI] 1169.86
 Al 6 2125 c [Al VI] 2124.95
 TOTL 556 i Al 11, Li seq 2s2p

 Allr 6 i these lines added to outlin in metdif - following must be false
 diel 1260 i SI II 1260, rough guess of dielec contribution
 diel 1909 i dielectronic recombination SiIII 1909
 rec 1207 i Si III 1207, dielectronic recombination only
 TOTL 1888 i Si III] 1892+1883, total intensity of both lines

```

Si 3 1883 i Si III] 1883 by itself
PHOT 1895 i photoproduction by inner shell removal
TOTL 1397 i Si IV 1397, collisionally excited
Inwd 1397 i inward part of SiIV 1397
Si 7 2148 c SI VII, 2148, O III like, collisionally excited

Si 7 2148 c
Si 8 1446 c SI VIII 1446, OIII like, collisionally excited
Si 9 1985 c SI IX 1985, 2150, collisionally excited
Si 9 949 c collisionally excited
Si 9 1815 c collisionally excited

Si 9 691 c both components of 5S-3P doublet
Si10 606 c SI 10 606A, actually group of 4 intercombination lines.
Si11 583 c SI XI 582.9, collisionally excited
TOTL 506 i
SiLr 6 i these lines added to outlin in metdif - following must be false

P15r 19 i these lines added to outlin in metdif - following must be false
S 1R 1807 i this is to check whether photoexcit of S II is ever important
S 2 6720 c S II 6731 + 6716 together
S 2 4074 c S II 4070 +4078 together
S 2 10330 c S II N=3 lines, all four lines together

S II 6731 i individual line from five level atom
S II 6716 i individual line from five level atom
S II 4070 i individual line from five level atom
S II 4078 i individual line from five level atom
S II 10323 i individual line from five level atom

S II 10289 i individual line from five level atom
S II 10373 i individual line from five level atom
S II 10339 i individual line from five level atom
S 3 9532 c [S III] 9532 alone
S 3 9069 c [S III] 9069 alone

S 3 6312 c [S III] 6312, transauroral temperature sensitive
S 3 3722 c [S III] 3722, same upper level as 6312
TOTL 1198 i S V 1198] both lines together
S 5 1188 i Be seq, weaker of the two transitions
TOTL 933 i total S VI 933+944

S 9 1715 c S IX 1715, 1987, collisionally excited
S 10 1213 c S X 1213, 1197, collisionally excited
S 11 1826 c S XI 1615, 1826, collisionally excited
S 12 520 c group of four intercombination lines
S 13 488 c S XIII 488.4, 1909 like, collisionally excited

TOTL 427 i S 14 506 li seq 2s2p
S LR 5 i these lines added to outlin in metdif - following must be false
S LR 5 i
Cl 2 8579 c Chlorine II 8581, 9127 doublet
Cl 2 9127 c Chlorine II 8581, 9127 doublet

Cl 2 9127 c
Cl 2 6164 c Chlorine II 6164 auroral line
Cl 2 3676 c Chlorine II 3679 auroral line
TOTL 5525 c Cl III 5519, 5539 doublet, both together
TOTL 3350 c Cl III 3354, 3344 doublet, both together

TOTL 8494 c Cl III 8504, 8436, 8552, 8483 multiplet, all together
Cl 3 5538 i Cl III 5538
Cl 3 5518 i Cl III 5518
Cl 3 3354 i Cl III 3354
Cl 3 3344 i Cl III 3344

Cl 3 8504 i Cl III 8504
Cl 3 8436 i Cl III 8436
Cl 3 8552 i Cl III 8552
Cl 3 8483 i Cl III 8483
Cl 4 8047 c ClIV 8047

Cl 4 7532 c ClIV 7532
Cl 4 3119 c ClIV 3119
Cl 4 5324 c ClIV 5324

```

6 THE EMISSION LINES

Cl 4 5324 c
ClRr 4 i Cl 17 ly a recombination 3.7A from fully stripped ion

Ar 3 7135 c Argon III 7135
Ar 3 7751 c Argon III 7751
Ar 3 5192 c Argon III 5192
Ar 3 3109 c Argon III 3109
Ar 3 3005 c Argon III 3005

TOTL 4725 i Argon IV 4711 + 4740 together, 4740=90%
TOTL 2860 i [ArIV] 2868, 2854 together
TOTL 7250 i [ArIV] auroral lines, 7237, 7331, 7171, 7263
Ar 4 4740 c [Ar IV] 4740
Ar 4 4711 c [Ar IV] 4711

Ar 4 2868 c [Ar IV] 2868
Ar 4 2854 c [Ar IV] 2854
Ar 4 7263 c [Ar IV] 7263
Ar 4 7171 c [Ar IV] 7171
Ar 4 7331 c [Ar IV] 7331

Ar 4 7237 c [Ar IV] 7237
Ar 5 7005 c Argon V, 3P lines, 7005, collisionally excited
Ar 5 6435 c Argon V, 3P lines, 6435, collisionally excited
Ar 5 6435 c
Ar14 4413 c Ar XIV 4413, predicted lambda, not observed(??)

Ar15 409 c collisionally excited
ArRr 4 i these lines added to outlin in metdif - following must be false
K19r 4 i these lines added to outlin in metdif - following must be false
Ca 2 3933 c coll excit calcium k+h
Ca 2 8579 c infrared triplet

Ca 2 7306 c forbidden lines, 7291+7324 together
Phot 3933 i fraction H Ly-alpha destruction of excited levels
Phot 7306 i fraction H Ly-alpha destruction of excited levels
Ca2K 3934 i individual lines from five level atom
Ca2H 3969 i individual lines from five level atom

Ca2X 8498 i individual lines from five level atom
Ca2Y 8542 i individual lines from five level atom
Ca2Z 8662 i individual lines from five level atom
CaF1 7291 i individual lines from five level atom
CaF2 7324 i individual lines from five level atom

Rec 3933 i recombination contribution to CaII emission
Ca 5 6087 c Ca V optical and uv lines, collisional excitation, 3-level atom
Ca 5 5311 c Ca V optical and uv lines, collisional excitation, 3-level atom
Ca 5 2414 c Ca V optical and uv lines, collisional excitation, 3-level atom
Ca 5 3997 c Ca V optical and uv lines, collisional excitation, 3-level atom

Ca 7 5620 c Ca VII optical and uv lines, collisional excitation, 3-level atom
Ca 7 4941 c Ca VII optical and uv lines, collisional excitation, 3-level atom
Ca 7 2112 c Ca VII optical and uv lines, collisional excitation, 3-level atom
Ca 7 3688 c Ca VII optical and uv lines, collisional excitation, 3-level atom
CaLr 3 i these lines added to outlin in metdif - following must be false

ScLr 3 i these lines added to outlin in metdif - following must be false
Sc 2 21 c Sc II 2.08 (1-3)
Sc 2 41 c Sc II 4.1 mic (1-2)
Sc 2 42 c Sc II 4.22 (2-3)
Sc 3 3933 c Sc III 3936

Sc 6 5054 c Sc VI 5054 (1-2)
Sc 6 3592 c Sc VI 3595 (2-3)
Sc 6 2100 c Sc VI 2100 (1-3)
TiLr 3 i these lines added to outlin in metdif - following must be false
Ti 3 12 c Ti III 1.21 micron, (actually multiplet) 2-1 transition from model atom

Ti 3 9594 c Ti III 9594, 3-1 transition, (actually multiplet) from model atom
Ti 3 45 c Ti III 4.57 micron, 3-2 transition, (actually multiplet) from model atom
V Lr 3 i these lines added to outlin in metdif - following must be false
V 3 8823 c V III 8823
V 3 8507 c V III 8507

V 3 8507 c

```

V 4 7735 c V IV 7741 1-3
V 4 9489 c V IV 9496 2-1
V 4 42 c V IV 4.19 mic 3-2
CrLr 3 i these lines added to outlin in metdif - following must be false

Cr 3 5828 c [CrIII] multiplet blend at 5828A
Cr 4 7267 c [CrIV] 2 - 1 multiplet blend at 7272
Cr 4 6801 c [CrIV] 3 - 1 multiplet blend at 6806
Cr 5 7979 c [CrV] 2 - 1 multiplet blend at 7985
Cr 5 6577 c [CrV] 3 - 1 multiplet blend at 6582

Cr 5 37 c [CrV] 3 - 2 multiplet blend at 3.75 microns
MnLr 3 i these lines added to outlin in metdif - following must be false
Fe 2 6200 i Fe 2 the 3-2 transition of Netzer's atom
Fe 2 4300 i Fe 2 forbidden 2-1 transition from Netzer's atom
Fe 2 2400 i Fe 2 UV3, 3-1 transition from Netzer's atom

Fe2c 0 c total of all UV+optical Fe 2 cooling
Fe2h 0 h
Fe 2 1100 i 1 to 6 transition of Fred's Fe 2 atom
Fe 2 1500 i 2 to 6 transition of Fred's Fe 2 atom
Fe 2 11500 i 3 to 4 transition of Fred's Fe 2 atom

Fe 2 2500 i 3 to 5 transition of Fred's Fe 2 atom
Fe 2 2300 i 4 to 6 transition of Fred's Fe 2 atom
Fe 2 8900 i 5 to 6 transition of Fred's Fe 2 atom
Fe 2 0 c all cooling due to 16 level atom
Fe 2 166 i Fe 2 1.664 microns 8-13

Fe 2 160 i Fe 2 1.599 microns 7-12
Fe 2 153 i Fe 2 1.534 microns 6-11
Fe 2 164 i Fe 2 1.644 microns 6-10
Fe 2 128 i Fe 2 1.279 microns 12-4
Fe 2 130 i Fe 2 1.295 microns 11-3

Fe 2 133 i Fe 2 1.328 microns 11-4
Fe 2 126 i Fe 2 1.257 microns 10-1
Fe 2 132 i Fe 2 1.321 microns 10-2
Fe 2 259 i Fe 2 25.988 microns 2-1
Fe 2 353 i Fe 2 35.348 microns 3-2

Fe 2 178 i Fe 2 17.936 microns 7-6, label is 178 to be unique
Fe 2 245 i Fe 2 24.518 microns 8-7
Fe 2 358 i Fe 2 35.776 microns 9-8
Fe 2 181 i Fe 2 1.810 microns 10-7
Fe 2 168 i Fe 2 1.677 microns 11-7

Fe 2 180 i Fe 2 1.800 microns 11-8
Fe 2 171 i Fe 2 1.712 microns 12-8
Fe 2 179 i Fe 2 1.798 microns 12-9
Fe 2 229 i Fe 2 22.902 microns 11-10
Fe 2 347 i Fe 2 34.660 microns 12-11

Fe 2 8619 i Fe 2 8619A 14-06
Fe 2 8894 i Fe 2 8894A 15-07
Fe 2 9229 i Fe 2 9229A 15-08
Fe 2 9270 i Fe 2 9270A 16-09
Fe2b 2 i emission from lage FeII atom, integrated over band

Fe 3 0 c sum of 3p and 3g states together
Fe 3 5270 c Fe 3 5270, predictions from garstang et al 78
Fe 3 4658 c Fe 3 5270, predictions from garstang et al 78
Fe 4 0 c total cooling due to 12-level Fe 4 atom
Fe 4 3096 i Fe 4 3096.A, 4-1 and 5-1 transitions together

Fe 4 2836 i Fe 4 2835.7A, 6-1 transition, 4P5/2 - 6S5/2
Fe 4 2829 i Fe 4 2829.4A, 7-1 transition, 4P3/2 - 6S5/2
Fe 4 2567 i Fe 4 2567.6+ 2567.4. 11-1 and 12-1 transitions
Fe 4 277 i Fe 4 2.774 microns 12-7 transition
Fe 4 271 i Fe 4 2.714 microns 12-6 transition

Fe 4 272 i Fe 4 2.716 microns 11-6 transition
Fe 4 281 i Fe 4 2.806 microns 10-7 transition
Fe 4 287 i Fe 4 2.865 microns 10-8 transition
Fe 4 284 i Fe 4 2.836 microns 9-6 transition
Fe 5 3892 c Fe 5 3892+3839

```

6 THE EMISSION LINES

```
Fe 6      0 c   all of 2G lines together first
Fe 6  5177 c   Fe 6 5177, approximate correct
Fe 7  6087 c   [Fe 7] 6087
Fe 7  5722 c   [Fe 7] 5722
Fe 7   242 c   Fe 9 242 j=1 slower decay

Fe11  2649 c   Fe 11 2649 collisional excitation
Fe11  1467 c   Fe 11 1467 collisional excitation
Fe12  1242 c   Fe 12, 1242, 1349 together, collisional excitation
Fe12  2170 c   Fe 12, 2170, 2406 together, collisional excitation
Fe12  2568 c   Fe12 2904, 2567, 3567, 3073 together, collisional excitation

Fe14  5303 i   Fe 14 optically thin in line 344
Coll  5303 c   contribution from collisional excitation
Pump  5303 r   continuum fluorescence
      347 5303 c66 error! put this in
Fe19   592 c   Fe 19 from loulergue et al '85

Fe19  7082 c   Fe 19 from loulergue et al '85
Fe19  1118 c   Fe 19 from loulergue et al '85
Fe19  1328 c   Fe 19 from loulergue et al '85
Fe22   846 c   Fe 22 845.6A
Fe23   263 c   Fe 23 1909-like 262.6

FeKa   2 i   total intensity of K-alpha line
FeLr   2 i   recombination from fully stripped ion
TotH   2 i   total hot iron Ka; Auger "hot" iron, plus recom
AugC   2 i   Auger production of "cold" iron, less than or 17 times ionized
CoLr   1 i   these lines added to outlin in metdif - following must be false

NiLr   1 i   these lines added to outlin in metdif - following must be false
CuLr   1 i   these lines added to outlin in metdif - following must be false
ZnLr   1 i   these lines added to outlin in metdif - following must be false
Stoy   0 i   optional sum of certain emission lines, set with "print sum"
```

6.5 Atomic data sources

Codes like Cloudy can only exist because of the large body of work done by the atomic and molecular physics community. This work will only continue to be supported if it is cited in the literature whenever it is used. The following is a partial list of citations for the atomic data used within the code.

abundance	D/H	Pettini, M., & Bowen, D.V., 2001, ApJ, 560, 41
AGN	cont	Mathews and Ferland ApJ Dec15 '87
Al	CT	Pequignot, D., & Aldrovandi, S.M.V., 1986, A&A, 161, 169-176
al10	cs	Keenan, F.P. Berrington, K.A., Burke, P.G., Dufton, P.L Kingston, A.E. 1986, PhyS 34, 216
al11	cs	Cochrane, D.M., & McWhirter, R.W.P. 1983, PhyS, 28, 25
al2	cs	Tayal, S.S., Burke, P.G., Kingston, A.E. 1985, J.Phys. B, 18, 4321
al2	cs	Tayal, S.S., Burke, P.G., Kingston, A.E. 1984, J.Phys. B, 17, 3847
al2	cs	Keenan, F.P., Harra, L.K., Aggarwal, K.M., Feibelman, W.A. 1992 ApJ, 385, 375
al3	as	Dufton, P.L., Brown, P.J.F., Lennon, D.J., Lynas-Gray, A.E. 1986 MNRAS, 222, 713
al3	cs	Dufton, P.L., & Kingston, A.E. 1987, J.Phys. B, 20, 3899
al5	cs	Saraph, H.E. & Tully, J.A. 1994, A&AS, 107, 29
al6	cs	Butler, K., & Zeippen, C.J. 1994, A&AS, 108, 1
al8	cs	Lennon, D.J. Burke, V.M. 1994, A&AS, 103, 273
all	all	Mendoza, C. 1982, in Planetary Nebulae, IAU Symp No. 103 ed by D.R. Flower, (D. Reidel: Holland), 143
	atomic	
all	weight	Coplen, T.B. 2001, J. Phys. Chem REf Data, 30, 701
all	auger	Kaastra, J.S., & Mewe, R. 1993, 97, 443-482
all	coll_ion	Voronov G.S., 1997, At. Data Nucl. Data Tables 65, 1
all	collion	Voronov, G. S., 1997, At. Data Nucl. Data Tables, 65, 1
all	cs	Mendoza, C. 1982, in Planetary Nebulae, IAU Symp No. 103 ed by D.R. Flower, (D. Reidel: Holland), 143
all	cs	Mendoza, C. 1982, in Planetary Nebulae, IAU Symp No. 103 ed by D.R. Flower, (D. Reidel: Holland), 143
all	cs	Van Regemorter, 1962, ApJ 136, 906
all	diel	Ali, B., Blum, R. D., Bumgardner, T. E., Cranmer, S. R., Ferland, G. J Haefner, R. I., & Tiede, G. P. 1991, PASP, 103, 1182
all	photocs	Verner, Ferland, Korista, Yakovlev, 1996, ApJ, in press
all	photoerde	Boyd and Ferland ApJ Let 318, L21
all	reccoef	Verner & Ferland, 1996, ApJS, 103, 467
all	recom	Shull & Van Steenberg, 1982, ApJS, 48, 95
Ar+1	CT	Butler, S.E., & Dalgarno, A., 1980b, ApJ, 241, 838
Ar+2	CT	Butler, S.E., & Dalgarno, A., 1980b, ApJ, 241, 838
Ar+3	CT	Butler, S.E., & Dalgarno, A., 1980b, ApJ, 241, 838
Ar+4	CT	Butler, S.E., & Dalgarno, A., 1980b, ApJ, 241, 838
Ar10	as	Froese Fischer, C. 1983, J.Phys. B, 16, 157

Ar10	cs	Saraph, H.E. & Tully, J.A. 1994, A&AS, 107, 29
ar16	??	Cochrane, D.M., & McWhirter, R.W.P. 1983, PhysS, 28, 25
Ar2	as	Nussbaumer, H., & Storey, P.J. 1988, A&A, 200, L25
Ar2	cs	Pelan, J., & Berrington, K.A. 1995, A&A Suppl, 110, 209
ar3	cs	Galavis, M.E., Mendoza, C., & Zeippen, C.J. 1995, A&AS, 111, 347
ar3	cs	Galavis, M.E., Mendoza, C., & Zeippen, C.J. 1995, A&AS, 111, 347
ar4	cs	Zeippen, C.J., Le Bourlot, J., Butler, K. 1987, A&A, 188, 251
ar4	cs	Ramsbottom, C.A., Bell, K.L., & Keenan, F.P., 1997 MNRAS 284, 754
ar4	cs	Ramsbottom, C.A., & Bell, K.L. 1997, At. Data Nucl. Data Tables, 66, 65
Ar5	as	Mendoza, C., & Zeippen, C.J. 1982, MNRAS, 199, 1025
Ar5	as	Mendoza, C. 1982, in Planetary Nebulae, IAU Symp No. 103 ed by D.R. Flower, (D. Reidel: Holland), 143
Ar5	cs	Galavis, M.E., Mendoza, C., & Zeippen, C.J. 1995, A&AS, 111, 347
Ar5	cs	Galavis, M.E., Mendoza, C., & Zeippen, C.J. 1995, A&AS, 111, 347
ar6	cs	Saraph, H.E., & Storey, P.J. A&AS, 115, 151
as	fe20	Merkelis, G., Martinson, I., Kisielius, R., & Vilkas, M.J., 1999 Physica Scripta, 59, 122
C+1	CT	Butler, S.E., Heil, T.G., & Dalgarno, A. 1980, ApJ, 241, 442
C+3	CT	Butler, S.E., & Dalgarno, A., 1980b, ApJ, 241, 838
C+4	CT	Butler, S.E., & Dalgarno, 1980b
c1	as	Mendoza, C. 1982, in Planetary Nebulae, IAU Symp No. 103 ed by D.R. Flower, (D. Reidel: Holland), 143
c1	cs	Tielens, A.G.G., & Hollenbach, D. 1985, ApJ, 291, 722
c1	cs	Johnson, C.T., Burke, P.G., Kingston, A.E. 1987, JPhB, 20, 2553
c1	cs	Launay & Roueff 1977, AA 56, 289
c1	cs	Schroeder et al. 1991, J.Phys.B 24, 2487
C1	rec	Escalante, Vladimir, & Victor, G.A., 1990, ApJS 73, 513
c2	as	Froese Fischer, C. 1983, J.Phys. B, 16, 157
c2	cs	Blum, R.D., & Pradhan, A.K. 1992, ApJS 80, 425
c2	cs	Tielens, A.G.G., & Hollenbach, D. 1985, ApJ, 291, 722
c2	cs	Blum, R.D., & Pradhan, A.K., 1992, ApJS 80, 425
c2	cs	Lennon, D.J., Dufton, P.L., Hibbert, A., Kingston, A.E. 1985, ApJ, 294, 200
c2	cs	Lennon, D.J., Dufton, P.L., Hibbert, A., Kingston, A.E. 1985, ApJ, 294, 200
c2	cs	Blum, R.D., & Pradhan, A.K. 1992, ApJS 80, 425
C3	13C As	Clegg, R.E.S., Storey, P.J., Walsh, J.R., & Neale, L 1997, MNRAS, 284, 348
c3	as	Kwong, V., Fang, Z., Gibbons, T.T., Parkinson, W.H., Smith, P.L 1993, ApJ, 411, 431
c3	as	Fleming, J., Bell, K.L, Hibbert, A., Vaeck, N., Godefroid, M.R 1996, MNRAS, 279 , 1289

c3	cs	Berrington, K.A., Burke, P.G., Dufton, P.L., Kingston, A.E. 1985 At. Data Nucl. Data Tables, 33, 195
c3	cs	Berrington, K.A., Burke, P.G., Dufton, P.L., Kingston, A.E. 1985 At. Data Nucl. Data Tables, 33, 195
c3	cs	Berrington, K.A. 1985, J.Phys. B, 18, L395
c4	cs	Cochrane, D.M., & McWhirter, R.W.P. 1983, PhyS, 28, 25
c6	cs	Aggarwal, K.M., & Kingston, A.E. 1991, J Phys B, 24, 4583
ca12	cs	Saraph, H.E. & Tully, J.A. 1994, A&AS, 107, 29
ca18	cs	Cochrane, D.M., & McWhirter, R.W.P. 1983, PhyS, 28, 25
ca2	as	Zeippen, C.J. 1990, A&A, 229, 248
ca2	cs	Saraph, H.E. 1970, J.Phys. B, 3, 952
ca2	cs	Chidichimo, M.C. 1981, J.Phys. B, 14, 4149
ca20	cs	Aggarwal, K.M., & Kingston, A.E. 1992, J Phys B, 25, 751
ca4	as	Mendoza, C. 1982, in Planetary Nebulae, IAU Symp No. 103 ed by D.R. Flower, (D. Reidel: Holland), 143
ca4	cs	Pelan, J., & Berrington, K.A. 1995, A&A Suppl, 110, 209
ca5	as	Mendoza, C. 1982, in Planetary Nebulae, IAU Symp No. 103 ed by D.R. Flower, (D. Reidel: Holland), 143
ca5	as	Mendoza, C. 1982, in Planetary Nebulae, IAU Symp No. 103 ed by D.R. Flower, (D. Reidel: Holland), 143
ca5	cs	Galavis, M.E., Mendoza, C., & Zeippen, C.J. 1995, A&AS, 111, 347
ca5	cs	Galavis, M.E., Mendoza, C., & Zeippen, C.J. 1995, A&AS, 111, 347
ca7	cs	Galavis, M.E., Mendoza, C., & Zeippen, C.J. 1995, A&AS, 111, 347
ca72	cs	Galavis, M.E., Mendoza, C., & Zeippen, C.J. 1995, A&AS, 111, 347
ca8	cs	Saraph, H.E., & Storey, P.J. A&AS, 115, 151
chem	rate	Hollenbach, D.J., Takahashi, T., & Tielens, A.G.G.M., 1991, ApJ, 377, 192-209
chemistry		Hollenbach and McKee ApJ 342, 306
Cl	CT	Pequignot, D., & Aldrovandi, S.M.V., 1986, A&A, 161, 169-176
cl3	all	Mendoza, C. 1982, in Planetary Nebulae, IAU Symp No. 103 ed by D.R. Flower, (D. Reidel: Holland), 143
cl3	as	Mendoza, C., & Zeippen, C.J. 1983, MNRAS, 202, 981
cl3	css	Krueger, T.K., & Czyzak, S.J. 1970, Pro Roy Soc Lond, 318, 531
cl4	cs	Galavis, M.E., Mendoza, C., & Zeippen, C.J. 1995, A&AS, 111, 347
cl5	cs	Saraph, H.E., & Storey, P.J., 1999, A&AS, 134, 369
cl9	as	Saraph, H.E. & Tully, J.A. 1994, A&AS, 107, 29
CO	collision	McKee, C.F., Storey, J.W.V., Watson, D.M., & Green, S., 1982, ApJ, 259, 647
	He+	
CO	destruction	Kwong, V.H.S., Chen, D., & Fang, Z. 2000, ApJ, 536, 954-958
CO	photodissoc	Hollenbach, D.J., Takahashi, T., & Tielens, A.G.G.M., 1991, ApJ, 377, 192-209
CO	photodissoc	van Dishoeck, E.F., & Black, J.H., 1988, ApJ, 334, 771

co	vib cool	Hollenbach & McKee 1979, ApJS, 41, 555
co11	as	Pelan, J., & Berrington, K.A. 1995, A&A Suppl, 110, 209
continuum	CrabNebula	Davidson, K., and Fesen, 1985, ARAA
continuum	synchrotron	Rybicki, G. B., & Lightman, A.P. 1979 Radiative Processes in Astrophysics (New York: Wiley
cosmic	background	Ostriker and Ikeuchi ApJL 268, L63
cosmic	background	Ikeuchi, S.; Ostriker, J. P., 1986, ApJ 301, 522
	ionization	
cosmic ray	rate	Tielens, A.G.G.M., & Hollenbach, D., 1998, ApJ, 291, 722
	ionization	
cosmic ray	rate	Tielens, A.G.G.M., & Hollenbach, D., 1998, ApJ, 291, 722
	ionization	
cosmic ray	rate	Tielens, A.G.G.M., & Hollenbach, D., 1998, ApJ, 291, 722
Cr16	cs	Saraph, H.E. & Tully, J.A. 1994, A&AS, 107, 29
Cr8	cs	Pelan, J., & Berrington, K.A. 1995, A&A Suppl, 110, 209
cs	fe10	Tayal, S.S., 2000, ApJ, 544, 575-580
cs	fe19	Butler, K., & Zeippen, C.J., 2001, A&A, 372, 1083
cs	fe20	Butler, K., & Zeippen, C.J., 2001, A&A, 372, 1078
cs	gbar	Fisher et al. (1996
cs	gbar	Gaetz & Salpeter (1983, ApJS 52, 155) and
cs	gbar	Mewe (1972, A&A 20, 215
ee	brems	Stepney and Guilbert, MNRAS 204, 1269 (1983
esc	prob	Bonilha et al. Ap.J. (1979) 233 649
f2	as	Buttler, K., & Zeippen, C.J., 1994, A&AS 108, 1
f2	cs	Galavis, M.E., et al. 1997, A&AS 123, 159
f4	cs	Lennon, D.J. Burke, V.M. 1994, A&AS, 103, 273
Fe	CT	Tielens, A.G.G.M., & Hollenbach, D., 1985a, ApJ, 294, 722-746
Fe	CT	Prasad, S.S., & Huntress, W.T., 1980, ApJS, 43, 1-35
Fe	CT	Pequignot, D., & Aldrovandi, S.M.V., 1986, A&A, 161, 169-176
fe10	as	Mason, H. 1975, MNRAS 170, 651
fe10	as	Pelan, J., & Berrington, K.A. 1995, A&A Suppl, 110, 209
fe10	cs	Mohan, M., Hibbert, A., & Kingston, A.E. 1994, ApJ, 434, 389
fe11	as	Mason, H. 1975, MNRAS 170, 651
fe11	as	Mendoza, C., & Zeippen, C.J. 1983, MNRAS, 202, 981
fe11	as	Fritzsche, S., Dong, C.Z., & Traebert, E., 2000, MNRAS, 318, 263

fe11	cs	Tayal, S.S., 2000, ApJ, 544, 575-580
fe11	cs	Kafatos, M., & Lynch, J.P. 1980, ApJS, 42, 611
fe11	cs	Tayal, S.S., 2000, ApJ, 544, 575-580
fe12	as	Tayal, S.S., & Henry, R.J.W. 1986, ApJ, 302, 200
fe12	cs	Tayal, S.S., Henry, R.J.W., Pradhan, A.K. 1987, ApJ, 319, 951
fe13	as	Shirai, T., Sugar, J., Musgrove, A., & Wiese, W.L., 2000 J Phys Chem Ref Data Monograph 8
fe13	cs	Tayal, S.S., 2000, ApJ, 544, 575-580
Fe14	cs	Storey, P.J., Mason, H.E., Saraph, H.E., 1996, A&A, 309, 677
fe14	cs	Storey, P.J., Mason, H.E., Saraph, H.E., 1996, A&A, 309, 677
Fe17-23	recom	Arnaud & Raymond, 1992, ApJ, 398, 394
fe18	cs	Saraph, H.E. & Tully, J.A. 1994, A&AS, 107, 29
fe2	as	Nahar, S., 1995, A&A 293, 967
fe2	as	Quinet, P., LeDourneuf, M., & Zeippen C.J., 1996, A&AS, 120, 361
fe2	as	Furh, J.R., Martin, G.A., & Wiese, W.L., 1988; J Phys Chem Ref Data 17, Suppl 4
fe2	as	Giridhar, S., & Arellano Ferro, A., 1995; Ref Mexicana Astron Astrofis 31, 23
fe2	as	Kurucz, R.L., 1995, SAO CD ROM 23
fe2	cs	Zhang, H.L., & Pradhan, A., 1995, A&A, 293, 953
fe2	cs	Zhang, H.L., & Pradhan, A.K., 1995, A&A 293, 953
fe2	cs	Bautista, M., (private communication)
fe2	cs	Mewe, R., 1972, A&AS 20, 215 (the g-bar approximation)
fe2	energy	Johansson, S., Brage, T., Leckrone, D.S., Nave, G Wahlgren, G.M. 1995, ApJ 446, 361
fe2	model	Wills, B.J., Wills, D., Netzer, H. 1985, ApJ, 288, 143
fe2	pump rate	Netzer, H., Elitzur, M., & Ferland, G.J., 1985, ApJ, 299, 752-762
Fe21	cs	Aggarwall, K.M., 1991, ApJS 77, 677
fe22	as	Dankwort, W., & Trefftz, E., 1978, A&A 65, 93-98
fe22	as	Froese Fischer, C. 1983, J.Phys. B, 16, 157
fe22	cs	Zhang, H.L., Graziani, M., & Pradhan, A.K., 1994, A&A 283, 319
fe23	cs	Bhatia, A.K., & Mason, H.E. 1986, A&A, 155, 413
fe24	cs	Cochrane, D.M., & McWhirter, R.W.P. 1983, Phys, 28, 25
fe26	cs	Aggarwal, K.M., & Kingston, A.E. 1993, ApJS, 85, 187
fe3	as	Garstang, R.H., 1957, Vistas in Astronomy, 1, 268
fe3	vs	Garstang, R.H., Robb, W.D., Rountree, S.P. 1978, ApJ, 222, 384
fe6	as	Garstang, R.H., Robb, W.D., Rountree, S.P. 1978, ApJ, 222, 384
fe7	as	Keenan, F.P., & Norrington, P.H. 1987 A&A, 181, 370

fe7	as	Nussbaumer, H., & Storey, P.J. 1982, A&A, 113, 21
fe7	cs	Keenan, F.P., & Norrington, P.H. 1987 A&A, 181, 370
fe9	all	Flower, D.R. 1976, A&A, 56, 451
gaunt	factor	Hummer, D.G., 1988, ApJ, 327, 477-484
gaunt	factor	Karzas, W.J., & Latter, R., 1961, ApJS, 6, 167
grain	phys	Hollenbach, D.J., & McKee, C.F., 1979, ApJS, 41, 555
grain	phys	Hollenbach, D.J., & McKee, C.F., 1979, ApJS, 41, 555
grain	physics	Bakes & Tielens, 1994, ApJ, 427, 822
grain	physics	Bakes & Tielens, 1994, ApJ, 427, 822
grain	physics	Weingartner & Draine, 2001, ApJS, 134, 263
grain	physics	Dwek E. & Smith R.K., 1996, ApJ, 459, 686
grain	physics	Draine & Sutin, 1987, ApJ, 320, 803
grain	physics	Bakes & Tielens, 1994, ApJ, 427, 822
grain	physics	Weingartner & Draine, 2000
grain	physics	Weingartner & Draine, ApJS, 2001, 134, 263
grain	physics	Spitzer, 1948, ApJ, 107, 6
grain	physics	Draine & Sutin, 1987, ApJ, 320, 803), PvH
grain	physics	Baldwin, Ferland, Martin et al., 1991, ApJ 374, 580
grain	physics	Draine and Salpeter 79 ApJ. 231, 77 (1979
grain	physics	Weingartner & Draine, 2000, ApJ
grain	physics	Guhathakurta & Draine, 1989, ApJ, 345, 230
grain	physics	Guhathakurtha & Draine, 1989, ApJ, 345, 230
grain	physics	Guhathakurtha & Draine, 1989, ApJ, 345, 230
grain	physics	Guhathakurtha & Draine, 1989, ApJ, 345, 230
grain	physics	Draine B.T., and Li A., 2001, ApJ, 551, 807
grain	physics	Guhathakurta & Draine, 1989, ApJ, 345, 230
grain	physics	Draine B.T., and Li A., 2001, ApJ, 551, 807
grain	physics	Dwek E., Arendt R.G., Fixsen D.J. et al., 1997, ApJ, 475, 565
grain	physics	Draine B.T., and Li A., 2001, ApJ, 551, 807
grain	physics	van Hoof et al., 2001, ASP Conf. Series 247, p. 353 (astroph/0107183
grain	rec	Draine and Sutin 1987 ApJ 320, 803 eqn 5.15
H	CT	Kingdon, J. B., & Ferland, G.J. 1996, ApJS, 106, 205
H	rec cooling	LaMothe, J., & Ferland, G.J., 2001, PASP, 113, 165
H	recom cool	LaMothe, J., & Ferland, G.J., 2001, PASP, in press

H1	21cm	Liszt, H., 2001, A&A, 371, 698
H1	21cm	Liszt, H., 2001, A&A, 371, 698
H1	21cm	Liszt, H., 2001, A&A, 371, 698
H1	21cm	Liszt, H., 2001, A&A, 371, 698
H1	A	Gould, ApJ 423, 522
H1	As	Johnson L.C., 1972 ApJ 174 227
H1	collision	Vriens, L., & Smeets, A.H.M. 1980, Phys Rev A 22, 940
H1	collision	Vriens, L., & Smeets, A.H.M. 1980, Phys Rev A 22, 940
H1	cs	Smith, F.J., 1966, Planet. Space Sci 14, 929
H1	cs	Smith, F.J., 1966, Planet. Space Sci 14, 929
H1	cs	Allison, A.C., & Dalgarno A., 1969, ApJ 158, 423
H1	cs	Anderson, H., Ballance, C.P., Badnell, N.R., & Summers, H.P 2000, J Phys B, 33, 1255; erratum, 2002
h1	cs	Callaway, J. 1983, Phys Let A, 96, 83
h1	cs	Zygelman, B., & Dalgarno, A. 1987, Phys Rev A, 35, 4085
h1	cs	Callaway, J. 1994, At. Data Nucl. Data Tables, 57, 9
H1	cs	Allison, A.C. & Dalgarno, A., 1969, ApJ 158, 423
H1	cs	Smith, F.J., 1966, Planet. Space Sci 14, 929
H2	coll disc	Dove and Mandy, Ap.J.(Let) 311, L93
H2	collision	de Jong, T., Chu, S-I., & Dalgarno, A. 1975, ApJ, 199, 69
H2	energies	Abgrall
H2	grain	
H2	formation	Hollenback, D., & McKee, C.F., ApJS, 41, 555 eq 3.4 3.8
H2	grain	
H2	physics	Jura, M., ApJ, 197, 581
H2	photo cs	Yan, M., Sadeghpour, H.R., & Dalgarno, A., 1998, ApJ, 496, 1044
H2	rates	Hollenback, D.J., and McKee, C.F., 1979, ApJS, 41, 555 eq 3.4 3.8
H2	rates	Latter, W.B., & Black, J.H., 1991, ApJ. 372, 161
H2	rates	Browne & Dalgarno J PHys B 2, 885
H2	rates	Lenzuni et al. apj sup 76, 759, quoted from Janev et al
H2	rates	Lenzuni et al. apj sup 76, 759
H2	rates	Janev et al
H2	rates	Dove and Mandy, Ap.J.(Let) 311, L93
H2	rot	Lepp and Shull ApJ 270, 578
H2	stat wght	Shull, J.M., & Beckwith, S., 1982, ARAA, 20, 163-188

HD	cooling	Puy, D., Grenacher, L., & Jetzer, P., 1999, A&A, 345, 723
He	CT	Zygelman, B., Dalgarno, A., Kimura, M., & Lane, N.F 1989, Phys. Rev. A, 40, 2340
He	I-mixing	Pengelly, R.M., & Seaton, M.J., 1964, MNRAS, 127, 165
he1	cs	Sawey, P.M.J., and Berrington, K.A., 1993 At. Data Nucl. Data Tables 55, 81
he1	cs	Aggarwal, K.M. 1983, MNRAS, 202, 15P
he1	cs	Sawey, P.M.J., and Berrington, K.A., 1993 At. Data Nucl. Data Tables 55, 81
he1	cs	Berrington, K.A., & Kingston, A.E. 1987, J.Phys. B, 20, 6631
he1	cs	Sawey, P.M.J., and Berrington, K.A., 1993 At. Data Nucl. Data Tables 55, 81
he1	cs	Seaton, M.S. 1964, Plan Sp Sci 12, 55
he1	cs	Seaton, M.S. 1964, Plan Sp Sci 12, 55
he1	cs	Berrington, Keith, 2001, private communication - email follows
He1	cs	Bray, I., Burgess, A., Fursa, D.V., & Tully, J.A., 2000, A&AS, 146, 481-498
he1	photo	Brown, Robert L., 1970, Phys Rev A, 1, 586
he1	photo	Brown, Robert L., 1970, Phys Rev A, 1, 341
He1	rec	Verner, D.A., & Ferland, G.J., 1996, ApJS, 103, 467
he2	cs	Aggarwal, K.M., Callaway, J., Kingston, A.E., Unnikrishnan, K 1992, ApJS, 80, 473
HeI	As	Lach, G., & Pachucki, K, 2001, Phys. Rev. A 64, 042510
HeI	As	Benjamin, Robert A., Skillman, Evan D Smits, Derck P., 1999, ApJ, 514, 307
Helike	2pho	Derevianko, A., & Johnson, W.R. 1997, Phys. Rev. A 56, 1288
He-like	As	Johnson, W.R., Savukov, I.M., Safronova, U.I Dalgarno, A., 2002, astro.ph. 0201454
He-like	As	Johnson, W.R., Savukov, I.M., Safronova, U.I Dalgarno, A., 2002, astro.ph. 0201454
He-like	As	Johnson, W.R., Savukov, I.M., Safronova, U.I Dalgarno, A., 2002, astro.ph. 0201454
He-like	As	Johnson, W.R., Savukov, I.M., Safronova, U.I Dalgarno, A., 2002, astro.ph. 0201454
HI	2nu	Spitzer, L., & Greenstein, J., 1951, ApJ, 114, 407
HI	2nu	Spitzer, L., & Greenstein, J., 1951, ApJ, 114, 407
HI	abs	Tielens & Hollenbach 1985 ApJ 291, 722
HI	cs	Allen 1973, Astro. Quan. for low Te
HI	cs	Sampson and Zhang 1988, ApJ, 335, 516 for High Te
Hlike	cs	Sampson and Zhang 1988, ApJ, 335, 516
k11	cs	Saraph, H.E. & Tully, J.A. 1994, A&AS, 107, 29
k3	cs	Pelan, J., & Berrington, K.A. 1995, A&A Suppl, 110, 209
k4	cs	Galavis, M.E., Mendoza, C., & Zeippen, C.J. 1995, A&AS, 111, 347
k6	cs	Galavis, M.E., Mendoza, C., & Zeippen, C.J. 1995, A&AS, 111, 347
k7	cs	Saraph, H.E., & Storey, P.J. A&AS, 115, 151

Klein-Nishina	cs	Rybicki and Lightman
la	esc	Hummer and Kunasz 1980 ApJ. 236,609
La	escp	Hummer, D.G., & Kunasz, P.B., 1980, ApJ, 236, 609
Li	CT	Stancil, P.C., & Zygelman, B., 1996, ApJ, 472, 102
line	desp	Netzer, H., Elitzur, M., & Ferland, G. J. 1985, ApJ, 299, 752
line	desp	Netzer, H., Elitzur, M., & Ferland, G. J. 1985, ApJ, 299, 752
line	escp	Hummer, D.G., xxxx, JQRST, 26, 187
many	recom	Landini & Monsignori Fossi, 1991, A&AS, 91, 183
mco	rot	Emerson, D., 1996, Interpreting Astronomical Spectra, p289
Mg+3	CT	Butler, S.E., & Dalgarno, A., 1980b, ApJ, 241, 838
Mg+4	CT	Butler, S.E., & Dalgarno, A., 1980b, ApJ, 241, 838
mg1	as	Mendoza, C. 1982, in Planetary Nebulae, IAU Symp No. 103 ed by D.R. Flower, (D. Reidel: Holland), 143
mg1	cs	Leep, D., & Gallagher, A. 1976, Phys Rev A, 13, 148
mg10	cs	Cochrane, D.M., & McWhirter, R.W.P. 1983, PhysS, 28, 25
mg2	cs	Sigut, A., & Pradhan, A.K., 1994, J Phys B sub
mg4	cs	Saraph, H.E. & Tully, J.A. 1994, A&AS, 107, 29
mg5	as	Mendoza, C., & Zeippen, C.J. 1987, MNRAS, 224, 7p
mg5	cs	Butler, K., & Zeippen, C.J. 1994, A&AS, 108, 1
mg5	cs	Butler, K., & Zeippen, C.J. 1994, A&AS, 108, 1
mg6	all	Kafatos, M., & Lynch, J.P. 1980, ApJS, 42, 611
mg6	as	Becker, Butler, Zeippen, 1989, A&A 221, 375
mg6	cs	Ramsbottom & Bell 1997, A&AS 125, 543
mg7	cs	Lennon, D.J. Burke, V.M. 1994, A&AS, 103, 273
mg8	as	Chandra, S. 1982, SoPh, 75, 133
mg8	cs	Zhang, H.L., Graziani, M., Pradhan, A.K. 1994, A&A, 283, 319
mg9	as	Muhlethaler, H.P., & Nussbaumer, H. 1976, A&A 48, 109
mg9	as	Fleming, J., Bell, K.L, Hibbert, A., Vaeck, N., Godefroid, M.R 1996, MNRAS, 279, 1289
mg9	cs	Keenan, F.P. Berrington, K.A., Burke, P.G., Dufton, P.L Kingston, A.E. 1986, PhysS 34, 216
mh2	cool	Lepp, S., & Shull, J.M. 1983, ApJ, 270, 578
mh2	fits	Tielens, A.G.G.M., & Hollenbach, D., 1985a, ApJ 291, 722
mheh+	rate	Zygelman, B., and Dalgarno, A. 1990, ApJ 365, 239
Mn	CT	Pequignot, D., & Aldrovandi, S.M.V., 1986, A&A, 161, 169-176
mn17	cs	Saraph, H.E. & Tully, J.A. 1994, A&AS, 107, 29
mn9	cs	Pelan, J., & Berrington, K.A. 1995, A&A Suppl, 110, 209

N+1	CT	Butler, S.E., & Dalgarno, A., 1980b, ApJ, 241, 838
N+2	CT	Sun, Sadeghpour, Kirby, Dalgarno, and Lafyatis, cfa preprint 4208
N+2	CT	Fand&Kwong, ApJ 474, 529
N+3	CT	Butler, S.E., & Dalgarno, A., 1980b, ApJ, 241, 838
N+4	CT	Feickert, Blint, Surratt, and Watson, (preprint Sep 84). Ap.J. in press
N+4	CT	Rittby et al J Phys B 17, L677, 1984
n1	as	Butler, K., & Zeippen, C.J. 1984, A&A, 141, 274
n1	cs	Tayal, S.S., 2000, ADNDT, 76, 191
n1	photo	Henry, R., ApJ 161, 1153
n2	as	Nussbaumer, H., & Rusca, C. 1979, A&A, 72, 129
n2	as	Brage, T., Hibbert, A., Leckrone, D.S. 1997, ApJ, 478, 423
n2	cs	Lennon, D.J., & Burke, V.M., 1994, A&AS, 103, 273-277
n2	cs	Stafford, R.P., Bell, K.L, Hibbert, A. & Wijesundera, W.P. 1994
n2	cs	Lennon, D.J., & Burke, V.M., 1994, A&AS, 103, 273-277
n2	CT	Sun Sadeghpour, Kirby Dalgarno and Lafyatis, cfa preprint 4208
n2	rec	Liu, X.W., Storey, P.J., Barlow, M.J., Danziger, I.J., Cohen, M & Bryce, M., 2000, MNRAS, 312, 585
n3	as	Froese Fischer, C. 1983, J.Phys. B, 16, 157
N3	cs	Blum, R.D., & Pradhan, A.K. 1992, ApJS 80, 425
n3	cs	Blum, R.D., & Pradhan, A.K. 1992, ApJS 80, 425
n4	as	Flemming, J., Brage, T., Bell, K.L., Vaeck, N., Hibbert, A Godefroid, M., & Froese Fischer, C., 1995, ApJ, 455, 758
n4	cs	Ramsbottom, C.A., Berrington, K.A., Hibbert, A., Bell, K.L. 1994 Physica Scripta, 50, 246
n4	cs	Ramsbottom, C.A., Berrington, K.A., Hibbert, A., Bell, K.L. 1994 Physica Scripta, 50, 246
n5	cs	Cochrane, D.M., & McWhirter, R.W.P. 1983, PhysS, 28, 25
Na, Al	recom	Landini & Monsignori Fossi, 1990, A&AS, 82, 229
Na0	CT	Dutta, C.M., Nordlander, P., Kimura, M., & Dalgarno, A., 2001, Phys REv A, 63, 022709
na3	cs	Saraph, H.E. & Tully, J.A. 1994, A&AS, 107, 29
na4	cs	Butler, K., & Zeippen, C.J. 1994, A&AS, 108, 1
na5	as	Kaufman, V., & Sugar, J. 1986, J Phys Chem Ref Dat, 15, 321
na5	cs	Mendoza, C. 1982, in Planetary Nebulae, IAU Symp No. 103 ed by D.R. Flower, (D. Reidel: Holland), 143
na7	cs	Lennon, D.J. Burke, V.M. 1994, A&AS, 103, 273
Ne+2	CT	Butler, S.E., & Dalgarno, A., 1980b, ApJ, 241, 838
Ne+3	CT	Butler, S.E., & Dalgarno, A., 1980b, ApJ, 241, 838
Ne+4	CT	Butler, S.E., & Dalgarno, A., 1980b, ApJ, 241, 838
ne10	cs	Aggarwal, K.M., & Kingston, A.E. 1991, PhysS, 44, 517

ne2	cs	Saraph, H.E. & Tully, J.A. 1994, A&AS, 107, 29
ne3	as	Mendoza, C. 1982, in Planetary Nebulae, IAU Symp No. 103 ed by D.R. Flower, (D. Reidel: Holland), 143
ne3	cs	Butler, K., & Zeippen, C.J. 1994, A&AS, 108, 1
ne3	cs	Butler, K., & Zeippen, C.J. 1994, A&AS, 108, 1
ne4	as	Zeippen, C.J. 1982, MNRAS 198 111
ne4	cs	Giles, K. 1981, MNRAS, 195, 63
ne4	cs	Ramsbottom, C.A., Bell, K.L., & Keenan, F.P. 1998, MNRAS, 293, 233
ne5	as	Baluja, K.L. 1985, J.Phys. B, 18, L413
ne5	as	Baluja, K.L. 1985, J.Phys. B, 18, L413
ne5	cs	Lennon, D.J. & Burke, V.M. 1991, MNRAS 251, 628
ne5	cs	Lennon, D.J. Burke, V.M. 1994, A&AS, 103, 273
ne5	cs	Lennon, D.J. Burke, V.M. 1994, A&AS, 103, 273
ne5	cs	Lennon, D.J. Burke, V.M. 1994, A&AS, 103, 273
ne5	cs	Mendoza, C. 1982, in Planetary Nebulae, IAU Symp No. 103 ed by D.R. Flower, (D. Reidel: Holland), 143
ne6	as	Froese Fischer, C. 1983, J.Phys. B, 16, 157
ne6	cs	Zhang, H.L., Graziani, M., Pradhan, A.K. 1994, A&A, 283, 319
ne7	as	Fleming, J., Bell, K.L, Hibbert, A., Vaeck, N., Godefroid, M.R 1996, MNRAS, 279, 1289
ne7	cs	Berrington, K.A., Burke, P.G., Dufton, P.L., Kingston, A.E. 1985 At. Data Nucl. Data Tables, 33, 195
ne7	cs	Dufton, P.L., Doyle, J.G., Kingston, A.E. 1979, A&A, 78, 318
ne7	cs	Ramsbottom, C.A., Berrington, K.A., Bell, K.L. 1995 At. Data Nucl. Data Tables, 61, 105
ne8	??	Cochrane, D.M., & McWhirter, R.W.P. 1983, Phys, 28, 25
Ni	CT	Pequignot, D., & Aldrovandi, S.M.V., 1986, A&A, 161, 169-176
ni12	cs	Pelan, J., & Berrington, K.A. 1995, A&A Suppl, 110, 209
ni12	cs	Mathews, A., Ramsbottom, C.A., Bell, K.L., & Keenan, F.P., 1998 ApJ 492, 415
O	abundance	Meyers, D.M., Jura, M., & Cardelli, J.A., 1998, ApJ, 493, 222-229
O+2	CT	Butler, S.E., & Dalgarno, A., 1980b, ApJ, 241, 838
O+3	CT	Butler, S.E., & Dalgarno, A., 1980b, ApJ, 241, 838
O+4	CT	Butler, S.E., & Dalgarno, A., 1980b, ApJ, 241, 838
o1	as	Berrington, K.A. 1988, J.Phys. B, 21, 1083
o1	cs	Berrington, K.A. 1988, J.Phys.B, 21, 1083 for Te > 3000K
o1	cs	Bell, Berrington & Thomas 1998, MNRAS 293, L83 for 50K <= Te <= 3000K
o1	cs	Launay & Roueff 1977, AA 56, 289
o1	cs	Berrington, K.A. 1988, J.Phys.B, 21, 1083 for Te > 3000K
o1	cs	Bell, Berrington & Thomas 1998, MNRAS 293, L83 for 50K <= Te <= 3000K

o2	as	Wiese, W.L., Fuhr, J.R., Deters, T.M. 1996, J Phys Chem Ref Data Monograph 7
O2	cr dest	Gredel et al. ApJ 347, 289
o2	cs	McLaughlin, B.M., & Bell, K.L. 1993, ApJ, 408, 753
o2	cs	McLaughlin, B.M., & Bell, K.L. 1998, J Phys B 31, 4317
o2	cs	McLaughlin, B.M., & Bell, K.L. 1993, ApJ, 408, 753
o3	as	Storey, P.J., & Zeippen, C.J., 2000, MNRAS, 312, 813-816
o3	as	Storey, P.J., & Zeippen, C.J., 2000, 312, 813-816
o3	as	Nussbaumer, H., & Storey, P., 1981, A&A, 99, 177
o3	as	Mathis, J.S., & Liu, X.-W., 1999, ApJ, 521, 212-216
o3	cs	Lennon, D.J. Burke, V.M. 1994, A&AS, 103, 273
o3	cs	Lennon, D.J. Burke, V.M. 1994, A&AS, 103, 273
o3	cs	Burke, V.M., Lennon, D.J., & Seaton, M.J. 1989, MNRAS, 236, 353
o3	cs	Lennon, D.J. Burke, V.M. 1994, A&AS, 103, 273
o3	cs	Aggarwal, K.M., 1985 A&A 146, 149
O3	CT	Dalgarno+Sternberg ApJ Let 257, L87
O3	CT	Gargaud et al AA 208, 251, (1989)
o4	as	Brage, T., Judge, P.G., & Brekke, P. 1996, ApJ. 464, 1030
o4	cs	Blum, R.D., & Pradhan, A.K. 1992, ApJS 80, 425
o4	cs	Blum, R.D., & Pradhan, A.K., 1992, ApJS 80, 425
o4	cs	Zhang, H.L., Graziani, M., Pradhan, A.K. 1994, A&A, 283, 319
o4	cs	Zhang, H.L., Graziani, M., Pradhan, A.K. 1994, A&A, 283, 319
o4	cs	Berrington, K.A., Burke, P.G., Dufton, P.L., Kingston, A.E. 1985 At. Data Nucl. Data Tables, 33, 195
o5	cs	Berrington, K.A., Burke, P.G., Dufton, P.L., Kingston, A.E. 1985 At. Data Nucl. Data Tables, 33, 195
o5	cs	Fleming, J., Bell, K.L, Hibbert, A., Vaeck, N., Godefroid, M.R 1996, MNRAS, 279, 1289
o6	vs	Cochrane, D.M., & McWhirter, R.W.P. 1983, PhyS, 28, 25
OH	cr dest	Gredel et al. ApJ 347, 289
oi	cs	Federman, S.R., & Shipsey, E.J. 1983, ApJ, 269, 791
oi	cs	Tielens, A.G.G., & Hollenbach, D. 1985, ApJ, 291, 722
oi	cs	Monteiro & Flower 1987, MNRAS 228, 101
oi	cs	Jaquet et al. 1992, J.Phys.B 25, 285
oi	cs	Pequignot, D. 1990, A&A 231, 499
oi	cs	Chambaud et al., 1980, J.Phys.B, 13, 4205 (upto 5000K
oi	cs	Roueff, private communication (10,000K and 20,000K
P	CT	Pequignot, D., & Aldrovandi, S.M.V., 1986, A&A, 161, 169-176

p2	as	Mendoza, C., & Zeippen, C.J., 1982, MNRAS 199, 1025
p2	as	Mendoza, C., & Zeippen, C.J., 1982, MNRAS 199, 1025
p2	cs	Krueger, T.K., and Czyzak, S.J., 1970, Proc Roy Soc London A 318, 531
p3	as	Kaufman, V., & Sugar, J., 1986, J Phys Chem Ref Data 15, 321
p3	cs	Krueger, T.K., and Czyzak, S.J., 1970, Proc Roy Soc London A 318, 531
p4	cs	Saraph, H.E. & Tully, J.A. 1994, A&AS, 107, 29
phys	const	Mohr P.J. & Taylor B.N., 1998 Codata, see Reviews of Modern Physics, Vol. 72, No. 2, 2000 or http://www.physics.nist.gov/constants
PN	abundances	Aller+Czyzak, ApJ Sup 51, 211
RT	wind	Castor, J.I., Abbott, D.C., & Klein, R.I., 1975, ApJ, 195, 157
S+1	CT	Butler, S.E., & Dalgarno, A., 1980b, ApJ, 241, 838
S+2	CT	Butler, S.E., & Dalgarno, A., 1980b, ApJ, 241, 838
S+3	CT	Butler, S.E., & Dalgarno, A., 1980b, ApJ, 241, 838
S+4	CT	Butler, S.E., & Dalgarno, A., 1980b, ApJ, 241, 838
s12	all	Saha, H.P., & Trefftz, E. 1983, SoPh, 87, 233
s12	as	Froese Fischer, C. 1983, J.Phys. B, 16, 157
s12	as	Saha, H.P., & Trefftz, E. 1983, SoPh, 87, 233
s12	cs	Oliva, E., Pasquali, A., & Reconditi, M. 1996, A&A, 305, 210
s14	cs	Cochrane, D.M., & McWhirter, R.W.P. 1983, PhyS, 28, 25
s2	as	trans Mendoza, C., & Zeippen, C.J., 1982, MNRAS, 198, 127
s2	cs	Ramsbottom, C.A., Bell, K.L., Stafford, R.P. 1996, At. Data Nucl. Data Tables, 63, 57
s2	cs	Ramsbottom, C.A., Bell, K.L., Stafford, R.P. 1996, At. Data Nucl. Data Tables, 63, 57
s2	cs	Ramsbottom, C.A., Bell, K.L., Stafford, R.P. 1996 At. Data Nucl. Data Tables, 63, 57
s2	cs	Tayal, S., 1997, ApJS, 111, 459
s2	cs	Ramsbottom, C.A., Bell, K.L., Stafford, R.P. 1996, ADNDT, 63, 57
s3	as	Mendoza, C. 1982, in Planetary Nebulae, IAU Symp No. 103 ed by D.R. Flower, (D. Reidel: Holland), 143
s3	as	Mendoza, C., & Zeippen, C.J. 1982, MNRAS, 199, 1025
s3	cs	Galavis, M.E., Mendoza, C., & Zeippen, C.J. 1995, A&AS, 111, 347
s3	cs	Tayal, S.S., and Gupta, G.P. 1999 ApJ 526, 544
s3	cs	Galavis, M.E., Mendoza, C., & Zeippen, C.J. 1995, A&AS, 111, 347
s3	cs	Tayal, S.S., and Gupta, G.P. 1999 ApJ 526, 544
s3	cs	Ho, Y.K., & Henry, R.J.W. 1984, ApJ, 282, 816
s3	cs	Tayal, S.S. 1997, ApJ 481, 550
s3	cs	Hayes, M.A., 1986, J Phys B 19, 1853
s3	cs	Tayal, S.S. 1997, ApJ 481, 550

s4	as	Johnson, C.T., Kingston, A.E., Dufton, P.L. 1986, 220, 155
s4	cs	Tayal, S.S., 2000, ApJ 530, 1091
s4	cs	Tayal, S.S., 2000, ApJ, 530, 1091
s4	cs	Tayal, S.S., 2000, ApJ 530, 1091
s5	as	Mendoza, C. 1982, in Planetary Nebulae, IAU Symp No. 103 ed by D.R. Flower, (D. Reidel: Holland), 143
s5	as	Dufton, P.L., Hibbert, A., Keenan, F.P, Kingston, A.E Doschek, G.A. 1986, ApJ, 300, 448
s5	cs	Dufton, P.L., & Kingston, A.E. 1984, J.Phys. B, 17, 3321
s5	cs	Dufton, P.L., & Kingston, A.E. 1984, J.Phys. B, 17, 3321
s6	as	Mendoza, C. 1982, in Planetary Nebulae, IAU Symp No. 103 ed by D.R. Flower, (D. Reidel: Holland), 143
s6	cs	Dufton, P.L., & Kingston, A.E. 1987, J.Phys. B, 20, 3899
s8	cs	Saraph, H.E. & Tully, J.A. 1994, A&AS, 107, 29
s9	all	Kafatos, M., & Lynch, J.P. 1980, ApJS, 42, 611
s9	cs	Butler, K., & Zeippen, C.J. 1994, A&AS, 108, 1
sc13	cs	Saraph, H.E. & Tully, J.A. 1994, A&AS, 107, 29
sc5	cs	Pelan, J., & Berrington, K.A. 1995, A&A Suppl, 110, 209
sec	ioniz	Xu and McCray 1991, ApJ. 375, 190
Si+1	CT	Butler, S.E., & Dalgarno, A., 1980b, ApJ, 241, 838
Si+2	CT	Gargaud, M., McCarroll, R., & Valiron, P. 1982, A&ASup, 45, 603
Si+3	CT	Butler, S.E., & Dalgarno, A., 1980b, ApJ, 241, 838
Si+3	CT	Fang, Z., & Kwong, H.S. 1997 ApJ 483, 527
Si+4	CT	Opradolce et al., 1985, A&A, 148, 229
Si0	CT	Prasad, S.S., & Huntress, W.T., 1980, ApJS, 43, 1-35
si10	as	Chandra, S. 1982, SoPh, 75, 133
si10	cs	Saha, H.P., & Treffitz, E. 1982, A&A, 116, 224
si10	cs	Zhang, H.L., Graziani, M., Pradhan, A.K. 1994, A&A, 283, 319
si10	cs	Bell, K.L., & Ramsbottom, C.A., 2000, ADNDT, 76, 176-190
si11	as	Muhlethaler, H.P., & Nussbaumer, H. 1976, A&A 48, 109
si11	cs	Berrington, K.A., Burke, P.G., Dufton, P.L., Kingston, A.E 1985, At. Data Nucl. Data Tables, 33, 195
si11	cs	Lennon, D.J. Burke, V.M. 1994, A&AS, 103, 273
si11	cs	Kafatos, M., & Lynch, J.P. 1980, ApJS, 42, 611
si12	cs	Cochrane, D.M., & McWhirter, R.W.P. 1983, Phys, 28, 25
si2	as	Dufton, P.L., Keenan, F.P., Hibbert, A
si2	as	morton et al 88 (apj sup
si2	cs	Dufton, P.L., & Kingston, A.E. 1994, At. Data Nucl. Data Tables 57, 273

si2	cs	Tielens, A.G.G., & Hollenbach, D. 1985, ApJ, 291, 722
si2	cs	Dufton, P.L., & Kingston, A.E., 1991, MNRAS, 248, 827
si2	cs	Dumont, A.M., & Mathez, G. 1981, A&A, 102, 1
si2	cs	Dufton, P.L., & Kingston, A.E. 1991, MNRAS, 248, 827
si2	cs	Mendoza, C. 1982, in Planetary Nebulae, IAU Symp No. 103 ed by D.R. Flower, (D. Reidel: Holland), 143
si2	cs	Dufton, P.L., & Kingston, A.E. 1991, MNRAS, 248, 827
si3	as	Callegari, F., & Trigueiros, A.G., 1998, ApJS, 119, 181
si3	cs	Callaway, J. 1994, At. Data Nucl. Data Tables, 57, 9
si3	cs	Dufton, P.L., & Kingston, A.E. 1989, MNRAS, 241, 209
si3	cs	Dufton, P.L., & Kingston, A.E. 1994, ADNDT, 57, 273
si4	as	Mendoza, C. 1982, in Planetary Nebulae, IAU Symp No. 103 ed by D.R. Flower, (D. Reidel: Holland), 143
si4	cs	Dufton, P.L., & Kingston, A.E. 1987, J.Phys. B, 20, 3899
si6	cs	Saraph, H.E. & Tully, J.A. 1994, A&AS, 107, 29
si7	cs	Kafatos, M., & Lynch, J.P. 1980, ApJS, 42, 611
si7	cs	Butler, K., & Zeippen, C.J. 1994, A&AS, 108, 1
si8	cs	Kafatos, M., & Lynch, J.P. 1980, ApJS, 42, 611
si9	as	Baluja, K.L. 1985, J.Phys. B, 18, L413
si9	as	Baluja, K.L. 1985, J.Phys. B, 18, L413
si9	cs	Aggarwal, K.M. 1983, J.Phys. B, 16, L59
si9	cs	Lennon, D.J. Burke, V.M. 1994, A&AS, 103, 273
si9	cs	Aggarwal, K.M. 1984, ApJS, 54, 1
Ti	CT	Pequignot, D., & Aldrovandi, S.M.V., 1986, A&A, 161, 169-176
ti14	cs	Saraph, H.E. & Tully, J.A. 1994, A&AS, 107, 29
ti6	cs	Pelan, J., & Berrington, K.A. 1995, A&A Suppl, 110, 209
v15	cs	Saraph, H.E. & Tully, J.A. 1994, A&AS, 107, 29
v7	cs	Pelan, J., & Berrington, K.A. 1995, A&A Suppl, 110, 209
XUV	extinction	Cruddace et al. 1974 ApJ 187, 497

7 CODING CONVENTIONS

Cloudy is large, complex, and as is any large code, it is the result of many hands. It is essential that clarity and integrity of purpose be sustained (Ferland 2001b). This can only be achieved by having the *self-restraint* to follow a coherent set of standards. These standards are outlined in this section. All are arbitrary standards, but these are the standards Cloudy follows. It is far better to follow a single set of standards than to have total anarchy.

7.1 Variable names and strong typing

Cloudy is evolving towards a simple formulation of the Hungarian naming convention (Simonyi 1977). In this convention the first few characters of a variable name indicate the type and function of that variable.

The naming convention used in the code today looks back to an under appreciated advantage in the FORTRAN II and FORTRAN 66 languages - the fully implicit designation of variable types by the first letter of its name. The naming convention forced by early versions of FORTRAN (integers begin with i-n, real numbers with other characters) is still useful since the type can be determined at a glance. The current is a mix of the two.

7.1.1 Integers

Integers begin with the characters i, j, k, l, m, or n.

Counters begin with n. Examples include *nLevel* or *nLoop*.

Loop indices are generally i, j, or k. Sometimes they are counters.

Indices within arrays begin with ip. Examples include *ipContinuum* or *ipCIV1549*.

7.1.2 Double or float variables

These begin with letters between a through h, and o through z. Examples include *PumpRate*, *DestRate*, or *CollisIoniz*.

At this time the naming convention does not distinguish between floats and doubles. Eventually the code will be totally double precision.

In some cases floating numbers naturally will have names beginning with one of the letters reserved for integers. In this case a lower case x is used as the first character. Examples include *xJumpDown*, *xMoleDen*.

7.1.3 Character strings

Character variables begin with "ch". Examples are *chName* or *chReadInput*.

7.1.4 Logical variables

These begin with "lg". Examples are *lgOK*, *lgDone*. These are of intrinsic type int.

7.2 Structure names

Variables with a common purpose are grouped together into structures. The electron density variable *eden* is an element of the structure *dense* with the name *dense.eden*. The declaration for a structure occurs within an included file with the same name ending with “.h” – the *dense* structure is in *phycon.h*.

7.3 Braces

The format of braces consumes a staggering amount of on-line debate and is important since the format must be followed consistently across the code for it to be instantly legible. There are three major styles of braces:

Style 1:

```
if( a>0 )
{
    b = 0.;
}
else
{
    b = 1.;
}
```

Style 2:

```
if( a>0 )
{
    b = 0.;
}
else
{
    b = 1.;
}
```

Style 3:

```
if( a>0 ) {
    b = 0.; }
else {
    b = 1.; }
```

The code uses the first style. Any one of the three could have been chosen, but the first one was chosen. We must have the *self-restraint* to follow this arbitrary choice, for the clarity of the overall code.

7.4 Changes to the code

A comment line just before the affected line indicates changes to logical flow within the code that could impact results or convergence. These have the following style:

```
/* >>chng 95 dec 20 eden had eold, was undefined here, affect electron density */
```

The flag **>>chng yy mmm dd** indicates a change. Here **yy** are the last two digits of the year, **mmm** is a 3-character abbreviation of the month, all in lower case, and **dd** is a two-digit date. It is important that this style be followed consistently so that changes within the code can be extracted with a pattern

matcher such as **grep**, and then sorted by date (as in, why did the Compton temperature change on March 21?).

7.5 Atomic data references

Codes such as Cloudy only exist because of the foundation of basic atomic and molecular data. It is important to the survival of this field that the original sources of the basic data be cited, since this in turn affects their ability to generate support. The code follows the convention of preceding all uses of atomic data with a citation to the original paper in the following form:

```
/* >>refer Si+2 AS Berrington, K., AtData Nuc Data Tab 33, 195.
```

This information is extracted from the source with a Perl script that creates a file giving all atomic data references.

The flag “>>refer” indicates a reference. The fields are delimited by the tab character, and indicate the species (c4, he2, etc) and process (cs for collision strength, As for transition probabilities, etc). If the reference cannot fit on a single line it may continue on the following line, starting with the flag “>>refercon” which is followed by a tab. This style must be followed consistently so that a pattern search will generate a list of references used.

7.6 Sanity checks and asserts

Sanity checks and asserts are redundant tests for variable values that are totally impossible (Maguire 1993). Examples include negative collision strengths or electron temperatures. A major improvement to Cloudy version 86 and later is the inclusion of large numbers of sanity checks, while in version 94 and later the *C assert* macro is used. These checks do not have a major impact on performance but they do slow the code down a bit. For production runs with a gold version of the code it is reasonable to not include these checks.

The asserts can be neglected, and the code run slightly faster without this checking, by defining the macro *NDEBUG* on the compiler command line, as in

```
cc -DNDEBUG file.c
```

For most compilers this happens automatically when higher levels of optimization are used.

7.7 Code in need of attention

broken() It is sometimes necessary to physically break the code, either by writing specific code to override the correct behavior or disable a physical process. Such code should be accompanied by a call to routine *broken*. This routine sets a flag showing that broken code is present. This flag generates a warning after the calculation is complete, to serve as a reminder of the presence of the broken code. This routine is not normally used.

TestCode() Test code is identified by a call to routine *TestCode*. This routine does nothing but set a flag that test code is present. This flag generates a comment after the calculation is complete, to serve as a reminder of the presence of the test code. This routine is not normally used.

fixit() sets a flag saying that the code needs to be fixed. A comment is generated at the end of the calculation.

*/*TODO ...*/* This is a comment within the source that indicates something that needs attention, but not serious enough to cause a comment to be generated.

TotalInsanity() This routine announces that total insanity has been encountered, and exits with appropriate warnings. This is called when a test indicates that an impossible condition has occurred. It causes the calculation to stop and indicate that a catastrophic condition has occurred.

cdEXIT(condition) This routine must be called to exit the code. It does several chores, including calling the MPI exit handler and closing open file handles. The argument is the exit condition – if the exit was intended and the calculation is valid then the argument should be the standard macro *EXIT_SUCCESS*. If the exit is the result of a failure then the argument should be *EXIT_FAILURE*.

NB – it is essential that the code exit with this routine when running in a multiprocessor environment – the version of MPI on our HP cluster will hang and require a reboot, resulting in a nasty phone call from the system manager, if the code exists with a without this call.

7.8 Version numbers

Cloudy uses version numbers to keep track of changes to the code. The version number is stored in *version*, in the structure *date*. The variable *chDate* contains the date of the last major revision, and the variable *chVersion* is a string giving the version of the code.

8 PROBLEMS

8.1 Overview

This section describes some of the errors that can cause Cloudy to stop. Floating point errors should never occur. Several other internal errors, which the code is designed to catch and then complain about, can occur. Finally, it is possible that the code will stop because of thermal stability problems. If the calculation aborts it will conclude with a request to send the information to me – please do – I can't fix it if I don't know it's broken.

The most important single thing to understand about any calculation is why it stopped, and whether this affects the predictions. This is discussed further in the section *Stopping Criteria* in Part I of this document.

8.2 Thermal stability and temperature convergence

This section describes thermal stability problems, how to identify them, and what to do about them.

8.2.1 Types of thermal maps

Three types of thermal maps, showing the heating or cooling of gas as a function of temperature, can be produced by Cloudy. Each is the answer to a different question.

Figure 10 shows the heating and cooling rates as a function of temperature for a photoionized gas in which the electron temperature was varied. This figure was produced by running the test case `map.in`, one of the standard test cases included

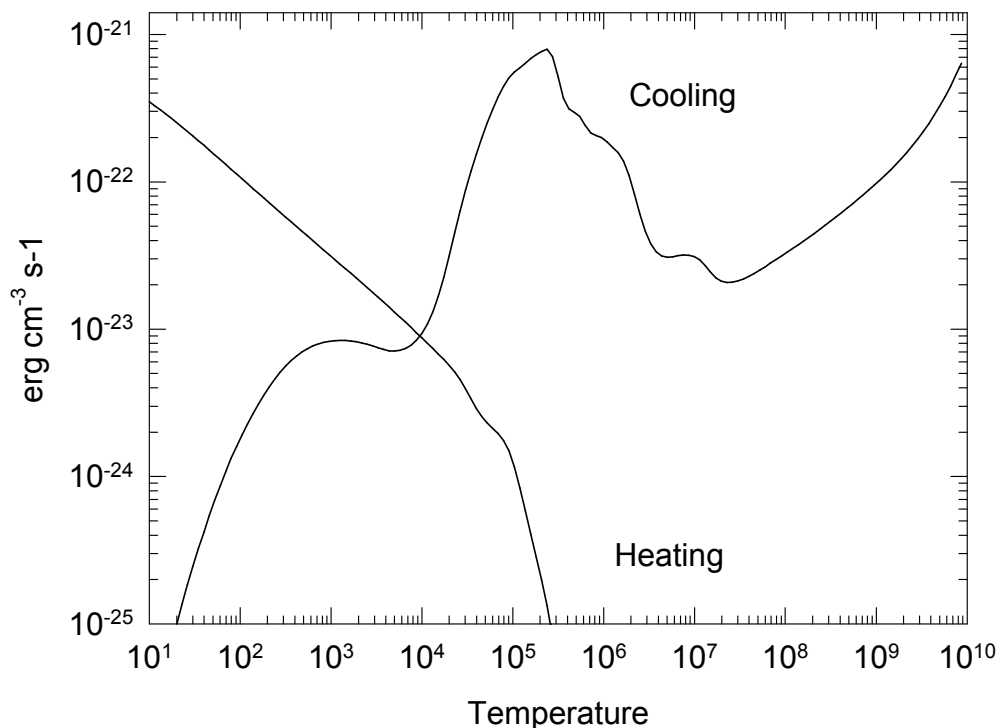


Figure 10 A typical cooling function for low density photoionized gas. The cooling and heating rates ($\text{erg cm}^{-3} \text{s}^{-1}$) are shown. Cooling – computed with `map.in` test case

in the code distribution. Both the gas density and the flux of ionizing photons were held constant, so only one temperature, the point where the two curves cross, is meaningful. The `map.in` file uses the `punch map` command to determine heating and cooling rates at a variety of temperatures. This is exactly what the code does to determine the equilibrium temperature, so this plot can be useful to find out why the code ran into problems. This is why the command was introduced. Note that the only valid solution, and the only one with physical meaning, is the one where heating and cooling match – the others are simple bookkeeping exercises.

Gas in collisional equilibrium has a well-defined cooling rate that is only a function of temperature. The sample program `coolcurve.c` (included in the source distribution) does such a calculation, and Figure 11 shows it. Here the electron temperature is set by some physics external to the problem. Each temperature, and the entire ionization solution, is valid for each temperature, under this assumption. The unspecified heat source would have to provide a local heating rate that is equal to the calculated cooling rate for the solution to be time steady.

The third map is the type of thermal stability map shown by Krolik, McKee, and Tarter (1981) and plotted in Figure 12. The program that generated these results is given in the file `kmt.c`. Here the equilibrium temperature is determined self-consistently for gas over a wide range of densities, but for a single flux of ionizing photons (or equivalently, distance from the central object).

8.2.2 No Temperature Convergence

A temperature failure occurs when the heating-cooling balance is not within a

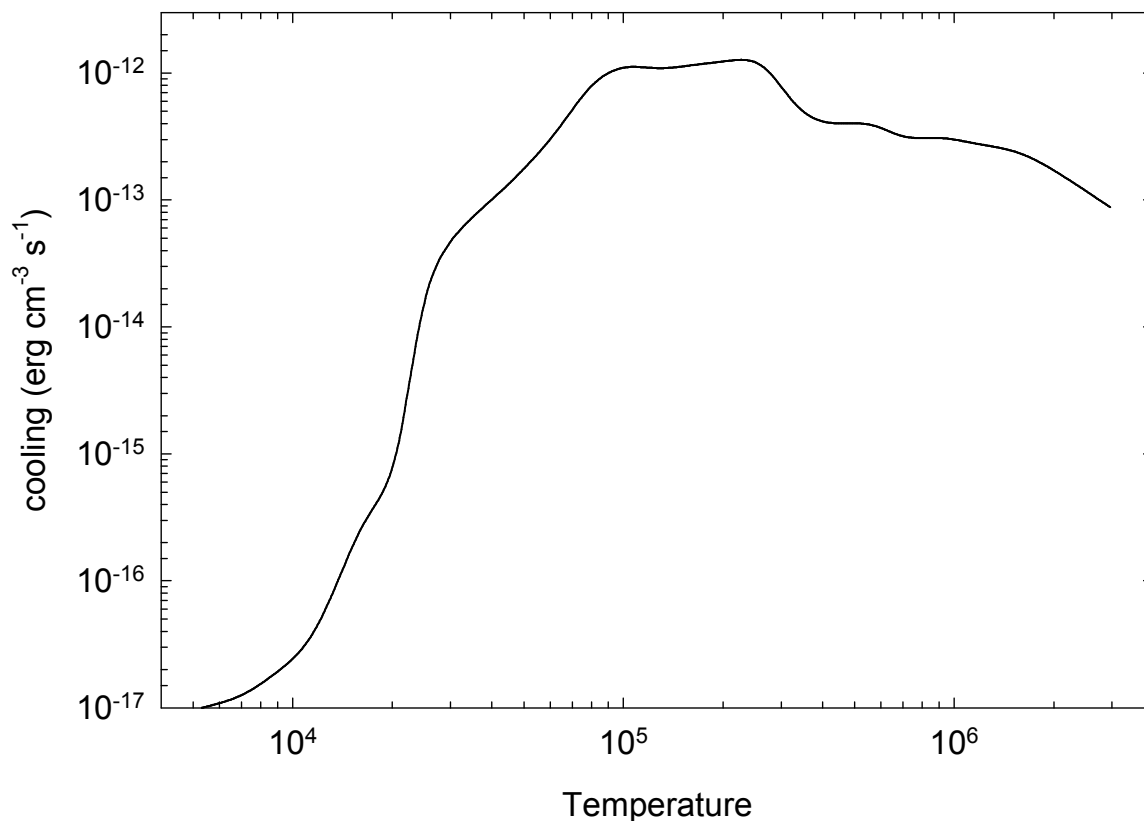


Figure 11 A typical cooling function for low density collisionally ionized gas. coolcurve

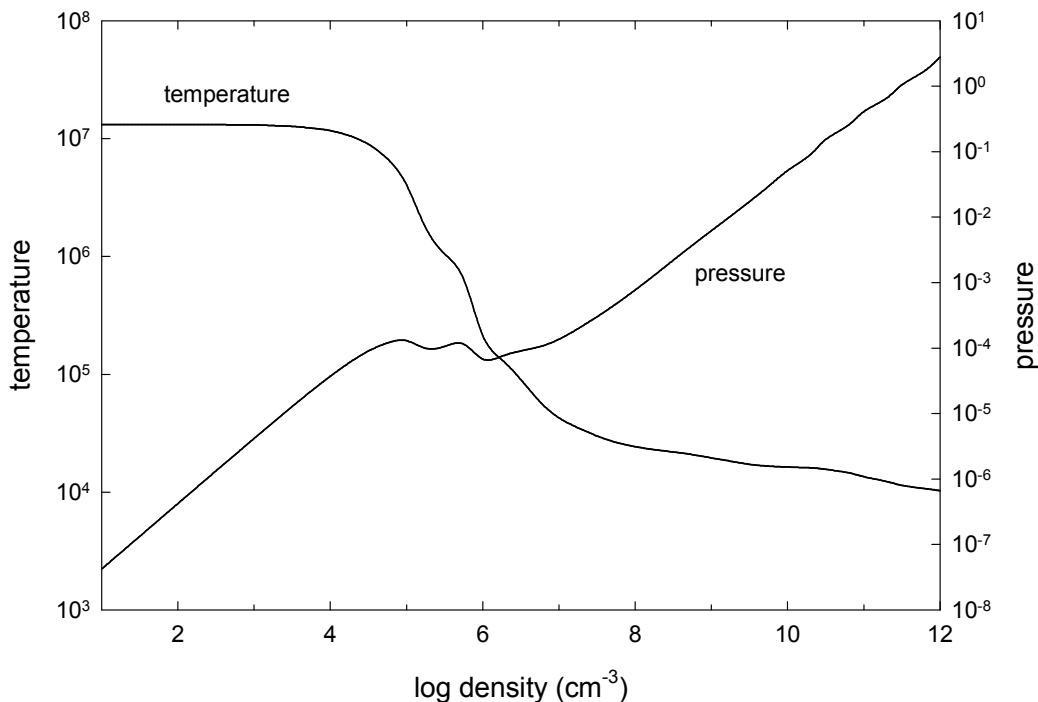


Figure 12 Equilibrium temperate as a function of density. Hazy_kmt

certain tolerance, set by the **set temperature error** command, after 20 tries. Normally Cloudy will punt after an excessive number of temperature failures occur. The limit to the number of failures is reset with the **failures** command. The default value is 20. (If the **failures map** command is entered then the code will first produce a map of heating-cooling space to give an indication of where the equilibrium temperature should have been when excessive failures occur.)

Temperature failures most often occur for temperatures in the range 1 to 4×10^3 K, and 10^5 to 10^6 K. These are ranges where the cooling function permits more than one thermal solution (see, for example, Williams 1967). Figure 10 shows a typical cooling function for gas in photoionization equilibrium, and there are regions where the gas is unstable.

A peak is reached at a temperature near 10^3 K. This can occur when the fine-structure lines are major coolants. At lower temperatures their cooling rate goes up exponentially (as expected), until roughly 10^3 K, when their Boltzmann factors are near unity. Above this temperature their cooling rate is nearly proportional to the Coulomb focusing factor $T^{-1/2}$, and the cooling *decreases* until the temperature is high enough for optical forbidden lines to become important (at roughly 4000 K). A similar phenomenon occurs near the $\sim 10^5$ to 10^6 K peak in the cooling function.

When failures occur because more than one temperature solution is possible, the reported failures are a physical (not numerical) problem. Cloudy will try to deal with this problem by forcing the temperature to values below the peak in the cooling function. Increasing the number of allowed failures (with the **failures** command) to prevent the code from stopping prematurely is permissible as long as the global

energy balance is preserved. A warning will be issued at the end of the calculation if the heating-cooling balance is not preserved.

8.2.3 Thermal Stability

The thermal solution may be unstable when the temperature derivative of the net cooling function (cooling minus heating) is negative (Field 1965). Possibly unstable solutions are indicated by a “u” just before the equilibrium temperature in the zone printout. The temperature derivative is for isochoric (constant density), not isobaric (constant pressure), conditions. Comments are printed at the end of the calculation if possibly unstable thermal solutions are present in the calculation.

8.2.4 Thermal fronts

Just as an ionization front is a region where the level of ionization changes dramatically over a small scale, a thermal front occurs where the temperature changes dramatically over a small scale. This can be caused by a real physical change of state of the gas such as those that occur near the peaks in the cooling curve. An example of a thermal front, taken from Ferland, Fabian, & Johnstone (2001), is shown in Figure 13. This type of jump is physical. The code will generate a caution or comment if the electron temperature changes discontinuously from one zone to the next.

A thermal front can lead to pressure convergence failures when the solution jumps between the high and low temperature branches. Figure 14 shows an example case, taken from *orion_hii_pdr_pp.in* in the test suite. This shows the pressure history (output with the **punch pressure history**

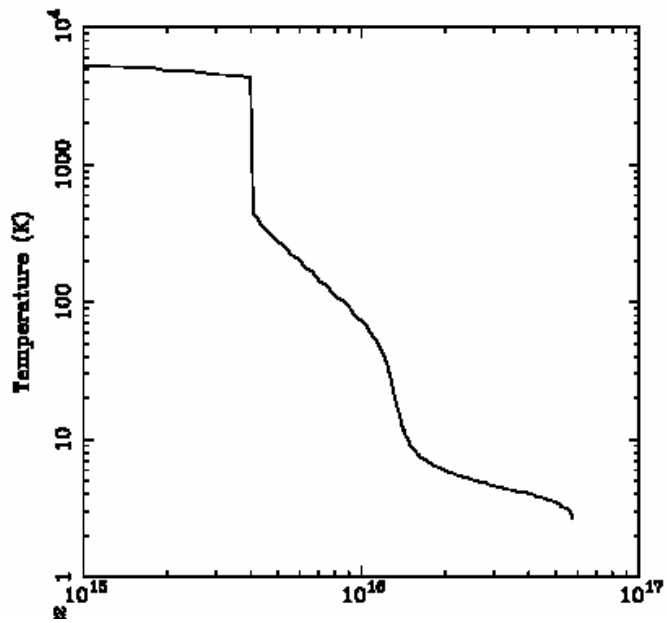


Figure 13 An example of a thermal front in a cooling flow cloud (Ferland, Fabian, & Johnstone 2001). The x-axis is the depth into the cloud. The thermal front at $\sim 4 \times 10^{15}$ cm is unresolved.

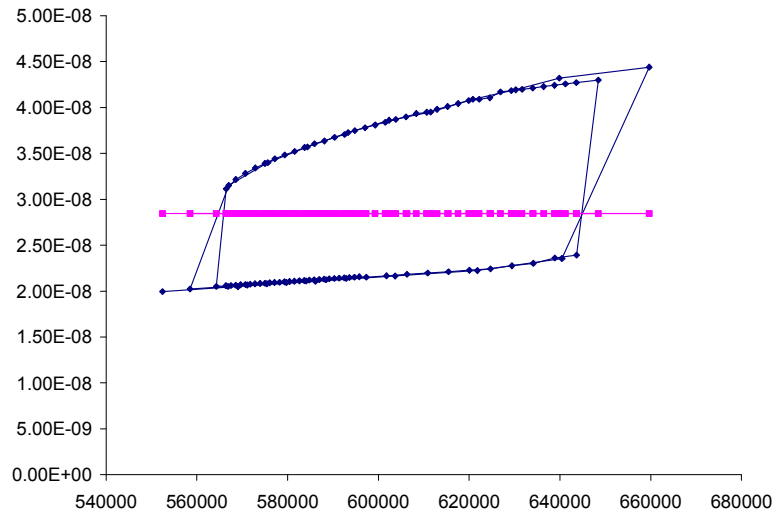


Figure 14 A thermal front in a constant pressure simulation. The x-axis gives the hydrogen density (cm^{-3}). The blue points are the resulting total gas pressure and (y-axis) the red points are the correct pressure. The solution jumps above and below the equilibrium value as the temperature jumps above and below the thermal front, leading to a pressure failure.

command). The solver adjusts the density trying to make the resulting pressure

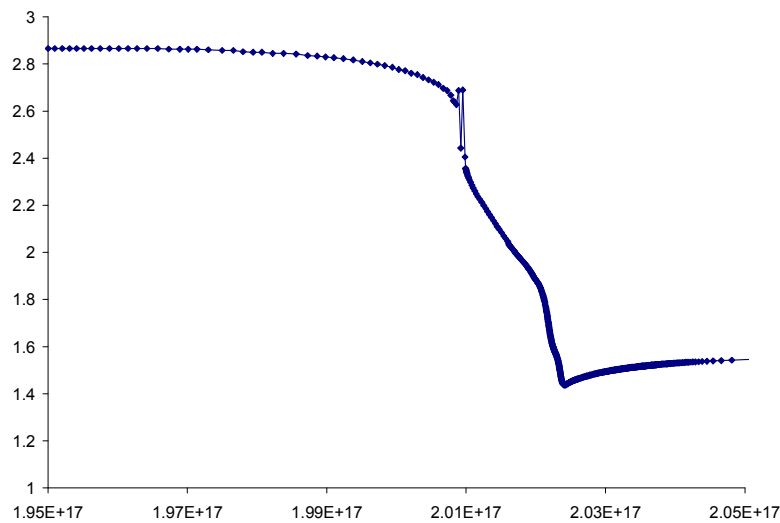


Figure 15 A constant-pressure thermal front in a temperature – radius plot. The x-axis gives the radius (cm). The y-axis gives the log of the temperature (K). The solution jumps above and below the equilibrium value, leading to a series of pressure failures, near a depth of 2×10^{17} cm, as it soldiers on through the thermal front.

agree with the desired pressure. The pressure changes continuously with density up to the point where the gas jumps over the front. No solution is possible, and the code announces a pressure failure.

A series of pressure failures occur in this simulation when the gas falls to a temperature of ~ 300 K, as shown in Figure 15. The code tries to simply press on with the goal of reaching the cold side of the front.

8.2.5 Map Output

If an excessive number of temperature failures occur (the default limit is 20) then the program stops. It will produce a map of the heating and cooling as a function of temperature for the last computed zone if the **map** option on the **failures** command is given. The limit to the number of failures allowed before the code punts is reset with the **failures** command. The map is described here. The start of the output from the test case **map** is shown below.

```
90.02x map of heating vs cooling
te, heating, cooling.
Cloudy punts, Te= 9.254E+03 HTOT= 9.123E-24 CTOT= 9.118E-24 nzone= 1
COOLNG array is
  O 4 25 0.340 O 3 5007 0.182 O 3 88 0.075 H FB 0 0.057 S 4 10 0.048 O 3 51 0.042 S 3 9532 0.035
  H ff 0 0.022 S 3 33 0.020 Ne 3 15 0.019 Hefb 0 0.015 N 3 57 0.015 Ne 3 3869 0.013 S 3 18 0.013
  Ne 5 24 0.010 Ne 5 14 0.009 C 3 1910 0.008 Heff 0 0.007 Si 2 34 0.006 Fe 5 3892 0.006 O 2 3727 0.005
Line heating array follows
  Te Heat-----> Cool-----> dH/dT dC/DT Ne NH HII Helium
1.0000E+01 3.4774E-22 1 1 0.636 4.6095E-26 H FB 0A 0.723 -8.19E-24 1.56E-27 9.1178E-01 1.0000E+00 -0.07 -0.40 -0.24 -1.75
1.0209E+01 3.4490E-22 1 1 0.635 4.6814E-26 H FB 0A 0.720 -7.98E-24 1.65E-27 9.1353E-01 1.0000E+00 -0.07 -0.40 -0.23 -1.73
1.0423E+01 3.4233E-22 1 1 0.635 4.7510E-26 H FB 0A 0.717 -7.74E-24 1.74E-27 9.1491E-01 1.0000E+00 -0.07 -0.41 -0.23 -1.73
```

The output begins with a listing of the strongest coolants for the last zone. Then the program steps through increasing temperatures and prints the heating, cooling, and ionization of the gas. From this information it should be possible to determine the temperature where the equilibrium thermal solution should have been. Each solution is completely self-consistent, except that heating and cooling do not balance. Both the local attenuated radiation field and collisional ionization contribute to the

ionization balance at each temperature. All processes contribute to the thermal balance, including collisional ionization. The map is at constant density.

The first column gives the temperature. Columns 2 and 6 give the volume heating and cooling. Both have units $\text{erg s}^{-1} \text{cm}^{-3}$. Columns 3 and 4 constitute an indication of the main heating source. Columns 7 and 8 give the label and wavelength of the strongest coolant. Columns 5 and 9 give the fraction of the total heating or cooling due to these agents. Columns 10 and 11 give the heating and cooling derivatives. Columns 12 and 13 give the electron and hydrogen densities (cm^{-3}) and the remaining columns give the logs of the hydrogen and helium ionization fractions. The location of the probable thermal solution is indicated by a comment surrounded by dashed lines.

8.3 Floating Point Errors

The code should be compiled and linked with options enabled so that the code will crash on overflow or division by zero, but ignore underflow. *Floating point errors should never occur.* The logic within the code is designed to identify problems, and complain, but not fail. The logic is only as good as the tests they were designed to pass. It is inevitable that circumstances will occur for which the logic now in the code is not sufficient. It is possible that the code will fail when these circumstances occur. I would be grateful for reports of any such failures, since they inevitably identify shortcomings in the code, and lead to its improvement. My email address is gary@pa.uky.edu.

8.4 Optical depth convergence problems

The code generally will not converge if it has not done so within ten or so iterations. Convergence problems most commonly occur when the specified column density or thickness is very near a prominent ionization front. In this case very small changes in the physical conditions results in large changes in the optical depths. The code will not have convergence problems if an optical depth is used as a stopping criterion instead.

8.5 Negative populations of H-like and He-like ions, and molecules

It is possible that the code will stop because negative level populations were predicted for atoms or ions of hydrogen and helium. This is not supposed to occur, but sometimes happens because of numerical instabilities in the matrix inversion routine. Please send me the input stream and version of Cloudy.

8.6 I can't fix it if I don't know it's broken.

Machines are growing faster far more rapidly than people are getting smarter. Reliability in the face of complexity is the major challenge to the development of any large-scale computer code (Ferland 2001b). There can be little doubt that Cloudy contains bugs.

The code is well tested in many limits, and behaves in the correct manner. Simulations of H II regions, planetary nebulae, and other simple objects, are in good

agreement with predictions of other photoionization codes (Ferland et al. 1995; Ferland & Savin 2001).

Bugs can be discovered by strange behavior or crashes in situations where the code has not been well-tested. The discovery of the existence of problems is itself a major challenge. If problems arise or the code crashes then it is likely that a problem has been isolated. I would appreciate learning about such problems since they identify shortcomings which usually lead to improvements in the code (or the documentation). My email address is gary@pa.uky.edu.

9 REVISIONS TO Cloudy

9.1 Overview

This section outlines some of the major versions of Cloudy, and gives an indication of the direction development will take in the next few years. Its development began in August of 1978, at the Institute of Astronomy, Cambridge, and has been continued at The University of Kentucky, The Ohio State University, and during extended visits to the Joint Institute for Laboratory Astrophysics, the Royal Greenwich Observatory, IOA Cambridge, Cerro Tololo Interamerican Observatory, and the Canadian Institute for Theoretical Astrophysics. Figure 16 shows the evolution of the code, as indicated by its size as a function of time⁷.

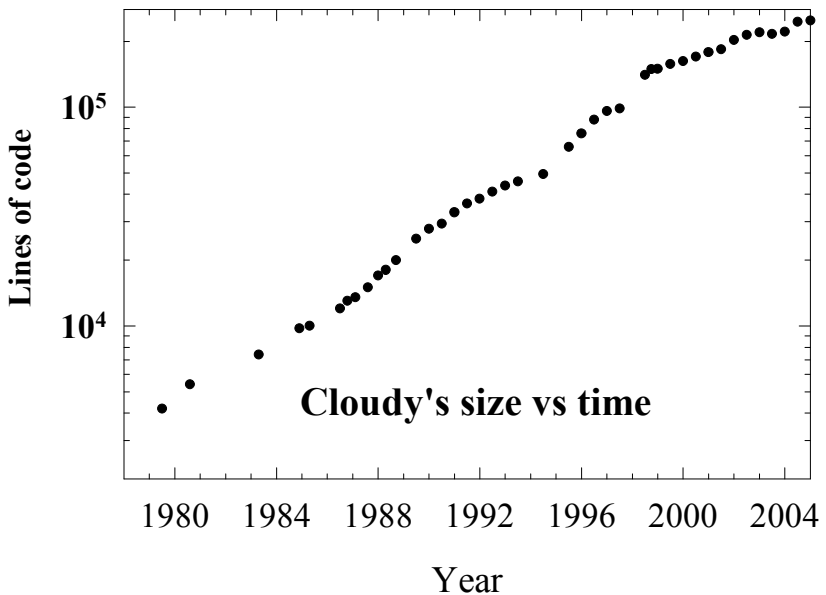


Figure 16 The size of the code as a function of time. The code grows roughly 7% larger per year, with growth spurts and slowdowns at times. There are several changes in slope evident – the year and cause are: 1985 – mainframe to Unix; 1993 – Unix to windows; the jump at 1999 – the Fortran to C conversion. size

9.2 Cloudy and Moore's Law

Moore's Law is due to Gordon Moore, one of the founders of Intel Corporation. He observed that modern CPU's become about twice as powerful every 18 months. This trend has held true for the past twenty years, shows no sign of failing, and seems to be associated with our ability to control complexity.

By this standard the growth of Cloudy has been conservative, in that it is growing slower and complex on the Moore's law timescale. As an example, the Meudon 1985 Meeting planetary nebula test (`parispn.in` in the distributed test cases) has always taken about one minute to compute.

9.3 Major Past Versions

- 67 August 1987. Hydrogen atom goes to LTE in limit of large electron densities. Many small bugs uncovered as result of careful comparison with Netzer's ION.

⁷ Before mid-1995 the size was the total number of lines in the distributed source. After 1995 the size only includes the number of lines excluding block datas. When the code was converted to C the block datas were converted to external data files. These external files are now far larger than the code itself.

- 68 Cambridge, Fall 1987. Development work in progress.
- 69 December 1987. Hydrogen atom goes to LTE in limit of large photon densities. Ferland and Rees (1988).
- 70 September 1988. He II $L\alpha$ transfer improved. Improved form of escape probabilities with explicit damping constants. H^- and improved free-free heating. Many high excitation metal lines transferred. (Rees, Netzer, and Ferland 1989; Ferland and Persson 1989).
- 71 December 1988. Photon array rewritten, now Compton exchange problem is exact for black bodies with temperatures between 2.7 K and 10^{10} K. He II $L\alpha$ radiation pressure included.
- 72 January 1989. Static version, minor bug fixes.
- 73 1989. Major rewrite of helium treatment. Dust changed to two populations, scattering and absorption included. Default radius and thickness increased by ten orders of magnitude. He^+ goes to LTE. Development work on getting helium to go to LTE. IR power law for default AGN continuum now $\nu^{+2.5}$ below 100 micron break. No *anumm* array, all continuum one array. **table star**. *coolr* broken up. Helium to LTE for high electron density.
- 74 1990 January. Hydrogen double precision, many bug fixes. 10 tables among the continua. Kurucz (1989) atmospheres. Improved dust treatment, including photoionization and charge.
- 75 1990, JILA visit. Cosmic abundances changed to Grevesse and Anders. Major bug in constant pressure for HII regions, PNs, etc; did not affect BLR. Calculation of ν_f ($H\beta$) was incorrect. Molecules at low temperatures. HDEN now $n(H^0) + n(H^+) + n(H^-) + 2n(H_2) + 2n(H_2^+)$. Improved Rayleigh scattering treatment. Dielectronic recombination for sulfur (guess). Many changes in dust; Orion paper (Baldwin et al. 1990). Subordinate lines changed to Hummer's K2 function.
- 76 1990, static version from end of JILA visit.
- 77 through Nov. 1990. **optimize** option added using Bob Carswell's code. Gaunt factor for brems input spectrum. Reflected continuum predicted. Frequency partition adjusted. X-Ray optical depth now at 0.5 keV. Read in table of points from previous calculation. *opsav* deleted, now single pointer *opsv* for all opacities. Numerical array to 100 MeV. Hummer $L\alpha$ escape destruction prob. *tautot* arrays now both in and outward directions. Bound Compton included for all ionization levels. Mean ionization arrays rewritten to make sense. Bug in wind velocity fixed, result now exact. C, O outward diffuse fields changed to OTS.
- 78 through May 91. Continuum escape probability formal H-only opacity. H recombination, cooling over wide range of temp. X-Ray optical depth back to 1 keV. **abundances no dust** no longer changes abundances of depleted elements. OI- $L\beta$ treatment is now six-level atom. Default table AGN changed. Continuum normalization rewritten. Milne relation for diffuse fields of H, all He. Fe $K\alpha$ divided into hot and cold. Beams paper (Ferland, Peterson, Horne,

et al. 1992) Many high ionization lines included as OTS and outward ionization sources.

- 79 Summer 91. H molecules completed, C, N, O molecules included. Continuum binning changed for Ca, Fe L-shell ionization potentials. Extensive testing.
- 80 July 91, static version .05. Version 80.06 fixed many small problems discovered by several people. New collision strength for [NeV] put in. This static version ended with 80.09, in January of 1993.
- 81 Late 1991. New collision strengths for [NeV] IR lines (10x larger). Also for [CII], [NIII], and [OIV]. Some are 2x larger. Opacity arrays totally rewritten with eye to Opacity Project data. NIII paper (Ferland 1992).
- 82 Early 1992. X-Ray opacity arrays rewritten. Improved pressure convergence. HJBAR now function. Error in cooling due to collisional ionization of H, He. Sodium and nickel added. /TAU/ array broken up. All heavy element opacities converted to table look-up. Revised collision strengths for NIII lines, improved treatment of atom. NLR abundances deleted, ISM put in their place. Summary comments now driven by subroutine. Cap on 911 OTS field. Note on [FeXI] maser (Ferland 1993). Luminosity command separated into luminosity and intensity commands.
- 83 Autumn 1992, Cambridge and CTIO visits. Hydrogen molecule network completed, Ferland, Fabian, and Johnstone (1993). Collision strengths for fine structure lines changed to Blum and Pradhan 1992, Hollenbach and McKee 89; these changed temperatures for cold ISM by factors of 2. Heavy element molecule network as in Hollenbach and McKee 1989. Code works in fully molecular limit. Kevin Volk's stars (Atlas 91, and Werner models). More accurate treatment of secondary ionization after Voit visit. [OI] lines each include escape prob. Opacities, destruction probabilities, evaluated within all loops, code far more stable, but roughly three times slower. Transferred HeI 2.06 line correctly, after Shields papers.
- 84 1993 Feb 13, Static version following CTIO visit.
- 85 1994, Revisions following Lexington meeting. Outward only now default continuum transport.
- 86 1995, All of first thirty elements are now in code. Photoionization database changed to Dima Verner's *phfit*.
- 87 1995 summer, Map now converges electron densities. Negative populations of OI and FeII atoms solved. Dima's 6k lines included in cooling and radiative acceleration. Total rewrite of *nextdr* logic. Ionization predictor corrector logic completely rewritten. Dima's *phfit* now fitted to all Opacity Project data.
- 88 1995 Fall-winter. Kirk's extensive grids of BLR models run. March 1996 visit to Tel Aviv to compare results with Hagai. Kirk carefully went over atomic data base. Iron recombination changed to Arnaud and Raymond (1992). Default iron abundance down 33%. Entire line data base revised.

- 89 1995 winter-spring. These were mainly beta versions with no major changes, but many fixes to problems.
- 90 1996 June 17, static version, extensive year of debugging. Ferland et al. (C90) paper.
- 91 1977, preparation of C version.
- 92 1998, sabbatical at CITA, revision and debugging of C version.
- 94 1999 December 24, gold version of C code.
- 96 2003 January, He isoelectronic sequence, CO multilevel molecule, pgrains distributed grains, atomic data update, H₂ molecule.

9.4 Version 96 vs 94

9.4.1 Commands

The **atom** command is now the primary method of changing treatments of H-like, he-like, and molecular species.

9.4.2 Physics

The helium isoelectronic sequence has been broken out.

H₂, ¹²CO and ¹³CO are now multi-level molecules with the full rotation spectrum predicted.

The **pgrains** treatment of grain physics has been incorporated, allowing fully resolved treatment of grains charging, collisions, and emission. It has been moved into the **grains** command with the final release. This effort was led by Peter van Hoof.

Two photon emission, and induced two photon emission, is fully treated for the complete H and He iso-electronic sequences.

The large H₂ molecule was incorporated by Gargi Shaw.

The CO network was updated by Nick Abel.

The code can now do dynamical flows. This effort was led by Robin Williams and Will Henney.

9.4.3 Miscellaneous

The ISM oxygen abundance was changed from 5.01e-4 to 3.19e-4 as recommended by Meyers et al. (1987).

9.5 Version 94 versus 90

9.5.1 Commands

The **hydrogen** and **feii** commands have been combined into the **atom** command, which has many options.

9.5.2 Hydrogen

The full hydrogenic isoelectronic sequence is now treated with a single model atom and code base. The model atom can have up to 400 levels.

9.5.3 Grains

Parameters used in the treatment of the old-style grains have been revised as per the Weingartner & Draine (2000) paper. This makes it possible to resolve the grain size distribution function, solving for grain properties and emission as a function of their size. This is described in van Hoof et al. (2000).

9.5.4 Other changes

The code is now ANSI 1989 C, making it especially gcc and Linux friendly.

9.6 Version 90 versus 84

9.6.1 Commands

The **abundances** command now needs 29 numbers by default. A new command “**init**” allows a commonly used set of commands to be saved as a single file and used by a variety of scripts.

9.6.2 Continuum Transport

Versions 86 and before used a modified version of on-the-spot approximation (OTS) for the Lyman continua of hydrogen and helium. This method was numerically stable and gave results in excellent agreement with Van Blerkom and Hummer (1967). This has been changed to outward-only to obtain better agreement with predictions of Pat Harrington’s and Bob Rubin’s codes (Ferland et al. 1995). The OTS code is still in place and will be used if the **diffuse OTS** command is entered, but outward-only is the default. The two methods result in temperatures at the illuminated face which can differ by as much as several thousand degrees, but the resulting spectra are surprisingly similar.

9.6.3 Hydrogen

The model hydrogen atom has been generalized to an arbitrary multi-level atom (Ferguson and Ferland 1996). The **hydrogen levels** command is used to specify the number of levels to be used. The collision strengths have been changed to Vriens and Smeets (1980) for levels higher than 3, and Callaway (1994) for collisions with 1, 2 and 3.

Predicted infrared line intensities are now correct for all densities and temperatures greater than 10^3 K. Versions before 89 used a well l-mixed hydrogen atom, and its predictions were not correct for some infrared lines at low densities.

The routine that computes the free-free gaunt factors has been extended to include the full range the code can handle.

9.6.4 The helium ion

The helium ionization balance at low photon and particle densities, and at high particle densities, has always been exact, and this continues to be the case. There was a problem in the helium ion for high radiation densities, in versions 87 and before. The code used three pseudo levels to represent the levels between 7 and 1000, for H, He, and He⁺. This seemed to work well for the atoms for the cases of high densities, but testing has shown that it did not represent the physics of the high radiation density limit well. The problem is that the pseudo-levels had very large statistical weights, they represented line energies in the far infrared, and had A’s appropriate

for lower levels. As a result they had very large induced rates when the photon occupation numbers were large, and this affected populations of lower levels. As a result the atom became too ionized - as much as a factor of two for He⁺. The following test illustrates this problem:

```
title helium ionization in high photon density limit
print departure coef
set dr 0
stop zone 1
constant temper 4
hden 11.000
phi(h) 20.750 range 1
stop thickness 11.7
table agn
```

In versions 88 and later no pseudo levels are used for any hydrogen or helium atom or ion.

9.6.5 Heavy elements

The atomic data base, the organization of aspects of the code dealing with storing heavy element ionization, and all the associated routines, have been totally rewritten. The lightest 30 elements are now included. Photoionization data are from Verner et al. (1996), recombination data partially from Verner and Ferland (1996), and roughly 10⁴ lines of the heavy elements have been added (Verner, Verner, and Ferland 1996).

The number of resonance lines has increased by more than an order of magnitude. All resonance lines listed by Verner, Verner, and Ferland (1996) are included. As a result of these many additional lines the cooling function tends to be larger and smoother.

All lines are now fully transferred, and include pumping by the attenuated incident continuum as a general excitation mechanism. Pumping can be a significant contributor to the formation of weak high excitation lines.

The default solar mixture has been changed to Grevesse and Noel (1993). The biggest change is in the iron abundance. Previous versions had used a higher photospheric abundance. The current version is the 1993 suggested meteoritic abundance.

9.6.6 Free-free, line heating and cooling

These are counted in a different but equivalent manner. Now the *difference* between cooling and heating is used, since this is more numerically stable at high radiation densities. This difference has no physical affect on the predictions, but the printed contributors to the total heating and cooling do appear different.

9.6.7 Excited state photoionization cross sections

OP data are now used. For the excited state of Mg⁺ this is nearly ten times smaller than old screened hydrogenic values. This affects the intensity of Mg II λ 2798 in some BLR calculations.

9.6.8 The O⁺ photoionization cross section

The Reilman and Manson photoionization cross sections, used before version 87, show a jump in the photoionization cross section at the 2s - 2p edge, and low values above that threshold extending up to the valence electron threshold. Opacity Project cross sections are used in the current version of the code, and these do not show the 2s edge (the OP calculations find that the 2s and 2p electrons are highly correlated). The cross section remains large up to the valence threshold. The difference approaches a factor of two, and this affects high ionization parameter clouds since O^+ is the dominant opacity for some energies.

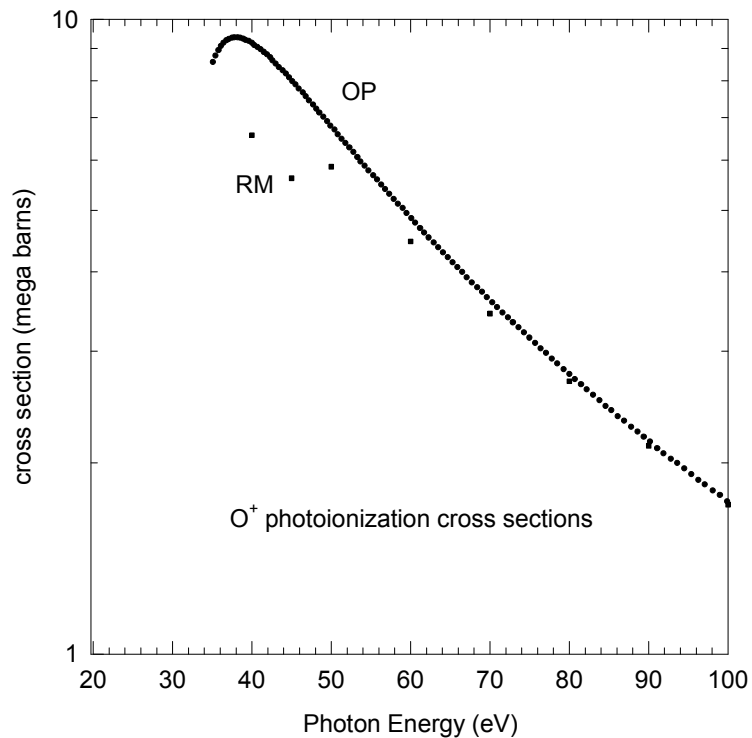


Figure 17 This figure shows the O^+ photoionization cross sections now used, compared to the Reilman and Manson values, and used in version 84 and before. o2photo

Verner, et al. (1996) comment on all other cases where the photoionization cross sections have changed. There are generally atoms and first ions where Opacity Project data are now available.

9.7 Version 84 versus 80

9.7.1 Commands

In previous versions of the code both luminosity (quantity radiated into 4π sr) and intensity (a surface flux) were specified with the same command. The code decided which was intended by checking the resulting ionization parameter. This method never failed to the best of my knowledge, but, as the code grows more capable of considering ever more extreme cases, there might eventually come a time when it made the wrong decision. All luminosity-intensity commands have now been split up. For instance, the Q(H) command is now two commands, Q(H) (for number of photons radiated into 4π sr) and ϕ (H), for the surface flux. These commands are all discussed in Part I of HAZY.

9.7.2 Mg II λ 2798

The biggest difference between the two versions is in the predicted intensity of Mg II λ 2798. The intensity of this line is now a factor of two stronger in many models. The new version uses L-shell photoabsorption cross sections from Reilman and Manson (1979), and the older version used inner shell cross sections extrapolated from the table in Weisheit (1974). The cross sections differ by a factor of nearly 3, in the sense that Mg now tends to be more neutral, and Mg II stronger. As a result of

the increased cooling by $\lambda 2798$ other lines formed in the same region tend to be weaker.

9.7.3 General Results

The following may affect certain specific models, but did not result in changes in any of the “standard” test cases.

The treatment of line-continuum fluorescence in the optically thin limit has been much improved, following Ferland (1992). This can affect hydrogen line emission in clouds that are optically thin in the Lyman continuum.

The treatment of molecules has been vastly improved. The code now goes to the fully molecular (H_2 and CO) limit, and reproduces the Tielens and Hollenbach (1985a, b) PDR results for Orion.

The elements Na and Ni have been added.

9.8 Known Modes for Cloudy 96

- Time dependent model turned off.

9.9 Making a Revision

9.9.1 The code

- Compile code with array bounds checking. Run all test cases.
- Run all test cases on Alpha, HP, Sparc, SGI, and PC.
- Confirm *fabden* stops immediately.
- Summarize changes in `c96rev.htm` in the web site. This is the primary documentation for changes to the code.
- Create the test case files for each of the platforms. Each lives in a separate subdirectory off the hazy directory. Create a compressed tar file with the name of the platform included.
- Tar all input files into single file with name `tests.tar`. The command is `tar -cvf tests.tar *.in *.for`. Compress and copy to `ftp`.

9.9.2 Printing Hazy

- *Update the list of subroutine names.* Do this by running `do.all` in the `include` directory. The list of routine names in is the file `routines.txt`, and this is automatically generated by `do.all`. This was probably done to update the source, as described in the previous section. Edit links in HAZY `routines.doc` to update this.
- *Update all comparison tables.* These are in the section starting on page 507. Go over these to confirm that line predictions are OK.
- *Update all test case input scripts.* These are listed in the section beginning on page 524 of this document. Edit the links to manually update them.
- *Confirm that all cross-linked variables are ok.* Change labels in HAZY `headinfo.doc`.

- *Summarize changes to the code.* These are listed in **version.for** and should go into the past major revisions in this section of HAZY.

10 COMPARISON CALCULATIONS

10.1 Overview

This section presents comparisons between the current predictions of the code, and results from other independent calculations. The “other” calculations are from the compendium resulting from the Lexington meeting on model nebulae (Ferland et al. 1995).

The scatter among the calculations, as well as the changes that have occurred in the predictions made by Cloudy, are in some sense an indication of the stability and reliability of these types of extreme non-LTE calculations. The largest discrepancies between current predictions made by Cloudy and the other models from the Meudon meeting (which were computed in 1985) are due to changes which have occurred in the atomic data base between 1985 and the present. In general, the strongest lines are in very good agreement (as they must because of energy conservation) while weak lines (which are very sensitive to changes in the computed temperature and ionization structure) scatter by nearly a factor of two.

10.2 Cool HII Region

This is an HII region ionized by a very cool star. It is one of the Lexington Meeting test cases and is computed with the input script `coolhii.in` in the code's test suite. This is the simplest model since helium is predominantly neutral. The entry $L(\text{total})$ comes from the "Stoy" printed entry.

Table 2 HII Region Ionized by Cool Star

		Mean	Ferland	Harrington	Netzer	Pequignot	Rubin
L(H γ)	E36	4.90	4.98	4.93	4.85	4.83	4.93
[NII]	6584+	0.87	0.91	0.82	0.97	0.82	0.84
[OII]	3727+	1.21	1.16	1.22	1.32	1.14	1.21
[NeII]	12.8 γ	0.30	0.35	0.29	0.29	0.29	0.29
[SII]	6720+	0.57	0.64	0.55	0.61	0.52	0.52
[SIII]	18.7 γ	0.31	0.27	0.36	0.17	0.37	0.37
[SIII]	34 γ	0.51	0.47	0.60	0.27	0.61	0.62
[SIII]	9532+	0.57	0.48	0.55	0.64	0.60	0.56
L(total)	E36	21.3	21.3	21.7	20.7	21.0	21.8
T(in)		6860	6952	6749	6980	6870	6747
T(H $^+$)		6767	6740	6742	6950	6660	6742
<He $^{+}$ >/<H $^{+}$ >		0.047	0.041	0.044	0.068	0.048	0.034
R(out)	E18	8.96	8.93	8.94	9.00	8.93	9.00

Table 3 Cool HII Region vs Cloudy

		Mean	STD	90.05	94.00	96.00
L(H \square)	E36	4.90	0.06	4.91	5.03	4.85
[NII]	6584	0.65	0.05	0.64	0.63	0.57
[OII]	3727+	1.21	0.07	1.08	1.04	1.01
[NeII]	12.8 \square	0.30	0.03	0.26	0.26	0.26
[SII]	6720+	0.57	0.05	0.45	0.44	0.49
[SIII]	18.7 \square	0.31	0.09	0.43	0.45	0.44
[SIII]	34 \square	0.51	0.15	0.61	0.64	0.90
[SIII]	9532	0.43	0.05	0.42	0.42	0.36
L(total)	E36	21.29	0.45	21.0	21.7	21.2
T(in)		6860	110	7261	7188	6790
T(H $^+$)		6767	108	6600	6530	6622
<He $^{+}$ >/<H $^{+}$ >		0.047	0.01	0.048	0.043	0.046
R(out)	E18	8.96	0.04	8.81	8.92	8.83

10.3 Paris HII Region

This compares current predictions of the code with those of other participants at the Meudon meeting on photoionization calculations for the case of a simple spherical HII region. The input used to generate this model HII region is contained in the sample input file *parishii.in*.

Table 4 Paris Meeting HII Region

		Meu	Lex	Ferland	Harrington	Netzer	Pequignot	Rubin
L(HI)	E37	2.06	2.04	2.06	2.04	2.02	2.02	2.05
HeI	5876	0.116	0.111	0.109	0.119	0.101	0.116	
CII	2326+	0.17	0.17	0.19	0.17	0.16	0.14	0.18
CIII	1909+	0.051	0.07	0.059	0.059	0.078	0.065	0.076
[NII]	122 H		0.031	0.033			0.036	0.031
[NII]	6584+	0.73	0.80	0.88	0.74	0.87	0.78	0.73
[NIII]	57 H	0.30	0.28	0.27	0.29	0.26	0.30	0.30
[OII]	3727+	2.01	2.20	2.19	2.14	2.3	2.11	2.26
[OIII]	51.8 H	1.10	1.06	1.04	1.11	0.99	1.08	1.08
[OIII]	88.4 H	1.20	1.20	1.07	1.28	1.16	1.25	1.26
[OIII]	5007+	2.03	2.09	1.93	1.96	2.29	2.17	2.10
[NeII]	12.8 H	0.21	0.21	0.23	0.19	0.22	0.20	0.20
[NeIII]	15.5 H	0.44	0.41	0.43	0.43	0.37	0.42	0.42
[NeIII]	3869+	0.096	0.091	0.103	0.086	0.100	0.079	0.087
[SII]	6720+	0.14	0.18	0.23	0.16	0.22	0.17	0.13
[SIII]	18.7 H	0.55	0.53	0.48	0.56	0.5	0.55	0.58
[SIII]	34 H	0.93	0.87	0.82	0.89	0.81	0.88	0.94
[SIII]	9532+	1.25	1.31	1.27	1.23	1.48	1.27	1.30
[SIV]	10.5 H	0.39	0.38	0.37	0.42	0.36	0.41	0.33
Sum	Sum	11.59	11.87	11.58	11.70	12.17	11.90	12.01
L(total)	E37	24.1	24.4	24.1	24.1	24.8	24.3	24.6
T(in)		7378	7655	7815	7741	7670	7650	7399
T(H+)		7992	8052	8064	8047	8000	8060	8087
He+>/<H+>			0.76	0.71	0.77	0.76	0.75	0.83
R(out)	E18	1.45	1.46	1.46	1.46	1.47	1.46	1.46

Table 5 Paris HII Region vs Cloudy

		Mean	STD	76.03	80.06	84.15	90.05	94.00	96.00
L(H β)	E37	2.04	0.02	2.06	2.04	2.01	2.05	2.02	2.04
HeI	5876	0.11	0.01	0.12	0.12	0.12	0.11	0.117	0.113
CII]	2326+	0.17	0.02	0.24	0.17	0.17	0.15	0.145	0.195
CIII]	1909+	0.07	0.01	0.06	0.11	0.09	0.063	0.060	0.051
[NII]	122 μ	0.03	0.00			0.03	0.028	0.028	0.027
[NII]	6584	0.60	0.05	0.58	0.60	0.58	0.58	0.57	0.519
[NIII]	57 μ	0.28	0.02			0.29	0.289	0.297	0.302
[OII]	3727+	2.20	0.08	2.29	2.43	2.31	2.02	1.996	2.00
[OIII]	51.8 μ	1.06	0.05	1.15	1.09	1.11	1.22	1.24	1.27
[OIII]	88.4 μ	1.20	0.09			1.06	1.11	1.13	1.16
[OIII]	5007	1.57	0.11	1.83	1.62	1.50	1.66	1.62	1.57
[NeII]	12.8 μ	0.21	0.02	0.22	0.23	0.23	0.18	0.18	0.17
[NeIII]	15.5 μ	0.41	0.02	0.47	0.45	0.45	0.28	0.29	0.29
[NeIII]	3869	0.0689	0.008	0.098	0.090	0.082	0.063	0.061	0.059
[SII]	6720+	0.18	0.04	0.27	0.29	0.129	0.126	0.12	0.153
[SIII]	18.7 μ	0.53	0.04	0.54	0.53	0.52	0.61	0.61	0.62
[SIII]	34 μ	0.87	0.05			0.88	0.85	0.86	1.21
[SIII]	9532	0.98	0.07	1.04	1.04	1.05	0.90	0.89	0.77
[SIV]	10.5 μ	0.38	0.04	0.09	0.11	0.36	0.53	0.53	0.56
Sum	Sum	11.87	0.24	10.0	9.9	11.8	11.9	11.8	12.1
L(total)	E37	24.44	0.31	20.9	20.4	23.9	24.5	24.3	24.1
T(in)		7655	157			6547	7822	7746	7524
T(H+)		8052	32			7530	7970	7920	7980
<He+>/<H+>		0.76	0.04			0.75	0.72	0.74	0.76
R(out)	E18	1.46	0.00			1.45	1.45	1.46	1.44

10.4 Blister HII Region

This is one of the Lexington Meeting test cases, and is meant to be similar to inner regions of the Orion Nebula and is called **blister.in** in the test suite.

Table 6 Blister HII Region

		Mean	Ferland	Harrington	Netzer	Pequignot	Rubin
I(H ⁺)		4.69	4.59	4.81	4.69	4.67	4.70
HeI	5876	0.12	0.13	0.11	0.12	0.12	
CII	2326+	0.16	0.14	0.20	0.10	0.15	0.23
CII	1335+	0.15	0.17	0.14	0.13	0.16	
CIII]	1909+	0.18	0.22	0.17	0.18	0.15	0.20
[NII]	6584+	0.81	0.58	0.94	0.74	0.90	0.87
[NIII]	57	.033	.035	.033	.033	.032	.034
[OII]	7330+	0.12	0.10	0.13	0.09	0.12	0.14
[OII]	3727+	0.86	0.73	0.98	0.69	0.86	1.04
[OIII]	51.8	0.29	0.31	0.29	0.28	0.28	0.28
[OIII]	5007+	4.18	4.74	3.90	4.40	3.90	3.96
[NeII]	12.8	0.34	0.32	0.33	0.35	0.33	0.35
[NeII]	15.5	1.06	1.24	1.07	0.96	1.04	1.00
[NeIII]	3869+	0.34	0.48	0.32	0.35	0.26	0.29
[SIII]	18.7	0.33	0.31	0.34	0.31	0.33	0.35
[SIII]	9532+	1.46	1.41	1.46	1.51	1.42	1.53
[SIV]	10.5	0.51	0.54	0.52	0.51	0.53	0.43
Sum	Sum	10.78	11.32	10.80	10.63	10.46	10.71
I(total)		51.3	52.6	52.4	50.4	49.4	50.3
T(in)		7911	8206	7582	8200	8200	7366
T(H ⁺)		8303	8324	8351	8310	8200	8328
<He ⁺ >/<H ⁺ >		0.85	0.94	0.78	0.93	0.79	0.84
R	E17	2.99	2.88	3.08	2.93	2.98	3.09

Table 7 Blister HII Region vs Cloudy

		Mean	STD	90.05	94.00	95.00
I(H β)		4.69	0.08	4.71	4.64	4.91
HeI	5876	0.12	0.01	0.129	0.132	0.132
CII]	2326+	0.16	0.05	0.133	0.124	0.135
CII	1335+	0.15	0.02	0.179	0.171	0.18
CIII]	1909+	0.18	0.03	0.222	0.234	0.26
[NII]	6584	0.54	0.09	0.468	0.417	0.40
[NIII]	57 μ	0.03	0.00	0.037	0.038	0.038
[OII]	7330+	0.12	0.02	0.115	0.113	0.127
[OII]	3727+	0.86	0.15	0.737	0.713	0.794
[OIII]	51.8 μ	0.29	0.01	0.303	0.309	0.307
[OIII]	5007	3.13	0.28	3.74	3.84	3.88
[NeII]	12.8 μ	0.34	0.01	0.140	0.141	0.14
[NeIII]	15.5 μ	1.06	0.11	0.458	0.462	0.466
[NeIII]	3869	0.34	0.08	0.157	0.159	0.166
[SIII]	18.7 μ	0.255	0.015	0.301	0.304	0.349
[SIII]	9532	1.09	0.037	0.950	.955	0.87
[SIV]	10.5 μ	0.51	0.04	0.68	0.68	0.665
Sum	Sum	10.78	0.32	10.6	10.7	10.8
I(total)		51.29	1.39	50.9	50.2	50.0
T(in)		7910	406	8447	8370	8430
T(H+)		8302	59	8325	8330	8429
<He+>/<H+>		0.85	0.07	0.895	0.90	0.916
ΔR	E17	2.99	0.09	2.99	2.94	2.94

10.5 Paris Planetary Nebula

This compares current predictions of the code with those of other participants at the Meudon (1985) and Lexington (1993) meetings on photoionization calculations, for the case of ionization by a very hot black body. The input used to generate this model planetary nebula is shown in the sample input section and is called **parispn.in** in the test suite. The model results are very sensitive to the detailed transfer of HeII $L\alpha$; this line is the dominant heat source across the He⁺⁺ region of the model nebula. The parameters were chosen to be roughly similar to NGC 7027, a very well studied object.

Table 8 Paris Meeting Planetary Nebula

Line		Meudon	Lexington	Ferland	Harrington	Netzer	Pequignot
L(H° J)	E35	2.60	2.68	2.63	2.68	2.73	2.68
HeII (35)	erg/s	0.87	0.88	0.83	0.88	0.94	0.85
He I	5876	0.11	0.11	0.11	0.10	0.10	0.11
He II	4686	0.33	0.33	0.32	0.33	0.35	0.32
C II]	2326+	0.38	0.33	0.33	0.43	0.27	0.30
C III]	1909+	1.70	1.77	1.82	1.66	1.72	1.87
C IV	1549+	1.64	2.33	2.44	2.05	2.66	2.18
[N II]	6584+	1.44	1.49	1.59	1.45	1.47	1.44
N III]	1749+	0.11	0.12	0.13	0.13	0.11	0.13
[NIII]	57 °		0.13	0.12	0.13	0.13	0.13
N IV]	1487+	0.12	0.19	0.20	0.15	0.21	0.19
N V	1240+	0.09	0.17	0.18	0.12	0.23	0.15
[O I]	6300+	0.15	0.14	0.15	0.12	0.14	0.14
[O II]	3727+	2.23	2.25	2.23	2.27	2.31	2.18
[O III]	5007+	20.9	20.76	21.1	21.4	19.4	21.1
[O III]	4363	0.16	0.15	0.16	0.16	0.14	0.16
[O III]	52 ° k	1.43	1.43	1.42	1.44	1.40	1.46
[O IV]	26 ° k	3.62	3.67	3.52	3.98	3.32	3.86
O IV]	1403+	0.13	0.26	0.20	0.23	0.26	0.33
O V]	1218+	0.09	0.20	0.20	0.11	0.29	0.19
[Ne III]	15.5 °	2.51	2.78	2.75	2.76	2.80	2.81
[Ne III]	3869+	2.59	2.69	3.33	2.27	2.74	2.44
Ne IV]	2423+	0.56	0.78	0.72	0.74	0.91	0.74
[Ne V]	3426+	0.73	0.67	0.74	0.60	0.73	0.61
[Ne V]	24.2 °	1.67	0.87	0.94	0.76	0.81	0.99
Mg II	2798+	1.48	1.58	2.33	1.60	1.22	1.17
[Mg IV]	4.5 ° j	0.09	0.12	0.12	0.13		0.12
[Si II]	34.8 °	0.13	0.19	0.16	0.26	0.19	0.17
Si II]	2335+	0.11	0.16	0.15		0.16	0.16
Si III]	1892+	0.20	0.41	0.39	0.32	0.46	0.45
Si IV	1397+	0.15	0.18	0.20	0.15	0.21	0.17
[S II]	6720+	0.39	0.35	0.21	0.45	0.33	0.43
[S III]	18.7 °	0.49	0.48	0.48	0.49	0.46	0.49
[S III]	9532+	2.09	1.96	2.04	1.89	2.05	1.87
[S IV]	10.5 °	1.92	1.98	1.92	2.21	1.81	1.98
L(total)	E35	129	137	139	136	135	136
T(in)	E4		1.81	1.83	1.78	1.84	1.78
T(H+)	E4		1.25	1.22	1.21	1.35	1.21
<He+>/<H+>			0.72	0.74	0.74	0.71	0.71
R(out)	E17		4.06	4.04	4.04	4.07	4.07

Table 9 Paris Planetary vs Cloudy

Line		Lexington	STD	74.23	76.03	80.06	84.15	90.05	94.00	96.00
L(H β)	E35	2.68	0.04	2.57	2.66	2.52	2.34	2.62	2.55	2.56
Hell (35)	erg/s	0.88	0.05				0.83	0.83	0.866	.873
He I	5876	0.11	0.01	0.11	0.11	0.11	0.11	0.111	0.108	0.108
He II	4686	0.33	0.01	0.29	0.32	0.35	0.36	0.319	0.343	0.345
C II]	2326+	0.33	0.07	0.36	0.35	0.37	0.35	0.286	0.289	0.294
C III]	1909+	1.77	0.09	1.57	1.48	1.72	1.72	1.88	1.83	1.90
C IV	1549+	2.33	0.27	2.24	2.76	2.48	2.19	2.65	2.63	2.61
[N II]	6584	1.12	0.05	1.06	1.05	1.08	1.11	0.978	1.00	0.885
N III]	1749+	0.12	0.01	0.10	0.08	0.10	0.11	0.123	0.118	0.121
[NIII]	57 μ	0.13	0.00				0.12	0.128	0.125	0.127
N IV]	1487+	0.19	0.03	0.16	0.12	0.11	0.15	0.242	0.238	0.241
N V	1240+	0.17	0.05	0.14	0.09	0.06	0.09	0.175	0.18	0.18
[O I]	6300	0.105	0.007	0.11	0.11	0.12	0.12	0.116	0.118	0.119
[O II]	3727+	2.25	0.06	2.24	2.19	2.35	2.40	2.22	2.32	2.36
[O III]	5007	15.6	0.68	15.9	15.8	15.3	15.6	17.0	16.3	16.4
[O III]	4363	0.15	0.01	0.14	0.13	0.15	0.16	0.174	0.166	0.167
[O III]	52 μ	1.43	0.03	1.40	1.35	1.37	1.35	1.32	1.28	1.28
[O IV]	26 μ	3.67	0.30			3.42	3.65	3.42	3.59	3.64
O IV]	1403+	0.26	0.05	0.19	0.22	0.11	0.15	0.248	0.25	0.225
O V]	1218+	0.20	0.07	0.17	0.11	0.07	0.11	0.200	0.20	0.20
[Ne III]	15.5 μ	2.78	0.03	2.77	2.70	2.67	2.71	1.90	1.87	1.87
[Ne III]	3869	2.01	0.35	2.41	2.25	2.43	2.49	2.15	2.09	2.11
Ne IV]	2423+	0.78	0.09	0.62	0.51	0.51	0.63	0.823	0.827	0.829
[Ne V]	3426	0.50	0.06	0.48	0.40	0.40	0.48	0.589	0.614	0.621
[Ne V]	24.2 μ	0.87	0.11	0.24	0.25	1.01	1.04	1.03	1.09	1.098
Mg II	2798+	1.58	0.54	0.83	1.82	1.96	2.33	2.26	2.27	2.29
[Mg IV]	4.5 μ	0.12	0.00	0.12	0.13	0.14	0.13	0.118	0.12	0.123
[Si II]	34.8 μ	0.19	0.04	0.16	0.16	0.16	0.17	0.157	0.16	0.159
Si II]	2335+	0.16	0.01	0.15	0.14	0.16	0.18	0.150	0.15	0.173
Si III]	1892+	0.41	0.07	0.32	0.42	0.42	0.42	0.526	0.49	0.499
Si IV	1397+	0.18	0.03	0.17	0.24	0.22	0.15	0.235	0.223	0.229
[S II]	6720+	0.35	0.11	0.38	0.68	0.66	0.36	0.354	0.354	0.356
[S III]	18.7 μ	0.48	0.02	0.58	0.71	0.67	0.47	0.467	0.472	0.556
[S III]	9532	1.47	0.075	1.27	1.58	1.55	1.48	1.34	1.35	1.17
[S IV]	10.5 μ	1.98	0.17	1.64	1.32	1.53	1.78	2.20	2.04	2.04
L(total)	E35	137	1.60	117	124	128	121	135		
T(in)	E4	1.81	0.03				1.49	1.828	1.80	1.808
T(H+)	E4	1.25	0.07				1.28	1.22	1.22	1.23
<He+>/<H+>		0.72	0.02				0.72	0.74	0.72	0.72
R(out)	E17	4.06	0.02				3.90	4.03	3.99	4.00

10.6 Paris NLR Model

This compares current predictions of the code with those of other participants at the Meudon meeting on photoionization calculations, for a model similar to the NLR of active nuclei. Results for other codes are from the 1985 Meudon meeting. The input stream is the file *parisnlr.in* in the test suite.

Table 10 Paris Meeting NLR Model

Line		Netzer	Pequignot	Binette	Kraemer	Mean
H β	erg/s/cm ²	0.129	0.134	0.124	0.12	0.127±0.006
H β	4861	1.00	1.00	1.00	1.00	1.00
L α	1216	35.3	33.1	-	24.0	30.8±6.0
He I	5876	0.095	0.098	0.092	0.090	0.094±0.004
He II	4686	0.36	0.32	0.38	0.37	0.358±0.026
C II]	2326	0.96	0.77	1.70	1.06	1.12±0.40
C II	1335	0.14	0.14	0.20	0.08	0.14±0.05
C III]	1909	4.59	4.99	6.50	4.91	5.25±0.85
C IV	1549	7.03	7.20	5.30	7.20	6.68±0.93
[N I]	5200	0.31	0.33	0.82	0.37	0.46±0.24
[N II]	6548	2.68	1.52	1.77	1.63	1.90±0.53
N III]	1749	0.40	0.40	0.43	0.48	0.428±0.038
N IV]	1487	0.45	0.43	0.51	0.48	0.468±0.035
N V	1240	0.32	0.30	0.32	0.28	0.305±0.019
[O I]	63.2 μ m	-	0.62	0.14	0.10	0.29±0.29
[O I]	6300	1.32	0.90	1.62	1.04	1.22±0.32
[O II]	7325	0.11	0.094	0.16	0.10	0.116±0.03
[O II]	3727	3.4	2.62	4.41	2.73	3.29±0.82
[O III]	52 μ m	2.5	2.54	2.31	2.65	2.50±0.14
[O III]	5007	27.36	27.36	23.28	27.76	26.44±2.11
[O III]	4363	0.42	0.41	0.44	0.44	0.428±0.015
O III]	1663	0.97	0.95	0.92	1.01	0.963±0.038
[O IV]	25.9 μ m	5.69	5.19	5.49	-	5.46±0.25
O IV]	1403	0.53	0.44	0.51	0.66	0.534±0.092
O V]	1218	0.33	0.32	0.45	0.24	0.335±0.086
O VI	1035	0.17	0.17	0.22	0.10	0.165±0.049
[Ne II]	12.8 μ m	0.28	0.18	0.48	0.13	0.268±0.155
[Ne III]	15.5 μ m	2.8	2.62	1.83	1.25	2.13±0.72
[Ne III]	3869	2.70	2.59	2.27	1.67	2.31±0.46
Ne IV]	2423	0.82	0.79	1.03	1.12	0.94±0.16
[Ne V]	24.2 μ m	3.54	2.64	3.54	-	3.24±0.52
[Ne V]	3426	1.17	1.02	1.13	1.05	1.095±0.066
Mg II	2798	1.58	1.43	1.51	1.10	1.40±0.21
Si II	34.8 μ m	1.73	0.97	0.51	-	1.07±0.62
Si II	2335	0.21	0.17	0.09	-	0.16±0.06
Si III]	1892	0.15	0.19	0.69	0.14	0.29±0.26
Si IV	1397	0.21	0.14	0.02	0.13	0.13±0.08
S II	6720	1.00	0.62	1.29	0.37	0.82±0.41
S II	4070	0.07	0.04	0.078	0.03	0.055±0.023
S III	18.7 μ m	0.75	0.49	0.68	0.65	0.64±0.11
S III	9532	2.25	1.38	1.73	1.62	1.74±0.37
S IV	10.5 μ m	1.39	0.73	0.94	1.57	1.16±0.39

Table 11 Paris NLR Model vs Cloudy

Line		Mean	84.15	90.05	94.00	96.00
H β	erg/s/cm ²	0.127±0.006	0.133	0.136	0.131	0.136
H β	4861	1.00	1.00	1.00	1.00	1.00
L α	1216	30.8±6.0	32.3	32.3	33.8	33.0
He I	5876	0.094±0.004	0.104	0.103	0.100	0.107
He II	4686	0.358±0.026	0.351	0.34	0.330	0.330
C II]	2326	1.12±0.40	0.766	0.652	0.693	0.754
C II	1335	0.14±0.05	0.126	0.141	0.142	0.145
C III]	1909	5.25±0.85	5.02	4.64	4.54	4.49
C IV	1549	6.68±0.93	8.42	7.47	7.15	6.84
[N I]	5200	0.46±0.24	0.14	0.144	0.151	0.154
[N II]	6548	1.90±0.53	2.32	2.36	2.50	2.52
N III]	1749	0.428±0.038	0.45	0.388	0.376	0.369
N IV]	1487	0.468±0.035	0.553	0.544	0.518	0.500
N V	1240	0.305±0.019	0.391	0.302	0.272	0.269
[O I]	63.2 μ m	0.29±0.29	0.36	0.439	0.464	0.476
[O I]	6300	1.22±0.32	1.02	1.02	1.08	1.19
[O II]	7325	0.116±0.03	0.111	0.106	0.117	0.125
[O II]	3727	3.29±0.82	2.99	2.69	2.97	3.32
[O III]	52 μ m	2.50±0.14	2.34	2.23	2.20	2.10
[O III]	5007	26.44±2.11	25.3	26.05	25.4	24.4
[O III]	4363	0.428±0.015	0.45	0.441	0.428	0.414
O III]	1663	0.963±0.038	1.05	1.03	1.00	0.973
[O IV]	25.9 μ m	5.46±0.25	5.76	5.91	5.79	5.59
O IV]	1403	0.534±0.092	0.54	0.517	0.490	0.419
O V]	1218	0.335±0.086	0.453	0.292	0.264	0.260
O VI	1035	0.165±0.049	0.222	0.142	0.120	0.123
[Ne II]	12.8 μ m	0.268±0.155	0.220	0.168	0.172	0.227
[Ne III]	15.5 μ m	2.13±0.72	3.13	2.12	2.12	2.13
[Ne III]	3869	2.31±0.46	3.99	3.22	3.19	3.12
Ne IV]	2423	0.94±0.16	1.19	1.16	1.12	1.09
[Ne V]	24.2 μ m	3.24±0.52	2.74	2.69	2.69	2.59
[Ne V]	3426	1.095±0.066	1.45	1.25	1.20	1.17
Mg II	2798	1.40±0.21	1.76	1.66	1.62	1.79
Si II	34.8 μ m	1.07±0.62	1.12	1.03	1.07	1.20
Si II	2335	0.16±0.06	0.218	0.191	0.201	0.239
Si III]	1892	0.29±0.26	0.401	0.501	0.474	0.464
Si IV	1397	0.13±0.08	0.140	0.215	0.188	0.185
[S II]	6720	0.82±0.41	1.50	0.988	0.958	1.21
[S II]	4070	0.055±0.023	0.1004	0.095		0.114
[S III]	18.7 μ m	0.64±0.11	0.625	0.685	0.715	0.837
[S III]	9532	1.74±0.37	1.92	1.67	1.74	1.57
[S IV]	10.5 μ m	1.16±0.39	1.73	1.44	1.32	1.27

10.7 Lexington NLR Model

This is the NLR model computed at the 1994 Lexington meeting, and is called `nlr.in` in the test suites.

Table 12 Lexington NLR Model

		Lexington	Binette	Ferland	Netzer	Pequignot	Viegas
I(H π)	E0	1.36	1.33	1.31	1.37	1.43	1.34
Ly π	1216	33.70	38.3	32.1	32.4	31.5	34.2
HeI	5876	0.12	0.11	0.13	0.12	0.13	0.13
HeII	4686	0.24	0.25	0.25	0.25	0.23	0.24
HeII	1640	1.62	1.60	1.74	1.53	1.56	1.67
CIII]	1909+	2.90	2.90	2.99	2.87	2.83	2.90
CIV	1549+	3.35	2.70	3.85	3.69	3.17	3.36
[NII]	6584+	2.55	1.40	3.20	3.10	2.67	2.40
NIII]	1749+	0.23	0.24	0.24	0.22	0.22	0.22
NIV]	1487+	0.21	0.20	0.23	0.22	0.21	0.21
[OI]	6300+	1.65	2.20	1.61	1.67	1.31	1.46
[OI]	63 π	1.12	0.25	1.13		1.44	1.64
[OII]	3727+	1.42	1.60	1.44	1.58	1.30	1.20
OIII]	1663+	0.56	0.35	0.63	0.61	0.57	0.63
[OIII]	5007+	33.54	31.4	34.5	33.0	32.8	36.0
[OIII]	4363	0.32	0.30	0.34	0.31	0.30	0.33
OIV	1403+	0.36	0.49	0.30	0.36	0.42	0.25
[NeIII]	15.5 π	1.89	1.50	2.01	1.94	2.05	1.95
[NeIII]	3869+	2.13	1.90	2.51	2.16	1.72	2.34
[Ne IV]	2423+	0.44	0.52	0.42	0.47	0.41	0.38
[NeV]	3426+	0.52	0.59	0.55	0.53	0.44	0.50
MgII	2798+	1.84	3.50	1.72	1.23	1.12	1.61
[SIII]	34.8 π	0.90	1.00	0.96	1.07	0.96	0.52
[SII]	6720+	1.29	2.40	1.01	0.93	0.99	1.10
[SIII]	9532+	1.91	1.60	2.15	2.06	1.67	2.08
[SIII]	18.7 π	0.49	0.36	0.61	0.57	0.52	0.37
[SIV]	10.5 π	1.02	0.86	1.24	0.82	0.94	1.22
I(total)	E0	130	131	128	128	131	133
T(in)	E4	1.70	1.71	1.70	1.72	1.68	1.68
T(H+)	E4	1.18		1.24	1.06	1.20	1.23

Table 13 Lexington NLR vs Cloudy

		Mean	STD	90.05	94.01	96.00
I(H β)	E0	1.36	0.05	1.38	1.33	1.39
L α	1216	33.70	2.76	30.0	31.6	29.7
HeI	5876	0.12	0.01	0.128	0.12	0.129
HeII	4686	0.24	0.01	0.24	0.24	0.232
HeII	1640	1.62	0.09	1.76	1.68	1.63
CIII]	1909+	2.90	0.06	2.62	2.55	2.52
CIV	1549+	3.35	0.45	3.99	3.78	3.64
[NII]	6584	1.91	0.52	2.26	2.39	2.448
NIII]	1749+	0.23	0.01	0.20	0.20	0.192
NIV]	1487+	0.21	0.01	0.286	0.27	0.260
[OI]	6300+	1.65	0.34	1.63	1.73	1.96
[OI]	63 μ	1.12	0.61	0.77	0.79	0.784
[OII]	3727+	1.42	0.17	1.33	1.45	1.60
OIII]	1663+	0.56	0.12	0.62	0.60	0.584
[OIII]	5007+	33.54	1.76	34.4	33.4	32.1
[OIII]	4363	0.32	0.02	0.327	0.32	0.306
OIV	1403+	0.36	0.09	0.35	0.38	0.326
[NeIII]	15.5 μ	1.89	0.22	1.43	1.44	1.42
[NeIII]	3869+	2.13	0.32	1.96	1.98	1.92
[Ne IV]	2423+	0.44	0.06	0.47	0.45	0.437
[NeV]	3426+	0.52	0.06	0.60	0.60	0.544
MgII	2798+	1.84	0.96	1.48	1.48	1.63
[SiII]	34.8 μ	0.90	0.22	0.87	0.90	0.935
[SII]	6720+	1.29	0.63	0.91	0.91	1.18
[SIII]	9532+	1.91	0.26	2.02	2.04	1.85
[SIII]	18.7 μ	0.49	0.12	0.68	0.72	0.928
[SIV]	10.5 μ	1.02	0.20	1.14	1.06	1.02
I(total)	E0	130	1.86	125	125	124
T(in)	E4	1.70	0.02	1.7	1.69	1.70
T(H+)	E4	1.18	0.08	1.24	1.23	1.02

10.8 The DQ Her Shell

This is more or less the model of the DQ Her nebula proposed by Ferland et al. (1984). The input stream for this model is called `dqher.in` in the test suite. The big difference between C90 and previous versions is in the intensity of H β predicted. The code no longer assumes case B when the temperature is too low to do the matrix solution. The nebula is optically thin to many Lyman lines and these escape, robbing flux from H β .

Table 14 The DQ Her Shell

Line		80.09	84.15	90.05	94.00	96.00
H β (+30)	4861	1.65	1.62	0.879	1.07	1.07
Totl	4861			0.649	0.883	0.887
Case B	4861			1.00	1.00	1.00
L α	1216	40.9	20.7	20.6	27.9	28.7
He I	5876	0.786	0.315	0.246	0.274	0.273
He II	4686	0.166	0.085	0.0877	0.052	0.054
C II	158 μ	0.777	0.62	0.092	0.102	0.103
C II	1335		0.062	0.0195	0.021	0.677
[N I]	5200	0.144		0.078	0.087	0.087
[N II]	122 μ	7.85	3.43	3.22	3.58	3.603
[N III]	57 μ	5.30	3.78	9.20	10.2	10.4
[O II]	3727	1.16	0.304	0.294	0.325	0.331
[O III]	88 μ	12.1	6.36	4.95	5.45	5.40
[O III]	52 μ	12.4	6.60	5.51	6.06	6.00
[Si II]	35 μ	0.586	0.79	0.83	0.92	0.93
[S III]	34 μ	0.114	0.167	0.230	0.258	0.398
[Fe II]		0.121	0.187	0.137	0.151	0.154
<Te>	K		643	862	853	860

10.9 The Kwan and Krolik Standard Model

Table 15. The Kwan and Krolik Standard Model.

Line	KK81	80	84.15	90.05	94.00	96.00
L α 1216	5.512+7 ⁸	5.78	5.59	6.03	5.98	6.03
L α 1216	100	100	100	100	100	100
H β 4861	10.3	6.37	6.05	5.85	5.55	5.97
H α 6563	42.8	19.9	19.56	24.4	17.2	18.2
BaC	47.0	38.8	39.5	59.6	58.5	64.6
PaC	30.7	20.2	20.0	37.4	34.1	39.8
2s-1s	3.3	2.35	3.19	2.70	2.95	2.78
free-free	29.0	25.3	23.3	40.5	39.2	43.9
He I 10830	4.4	2.86	2.84	3.30	2.96	3.30
He I 5876	0.9	0.697	0.845	0.68	0.64	0.690
He II 4686	-	0.365	0.316	0.29	0.27	0.272
He II 1640	2.5	3.17	2.77	2.49	2.29	2.29
C II] 2326	3.3	2.70	0.686	3.17	3.70	4.83
C II 1335	-	0.661	0.611	0.68	0.71	0.587
C III 977	5.1	7.53	6.52	5.58	5.47	5.76
C III] 1909	13.0	20.7	15.9	13.5	13.2	13.2
C IV 1549	67.0	95.7	76.3	70.2	68.1	68.1
N III] 1750	1.5	4.26	4.95	4.23	4.17	3.67
N III 990	-	0.324	1.35	1.40	1.35	1.35
N IV] 1486	5.8	4.88	5.24	5.27	5.13	5.13
N V 1240	8.4	3.61	4.95	3.78	3.72	3.72
O I 1304	6.9	4.01	3.93	5.13	8.21	6.44
O III] 1663	9.5	18.4	18.3	18.6	18.3	18.6
O IV] 1402	5.2	4.81	5.84	6.20	6.04	5.15
O V] 1218	6.7	3.07	4.63	3.23	3.15	3.25
O VI 1034	15.0	2.85	4.71	2.92	2.85	2.98
Mg II 2798	18.0	17.6	9.71	30.0	33.8	34.6
Si III] 1892	-	14.6	15.7	11.6	12.2	12.6
Si IV 1397	5.5	14.2	9.77	8.54	7.60	7.75
Fe II	23.9	9.58	11.3	13.6	15.5	13.2
Fe K α		2.11	1.74	1.78	1.81	1.80

Table 15 gives the spectrum of the Kwan and Krolik (1981) standard model, called **kk.in** in the test suite.

⁸Line intensity in $\text{erg s}^{-1} \text{cm}^{-2}$. The entries which follow are relative to a scale where $\text{Ly}\alpha=100$.

10.10 Rees, Netzer, and Ferland, low density

This is the lower density model listed in Table 1 of Rees et al. (1989). It is `rnfa.in` in the sample input streams.

Table 16 Rees, Netzer, and Ferland, low density case.

	1989	90.05	94.00	95.00	Ion
log n = 10					
L α	1.000	100	100	100	1.000
H β	0.030	2.76	3.18	3.44	0.026
H α	0.197	13.0	12.1	12.5	0.180
P α	0.022	1.45	1.43	1.31	0.020
Ba C	0.127	13.3	12.1	12.9	0.125
Pa C	0.052	5.01	4.54	4.90	0.025
ff	0.082	8.38	8.24	8.61	0.089
HeI 5876	0.007	0.656	0.584	0.623	0.008
HeII 4686	0.005	0.39	0.392	0.397	0.004
HeII 1640	0.039	3.44	3.38	3.42	0.034
CII 1335	0.009	1.04	1.00	0.880	0.008
CII] 2326	0.014	1.05	0.96	1.59	0.011
CIII 977	0.030	2.59	2.52	2.58	0.035
CIII] 1909	0.106	9.91	9.66	9.96	0.103
CIV 1549	0.424	44.8	42.9	42.3	0.453
NIII] 1750	0.012	1.31	1.26	1.06	0.014
NIV] 1486	0.009	1.19	1.14	1.13	0.009
NV 1240	0.002	0.235	0.22	0.225	0.003
OI 1304	0.033	0.91	0.915	1.27	0.013
OI 8446	0.005	0.0579	0.064	0.066	0.005
OIII] 1663	0.055	6.17	5.92	6.00	0.060
OIV] 1402	0.011	1.41	1.35	1.18	0.017
Mg II 2798	0.076	19.2	18.4	21.5	0.160
SIII 1207	0.012	1.04	1.05	1.07	0.013
SIII] 1892	0.085	8.56	8.51	9.13	0.090
SIV 1397	0.048	4.47	4.10	4.16	0.044
FeII	0	1.79	2.77	3.46	0.052
K α	0	0.098	0.102	0.103	0.001
sum	2.492	254.2169	248.787	255.764	2.602
L α	4.85E+07	4.54+07	4.42+7	4.39	4.55+07
I(total)	6.03E+07	1.15+8	1.09+8		6.02+07

10.11 Rees, Netzer, and Ferland, high density

Table 17 Rees, Netzer, and Ferland, high density case.

	1989	90.05	94.00	96.00	Ion
log n = 12					
L α	1.000	100	100	100	1.000
H β	0.063	1.99	1.66	1.62	0.054
H α	0.175	5.87	3.00	2.94	0.134
P α	0.009	0.45	0.22	0.212	0.008
Ba C	2.938	230	234	233	2.680
Pa C	1.313	104	104	107	0.590
ff	1.563	114	120	119	1.300
HeI 5876	0.038	3.13	3.42	3.27	0.032
HeII 4686	0.030	2.78	2.76	2.69	0.017
HeII 1640	0.266	17.5	18.3	17.8	0.140
CII 1335	0.082	4.67	4.84	4.34	0.099
CII] 2326	0.003	0.14	0.18	0.312	0.002
CIII 977	0.225	9.95	11.5	11.2	0.150
CIII] 1909	0.023	0.85	0.92	0.895	0.014
CIV 1549	0.938	55.4	62.7	59.9	0.860
NIII] 1750	0.006	0.26	0.28	0.182	0.004
NIV] 1486	0.006	0.35	0.36	0.341	0.004
NV 1240	0.031	2.15	2.34	2.20	0.021
OI 1304	0.033	2.01	1.98	2.05	0.028
OI 8446	0.006	0.26	0.27	0.276	0.005
OIII] 1663	0.039	1.77	1.90	1.82	0.024
OIII 835	0.041	1.90	0.043	2.03	0.002
OIV] 1402	0.023	1.62	1.69	1.60	0.020
Mg II 2798	0.088	12.6	13.6	13.0	0.170
SiIII 1207	0.088	4.46	4.70	4.37	0.068
SiIII] 1892	0.113	3.37	3.72	6.79	0.061
SiIV 1397	0.300	17.5	18.9	18.3	0.230
FeII		0.77	0.99	0.832	0.015
K α		0.38	0.42	0.405	0.003
sum	8.188	700.13	718.693	718.375	7.521
L α	8.54+08	1.17+09	1.08+09	1.11+09	1.08+09
I(total)	7.00+09	8.19+09	7.74+09		7.04+09

This is the higher density model listed in Table 1 of Rees et al. (1989). It is **rnfb.in** in the sample input streams.

11 THE TEST SUITE

The code must be completely tested every time anything is changed (Ferland 2001b). This is done with the test suite that is included in the distribution. In versions 90 and before this section listed all the test cases and discussed the motivations for each. Now each input file is self-descriptive, and should be consulted to use as examples and understand how the code is run.

The test suite contains a series of Perl scripts that automate several tasks. The *readme_tests.htm* file included with the tests describes these. The script *doc_tsuite.pl* extracts the test names and the description of each, and creates two files, *doc_tsuite.html*, a formatted description of each test, and *doc_tsuite.txt*, the table that follows this discussion. Column 1 of the following table lists the name of each test case and the second column gives a brief description of it.

This list is generated with the

Table 18 The single-model standard test cases

<i>agn_blr_albedo.in</i>	measure rayleigh scattering of Ly α
<i>agn_reflector.in</i>	model of Compton reflector
<i>agn_warm_absorber.in</i>	simple warm absorber model
<i>aperture_beam_int.in</i>	test aperture beam command with intensity
<i>aperture_beam_lum.in</i>	test aperture beam command with luminosity
<i>aperture_slit.in</i>	test aperture slit command with luminosity
<i>blr_f92.in</i>	standard blr cloud in Ferland et al. 1992
<i>blr_fp89.in</i>	final F+P 1989 BLR model table 3
<i>blr_hizqso.in</i>	high Z quasar cloud
<i>blr_kk81.in</i>	old blr
<i>blr_level2.in</i>	test dominant blr_level2 lines
<i>blr_n09_p18.in</i>	BLR model, density 1e09 cm ⁻³ , flux of H-ion photos 1e18 cm ² s ⁻¹
<i>blr_n09_p18_Z20.in</i>	BLR model, density 1e09 cm ⁻³ , flux of H-ion photos 1e18 cm ² s ⁻¹ , Z = 20
<i>blr_n09_p20.in</i>	BLR model, density 1e09 cm ⁻³ , flux of H-ion photos 1e20 cm ² s ⁻¹
<i>blr_n09_p20_Z20.in</i>	BLR model, density 1e09 cm ⁻³ , flux of H-ion photos 1e20 cm ² s ⁻¹
<i>blr_n09_p22.in</i>	BLR model, density 1e09 cm ⁻³ , flux of H-ion photos 1e20 cm ² s ⁻¹
<i>blr_n09_p22_Z20.in</i>	BLR model, density 1e09 cm ⁻³ , flux of H-ion photos 1e22 cm ² s ⁻¹
<i>blr_n11_p20.in</i>	BLR model, density 1e11 cm ⁻³ , flux of H-ion photos 1e20 cm ² s ⁻¹
<i>blr_n11_p20_Z20.in</i>	BLR model, density 1e11 cm ⁻³ , flux of H-ion photos 1e20 cm ² s ⁻¹ , Z=20
<i>blr_n12_p19.in</i>	BLR model, density 1e12 cm ⁻³ , flux of H-ion photos 1e19 cm ² s ⁻¹
<i>blr_n12_p19.in</i>	BLR cloud for standard grid
<i>blr_n12_p19_Z20.in</i>	BLR model, density 1e12 cm ⁻³ , flux of H-ion photos 1e19 cm ² s ⁻¹ , Z=20
<i>blr_n13_p18.in</i>	BLR model, density 1e13 cm ⁻³ , flux of H-ion photos 1e18 cm ² s ⁻¹
<i>blr_n13_p18_Z20.in</i>	BLR model, density 1e13 cm ⁻³ , flux of H-ion photos 1e18 cm ² s ⁻¹
<i>blr_n13_p22.in</i>	BLR model, density 1e13 cm ⁻³ , flux of H-ion photos 1e22 cm ² s ⁻¹
<i>blr_n13_p22_Z20.in</i>	BLR model, density 1e13 cm ⁻³ , flux of H-ion photos 1e18 cm ² s ⁻¹
<i>blr_nf84.in</i>	early model of blr
<i>blr_nf84_45deg.in</i>	early model of BLR, with illumination at 45 degree angle
<i>blr_rnfa.in</i>	table 1 of Rees et al. ApJ 347, 648
<i>blr_rnfb.in</i>	table 1 of Rees et al. ApJ 347, 648
<i>c6_caseb.in</i>	c6_caseb C VI case B
<i>coll_coronal.in</i>	model of active region of solar corona
<i>coll_t4.in</i>	coronal equilibrium at 10 ⁴ K
<i>coll_t5.in</i>	coronal equilibrium at 10 ⁵ K

coll_t6.in	coronal equilibrium at 10^6 K
coll_t7.in	coronal equilibrium at 10^7 K
feii_hin.in	test feii in high density limit
feii_hirad.in	feii in case of high radiation density limit
feii_pump.in	test feii in continuum pumped limit
feii_ste.in	thermal equilibrium of FeII in STE limit
func_distance.in	check that distance and "print flux earth" commands work
func_globule.in	test of globule command
func_hotgas_coolstar.in	test very soft continuum, very hot gas
func_ion_increase.in	test model where ionization increases with depth
func_map.in	map of heating vs cooling
func_set_ion.in	test impact of setting ionization
func_stopline.in	test stop line command
func_test.in	this runs the standard, one command, test, which contains many asserts
func_trans_punch.in	first of func_trans_punch/transread pair, punch continuum
func_trans_read.in	first of transpunch/transread pair, punch continuum
grains_hot.in	test temperature of gas and dust in high energy density environment
grains_lte.in	check that grains equilibrate at correct temp in ste limit
grains_qheat.in	cool atomic ISM with Si grain quantum heating
grains_temp.in	test all grain species temperature
grains_temp_all.in	test all grain species temperature
h2_cr.in	background cosmic ray ionization by suprathemal electrons only
h2_t500.in	test large H2 molecule in PDR-like conditions
h_casea.in	case A
h_caseb_lon.in	low density case b
h_caseb_lot.in	log density case B, $T=5000$, $\log n=2$
h_caseb_n8.in	h_caseb_n8 high density case B
h_casebn2.in	log density case B, $T=5000$, $\log n=2$
h_casec.in	case C
h_induc.in	constant temper black body limit from Ferland and Rees 1988
h_lrg_atom.in	h_lrg_atom case B with largest possible H atom
h_lym_thin.in	H only optically thin in Lyman continuum
h_otsopen.in	test ots, inward fractions for pure hydrogen, open geo, filling factor
h_otspp.in	plane parallel conservation and hydrogenic emission for pure hydrogen
h_otssp.in	spherical conservation and hydrogenic emission for pure hydrogen
h_outopen.in	test inward fractions, open geo, filling factor, 2-photon emission
h_outpp.in	plane parallel H-only, close, test hydrogenic emission
h_outsp.in	spherical conservation and hydrogenic emission for pure hydrogen
h_t4_conemis.in	test continuous emission from model H atom
h_t4_conemis.in	punch continuum "h_t4_conemis.con" last no units microns
h_t4_conemis.in	punch spectrum "h_t4_conemis.ncon" last no units microns
h_t4_conemis_lon.in	test low-den continuous emission from H atom, 2-nu is important
h_t4_conemis_thick.in	test hydrogen atom continuous emissivity, used for plot in hazy
he1n2t4.in	test hei atom vs Benjamin et al. 99
he1n2t4_best.in	test hei atom vs Benjamin et al. 99
he1n2t4_Smits96.in	test hei atom vs Smits 96
he1n4t4.in	test hei atom vs Benjamin et al. 99
he1n4t4.in	punch diffuse continuum "he1n4t4.dif" last no units microns
he1n4t4.in	punch continuum "he1n4t4.con" last no units microns
he1n4t4_best.in	the best we can do to predict the HeI emission spectrum
he1n4t4_best.in	punch diffuse continuum "he1n4t4_best.dif" last no units microns
he1n4t4_best.in	punch continuum "he1n4t4_best.con" last no units microns
he1n6t4.in	test hei atom vs Benjamin et al. 99
he1n6t4_best.in	test hei atom vs Benjamin et al. 99
he1n6t4_Smits96.in	test hei atom vs Smits 96

he2_caseb.in	he2_caseb He II case B
heatomt10.in	continuous emission from HeI
heatomt10.in	punch spectrum "heatomt10.spc" last no units microns
heatomt10.in	punch continuum "heatomt10.con" last no units microns
heatomt10.in	punch diffuse continuum "heatomt10.dif" last no units microns
heatomt10lon.in	test low-den continuous emission from H atom, 2-nu is important
heiont10.in	continuous emission from HeII
heiont10.in	punch continuum "heiont10.con" last no units microns
heiont10.in	punch spectrum "heiont10.spc" last no units microns
helike_ar.in	test he-like argon ion
helike_c.in	test he-like carbon ion
helike_fe.in	test he-like iron ion
helike_mg.in	test he-like magnesium ion
helike_n.in	test he-like nitrogen ion
helike_ne.in	test he-like neon ion
helike_o.in	test he-like oxygen ion vs. Bautista & Kallman 2000 Table 1, column 3
helike_si.in	test he-like silicon ion
hhe_otssp.in	plane parallel conservation and hydrogenic emission for pure H, He
hhe_otssp.in	spherical conservation and hydrogenic emission for hydrogen and helium
hhe_outpp.in	plane parallel conservation and H, He emission for pure H, He gas
hhe_outppff.in	plane parallel filling factor for pure H, He gas
hhe_outsp.in	spherical conservation and hydrogenic emission for hydrogen and helium
hii_blister.in	conditions similar to Orion nebula hii_blister
hii_coolstar.in	cool HII region model from Lexington Meeting
hii_icf.in	HII region with negative He/H ICF
hii_paris.in	"New" Paris meeting HII region
igm_alpha.in	Ly alpha forest cloud
igm_primal.in	cloud with primordial abundances exposed to background at Z=10
igm_z3.in	redshift 1000 recombination epoch
ism.in	interstellar cloud irradiated by ism background
ism_cosmicray.in	background cosmic ray ionization by suprathermal electrons only
ism_hot_brems.in	generate continuum due to hot ism in high Z,z starburst
ism_hot_brems.in	punch continuum last "ism_hot_brems.con" no title, units keV
ism_jura.in	check rate H2 forms on grain surfaces
ism_opacity.in	generate standard ISM opacity curve
limit_compton_hi_t.in	compton exchange in high temper limit
limit_compton_lo_t.in	compton exchange near low temperature limit
limit_compton_mid_t.in	Compton limit, test continuum partition
limit_conserve.in	test that energy is limit_conserved
limit_eden.in	Martin Gaskell's funny model
limit_laser_1.in	test of H ionization in optically thin limit
limit_laser_2.in	test of H and HeI ionization in optically thin limit
limit_laser_200.in	test of ionization in optically thin Auger-dominated limit
limit_laser_200_low.in	test of ionization in optically thin Auger-dominated limit
limit_laser_3.in	test of H, HeI, and HeII ionization in optically thin limit
limit_lowd0.in	test low density limit, this and lowdm6 should get same results
limit_lowden.in	test optically thin model that extends to very low densities
limit_lowdm6.in	test low density limit, this and limit_lowdm6 should get same results
limit_lowion_low.in	test conditions of very low ionization matrix/simple solver
limit_lowion_pops.in	test conditions of very low ionization matrix/simple solver
limit_lte_h_t50_cion.in	test collisional ionization only, no excitation, should be in lte
limit_lte_h_t50_coll.in	test collisional excitation only, very high density to force H to LTE
limit_lte_he1_coll.in	test hei atom at high densities
limit_lte_hhe.in	thermal equil black body limit from Ferland and Rees 1988
limit_lte_hhe_coll_t50.in	high electron density approach to lte

limit_lte_hhe_induc.in	half H, He gas with induced BF processes dominate
limit_lte_hminus.in	hminus test of lte
limit_lte_metal.in	thermodynamic equilibrium with metals
limit_recoil_ion.in	test compton recoil ionization of hydrogen
limit_strom.in	check pure hydrogen Stromgren sphere
limit_supra.in	test very high levels of secondary ionization, like SN envelope
limit_vbhum.in	test against Van Blerkom and Hummer, fig 4
limit_veryfast.in	very fast dusty windy model
limit_veryveryfast.in	very fast model for running with debuggers
limit_wind.in	test of equations of motion in a wind
lines.in	create output file with list of lines
nlr_lex00.in	Hagai's nlr_lex00 model for Lexington Meeting
nlr_liner.in	nlr_liner model
nlr_liner_grains.in	liner model with grains
nlr_paris.in	paris meeting NLR model
nova_dqher.in	(roughly) Ferland et al. DQ Her model
nova_photos.in	dense nova_photos shell
o8_caseb.in	o8_caseb O VIII case B
optimal.in	test optimizers, spectrum computed with hden 5, temp 4
optimize_amoeba.in	test optimizers, spectrum computed with hden 5, temp 4
optimize_phymir.in	test optimizers, spectrum computed with hden 5, temp 4
optimize_powell.in	test optimizers, spectrum computed with hden 5, temp 4
optimize_subplex.in	test optimizers, spectrum computed with hden 5, temp 4
orion_hii_dist_grn.in	conditions similar to Orion nebula blister
orion_hii_pdr.in	constant gas pressure orion into pdr
orion_hii_pdr_fast.in	constant gas pressure orion into pdr
orion_hii_pdr_pp.in	constant pressure orion into pdr
orion_hii_single_grn.in	conditions similar to Orion nebula blister
orion_wind.in	Orion nebula blister with wind
pdr_co_fully.in	test case where H2 and CO go into fully molecular limit
pdr_HTT91.in	Hollenbach et al. 1991 low-density PDR
pdr_leiden_f1.in	model 1 as defined in e-mail
pdr_leiden_f2.in	model 2 as defined in e-mail
pdr_leiden_f3.in	model 3 as defined in e-mail
pdr_leiden_f4.in	model 4 as defined in e-mail
pdr_leiden_hack_f1.in	model 1 as defined in e-mail
pdr_leiden_hack_f2.in	model 2 as defined in e-mail
pdr_leiden_hack_f3.in	model 3 as defined in e-mail
pdr_leiden_hack_f4.in	model 4 as defined in e-mail
pdr_leiden_hack_v1.in	model 5 as defined in e-mail
pdr_leiden_hack_v2.in	model 6 as defined in e-mail
pdr_leiden_hack_v3.in	model 7 as defined in e-mail
pdr_leiden_hack_v4.in	model 8 as defined in e-mail
pdr_leiden_v1.in	model 5 as defined in e-mail
pdr_leiden_v2.in	model 6 as defined in e-mail
pdr_leiden_v3.in	model 7 as defined in e-mail
pdr_leiden_v4.in	model 8 as defined in e-mail
pdr_orion_veil.in	model like Orion's veil
pdr_th85ism.in	Tielens and Hollenbach pdr model with ism grains, Table 2, paper b
pdr_th85orion.in	Tielens and Hollenbach pdr model with orion grains, Table 2, paper b
pn_fluc.in	Paris meeting Planetary nebula with density fluctuations
pn_ots.in	Paris meeting Planetary nebula with ots
pn_paris.in	pn_paris.in Meudon Planetary nebula
pn_paris_fast.in	pn_paris_fast.in Meudon Planetary nebula
pn_sqrden.in	test with density falling as R^{-2} , and filling factor

11 THE TEST SUITE

stars_atlas.in	Model of a Compact HII Region
stars_costar.in	test costar continuum
stars_costarhalo.in	test costar halo abundances continuum
stars_rauch.in	hot PN model
stars_rauchold.in	very hot PN model
stars_starburst99.in	demonstate use of Starburst 99 spectrum
stars_werner.in	test run with Werner stellar atmosphere

12 REFERENCES

- Abbott, D. C. 1982, ApJ, 259, 282
- Adams, T. 1972, ApJ, 174, 439
- Aldrovandi, S., & Péquignot, D. 1972, A&A, 17, 88
- Aldrovandi, S., & Péquignot, D. 1974, Revista Brasileira de Fisica, 4, 491
- Ali, B., Blum, R. D., Bumgardner, T. E., Cranmer, S. R., Ferland, G. J., Haefner, R. I., & Tiede, G. P. 1991, PASP, 103, 1182
- Allen, C. W. 1976, *Astrophysical Quantities*, Third Edition (London: Athlone Press)
- Allende Prieto, C., Lambert, D.L., & Asplund, M., 2001, ApJ, 556, L63
- Allende Prieto, C., Lambert, D.L., & Asplund, M., 2002, ApJ, 573, L137
- Aller, L. H. 1984, in *Physics of Thermal Gaseous Nebulae*, (Dordrecht: Reidel)
- Aller, L. H., & Czyzak, S. J. 1983, ApJS, 51, 211.
- Anderson, H., Ballance, C.P., Badnell, N.R., & Summers, H.P., 2000, J Phys B, 33, 1255
- Arimoto, N., & Yoshii, Y. 1987, A&A, 173, 23
- Antonucci, Robert, 1993, ARA&A, 31, 473
- Aviv N., Barlow, T.A., Laor, A., Sargent, W.L.W., & Blandford, R.D. 1998, MNRAS 297, 990
- Armour, Mary-Helen, Ballantyne, D.R., Ferland, G.J., Karr, J., & Martin, P.G., 1999, PASP 111, 1251-1257
- Arnaud, M., & Raymond, J. 1992, ApJ, 398, 394
- Arnaud, M., & Rothenflug, R. 1985, A&AS, 60, 425
- Asplund, M., Grevesse, N., & Sauval, A.J. 2005, in *Cosmic Abundances as Records of Stellar Evolution and Nucleosynthesis*, ASP Conf Ser, F.N. Bash & T.G. Barnes, editors (astro-ph 0410214)
- Avni, Y., & Tananbaum, H. 1986, ApJ, 305, 83
- Avni, Y., Worrall, D. M., & Morgan, W. A. ApJ, 1995, 454, 673
- Avrett, E. H., & Loeser, R. 1988, ApJ, 331, 211
- Bahcall, J.H., & Kozlovsky, B.-Z. 1969, ApJ, 155, 1077
- Bajtlik, S., Duncan, R. C., & Ostriker, J. P. 1988, ApJ, 327, 570
- Bakes, E.L.O. & Tielens, A.G.G.M. 1994, ApJ, 427, 822
- Balbus, S. A., & McKee, C. F. 1982, ApJ, 252, 529
- Baldwin, J., Ferland, G. J., Martin, P. G., Corbin, M., Cota, S., Peterson, B. M., & Slettebak, A. 1991, ApJ, 374, 580
- Baldwin J. A., Ferland, G. J., Korista, K. T., Carswell, R., Hamann, F., Phillips, M., Verner, D., Wilkes, B., & Williams, R. E. 1996, ApJ, 461, 683
- Baldwin, J. A., Ferland, G. J., Korista, K. T., & Verner, D. 1995, ApJ, 455, L119
- Baldwin, J.A., Ferland, G.J., Korista, K.T., Hamann, F., & Dietrich, M. 2003, ApJ, 582, 590
- Baldwin, J.A., Verner, E.M., Verner, D.A., Ferland, G.J., Martin, P.G., Korista, K.T., & Rubin, R. H., 2000, ApJS, 129, 229-246
- Baldwin, J., Wampler, J., & Gaskell, C. M. 1989, ApJ, 338, 630
- Balick, B., Gammon, R. H., & Hjellming, R. 1974 PASP, 86, 616
- Ballantyne, D.R., Ferland, G.J., & Martin, P.G., 2000, ApJ 536, 773-777
- Bässgen, G., Bässgen, M., & Grewing, M. 1988, A&A, 200, 51
- Bates, D. R., Kingston, A. E., & McWhirter, R. W. P. 1962, Proc R Soc, A267, 297
- Bechtold, J., Weymann, R. J., Lin, Z., & Malkan, M. A. 1987, ApJ, 315, 180
- Behar, E., Sako, M, Kahn, S.M., 2001, ApJ, 563, 497-504
- Behar, E., & Netzer, H., 2002, ApJ, 570, 165-170
- Bell, K. L., Kingston, A. E., & McIlveen, W. A. 1975, J. Phys. B 8, 358
- Benjamin, Robert A., Skillman, Evan D., & Smits, Derek P., 1999, ApJ, 514, 307
- Berger, M. J., & Seltzer, S. M. 1965, NASA SP-3012
- Bergeron, J., & Collin-Souffrin, S. 1971, A&A, 14, 167
- Berrington, K., & Pelan, A. 1995, A&AS, 114, 367
- Bertoldi, F., & Draine, B. T. 1996, ApJ, 458, 222
- Bethe, H. 1930, Ann. Phys. 5, 325
- Bica, E. 1988, A&A, 195, 76

- Bieniek, R. J., & Dalgarno, A. 1979, ApJ, 228, 635
- Binette, L., Prieto, A., Szuszkiewicz, E., & Zheng, W. 1989, ApJ, 343, 135
- Black, J. H. 1978, ApJ, 222, 125
- Black, J. H. 1987, in *Interstellar Processes*, ed. D.J. Hollenbach & H.A. Thronson, (Dordrecht: Reidel), p 731
- Bohm, D., & Aller, L. H. 1947, ApJ, 105, 131
- Bonihala, J. R. M., Ferch, R., Salpeter, E. E., Slater, G., & Noerdlinger, P. 1979, ApJ, 233, 649
- Borkowski, K. J., & Harrington, J. P. 1991, ApJ, 379, 168
- Bottorff, M., Lamothe, J., Momjian E., Verner, E., Vinkovic, D. & Ferland, G. 1998 PASP, 110, 1040
- Bottorff, M. C., Ferland, & Gary J., 2000, MNRAS 316, 103-106
- Bottorff, Mark & Ferland, Gary 2001a, ApJ, 549, 118-132
- Bottorff, M. C., Ferland, & Gary J., 2002, ApJ 568, 581-591
- Bottorff, Mark, Ferland, Gary, Baldwin, Jack, & Korista, Kirk, 2000, ApJ, 542, 644-654
- Boyd, R., & Ferland, G.J. 1987, ApJ, 318, L21
- Bowen, I. S. 1960, ApJ, 132, 1
- Bray, I., Burgess, A., Fursa, D.V., & Tully, J.A., 2000, A&AS, 146, 481
- Bregman, J. D., Allamandola, L. J., Tielens, A. G. G. M., Geballe, T. R., & Witteborn, F. C. 1989, ApJ, 344, 791
- Broad, J. T., & Reinhardt, W. P. 1976, Phys Rev A 14, 2159
- Brocklehurst, M., 1970, MNRAS, 148, 417
- Brocklehurst, M., 1972, MNRAS, 157, 211
- Brooks, Frederick P., 1995, *The Mythical Man-Month, Essays on Software Engineering*, (Reading: Addison-Wesley)
- Brown, R. L., & Mathews, W. G. 1970, ApJ, 160, 939
- Burgess, A. 1965, ApJ, 141, 1588
- Burgess, A., & Summers, H. P. 1969, ApJ, 157, 1007
- Burgess, A., & Summers, H. P. 1976, MNRAS, 174, 345
- Burgess, A., & Tully, J. A. 1992, A&A, 254, 436
- Butler, S. E., Bender, C. F., & Dalgarno, A. 1979, ApJ, 230, L59
- Butler, S. E., & Dalgarno, A. 1979, ApJ, 234, 765
- Butler, S. E., Heil, T. G., & Dalgarno, A. 1980, ApJ, 241, 442
- Butler, S. E., & Dalgarno, A. 1980, ApJ, 241, 838
- Callaway, J. 1994, At Dat Nuc Dat Tab 57, 9
- Cameron, A.G.W. 1982, in *Essays in Nuclear Astrophysics*, ed CA Barnes, DD Clayton, & DN Schramm, (Cambridge: Cambridge Univ Press)
- Canfield, R. C., & Puetter, R. C. 1980, ApJ, 236, L7
- Cardelli, J. A. 1994, Science 264, 209
- Cardelli, J. A., et al. 1991, ApJ, 377, L57
- Castor, J.I., Abbott, D.C., & Klein, R.I., 1975, ApJ, 195, 157-174
- Carswell R. F. & Ferland, G. J. 1988, MNRAS, 235, 1121
- Castor, J. I. 1970, MNRAS, 149, 111
- Cazaux, S., & Tielens, A.G.G.M., 2002, ApJ, 575, L29-L32
- Chaffee, F. H., & White, R. E. 1982, ApJS, 50, 169
- Chamerlain, J.W., 1956, ApJ, 124, 390
- Chan, E. S., Avrett, E. H., & Loeser, R. 1991, A&A, 247, 580
- Chapman, R. D., & Henry, R. J. W. 1971, ApJ, 168, 169
- Chidichimo, M. C. 1981, J. Phys. B., 14, 4149
- Clavel, J., & Santos-Lleo, M. 1990, A&A, 230, 3
- Clegg, R. E. S. 1987, MNRAS, 229, 31p
- Clegg, R. E. S., & Harrington, J. P. 1989, MNRAS, 239, 869
- Clegg, R.E.S., Storey, P.J., Walsh, J.R., & Neale, L. 1997, MNRAS, 284, 348
- Cohen, E. R., & Taylor, B. N. 1987, Rev Mod Phys 57, 1121
- Cota, S. A. 1987, Ph.D. Thesis, OSU
- Cota, S. A., & Ferland, G. J. 1988, ApJ, 326, 889
- Cowie, L. L., & Songaila, A. 1986, ARA&A 24, 499

- Cowling, T.G., 1976, *Magnetohydrodynamics*, (Hilger; Bristol)
- Craig, I.J.D., & Brown, J.C., 1986, *Inverse Problems in Astronomy* (Adam Hilger: Bristol)
- CrinkLaw, G., Federman, S. R., & Joseph, C. L. 1994, *ApJ*, 424, 748
- Crosas, M., & Weisheit, J.C. 1993, *MNRAS*, 262, 359
- Cruddace, R., Paresce, F., Bowyer, S., & Lampton, M. 1974, *ApJ*, 187, 497
- Cunto, W., Mendoza, C., Ochsenbein, F., Zeippen, C. J. 1993, *A&A* 275, L5
- Dalgarno, A., & Kingston, A. E. 1963, *Observatory*, 83, 39
- Dalgarno, A., & McCray, R. A. 1973, *ApJ*, 181, 95
- Dalgarno, A., & Roberge, W. G. 1979, *ApJ*, 233, L25
- Dalgarno, A., Yan, Min, & Liu, Weihong 1999, *ApJS*, 125, 237
- Davidson, K. 1972, *ApJ*, 171, 213
- Davidson, K. 1975, *ApJ*, 195, 285
- Davidson, K. 1977, *ApJ*, 218, 20
- Davidson, K., & Netzer, H. 1979, *Rep. Prog. in Physics* 51, 715
- Davidson, K., & Fesen, R.A. 1985, *ARA&A*, 23, 119
- de Jong, T., Chu, S-I., & Dalgarno, A. 1975, *ApJ*, 199, 69
- Deguchi, S., & Watson, W.D. 1985, *ApJ*, 290, 578-586
- Desert, F.-X., Boulanger, F., & Puget, J. L. 1990, *A&A*, 237, 215
- Dove, J. E., Rush, A., Cribb, P., & Martin, P. G. 1987, *ApJ*, 318, 379
- Dove, J. E., & Mandy, M. E. 1986, *ApJ*, 311, L93
- Draine, B. T. 1978, *ApJS*, 36, 595
- Draine, B.T., & Bertoldi, Frank, 1996, *ApJ*, 468, 269-289
- Draine, B. T., & Lee, H. M. 1984, *ApJ*, 285, 89
- Draine, B. T., & Salpeter, E. E. 1979, *ApJ*, 231, 77
- Draine, B. T., & Sultin, B. 1987, *ApJ*, 320, 803
- Drake, G., 1993, Chapt 3 in *Long Range Casimir Forces, theory and recent experiments on atomic systems*, edited by Levin & Mihca, Plenum Press
- Drake, G., 1996, *Atomic Molecular Physics Handbook*, ed by Gordon Drake (AIP Press,)
- Drake, S. A., & Ulrich, R.K. 1980, *ApJS*, 42, 351
- Dyson, J.E., & Williams, D.A. 1997, *The Physics of the Interstellar Medium* (Bristol; Institute of Physics Publishing)
- Elitzur, M. 1982, *Rev. Mod. Phys* 54, 1125
- Elitzur, M. 1984, *ApJ*, 280, 653
- Elitzur, M, 1992, *Astronomical Masers*, (Dordrecht: Kluwer)
- Elitzur, M., Ferland, G. J., Mathews, W. G., & Shields, G. 1983, *ApJ*, 272, L55
- Elitzur, M., & Ferland, G. J. 1986, *ApJ*, 305, 35
- Elvis, M. et al. 1994, *ApJS*, 95, 1
- Emerson, D. 1996, *Interpreting Astronomical Spectra*, (Chichester: John Wiley & Sons)
- Fabian, A. C., Pringle, J. E., & Rees M. J. 1976, *MNRAS*, 175, 43
- Federman, S.R., Glassgold, A.E., & Kwan, J. 1979, *ApJ*, 227, 466
- Federman, S. R., et al. 1993, *ApJ*, 413, L51
- Fenley, J.A., Taylor, K.T., & Seaton, M.J. 1987, *J. Phys. B.* 20, 6457-6476
- Ferguson, J. W., Ferland, G. J., & A. K. Pradhan, 1995, *ApJ*, 438, L55
- Ferguson, J. W., & Ferland, G.J. 1997, *ApJ*, 479, 363
- Ferguson, J. W., Korista, K. T., Baldwin, J. A., & Ferland, G. J. 1997, *ApJ*, 487, 122
- Ferguson, J W., Korista, Kirk. T., and Ferland, Gary J., 1997, *ApJS* 110, 287-297
- Ferguson, J W., Korista, Kirk. T., Verner, D.A., & Ferland, Gary J., 2001, *ASP Conference Series, Vol 247, Spectroscopic Challenges of Photoionized Plasmas*, G Ferland & D Savin, editors.
- Ferland, G. J. 1977, *ApJ*, 212, L21
- Ferland, G. J. 1979, *MNRAS*, 188, 669
- Ferland, G. J. 1980a, *MNRAS*, 191, 243
- Ferland, G. J. 1980b, *BAAS*, 12, 853
- Ferland, G. J. 1980c, *PASP*, 92, 596
- Ferland, G. J. 1986, *PASP*, 98, 549
- Ferland, G. J. 1986, *ApJ*, 310, L67

12 REFERENCES

- Ferland, G. J. 1992, ApJ, 389, L63 NIII
Ferland, G. J. 1993, ApJS, 88, 49
Ferland, G. J. 1999, PASP, 111, 1524
Ferland, G. J. 1999a, in Quasars and Cosmology, ASP 162, p 147 ed G Ferland & J Baldwin (astro-ph/0307450)
Ferland, G. J., 1999b, ApJ 512 247-249
Ferland, G.J., 2000, RMxAC, 9, 153
Ferland, G.J., 2001a, PASP, 113, 41
Ferland, G.J., 2001b, ASP Conference Series, Vol 247, *Spectroscopic Challenges of Photoionized Plasmas*, G Ferland & D Savin, editors (astro-ph/0210161)
Ferland, G.J., 2003a, in *Star formation through time*, 2003, by Gary J. Ferland, ASP Conf 297, E. Pérez, R.M. González Delgado, & G. Tenorio-Tagle, eds, p 69
Ferland, G.J., 2003b, ARA&A, 41, 517
Ferland, G. J., Baldwin J. A., Korista, K. T., Hamann, F., Carswell, R., Phillips, M., Wilkes, B., & Williams, R. E. 1996, ApJ, 461, 683
Ferland, G., Binette, L., Contini, M., Harrington, J., Kallman, T., Netzer, H., Péquignot, D., Raymond, J., Rubin, R., Shields, G., Sutherland, R., & Viegas, S. 1995, in *The Analysis of Emission Lines*, Space Telescope Science institute Symposium Series, R. Williams & M. Livio, editors (Cambridge: Cambridge University Press)
Ferland, G. J., & Elitzur, M. 1984, ApJ, 285, L11
Ferland, G. J., Fabian, A. C., & Johnstone, R.M. 1994, MNRAS, 266, 399
Ferland, G. J., Fabian, A. C., & Johnstone, R.M. 2002, MNRAS, 333, 876
Ferland, G. J., Henney, W. J., Williams, R. J. R., Arthur, S. J. 2002, RMxAC, 12, 43
Ferland, G. J., Korista, K.T. & Peterson, B.M. 1990, ApJ, 363, L21
Ferland, G. J., Korista, K.T., Verner, D. A., & Dalgarno, A. 1997, ApJ, 481, L115
Ferland, G. J. Korista, K.T. Verner, D.A. Ferguson, J.W. Kingdon, J.B. Verner, & E.M. 1998, PASP, 110, 761
Ferland, G. J., Lambert, D. L., Netzer, H., Hall, D. N. B., & Ridgway, S. T. 1979a, ApJ, 227, 489
Ferland, G. J., Lambert, D. L., Slovak, M., Shields, G. A., & McCall, M. 1982, ApJ, 260, 794
Ferland, G. J., & Mushotzky, R. F. 1982, ApJ, 262, 564
Ferland, G. J., & Mushotzky, R. F. 1984, ApJ, 286, 42
Ferland, G. J., & Netzer, H. 1979, ApJ, 229, 274
Ferland, G. J., & Netzer, H. 1983, ApJ, 264, 105
Ferland, G. J., Netzer, H., & Shields, G. A. 1979, ApJ, 232, 382
Ferland, G. J., Peterson, B. M., Horne, K., Welsh, W. F., & Nahar, S. N. 1992, ApJ, 387, 95
Ferland, G. J., & Persson, S. E. 1989, ApJ, 347, 656
Ferland, G. J., & Rees, M. J. 1988, ApJ, 332, 141
Ferland, G. J., & Shields, G. A. 1978, ApJ, 226, 172
Ferland, G. J., & Shields, G. A. 1985, in *Astrophysics of Active Galaxies & Quasi-stellar Objects*, J.S. Miller, Ed.
Ferland, G. J., & Truran, J. W. 1981, ApJ, 244, 1022
Ferland, G. J., Williams, R. E., Lambert, D. L., Shields, G. A., Slovak, M., Gondhalekar, P. M., & Truran, J. W. 1984, ApJ, 281, 194
Field, G. B. 1965, ApJ, 142, 431
Francis, P. J. 1993, ApJ, 407, 519
Friedrich, H. 1998, *Theoretical Atomic Physics*, (Berlin: Springer)
Fuhr, J. R., Martin, G. A., & Wiese, W. L. 1988, J. Phys. Chem. Ref. Data, 17, Suppl. 4
Gaetz, T. J., & Salpeter, E. E. 1983, ApJS, 52, 155
Garstang, R.H. 1958, MNRAS, 118, 57
Gavrila, M. 1967, Phys Rev 163, 147, also JILA Report #86, Sept 19, 1966
Ginzburg, V. I., & Syrovatskii, S. I. 1964, *The Origin of Cosmic Rays*, (Oxford: Pergamon)
Gould, R. S. 1978, ApJ, 219, 250
Grandi, S.A., 1975, ApJ, 196, 465
Grandi, S.A., 1975, ApJ, 199, 43
Grandi, S.A., 1976, ApJ, 206, 658

- Gredel, R., Lepp, S., & Dalgarno, A. 1987, ApJ, 323, L137
- Gredel, R., Lepp, S., Dalgarno, A., & Herbst, E. 1989, ApJ, 347, 289
- Greenhouse, M., et al. 1993, ApJS, 88, 23
- Grevesse, N., & Anders, E. 1989, *Cosmic Abundances of Matter*, AIP Conference Proceedings 183, p. 1, Ed. C. J. Waddington, (New York: AIP)
- Grevesse, N. & Noels, A. 1993 in *Origin & Evolution of the Elements*, ed. N. Prantzos, E. Vangioni-Flam, & M. Casse p. 15 (Cambridge: Cambridge Univ. Press)
- Grevesse, N., & Sauval, A.J., 1998, Space Science Review, 85, 161-174
- Guhathakurta, P., & Draine, B. T. 1989, ApJ, 345, 230
- Guilbert, P. W. 1986, MNRAS, 218, 171
- Guilbert, P., & Rees, M. J. 1988, MNRAS, 233, 475
- Haardt, Francesco, & Madau, Piero, 1996, ApJ, 461, 20
- Habing, H. J. 1968, Bull. Astr. Inst. Netherlands 19, 421
- Habart, E. Boulanger, F. Verstraete, L. Walmsley, C.M., & Pineau des Forets G., 2003, A&A in press, astro-ph/ 0311040
- Halpern, J. P., & Grindlay, J. E. 1980, ApJ, 242, 1041
- Hamann, F., & Ferland, G. J. 1992, ApJ, 391, L53
- Hamann, F., & Ferland, G. J. 1993, ApJ, 418, 11
- Hamann, F., & Ferland, G. J. 1999, ARAA, 37, 487
- Harrington, J. P. 1969, ApJ, 156, 903
- Harrington, J. P. 1973, MNRAS, 162, 43
- Hauschildt, P.H., & Baron, E., 1999, J. Comp. Appl. Math, 109, 41-63
- Heitler, W. 1954, *The Quantum Theory of Radiation* (Oxford: Oxford University Press)
- Hilborn, Robert C., 1982, American Journal of Physics, 50, 982-986, erratum, 51 471
- Hjellming, R. M. 1966, ApJ, 143, 420
- Hollenbach, D., & McKee, C. F. 1979, ApJS, 41, 555
- Hollenbach, D., & McKee, C. F. 1989, ApJ, 342, 306
- Hollenbach, D.J., Takahashi, T., & Tielens, A.G.G.M., 1991, ApJ, 377, 192-209
- Hollenbach, D.J., & Tielens, A. G. G. M. 1997, ARA&A, 35, 179
- Hollenbach, D.J., & Tielens, A.G.G.M. 1999, Rev Mod Phys 71, 173
- Holweger, H., 2001, Joint SOHO/ACE workshop "Solar and Galactic Composition". Edited by Robert F. Wimmer-Schweingruber. Publisher: American Institute of Physics Conference proceedings vol. 598 location: Bern, Switzerland, March 6 - 9, 2001, p.23
- Hubbard, E. N., & Puetter, R. C. 1985, ApJ, 290, 394
- Hubeny, I. 2001, Hubeny 2001 Spectroscopic Challenges of Photoionized Plasmas, ASP Conference Series Vol. 247. Edited by Gary Ferland and Daniel Wolf Savin. San Francisco: Astronomical Society of the Pacific, p.197
- Hummer, D. G. 1962, MNRAS, 125, 21
- Hummer, D. G. 1968, MNRAS, 138, 73
- Hummer, D. G. 1988, ApJ, 327, 477
- Hummer, D. G, Berrington, K. A., Eissner, W., Pradhan, A. K., Saraph H. E., Tully, J. A. 1993, A&A, 279, 298
- Hummer, D. G., & Kunasz, 1980, ApJ, 236, 609
- Hummer, D. G., & Seaton, M. J. 1963, MNRAS, 125, 437
- Hummer, D. G., & Storey, P. J. 1987, MNRAS, 224, 801
- Hummer, D. G., & Storey, P. J. 1992, MNRAS, 254, 277
- Hutchings, J.B. 1976, ApJ, 205, 103
- Ikeuchi, S., & Ostriker, J. P. 1986, ApJ, 301, 522
- Jackson, J. D. 1975, *Classical Electrodynamics* (New York: Wiley)
- Kaler, J., & Jacoby, G. 1991, ApJ, 372, 215
- Janev, R. K., Langer, W. D., Post, D. E., & Evans, K. 1987, *Elementary Processes in Hydrogen-Helium Plasmas* (Berlin: Springer-Verlag)
- Jenkins, E. B. 1987, in *Interstellar Processes*, D. Hollenbach & H. Thronson, Eds, (Dordrecht: Reidel), p.533
- Johnson, L. C. 1972, ApJ, 174, 227

- Johnstone, R. M., Fabian, A. C., Edge, A. C., & Thomas, P. A. 1992, MNRAS, 255, 431
- Jones, A.P., Tielens, A. G. G. M., & Hollenbach, D.J. 1996, 469, 740-764
- Jura, M., 1974, ApJ, 191, 375-379
- Jura, M., 1975, ApJ, 197, 575-580
- Kaler, J., 1978, ApJ, 220, 887
- Kallman, T. R., & McCray, R. 1982, ApJS, 50, 263
- Karzas, W. J., & Latter, R. 1961, ApJS, 6, 167
- Kaastra, J. S., & Mewe, R. 1993, A&AS, 97, 443
- Kato, T. 1976, ApJS, 30, 397
- Kellerman, K. I. 1966, ApJ, 146, 621
- Khromov, G. S. 1989, Space Science Reviews 51, 339
- Kingdon, J. B., & Ferland, G. J. 1991, PASP, 103, 752
- Kingdon, J. B., & Ferland, G. J. 1993, ApJ, 403, 211
- Kingdon, J. B., & Ferland, G. J. 1995, ApJ, 450, 691
- Kingdon, J. B., & Ferland, G. J. 1996, ApJS, 106, 205
- Kingdon, J. B., Ferland, G. J., & Feibelman, W.A. 1995, ApJ, 439, 793
- Kingdon J.B., & Ferland, G.J., 1998, ApJ 506, 323-328
- Kingdon, J. B., & Ferland, G. J. 1998, ApJ, 516, L107-109
- Korista, K. T., Baldwin, J. A., & Ferland, G. J. 1998, ApJ, 507, 24
- Korista, K. T., & Ferland, G. J. 1989, ApJ, 343, 678
- Korista, K. T., & Ferland, G. J. 1998, ApJ, 495, 672
- Korista, K. T., Ferland, G. J., & Baldwin, J. 1997, ApJ, 487, 555
- Kraemer, S.B., Ferland, G.J., & Gabel, J.R. 2004, ApJ in press
- Krolik, J., McKee, C. M., & Tarter, C.B. 1981, ApJ, 249, 422
- Kurucz, R. L. 1970, SAO Special Reports 309
- Kurucz, R. L. 1979, ApJS, 40, 1
- Kurucz, R. L. 1991, in *Proceedings of the Workshop on Precision Photometry: Astrophysics of the Galaxy*, ed. A. C. Davis Philip, A. R. Upgren, & K. A. James, (Schenectady: Davis), 27
- Kwan, J., & Krolik, J. 1981, ApJ, 250, 478
- Lambert, D. L., & Pagel, B. E. J. 1968, MNRAS, 141, 299
- La Franca, Franceshini, A., Cristiani, S., & Vio, R. 1995, A&A, 299, 19
- Lame N. J., & Ferland, G. J. 1991, ApJ, 367, 208
- LaMothe, J., & Ferland, G.J., 2001, PASP, 113, 165
- Landini, M., & Monsignori Fossi, B. 1990, A&AS, 82, 229
- Landini, M., & Monsignori Fossi, B. 1991, A&AS, 91, 183
- Lanzafame, A., Tully, J. A., Berrington, K. A., Dufton, P. L., Byrne, P. B., & Burgess, A. 1993, MNRAS, 264, 402
- Laor, A., & Draine, B. T. 1993, ApJ, 402, 441
- Latter, W. B., & Black, J. H. 1991, ApJ, 372, 161
- Lea, S., & Holman, G. 1978, ApJ, 222, 29
- Le Bourlot, J., 2000, A&A, 360, 656-662
- Leitherer, Claus; Schaerer, Daniel; Goldader, Jeffrey D.; Delgado, Rosa M. González; Robert, Carmelle; Kune, Denis Foo; de Mello, Duília F.; Devost, Daniel; Heckman, Timothy M. 1999, ApJS, 123, 3
- Lennon, D. J., & Burke, V. M. 1991, MNRAS, 251, 628
- Lenzuni, P., Chernoff, D. F., & Salpeter, E. E. 1991, ApJS, 76, 759
- Levich, E. V., & Sunyaev, R.A. 1970, Astrophysical Letters 7, 69
- Lepp, S., & Shull, J. M. 1983, ApJ, 270, 578
- Lightman, A. P., & White, T.R. 1988, ApJ, 335, 57
- Liske, J., 2000, MNRAS, 319, 557-561
- Lites, B. W., & Mihalas, D. 1984, Solar Physics 93, 23
- Liu, X.-W., Storey, P. J., Barlow, M. J., & Clegg, R. E. S. 1995, MNRAS, 272, 369
- Longair, M. S. 1981, *High Energy Astrophysics*, (Cambridge: Cambridge University Press)
- Lotz, W. 1967, ApJS, 14, 207
- Launay, J.R., Le Dourneuf, M., & Zeippen, C.J., 1991, A&A, 252, 842-852
- MacAlpine, G. M. 1971, ApJ, 175, 11

- Maguire, S. 1993, *Writing Solid Code*, (Redmond: Microsoft Press)
- Maguire, S. 1994, *Debugging the Development Process*, (Redmond: Microsoft Press)
- Mallik, D. C. V., & Peimbert, M. 1988, *Rev Mexicana* 16, 111
- Maloney, P.R., Hollenbach, D.J., & Tielens, A. G. G. M., 1996, *ApJ*, 466, 561
- Martin, P. G. 1979, *Cosmic Dust* (Oxford: Clarendon Press)
- Martin, P. G. 1988, *ApJS*, 66, 125
- Martin, P. G., & Ferland, G. J. 1980, *ApJ*, 235, L125
- Martin, P.G., & Rouleau, F., 1991, in Malina R.F., Bowyer S., eds, *Extreme Ultraviolet Astronomy*, Pergamon Press, Oxford, p. 341
- Martin, P. G., & Whittet, D. C. B. 1990, *ApJ*, 357, 113
- Masters, A. R., Pringle, J. E., Fabian, A. C., & Rees, M. J. 1977, *MNRAS*, 178, 501
- Mather, J.C., Fixsen, D.J., Shafer, R.A., Mosier, C., & Wilkinson, D.T. 1999, *ApJ*, 512, 511
- Mathews, W. G., Blumenthal, G. R., & Grandi, S. A. 1980, *ApJ*, 235, 971
- Mathews, W. G., & Ferland, G. J. 1987, *ApJ*, 323, 456
- Mathis, J. S. 1982, *ApJ*, 261, 195
- Mathis, J. S. 1985, *ApJ*, 291, 247
- Mathis, J. S., Rumpl, W., & Nordsieck, K. H. 1977, *ApJ*, 217, 425
- Mathis, J. S., & Wallenhorst, S. G. 1981, *ApJ*, 244, 483
- Matteucci, F., & Tornambe, A. 1987, *A&A*, 185, 51
- Matteucci, F., & Greggio, A. 1986, *A&A*, 154, 279
- Mazzotta, P., Mazzitelli, G., Colafrancesco, C., & Vittorio, 1998, *A&AS* 133, 403-409
- McKee, C. F. 1999, preprint, Astro-ph 9901370
- Mendoza, C. 1983, in *Planetary Nebulae*, IAU Sym 103, D. R. Flower, Ed., p 143, (Dordrecht: Reidel)
- Meyer, D.M., Jura, M., & Cardelli, J.A. 1998, *ApJ*, 493, 222-229
- Mewe, R. 1972, *A&A*, 20, 215
- Mihalas, D. 1972, *Non-LTE Model Atmospheres for B & O Stars*, NCAR-TN/STR-76
- Mihalas, D. 1978, *Stellar Atmospheres*, 2nd Edition (San Francisco: W.H. Freeman)
- Mihalszki, J. S., & Ferland, G. J. 1983, *PASP*, 95, 284
- Mohr P.J. & Taylor B.N., 1998 *Codata*, see *Reviews of Modern Physics*, Vol. 72, No. 2, 2000
- Morrison, R., & McCammon, D. 1983, *ApJ*, 270, 119
- Morton, D. C., York, D. G., & Jenkins, E. B. 1988, *ApJS*, 68, 449
- Nahar, S. N., & Pradhan, A. K. 1992, *ApJ*, 397, 729
- Netzer, H. 1990, in *Active Galactic Nuclei, Saas-Fee Advanced Course 20*, Courvorsier, T.J.-L., & Mayor, M., (Springer-Verlag; Berlin)
- Netzer, H., Elitzur, M., & Ferland, G. J. 1985, *ApJ*, 299, 752
- Netzer, H., & Ferland, G. J. 1984, *PASP*, 96, 593
- Neufeld, D. A. 1989, Harvard Research Exam
- Neufeld, D.A., 1990, *ApJ*, 350, 216
- Neufeld, D. A., & Dalgarno, A. 1989, *Phys Rev A*, 35, 3142
- Novotny, Eva, 1973, *Introduction to Stellar Atmospheres*, (New York; Oxford University Press)
- Nussbaumer, H., & Storey, P. J. 1983, *A&A*, 126, 75
- Nussbaumer, H., & Storey, P. J. 1984, *A&AS*, 56, 293
- Nussbaumer, H., & Storey, P. J. 1986, *A&AS*, 64, 545
- Nussbaumer, H., & Storey, P. J. 1987, *A&AS*, 69, 123
- O'Dell, C.R., 2001, *ARAA*, 39, 99
- Oliveira, S., & Maciel, W. J. 1986, *Ap&SS*, 126, 211
- Oliva, E., Pasquali, A., & Reconditi, M. 1996, *A&A*, 305, 210
- Olive, K.A., Steigman, G., & Walker, T.P., 2000, *Physics Reports*, 333-334, 389-407
- Osterbrock, D. E. 1951, *ApJ*, 114, 469
- Osterbrock, D. E. 1989, *Astrophysics of Gaseous Nebulae & Active Galactic Nuclei*, (Mill Valley; University Science Press)
- Osterbrock, D. E., & Flather, E. 1959, *ApJ*, 129, 26
- Osterbrock, D. E., Tran, H. D., & Veilleux, S. 1992, *ApJ*, 389, 305
- Ostriker, J. P., & Ikeuchi, S. 1983, *ApJ*, 268, L63
- Pacholczyk, A. G. 1970, *Radio Astrophysics* (San Francisco: Freeman)

- Pagel, B. E. J. 1997, *Nucleosynthesis and Chemical Evolution of Galaxies*, (Cambridge: Cambridge University Press)
- Palla, F., Salpeter, E. E., & Stahler, S. W. 1983, *ApJ*, 271, 632
- Peebles, P. J. E. 1971, *Physical Cosmology*, (Princeton: Princeton U. Press)
- Peimbert, M. 1967, *ApJ*, 150, 825
- Pengelly, R. M. 1964, *MNRAS*, 127, 145
- Pengelly, R.M., & Seaton, M.J., 1964, *MNRAS*, 127, 165
- Péquignot, D. 1986, *Workshop on Model Nebulae*, (Paris: l'Observatoire de Paris) p363
- Péquignot, D., & Aldrovandi, S.M.V. 1986, *A&A*, 161, 169
- Péquignot, D., Ferland, G.J., et al., in ASP Conference Series, Vol 247, *Spectroscopic Challenges of Photoionized Plasmas*, G Ferland & D Savin, editors
- Péquignot, D., Petitjean, P., & Boisson, C. 1991, *A&A*, 251, 680
- Péquignot, D., Stasinska, G., & Aldrovandi, S. M. V. 1978, *A&A*, 63, 313
- Percival, I.C., & Richards, D., 1978, *MNRAS*, 183, 329
- Peterson, B.M. 1993, *PASP*, 105, 247
- Peterson, J. R., Aberth, W., Moseley, J., & Sheridan, J. 1971, *Phys Rev A*, 3, 1651
- Pettini, M., & Bowen, D.V., 2001, *ApJ*, 560, 41
- Porquet, D., & Dubau, J. 2000, *A&AS*, 143, 495
- Prasad, S.S., & Huntress, W.T., 1980, *ApJS*, 43, 1-35
- Press W. H., Teukolsky, S.A., Vetterling, W. T., & Flannery, B. P. 1992, *Numerical Recipes*, (Cambridge: Cambridge University Press)
- Puetter, R. C. 1981, *ApJ*, 251, 446
- Puy, D., Alecian, G., Le Bourlot, J., Leorat, J., & Pineau des Forets, G. 1993, *A&A*, 267, 337
- Puy, D., Grenacher, L., & Jetzer, P., 1999, *A&A*, 345, 723
- Rauch, T. 1997 *A&A*, 320, 237
- Rauch, T. 2002, H-Ni grid, available at <http://astro.uni-tuebingen.de/~rauch>
- Raymond, J. C., Cox, D. P., & Smith, B. W. 1976, *ApJ*, 204, 290
- Rees, M. J., Netzer, H., & Ferland, G. J. 1989, *ApJ*, 347, 640
- van Regemorter, H. 1962, *ApJ*, 136, 906
- Rephaeli, Y. 1987, *MNRAS*, 225, 851
- Reilman, R. F., & Manson, S. T. 1979, *ApJS*, 40, 815, errata 46, 115; 62, 939
- Roberge, W. G., Jones, D., Lepp, S., & Dalgarno, A. 1991, *ApJS*, 77, 287
- Rossi, B. 1952, *High-Energy Particles* (New York; Prentice-Hall)
- Rouleau, F., & Martin, P.G. 1991, *ApJ*, 377, 526
- Rowan, T. 1990, *Functional Stability Analysis of Numerical Algorithms*, Ph.D. Thesis, Department of Computer Sciences, University of Texas at Austin
- Rubin, R. H. 1968, *ApJ*, 153, 671
- Rubin, R. H. 1983, *ApJ*, 274, 671
- Rubin, R. H. Martin, P. G. Dufour, R. J. Ferland, G. J Baldwin, J. A. Hester, J. J. & Walter, D. K. 1998, *ApJ*, 495, 891
- Rubin, R. H., Simpson, J. R., Haas, M. R., & Erickson, E. F. 1991, *ApJ*, 374, 564
- Rutten, Rob, 2002, Radiative transfer in stellar atmospheres, at <http://www.fys.ruu.nl/~rutten/node20.html>
- Rybicki, G. B., & Hummer, D. G. 1991, *A&A*, 245, 171
- Rybicki, G. B., & Hummer, D. G. 1992, *A&A*, 262, 209
- Rybicki, G. B., & Hummer, D. G. 1994, *A&A*, 290, 553
- Rybicki, G. B., & Lightman, A.P. 1979, *Radiative Processes in Astrophysics* (New York: Wiley)
- Sanders, D. B., et al. 1989, *ApJ*, 347, 29
- Saraph, H. E. 1970, *J.Phys.B.*, 3, 952
- Savage, B. D., & Sembach, K. R. 1996, *ARA&A*, 34, 279
- Savin, Daniel Wolf, 2000, *ApJ*, 533, 106
- Savin, D. W.; Kahn, S. M.; Linkemann, J.; Saghiri, A. A.; Schmitt, M.; Grieser, M.; Repnow, R.; Schwalm, D.; Wolf, A.; Bartsch, T.; Brandau, C.; Hoffknecht, A.; Müller, A.; Schippers, S.; Chen, M. H.; Badnell, N. R., 1999, *ApJS*, 123, 687
- Sciortino, S., et al. 1990, *ApJ*, 361, 621

- Scott, J. S., Holman, G. D., Ionson, J. A., & Papadopoulos, K. 1980, *ApJ*, 239, 769
- Schaerer D., de Koter, A., Schmutz, W., & Maeder, A. 1996ab, *A&A*, 310, 837, & *A&A*, 312, 475
- Schaerer D., & de Koter A. 1997, *A&A*, 322, 592
- Schuster, A. 1905, *ApJ*, 21, 1
- Schutte, W. A., Tielens, A. G. G. M., & Allamandola, L. J. 1993, *ApJ*, 415, 397
- Schwarzschild, M. 1965, *Structure & Evolution of the Stars*, (New York: Dover)
- Seaton, M. J. 1959, *MNRAS*, 119, 81
- Seaton, M. J. 1959, *MNRAS*, 119, 90
- Seaton, M. J. 1987, *J.Phys. B*, 20, 6363
- Sellgren, K., Tokunaga, A. T., & Nakada, Y. 1990, *ApJ*, 349, 120-125
- Sellmaier, F. H., Yamamoto, T., Pauldrach, A. W. A., & Rubin, R. H. 1996, *A&A*, 305, L37
- Shields, G. A. 1976, *ApJ*, 204, 330
- Shine, R. A., & Linsky, J. L. 1974, *Solar Physics* 39, 49
- Shull, J. M. 1979, *ApJ*, 234, 761
- Shull, J.M., & Beckwith, S. 1982, *ARA&A*, 20, 163
- Shull, J. M., & Van Steenberg, M. E. 1982, *ApJS*, 48, 95
- Shull, J. M., & Van Steenberg, M. E. 1985, *ApJ*, 298, 268
- Sellgren, K., Tokunaga, A. T., & Nakada, Y. 1990, *ApJ*, 349, 120
- Sellmaier, F.H., Yamamoto, T., Pauldrach, A.W.A., Rubin, R.H 1996, *A&A*, 305, 37
- Sikora, M., Begelman, M. C., & Rudak, B. 1989, *ApJ*, 341, L33
- Simonyi, C. 1977, *Meta-Programming: A Software Production Method*, Thesis, Stanford University
- Simpson, J. P. 1975, *A&A*, 39, 43
- Smits, D.P., 1996, *MNRAS*, 278, 683
- Snow, T. P., & Dodger, S. L. 1980, *ApJ*, 237, 708
- Snow, T. P., & York, D. G. 1981, *ApJ*, 247, L39
- Snow, T.P., & Witt, A. 1996, *ApJ*, 468, L65
- Spitzer, L. 1948, *ApJ*, 107, 6
- Spitzer, L. 1962, *Physics of Fully Ionized Gasses*, (New York: Interscience)
- Spitzer, L. 1978, *Physical Processes in the Interstellar Medium*, (New York: Wiley)
- Spitzer, L. 1985, *ApJ*, 290, L21
- Spitzer, L., & Tomasko, M. G. 1968, *ApJ*, 152, 971
- Stecher, T. P., & Williams, D. A. 1967, *ApJ*, 149, 29
- Sternberg, A., & Neufeld, D.A. 1999, *ApJ*, 516, 371-380
- Stoy, R. H. 1933, *MNRAS*, 93, 588
- Storey, P. J. 1981, *MNRAS*, 195, 27p
- Storey, P. J. 1994, *A&A*, 282, 999
- Storey, P. J., & Hummer, D. G. 1991, *Comput. Phys. Commun.* 66, 129
- Storey, P. J., & Hummer, D. G. 1995, *MNRAS*, 272, 41 (on the web at <http://adc.gsfc.nasa.gov/adc-cgi/cat.pl?/catalogs/6/6064/>)
- Suchkov, A., Allen, R.J., & Heckman, T. M. 1993, *ApJ*, 413, 542-547
- Swings, P., & Struve, O. 1940, *ApJ*, 91, 546
- Takahashi, Junko, 2001, *ApJ*, 561, 254-263
- Tarter, C. B., & McKee, C. F. 1973, *ApJ*, 186, L63
- Tarter, C.B., Tucker, W.H., & Salpeter, E.E., 1969, *ApJ*, 156, 943
- Tielens, A. G. G. M., & Hollenbach, D. 1985a, *ApJ*, 291, 722
- Tielens, A. G. G. M., & Hollenbach, D. 1985b, *ApJ*, 291, 746
- Tinsley, B. 1979, *ApJ*, 229, 1046
- Tout, C. A., Pols, O. R., Eggleton, P. P. & Han, Z. 1996, *MNRAS*, 281, 257
- Turner, J., & Pounds, K. 1989, *MNRAS*, 240, 833
- Van Blerkom, D., & Hummer, D. G. 1967, *MNRAS*, 137, 353
- Vegele, WM. J. 1973, *Atomic Data Tables*, 5, 51
- van Dishoeck, E.F., & Black, J.H., 1988, *ApJ*, 334, 771
- van Hoof, P. A. M. 1997, PhD Thesis, University of Groningen
- van Hoof, P.A.M., Beintema, D.A., Verner D.A., & Ferland, G.J., 2000a, *A&A* 354, L41-L44

- van Hoof, P.A.M., Van de Steene, G.C., Beintema, D.A., Martin, P.G., Pottasch, S.R., Ferland, G. J., 2000b, *ApJ* 532, 384-399
- van Hoof, P.A.M., Weingartner, J.C., Martin, P.G., Volk, K., & Ferland, G.J., 2001, in *Challenges of Photoionized Plasmas*, (G Ferland & D. Savin, eds) ASP Conf Ser 247, 363-378 (astro-ph/0107183)
- van Hoof, P.A.M., Weingartner, J.C., Martin, P.G., Volk, K., & Ferland, G.J., 2004, *MNRAS* in press (astro-ph/0402381)
- van Regemorter, H. 1962, *ApJ*, 136, 906
- Vedel, H., Hellsten, U., & Sommer-Larsen, J. 1994, *MNRAS*, 271, 743
- Vernazza, J. E., Avrett, E. H., & Loeser, C. B. 1981, *ApJS*, 45, 635
- Verner, D. A., Yakovlev, D. G., Band, I. M., & Trzhaskovshaya, M. B. 1993, *ADNDT*, 55, 233
- Verner, D. A., & Yakovlev, 1995, *A&AS*, 109, 125
- Verner, D. A., & Ferland, G. J. 1996, *ApJS*, 103, 467
- Verner, D. A., Ferland, G. J., Korista, K., & Yakovlev D. G. 1996, *ApJ*, 465, 487
- Verner, D. A., Verner, K., & Ferland, G. J. 1996, *ADNDT*, 64, 1
- Verner, E.M. Verner, D.A. Korista, K.T. Ferguson, J.W. Hamann, F. & Ferland, G.J. 1999, *ApJS* 120, 101
- Voronov, G. S. 1997, *ADNDT*, 65, 1
- Voit, G. M. 1991, *ApJ*, 377, 1158
- Volk, K., and Kwok, S. 1988, *ApJ*, 331, 435
- Vriens, L., & Smeets, A. H. M. 1980, *Phys Rev A*, 22, 940
- Vrinceanu, D. & Flannery, M. R. 2001, *PhysRevA* 63, 032701
- Watson, W. D. 1972, *ApJ*, 176, 103
- Weingartner, J.C., & Draine, B.T., 2001a, *ApJS*, 134, 263
- Weingartner, J.C., & Draine, B.T., 2001b, *ApJ*, 548, 296
- Weingartner, J.C., & Draine, B.T., 2001c, *ApJ*, 563, 842
- Weisheit, J. C. 1974, *ApJ*, 190, 735
- Weisheit, J. C., & Collins, L. A. 1976, *ApJ*, 210, 299
- Weisheit, J. C., & Dalgarno, A. 1972, *Astrophysical Letters*, 12, 103
- Weisheit, J., Shields, G. A., & Tarter, C. B. 1981, *ApJ*, 245, 406
- Wen, Z., & O'Dell, C.R. 1995, *ApJ*, 438, 784-793
- Werner, K., & Heber, U. 1991, in *Stellar Atmospheres: Beyond Classical Models*, p 341, NATO ASI Series C, eds. L. Crivellari, I. Hubney, & D. G. Hummer, (Dordrecht: Kluwer)
- White, R. E. 1986, *ApJ*, 307, 777
- Wiese, W.L., Fuhr, J.R., & Deters, T.M., 1996, *J Phys Chem Ref Data*, Monograph 7
- Wiese, W. L., Smith, M. W., & Glennon, B. M. 1966, *NSRDS-NBS* 4
- Wilkes, B. J., Ferland, G. J., Truran, J., & Hanes, D. 1981, *MNRAS*, 197, 1
- Wilkes, et al 1994, *ApJS*, 92, 53
- Wilkinson, D. T. 1987, in *13th Texas Symposium on Relativistic Astrophysics*, M. P. Ulmer, ed., (Singapore: World Scientific), p209
- Williams, J.P., Bergin, E.A., Caselli, P., Myers, P.C., & Plume, R. 1998, *ApJ*, 503, 689
- Williams, R. E. 1967, *ApJ*, 147, 556
- Williams, R. E. 1992, *ApJ*, 392, 99
- Wills, B., Netzer, H., & Wills, D. 1985, *ApJ*, 288, 94
- Wing, W.H., & MacAdam, K.B., 1978, in *Progress in Atomic Spectroscopy*, Part A, W. Hanle & H. Kleinpopper, eds
- Winslow, A. M. 1975, Lawrence Livermore Lab. report UCID-16854
- Wishart, A. W. 1979, *MNRAS*, 187, 59p
- Wolfire, M. G., Tielens, A., & Hollenbach, D. 1990, *ApJ*, 358, 116
- Worral et al. 1987, *ApJ*, 313, 596
- Wyse, A. B. 1941, *PASP*, 53, 184
- York, D. G., Meneguzzi, M., & Snow, T. 1982, *ApJ*, 255, 524
- Xu, Y., & McCray, R. 1991, *ApJ*, 375, 190
- Zamorani, G., et al. 1981, *ApJ*, 245, 357
- Zheng, W., Kriss, G.A., Telfer, R.C., Grimes, J.P. & Davidsen, A.F. 1997, *ApJ*, 475, 469
- Zuckerman, B. 1973, *ApJ*, 183, 863
- Zycki, P. T., Krolik, J. H., Zdziarski, A. A., & Kallman, T. R. 1994, 437, 597

Zygelman, B., & Dalgarno, A. 1990, ApJ, 365, 239

13 INDEX

— 2 —

21 cm
temperature with Ly α , 446

— A —

abundances
printed, 435
variables used, 412
alpha ox
printed, 433
apparent helium abundance, 447
atomic data references, 492

— B —

blister.in
predictions, 516
braces, 491
brightness temperature, 435
broken code, 493

— C —

cautions
printed, 442
routine to print, 427
cdCautions, 427
cdCO_colden, 423
cdColm, 422
cdDrive, 419
cdEms, 422
cdGett, 431
cdH2_colden, 423
cdInit, 417
cdIonFrac, 424
cdLine, 420
cdNoExec, 419
cdNotes, 428
cdNwcns, 427
cdOutp, 418
cdRead, 418
cdSurprises, 428
cdTalk, 418
cdTemp, 424
cdWarnings, 427
changes to code, 492
chemical composition
printed, 435
Cloudy
84 vs 80, 509
90 vs 84, 507
braces, 491
changes to code, 492
date, 426, 494
execution time, 426
flowchart, 401
history, 503
known modes, 510
making a revision, 510
revision history, 504
running 1 model, 415

search phase, 411
size, 503
structure, 401
version number, 426
version numbers, 494
CO
column densities, 423
coding conventions, 490
braces, 491
broken code, 493
changes to code, 492
characters, 491
exit handler, 493
fixit code, 493
insane code, 493
integers, 490
logical variables, 491
real numbers, 490
sanity checks, 492
strong typing, 490
test code, 493
TODO code, 493
column densities
CO, 423
H2, 423
column density
effective
printout, 446
excited state, 450
predicted, 458
printed, 450
total
printed, 437
comparison calculations, 512
Compton
cooling
output, 437
heating
output, 437
temperature
output, 434
timescale
output, 447
continuum
diffuse printed, 453
incident printed, 453
occupation number, 434
surface brightness, 455
ConvPresTempEdenIoniz
flowchart, 402
ConvTempEdenIoniz
flowchart, 402
coolcurve.for, 496
coolhii.in
predictions, 513
cooling
Compton, 437
error, 446
getting from code, 425

grain, 438
printout, 445
covering factor
computational details, 413
geometric, 413
radiative transfer, 413

— D —

date of code, 426
density
electron
evaluated, 409
output, 436
hydrogen
output, 436
particle, 409
structure
output, 444
structure saved, 410
density per particle, 409
dqher.in
predictions, 526

— E —

electron
density
evaluated, 409
saved, 410
emission line list, 460
emission measure, 446
H+, 446
He+, 446
He2+, 446
equivalent width
computing, 453
execution time, 448

— F —

file
BLRLineList.dat, 421
file buffering, 428
filling factor, 437, 446
fixit code, 493
floating point errors, 414
flowcharts, 401
Cloudy, 401
ConvPresTempEdenIoniz, 402
ConvTempEdenIoniz, 402
main, 401
Taulnc, 407
flux
converting to luminosity, 456

— G —

G0
printed, 445
gas
particle density, 409
geometry
closed, 444

- details, 407
 - open, 444
 - plane parallel, 442
 - printed, 442
 - spherical, 442
 - thick shell, 442
 - wind, 447
 - grain
 - abundances printed, 435
 - dust to gas ratio printed, 449
 - extinction per H printed, 449
 - mean charge printed, 449
 - mean drift velocity printed, 449
 - mean temperature printed, 449
 - ratio total to selective extinction printed, 449
- H —
- H2
 - column densities, 423
 - Hazy
 - printing, 510
 - heating
 - Compton, 434, 437
 - extra, 439
 - free-free, 446
 - getting from code, 425
 - grain, 438
 - photoelectric, 461
 - printout, 445
 - structure saved, 410
 - total, 436, 445
 - helium
 - printout
 - ionization, 437
 - lines, 464
 - Hungarian naming convention, 490
 - hydrogen
 - 21 cm mean temperature, 425
 - density
 - saved, 410
 - line intensities, 456
 - model printed, 448
- I —
- insane code, 493
 - iteration
 - last, 411
 - variables, 411
- J —
- Jeans length, 448
 - Jeans mass, 448
- K —
- kk.in
 - predictions, 527
 - kmt.for, 496
- L —
- line
 - profile, 459
 - line
 - asymmetries, 454
 - beaming, 454
 - continuum contrast, 454
 - continuum pumping contribution, 458
 - equivalent width, 453
 - intensities
 - with grains, 457
 - list
 - BLRLineList.dat, 421
 - radiation pressure
 - maximum printed, 446
 - printed, 436
 - stop, 439
 - standard list, 421
 - surface brightness, 455
 - transfer flowchart, 407
 - line
 - list, 460
 - line
 - intensities with grains, 460
 - line
 - wavelength convention, 460
 - line
 - output, 466
 - luminosity
 - converting to flux, 456
 - Ly α
 - temperature with 21 cm, 446
- M —
- main
 - flowchart, 401
 - map
 - output, 500
 - map.in, 496
 - mass of computed structure
 - printed, 447
 - molecular weight, 409
 - molecules
 - column densities, 422
 - printed, 438
 - Moore's Law, 503
- N —
- naming convention, 490
 - negative line intensities, 445
 - nlr.in
 - predictions, 524
 - notes
 - printed, 442
 - routine to print, 428
- O —
- observed quantities, 453
 - occupation number
 - continuum, 434
 - optical depth
 - output, 449
 - outward
 - first estimate, 410
 - incrementing, 410
 - reseting, 410
 - test for definition, 411
 - stopped because of, 441
 - updated, 411
 - optical to X-ray ratio, 433
 - output
 - apparent helium abundance, 446
 - cautions, 442
 - comments, 442
 - continuum, 452
 - emission lines, 444
 - header, 432
 - line, 466
 - map, 500
- P —
- Paris
 - H II region, 514
 - parishii.in
 - predictions, 514
 - parisnlr.in
 - predictions, 521
 - parispn.in
 - predictions, 518
 - particle density, 409
 - PDR
 - G0 printed, 445
 - Peimbert temperature fluctuations, 448
 - photoerosion, 447
 - plot
 - printed, 443
 - pressure
 - gas, 437
 - getting from code, 425
 - instability, 439
 - printed, 437
 - radiation, 436, 437, 438, 446
 - total, 437
 - printed, 437
 - producing a synthetic spectrum, 458
 - punch
 - line
 - contrast, 454
 - results
 - using, 431
- Q —
- quiet mode
 - setting, 418
- R —
- radiation pressure
 - maximum printed, 446
 - printed, 436
 - stop, 439
 - radiative acceleration
 - printed, 438
 - wind, 436
 - radius
 - saved, 410
 - Rayleigh scattering, 450
 - reageo, 427
 - redirecting output, 418
 - reflector.in
 - plotted, 454
 - revision history, 504
 - rfa.in
 - predictions, 528
 - rnf.in
 - predictions, 529
 - routine
 - boltgn, 403
 - broken, 493
 - cdCautions, 427
 - cdColm, 422

cdDate, 426
 cdDrive, 401, 419
 cdEms, 422
 cdErrors, 428
 cdExecTime, 426
 cdEXIT, 493
 cdGetCooling_last, 425
 cdGetDepth_depth, 426
 cdGetHeating_last, 425
 cdGetLineList, 421
 cdGetnZone, 425
 cdGetPressure_depth, 425
 cdGetPressure_last, 425
 cdGett, 431
 cdGetTemp_last, 425
 cdInit, 401, 417
 cdIonFrac, 424
 cdLine, 420
cdNoExec, 419
 cdNotes, 428
 cdNwcns, 401, 427
 cdOutp, 418
 cdPrintCommands, 428
 cdRead, 401, 418
 cdSPEC, 426
 cdSurprises, 428
 cdTalk, 418
 cdTemp, 424
 cdTimescales, 426
 cdVersion, 426
 cdWarnings, 427
 Cloudy, 401
 ConvPresTempEdenIoniz, 402
 ConvTempEdenIoniz, 402
 DoOptimize, 401
 esum, 409
 fixit, 493
 insane, 493
 main, 401
 NextDR, 408
 PresChng, 402
 PrintElem, 412
 reageo, 427
 RTOptDepthIncr, 410
 RTOptDepthInit, 410
 RTOptDepthReset, 411
 RTOptDepthReset, 410
 setbuf, 428
 TauInc, 407
 TestCode, 493
 tfidle, 409, 410
 TotalPressure, 409
 update, 501
 ZoneStart, 410
 zonsrt, 407
 running Cloudy, 415

— S —

size of code, 503
 sound travel time, 446
 spectral index
 incident continuum, 433
 transmitted continuum, 448
 sphericity ratio, 408
 stability
 thermal, 436
 stop
 code returned busted, 440
 column density reached, 441

dr small rel to thick, 440
 drad small, 440
 highest Te reached, 441
 internal error, 442
 line ratio reached, 442
 low electron fraction, 440
 low H₂/H fraction, 440
 lowest EDEN reached, 439
 lowest Te reached, 441
 nzone reached, 441
 optical depth reached, 441
 outer radius reached, 441
 radiation pressure, 439
 reason, 439
 temperature out of bounds, 442
 wind velocity < 0, 440
 zero electron density, 442
 storing many models, 430
 strong typing, 490
 structure variables, 410
 style conventions for coding, 490
 subroutine
 calling from Fortran, 416
 use as a, 416
 surface brightness
 computing, 455
 surprises
 printed, 442
 routine to print, 428
 synthetic spectrum
 predicted, 458, 459

— T —

TauInc
 flowchart, 407
 temperature
 21 cm, 425
 21 cm/Ly α , 446
 21cm spin, 425
 brightness, 435
 Compton
 output, 434
 electron
 output, 435
 energy density
 output, 434, 438
 failure, 497
 fluctuations, 448
 getting 21cm/Ly α temperature,
 425
 getting from code, 425
 grain
 output, 438
 jumps, 499
 La excitation, 438
 last, 409
 mean grain
 output, 449
 multi-phase, 498
 obtaining mean, 424
 proposed, 410
 saved, 410
 stability, 498
 t2, 448
 unstable, 435
 variables, 409
 test code, 493
 tests

coolcurve.for, 496
 kmt.for, 496
 map.in, 496
 reflector.in, 454
 thermal stability, 436
 timescale
 Compton, 447
 photoerosion, 447
 sound travel, 446
 thermal, 447
 with cdTimescales, 426
 TODO code, 493
 turbulence, 439

— V —

variable
 abundances, 412
 alogete, 409, 410
 alogte, 409
 autocv, 501
 cdGetchLabel, 421
 cdsqte, 409
 character, 491
 chDate, 494
 chVersion, 494
 conv, 412
 covgeo, 413
 covrt, 413
 depset, 412, 413
 depth, 408, 440
 drad, 407, 440
 dReff, 408, 410
 drNext, 408
 dVeff, 408, 410
 eden, 409
 EdenError, 409
 edensqte, 409
 EdenTrue, 409
 ednstr, 410
 floating, 490
 getpar, 431
 heatstr, 410
 hiistr, 410
 histr, 410
 integers, 490
 iter, 402
 iteration, 411
 itermx, 411
 lgAbnSolar, 413
 lgElmtOn, 412
 lgLastIt, 411
 lgSearch, 412
 lgTauOutOn, 411
 limfal, 497
 logical, 491
 naming convention, 490
 nend, 411
 nPres2Ioniz, 412
 nzone, 402, 411
 pden, 409
 pdenstr, 410
 pirsq, 408
 r1r0sq, 408
 Radius, 408
 radstr, 410
 real, 490
 rinner, 407
 router, 408
 ScaleElement, 413

ScaleMetals, 412
SetAbundances, 412
solar, 412
SolarSave, 412
struc, 410
te, 409
telogn, 409, 410
TeProp, 410
testr, 410
tfail, 403
tlast, 409

volstr, 410
wmole, 409
xIonFrac, 413
xMassDensity, 409
variable naming convention, 490
version number, 426
version numbers, 494

— W —
warnings
 printed, 442
 routine to print, 427

wind, 436

— X —
X-ray to optical ratio, 433

— Z —
zone
 output, 435
 thickness, 407
 variables, 411